CHARACTERIZATION OF TRANSEPITHELIAL TRANSPORT IN THE OSMOREGULATION OF FRESHWATER DIPTERAN LARVAE

Sima Jonusaite

A DISSERTATION SUBMITTED TO THE FACULTY OF GRADUATE STUDIES
IN PARTIAL FULFILMENT OF THE REQUIREMENTS FOR THE DEGREE OF
DOCTOR OF PHILOSOPHY

GRADUATE PROGRAM IN BIOLOGY
YORK UNIVERSITY,
TORONTO, ONTARIO

DECEMBER 2016

ABSTRACT

In the osmoregulatory epithelia of freshwater (FW) animals, transcellular solute transport relies on at least one of the primary ionomotive pumps, Na^+/K^+-ATPase (NKA) and V-type H^+-ATPase (VA), but there are no data on their distribution in FW chironomid larvae. The paracellular solute movement in invertebrate epithelia is controlled by the septate junctions (SJs). However, nothing is known about the SJ components in aquatic insects. In the present set of studies, larvae of the FW chironomid *Chironomus riparius* and FW mosquito *Aedes aegypti* were used to examine a role for NKA and VA and SJ proteins, respectively, in the maintenance of salt and water balance in aquatic dipterans. Spatial distribution and activity of NKA and VA along the alimentary canal of *C. riparius* larvae revealed the importance of the rectum in the ionoregulatory homeostasis. It was found that the rectum absorbed relatively high amounts of K^+ into the hemolymph under dilute conditions and decreased K^+ absorption in brackish water (BW). This rectal K^+ absorption was dependent on the activities of both NKA and VA. Next, genes encoding transmembrane SJ proteins megatrachea, sinuous, kune-kune (Kune), neurexin IV, snakeskin (Ssk), mesh and gliotactin (Gli) were identified in *A. aegypti* and shown to exhibit tissue specific transcript abundance in larval osmoregulatory epithelia. Ssk and mesh expression was restricted to smooth SJ bearing midgut and Malpighian tubules (MT) whereas Gli was detected in all tissues examined. Kune was confined to SJs in the posterior midgut and rectum and apical membrane domain of the syncytial anal papilla epithelium. Rearing *A. aegypti* larvae in BW caused an increase in Kune and Gli protein and Ssk and mesh mRNA abundance in the midgut and MT which occurred in conjunction with increased midgut and decreased MT permeability. Paracellular MT permeability was further modulated by leucokinin. When dsRNA was used to reduce Gli abundance in the midgut, paracellular permeability was decreased. Together, this research provides a better understanding of the physiology of transepithelial ion and water

transport in aquatic insects and offers significant insight into the role of NKA, VA and SJ proteins in the osmoregulation of FW dipteran larvae.

ACKNOWLEDGMENTS

Firstly, I would like to express my sincerest thanks to my supervisors Dr. Andrew Donini and Dr. Scott Kelly. It has been an honor to be your student. You both have contributed immensely to my professional as well as personal growth. I truly could have not imagined having more caring, supportive and inspirational mentors as well as friends. I am eternally grateful for your trust in me.

I would also like to thank my advisors, Dr. Amro Zayed and Dr. Barry Loughton, for their time, insightful comments and encouragement.

My time at York was made enjoyable in large part due to the Donini and Kelly lab people, most of whom I now call my friends. I thank you, my fellow past and present labmates, for the stimulating discussions, late nights we were working together before deadlines, and all the fun we have had in the last six years. In particular, I thank my old friends and partners-in-crime Dennis, Helen, Phuong, Adrian and Lisa, and my new "gang" Andrea, Lidiya, Gil and Fargol!

I also thank members of the Paluzzi lab for their expertise and equipment as well as enjoyable conversations.

I owe special thanks to my family for all their love and understanding. For my parents and my big sister who supported me in all my pursuits.

Lastly, I have to thank my beloved Sophie Kelly, one of the greatest dog friends I have ever had. You have been my dose of oxytocin and have helped me keep my sanity in place throughout grad school. I love you and I will miss you!

TABLE OF CONTENTS

LIST OF TABLES

LIST OF FIGURES

Chapter One

Chapter Two

Chapter Three

Chapter Four

Appendix A

LIST OF ABBREVIATIONS

ADB – antibody dilution buffer
ADP – adenosine diphosphate
*Ae*AE – *Aedes aegypti* anion exchanger
AJM – apical junction molecule
Aka – anakonda
AMG – anterior midgut
ANOVA – analysis of variance
AP – anal papillae
ASET – automated scanning electrode technique
Bark – bark beetle
BLAST – Basic Local Alignment Search Tool
BSA – bovine serum albumin
BW – brackish water
CA – carbonic anhydrase
CAM – cell adhesion molecule
cDNA – complementary deoxyribonucleic acid
CDS – coding sequence
CeAJ – *Caenorhabditis elegans* apical junction
ChTX – charybdotoxin
CLAMS – cholinesterase-like adhesion molecules
Cldn – claudin
Cont – contactin
Cora/Cor – coracle
Cy-2 – cyanine-2
Da – dalton
DAPI – 4',6-diamidino-2-phenylindole
Dlg – discs large
DMSO – dimethyl sulfoxide
DNA – deoxyribonucleic acid
dNTP – deoxynucleotide triphosphate
dsRNA – double stranded RNA
DTT – dithiothreitol
ECL – enhanced chemiluminescence
ECL1/2 – extracellular loop 1/2
EDTA - ethylenediaminetetraacetic acid
EGF – epidermal growth factor
EM – electron microscopic
EST – expressed sequence tag
FAMG – foregut and anterior midgut
FasIII – fasciclin III
FG – foregut
FITC – fluorescein isothiocyanate
FRAP – fluorescence recovery after photobleaching
FW – freshwater

GAPDH – glyceraldehyde 3-phosphate dehydrogenase
GC – gastric caeca
Gli – gliotactin
Grh – grainy head
HEPES – 4-(2-hydroxyethyl)-1-piperazineethanesulfonic acid
HG – hindgut
IPW – ion-poor water
ISME – ion-selective microelectrode
kDa – kilodalton
Kune – kune-kune
Lac – lachesin
βLac – β-lactamase
Lgl – lethal giant larva
LKVIII – leucokinin-VIII
MAGUK – membrane-associated guanylate kinase
Mcr – macroglobulin complement-related
Mega – megatrachea
mRNA – messenger RNA
MT – Malpighian tubules
MTf – melanotransferrin
MW – molecular weight
NCBI – National Center for Biotechnology Information
NCP1 – neurexin IV/Caspr/paranodin
ND – not detected
NKA – Na^+-K^+-ATPase
Nrg – neuroglian
Nrv2 – NKA β subunit
Nrx IV – neurexin IV
ORF – open reading frame
PBS – phosphate-buffered saline
PCR – polymerase chain reaction
PEG-400 – polyethylene glycol-400
PJ – paranodal junction
PMSF – phenylmethylsulfonyl fluoride
pSJ – pleated septate junction
Pt – peptide
qRT-PCR – quantitative real-time PCR
RNA – ribonucleic acid
RNAi – RNA interference
Rp49 – ribosomal protein 49
RT – room temperature
RT-PCR – reverse transcriptase PCR
Scrib – scribble
SDS-PAGE – sodium dodecyl sulfate polyacrylamide gel electrophoresis
SEI – homogenization buffer containing sucrose, EDTA and imidazole
SEID – SEI with sodium deoxycholate
SEM – standard error of the mean

SIET – scanning ion-selective electrode technique
SJ – septate junction
sSJ – smooth septate junction
Ssk – snakeskin
SW – seawater
TBS – Tris-buffered saline
TBS-T – TBS with Tween-20
TCJ – tricellular junction
TJ – tight junction
TRITC – tetramethyl rhodamine isothiocyanate
Tsp2A – tetraspanin 2A
VA – V-type H^+-ATPase
Vari – varicose
WVS – water vascular system
ZO-1 – zonula occludens-1
18S rRNA – 18S ribosomal RNA

STATEMENT OF CONTRIBUTION

Chapter Two
This chapter was written by S. Jonusaite with valuable guidance and editorial support from Dr. S.P. Kelly and Dr. A. Donini. All of the experiments were executed by S. Jonusaite.

Chapter Three
This chapter was co-written by S. Jonusate, Dr. S.P. Kelly and Dr. A. Donini.

Chapter Four
This chapter was written by S. Jonusaite with valuable guidance and editorial support from Dr. S.P. Kelly and Dr. A. Donini. Megatrachae, sinuous, neurexin IV and kune-kune gene identification and real-time PCR analyses were executed by S. Jonusaite with valuable assistance from Dr. E. Clelland. Kune-kune immunochistochemistry and western blotting were executed by S. Jonusaite.

Chapter Five
This chapter was written by S. Jonusaite with valuable guidance and editorial support from Dr. S.P. Kelly and Dr. A. Donini. All of the experiments were executed by S. Jonusaite.

Chapter Six
This chapter was written by S. Jonusaite with valuable guidance and editorial support from Dr. S.P. Kelly and Dr. A. Donini. Gliotactin gene identification, assembly and analysis were executed by S. Jonusaite with valuable assistance from Dr. D. Kolosov. Gliotactin immunochistochemistry, western blotting, real-time PCR analyses were executed by S. Jonusaite. dsRNA knockdown and midgut permeability experiments were also executed by S. Jonusaite.

Chapter Seven
This chapter was written by S. Jonusaite with valuable guidance and editorial support from Dr. S.P. Kelly and Dr. A. Donini. All of the experiments were executed by S. Jonusaite.

Appendix A
All supplementary experiments and analyses described in this section were executed by S. Jonusaite.

_____ _____

Sima Jonusaite (PhD Candidate) Dr. Andrew Donini (PhD Supervisor)

_____

Dr. Scott P. Kelly (PhD Co-Supervisor)

CHAPTER 1: Overview

1.1 Environmental challenges and fundamental osmoregulatory strategies in aquatic dipteran larvae

Aquatic life demands special osmoregulatory adaptations for maintaining a relatively constant internal environment. The problems encountered in the homeostatic control of the ionic and osmotic composition of the blood/hemolymph relate to the nature of the external surrounding. Aquatic dipterans such as larval chironomids and mosquitoes live in a variety of habitats ranging from freshwater (FW) lakes, rivers and ponds (< 300 mOsm) to brackish water (BW) ditches, coastal salt marshes (300-1000 mOsm) and hypersaline pools (> 1000 mOsm; Driver 1977; Parma and Krebs 1977; Pinder 1995; Colbo 1996; Clements 1992; Bradley 1994; Williams and Williams 1998). One of the challenges faced by larvae is the tendency for their habitats to fluctuate in salinity. For instance, heavy rain can significantly reduce salt content in the relatively low volume habitats. By contrast, evaporation can lead to increased salinity. Environmental salt content may also change as a consequence of municipal effluents, irrigation and winter road salting and as a result of global warming causing a rise in sea levels in the coastal zones (Bervoets et al. 1995; Hassell et al. 2006; Cañedo-Argüelles et al. 2013; Silver et al. 2009; Ramasamy and Surendran 2012).

In these changing aquatic environments, larvae must be capable of regulating their hemolymph composition. The physiological challenges facing the larvae in FW are very different from those that arise in saline environments. Larvae of mosquitoes and chironomids found in FW are osmoregulators, that is, they maintain relatively constant hemolymph ionic concentrations which are much higher compared to those of the external medium (Lauer 1969; Wright 1975; Greenaway 1979; Barker and Wilhm 1982; Bradley 1994; Grueber and Bradley 1994; Patrick et al. 2001; Albers and Bradley 2011). The FW larvae whose hemolymph osmotic concentration is

in the range of approximately 200-350 mOsm kg^{-1} (Edwards 1982; Scholz and Zerbst-Boroffka 1998, Patrick and Bradley 2000) are hyperosmotic to the FW environment and thus tend to gain water by osmosis and risk losing essential ions to the surrounding. In addition to water entering larvae osmotically across the integument, body fluids are also diluted by water ingested along with food (Aly and Dadd 1989). Removal of excess water and ion conservation are achieved by the combined actions of key osmoregulatory organs such as the midgut, Malpighian tubules, hindgut and anal papillae (Fig. 1-1; Bradley 1994; Donini and O'Donnell 2005; Donini et al. 2006; Nguyen and Donini 2010; Zadeh-Tahmasebi et al. 2016).

The midgut is the site of nutrient and ion absorption from the food to the hemolymph (Jonusaite et al. 2011; Linser and Dinglasan 2014). The Malpighian tubules, which open into the alimentary canal at the junction of the midgut and the hindgut (Fig. 1-1), produce the primary urine through secretion of ions (Na^+, K^+, Cl^-) and the subsequent osmotic influx of water into their lumen from the hemolymph (Clark and Bradley 1996; Donini et al. 2006; Zadeh-Tahmasebi et al. 2016). The modification of this primary urine to meet the ionic and osmotic regulatory needs of the larvae is carried out in the rectal segment of the hindgut. The rectum is responsible for selective reabsorption of ions from the primary urine into the hemolymph which ultimately results in the formation of a dilute urine (Bradley 1987). The importance of the rectum in osmoregulation is also evident in the salt tolerant mosquito species which possess a specialized rectal segment that secretes ions into the rectal lumen where a final concentrated urine is formed (Bradley and Phillips 1975; Smith et al. 2008). Production of a hypertonic urine enables these mosquito larvae to survive in habitats of high salt content (Bradley and Phillips 1975). Lastly, larval chironomids and mosquitoes possess four externally protruding anal papillae (Fig. 1-1) which are sites of uptake of Na^+, Cl^- and K^+ from dilute environments (Credland 1976; Edwards and Harrison 1983; Donini and O'Donnell 2005; Nguyen and Donini 2010). Variations in

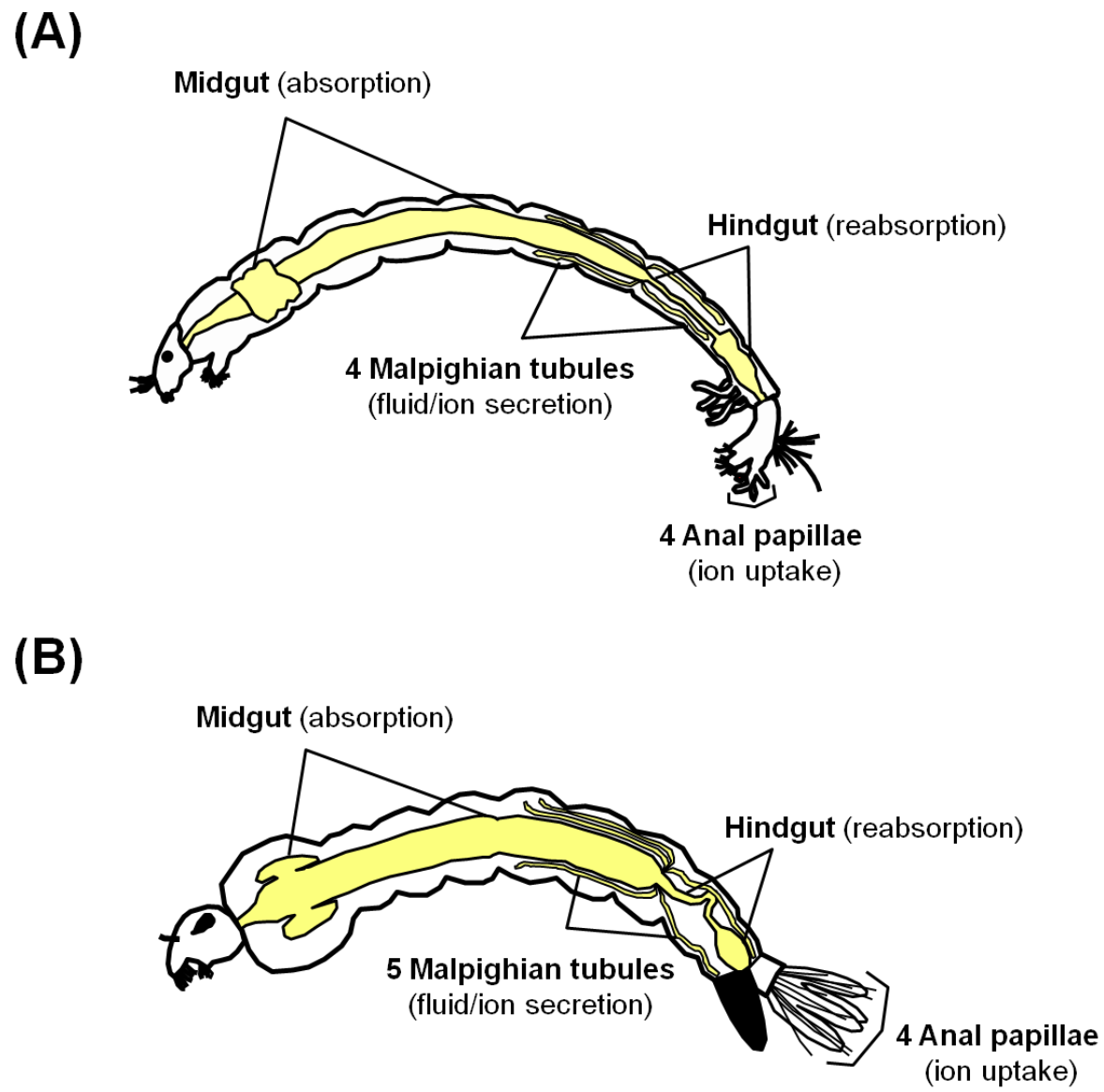

Figure 1-1: Structures associated with ion and water transport in freshwater (**a**) chironomid and (**b**) mosquito larva. The midgut is the site of ion absorption from the food sources. The Malpighian tubules produce primary urine by actively secreting ions from the haemolymph into their lumen. The hindgut is responsible for reabsorption of ions from the primary urine into the hemolymph which results in formation of a dilute urine for excretion. The anal papillae are sites of ion uptake from dilute external media.

external salinity affect both the size and the epithelial fine structure of the anal papillae. When mosquito larvae are reared in BW, the papillae are shorter, have less apical plasma membrane infolds and fewer mitochondria relative to those of larvae reared in FW, suggesting a reduction in ion uptake in saline conditions (Sohal and Copeland 1966; Edwards and Harrison 1983).

1.2 Ion and water movement across the osmoregulatory epithelia of freshwater larval chironomid and mosquito

1.2.1 Role of transcellular transport

In order for the larvae to maintain hemolymph homeostasis in FW, ions must be transported against their electrochemical gradients. The Na^+/K^+-ATPase (NKA) and V-type H^+-ATPase (VA) are well-known primary ionomotive pumps implicated in driving transepithelial solute movement across osmoregulatory epithelia in many aquatic FW animals including larval insects (Khodabandeh 2006; Marshall 2002; Lockwood APM 2008). In the gills of crustaceans a role for VA and NKA in ion uptake is well documented (Tsai and Lin 2007) and alterations in external salinity result in changes in the expression and/or activity of both ATPases (Lovett et al. 2006; Weihrauch et al. 2001). The function of fish gills also relies on the actions of these pumps (Marshall 2002; Hwang and Lee 2007).

The presence and localization of both ATPases have been established in all of the major osmoregulatory tissues of FW mosquito larvae, where they are proposed to play an integral role in ion transport (Patrick et al. 2006; Smith et al. 2008; Okech et al. 2008; Xiang et al. 2012). In the anterior midgut of larval mosquitoes, VA is responsible for maintaining high pH in the lumen which is essential for the function of digestive enzymes (Onken and Moffett 2009; Dadd 1975). The voltage gradient produced by VA is also responsible for driving Na^+/amino acid co-transporters (Harvey et al. 2009). In larval posterior midgut, NKA has been suggested to power Na^+ absorption, especially in dilute FW environments (Patrick et al. 2006; Okech et al. 2008).

The Malpighian tubules are responsible for producing the primary urine where the activity of VA on the apical side of the tubule epithelium is believed to drive Na^+ and K^+ transport and the subsequent osmotic influx of water into the lumen of the tubules (Weng et al. 2003; Patrick et al. 2006; Xiang et al. 2012). The rectum, which is responsible for reabsorption of ions from the primary urine, expresses both VA and NKA on the apical and basal sides, respectively (Patrick et al. 2006; Smith et al. 2008). When mosquito larvae are subjected to higher salinity there are apparent shifts in the localization of VA and/or NKA in the rectum, although it is unclear whether overall activity of these pumps changes (Smith et al. 2008). Lastly, both NKA and VA are expressed in the epithelium of anal papillae of FW mosquito larvae where VA is present on the apical plasma membrane and drives ion uptake from FW environments (Patrick et al. 2006; Del Duca et al. 2011). Ion transport at the anal papillae can alter with changes in external salinity such that there is a decrease in NaCl uptake if the larvae are acutely transferred from FW to 30% seawater (Donini et al. 2007).

Very little is known about the ion and water transport mechanisms and regulation in FW chironomid larvae. It has been shown that despite a substantial reduction in external ion levels, larvae of FW chironomid *Chironomus riparius* reared in ion-poor water (IPW) maintain hemolymph NaCl and pH at the same levels as larvae reared in FW (Nguyen and Donini 2010). This is partially attributed to the anal papillae, which are sites of net NaCl absorption and H^+ secretion under ion-poor conditions (Nguyen and Donini 2010). In a more recent study that examined the effects of increased external salinity on ionoregulatory homeostasis in larval *C. riparius*, it was demonstrated that larvae respond to an acute exposure to BW (20% SW) with a corresponding increase in hemolymph Na^+ and Cl^-, a decrease in hemolymph pH and a reduction in whole body NKA and VA activities (Jonusaite et al. 2011). In addition, VA activity in the gut (which included the Malpighian tubules) was considerably higher than whole body VA activity in

FW-reared larvae (Jonusaite et al. 2011). Combined, these findings have suggested that the ionomotive enzymes may play a regulatory role in ion transport activities across the gut and Malpighian tubules of *C. riparius* larva in response to changing salinity (Jonusaite et al. 2011).

1.2.2 Role of paracellular transport

In the epithelia of insects and more broadly arthropods, the paracellular route of solute and water transport is regulated by specialized intercellular occluding junctions, the septate junctions (SJs; Lane and Skaer 1980; Noirot-Timothee and Noirot 1980). SJs typically form circumferential belts around the apicolateral regions of epithelial cells. In electron micrographs of cross-sectional view, SJs show a characteristic ladder-like arrangement of distinct septa that span the lateral plasma membranes of epithelial cells and maintain a constant 15-20 nm distance between them (Green and Bergquist 1982). Two morphological variants of SJs have been described in the epithelia of arthropods on the basis of their ultrastructural appearance in oblique sections: the pleated SJs (pSJs) and the smooth SJs (sSJs). The septa of pSJs form regular undulating rows and those in sSJs are arranged in regularly spaced parallel lines (Noirot-Timothee and Noirot 1980). pSJs are generally observed in ectodermally derived epithelia such as the epidermis, foregut, hindgut, trachea and salivary glands, while sSJs are found mainly in the endodermally derived midgut epithelium and its derivatives as well as Malpighian tubules (Lane and Skaer 1980; Green and Bergquist 1982). Biological significance and functional properties of the two types of SJs in arthropods are still not well understood largely because of a paucity of information on their molecular physiology.

The molecular physiology of arthropod SJs is only known to any extent in *Drosophila* where over twenty pSJ-associated transmembrane and cytoplasmic proteins have been identified (Izumi and Furuse 2014; Deligiannaki et al. 2015). Loss-of-function mutations in most of these proteins prevent the formation of septa or SJ organization which in turn disrupts the

transepithelial barrier properties of ectodermally derived epithelia (for review see Izumi and Furuse 2014). In addition, three *Drosophila* sSJ-specific membrane proteins, snakeskin (Ssk), mesh and Tsp2A, have recently been discovered (Yanagihashi et al. 2012; Izumi et al. 2012; Izumi et al. 2016). All three proteins localize specifically to sSJs in the midgut and Malpighian tubules and are required for sSJ formation and intestinal barrier function (Yanagihashi et al. 2012; Izumi et al. 2012; Izumi et al. 2016).

Although evidence is growing to suggest that proteins of both pSJs and sSJs play a role in regulating paracellular solute movement in the epithelia of insects, nothing is known about the contribution of pSJs and/or sSJs to salt and water balance in aquatic insects such as FW larval mosquitoes and chironomids or more specifically whether SJ proteins play a role in reducing ion loss to a hypoosmotic FW environment. Similarly, nothing is known about the role of SJ proteins in maintaining salt and water balance in mosquito and chironomid larvae when the animals face changes in water salt content. Salinity-induced changes in the ultrastructure of pSJs have been reported for the gill epithelium of euryhaline crabs (Luquet et al. 1997, 2002). In low-salinity acclimated crabs, the pSJs between the gill ionocytes are long, highly-developed and have numerous, closely packed septa (Luquet et al. 1997, 2002). At higher salinities, the SJs of the crab gill epithelium become significantly shorter and confined to the apical region of the ionocytes, suggesting an increase in junctional permeability under high salinity conditions (Luquet et al. 1997, 2002). Salinity-induced alterations in junctional morphology have also been seen in the teleost fish gill epithelium which possesses tight junctions (TJs) as occluding junctions (for review see Chasiotis et al. 2012b). More specifically, gill cells of FW teleost fishes are linked by deep TJs, whereas in the saline water teleost fish gill epithelium only shallow TJs are present (Duffy et al. 2011; Chasiotis et al. 2012b). In addition to ultrastructure, the abundance of TJ proteins in fishes and amphibians alters in response to changes in environmental ion levels,

and in dilute conditions these changes are proposed to limit ion loss (Bagherie-Lachidan et al. 2008; Chasiotis and Kelly 2009; Chasiotis et al. 2012a; Duffy et al. 2011; Kwong and Perry 2013; Tipsmark et al. 2008).

1.3 Research objectives

As mentioned in Section 1.1, habitats of FW chironomid and mosquito larvae may fluctuate in salinity due to natural and anthropogenic factors. In order to understand what enables these larvae to survive in conditions of varying environmental ion levels, it is necessary to characterize both transcellular and paracellular pathways in the osmoregulatory organs.

1.3.1 PART1: The FW larval chironomid *C. riparius* was selected to gain a more profound understanding of the transcellular ion transport mechanisms within larval osmoregulatory tissues. Although larval *C. riparius* are ubiquitous benthic inhabitants of FW ecosystems throughout the northern hemisphere (Pinder 1995), they are also known to thrive in natural BW environments as well as polluted FW habitats exposed to salinated industrial effluents and road salts (Driver 1977; Colbo 1996; Parma and Krebs 1977; Bervoets et al. 1995; Lob and Silver 2012). The importance of studying these larvae is primarily associated with their ecological values as items of the food chain and detritus-feeding recyclers of the aquatic ecosystems. Climate change and human activities are predicted to continue damaging FW ecosystems and as a result, understanding the physiological mechanisms that permit larval *C. riparius* to thrive in different environmental conditions is important.

As reviewed in Section 1.2.1, it has been shown that acute exposure to BW decreased whole body activities of primary ionomotive enzymes NKA and VA in *C. riparius* larvae. In addition, in FW-reared *C. riparius* larvae the bulk of VA activity was found to be in the alimentary canal (i.e. gut and Malpighian tubules). Based on this information, the working hypothesis was that modulation of ionomotive enzyme activity in one or more regions of the

alimentary canal would be important in order for larval *C. riparius* to acclimate to changes in environmental salinity. The aims of this research were as follows:

1) Examine spatial distribution and activity of NKA and VA along the alimentary canal of larval *C. riparius* under varying salinity.

2) Establish a potential role for specific segments of the gut as well as the Malpighian tubules in ion regulation of *C. riparius* larvae upon exposure to different ionic conditions.

1.3.2 PARTII: At the beginning of the current studies, there was no information on the molecular and functional details of the paracellular route in the epithelia of aquatic arthropods. As such, nothing was known about SJs or SJ proteins with respect to epithelial permeability and osmoregulation in aquatic arthropods beyond the ultrastructural observations of salinity-induced changes in SJs in the crab gill epithelium (as reviewed in Section 1.2.2). Given the importance of TJ proteins in the maintenance of salt and water balance in FW vertebrates such as fishes (see Chasiotis et al. 2012b) and that invertebrate SJs are functional counterparts of vertebrate TJs, characterization of the molecular SJ physiology within the osmoregulatory tissues of FW insect was clearly needed.

The FW larval mosquito *Aedes aegypti* was chosen to identify and characterize SJ proteins in the osmoregulatory epithelia and determine whether SJ proteins play a role in larval osmoregulation by examining their contribution to the modulation of the permeability of osmoregulatory tissues. The larvae of *A. aegypti* are readily available and easily maintained in a laboratory setting in addition to being a good model for genetic studies due to available genome sequence. Studying the potential contribution of SJ proteins to the maintenance of salt and water balance in larval *A. aegypti* is of additional significance because this species is a vector of re-emerging viral diseases, Dengue, Chikungunya, Yellow fever and Zika, and mounting evidence suggests that these animals successfully breed in salinated water in addition to FW (Ramasamy

and Surendran 2012). Therefore, a more complete understanding of their osmoregulatory physiology may provide new and specific strategies for controlling their populations.

As discussed in Section 1.2.2, over twenty pSJ-associated proteins and three sSJ-specific proteins have been characterized and shown to contribute to the barrier function of *Drosophila* epithelia. With this background information in mind, homologs of seven transmembrane *Drosophila* SJ proteins megatrachea, sinuous, kune-kune, neurexin IV, snakeskin, mesh and gliotactin were selected for studies in larval *A. aegypti*. It was hypothesized that these SJ proteins would be expressed in larval mosquito osmoregulatory epithelia and their abundance would alter in response to changes in salinity and that these SJ protein alterations would occur in conjunction with changes in the paracellular permeability of osmoregulatory organs. The principal aims of this research were as follows:

1) Consolidate what is currently known about the occluding junctions of invertebrate epithelia.

2) Identify SJ proteins in larval *A. aegypti* osmoregulatory epithelia.

3) Establish a potential role for SJ proteins in the regulation of salt and water balance in *A. aegypti* larvae.

4) Determine the contribution of SJ proteins to the modulation of the permeability of larval *A. aegypti* osmoregulatory epithelia.

1.4 References

Albers MA, Bradley TJ (2011) On the evolution of saline tolerance in the larvae of mosquitoes in the genus *Ochlerotatus*. Physiol Biochem Zool 84:258-267

Aly C, Dadd RH (1989) Drinking rate regulation in some fresh-water mosquito larvae. Physiol Entomol 14:241-256

Bagherie-Lachidan M, Wright SI, Kelly SP (2008) Claudin-3 tight junction proteins in *Tetraodon nigroviridis*: cloning, tissue-specific expression, and a role in hydromineral balance. Am J Physiol Regul Integr Comp Physiol 294:R1638-R1647

Barker DM, Wilhm J (1982) Osmoregulation in *Chironomus tentans* (Fabr.), *Chironomus riparius* meigen, and *Chaoborus punctipennis* (say). Comp Biochem Physiol A 73:719-724

Jonusaite S, Kelly SP, Donini A (2011) The physiological response of larval *Chironomus riparius* (Meigen) to abrupt brackish water exposure. J Comp Physiol B 181:343-352

Bervoets L, Baillieul B, Blust R, Verheyen R (1995) Evaluation of effluent toxicity and ambient toxicity in a polluted lowland river. Environ Pollut 91:333-341

Bradley TJ (1987) Physiology of osmoregulation in mosquitoes. Annu Rev Entomol 32:439-462

Bradley TJ (1994) The role of physiological capacity, morphology and phylogeny in determining habitat use in mosquitoes. In: Wainwright PC and Reilly MS (eds) Ecological Morphology: Integrative Organismal Biology. University of Chicago Press, Chicago, IL, pp 303-318

Bradley TJ, Phillips JE (1975) The secretion of hyperosmotic fluid by the rectum of a saline-water mosquito larva *Aedes taeniorhynchus*. J Exp Biol 63:331-342

Cañedo-Argüelles M, Kefford BJ, Piscart C, Prat N, Schäfer RB, Schulz CJ (2013) Salinisation of rivers: an urgent ecological issue. Environ Pollut 173:157-167

Chasiotis H, Kelly SP (2009) Occludin and hydromineral balance in *Xenopus laevis*. J Exp Biol 212:287-296

Chasiotis H, Kolosov D, Kelly SP (2012a) Permeability properties of the teleost fish gill epithelium under ion-poor conditions. Am J Physiol Regul Integr Comp Physiol 302:R727-R739

Chasiotis H, Kolosov D, Bui P, Kelly SP (2012b) Tight junctions, tight junction proteins and paracellular permeability across the gill epithelium of fishes: a review. Resp Physiol Neurobiol 184:269-281

Clark TM, Bradley TJ (1996) Stimulation of Malpighian tubules from larval *Aedes aegypti* by secretagogues. J Insect Physiol 42:593-602

Clements AN (1992) The biology of mosquitoes, vol 1. Chapman & Hall, London

Colbo MH (1996) Chironomidae from marine coastal environments near St. John's, Newfoundland, Canada. Hydrobiologia 318:117-122

Credland PF (1976) A structural study of the papillae of the midge *Chironomus riparius Meigen* (Diptera: Chironomidae). Cell Tissue Res 166: 531-540

Dadd RH (1975) Alkalinity within the midgut of mosquito larvae with alkaline-active digestive enzymes. J Insect Physiol 21:1847-1853

Del Duca O, Nasirian A, Galperin V, Donini A (2011) Pharmacological characterisation of apical Na^+ and Cl^- transport mechanisms of the anal papillae in the larval mosquito *Aedes aegypti*. J Exp Biol 214:3992-3999

Deligiannaki M, Casper AL, Jung C, Gaul U (2015) Pasiflora proteins are novel core components of the septate junction. Development 142:3046-3057

Donini A, Gaidhu MP, Strasberg D, O'Donnell MJ (2007) Changing salinity induces alterations in hemolymph ion concentrations and Na^+ and Cl^- transport kinetics of the anal papillae in the larval mosquito, *Aedes aegypti*. J Exp Biol 210:983-992

Donini A, O'Donnell MJ (2005) Analysis of Na^+, Cl^-, K^+, H^+ and NH_4^+ concentration gradients adjacent to the surface of anal papillae of the mosquito *Aedes aegypti*: application of self referencing ion-selective microelectrodes. J Exp Biol 208:603-610

Donini A, Patrick ML, Bijelic G, Christensen RJ, Ianowski JP, Rheault MR, O'Donnell MJ (2006) Secretion of water and ions by Malpighian tubules of larval mosquitoes: Effects of diuretic factors, second messengers, and salinity. Physiol Biochem Zool 79:645-655

Driver EA (1977) Chironomid communities in small prairie ponds: some characteristics and controls. Freshw Biol 7:121-133

Duffy NM, Bui P, Bagherie-Lachidan M, Kelly SP (2011) Epithelial remodeling and claudin mRNA abundance in the gill and kidney of puffer fish (*Tetraodon biocellatus*) acclimated to altered environmental ion levels. J Comp Physiol B 181:219-238

Edwards HA (1982) Free amino acids as regulators of osmotic pressure in aquatic insect larvae. J Exp Biol 101:153-160

Edwards HA, Harrison JB (1983) An osmoregulatory syncytium and associated cells in a freshwater mosquito. Tissue Cell 15: 271-280

Green CR, Bergquist PR (1982) Phylogentic relationships within the invertebrates in relation to the structure of septate junctions and the development of 'occluding' junctional types. J Cell Sci 53: 279-305

Greenaway P (1979) Fresh water invertebrates. In: Maloiy GMO (ed) Comparative physiology of osmoregulation in animals, vol. 1. Academic Press, New York, pp 117-174

Grueber WB, Bradley TJ (1994) The evolution of increased salinity tolerance in larvae of *Aedes* mosquitoes: a phylogenetic analysis. Physiol Zool 67:566-579

Harvey WR, Boudko DY, Rheault MR, Okech BA (2009) NHE (VNAT): an H^+ V-ATPase electrically coupled to a Na^+:nutrient amino acid transporter (NAT) forms an Na^+/H^+ exchanger (NHE). J Exp Biol 212(3):347-357

Hassell KL, Kefford BJ, Nugegoda D (2006) Sub-lethal and chronic salinity tolerances of three freshwater insects: *Cloeon* sp. and *Centroptilum* sp. (Ephemeroptera: Baetidae) and *Chironomus* sp. (Diptera: Chironomidae). J Exp Biol 209:4024-4032

Hwang PP, Lee TH (2007) New insights into fish ion regulation and mitochondrion rich cells. Comp Biochem Physiol A 148:479-497

Izumi Y, Furuse M (2014) Molecular organization and function of invertebrate occluding junctions. Semin Cell Dev Biol 36:186-193

Izumi Y, Motoishi M, Furuse K, Furuse M (2016) A tetraspanin regulates septate junction formation in Drosophila midgut. J Cell Sci 129:1155-1164

Izumi Y, Yanagihashi Y, Furuse M (2012) A novel protein complex, Mesh-Ssk, is required for septate junction formation in the *Drosophila* midgut. J Cell Sci 125:4923-4933

Jonusaite S, Kelly SP, Donini A (2011) The physiological response of larval *Chironomus riparius* (Meigen) to abrupt brackish water exposure. J Comp Physiol B 181:343-352

Khodabandeh S (2006) Na^+,K^+-ATPase in the gut of larvae of the Zygopteran, *Ischnura elegans*, and the Anisoptera, *Libellula lydia*, (Odonata): activity and immunocytochemical localization. Zool Stud 45: 510-516

Kwong RM, Perry SF (2013) The tight junction protein claudin-b regulates epithelial permeability and sodium handling in larval zebrafish, *Danio rerio*. Am J Physiol Regul Integr Comp Physiol 304:R504-R513

Lane NJ, Skaer HB (1980) Intercellular junctions in insect tissues. In: Berridge MJ, Treherne JE, Wigglesworth VB (eds) Advances in Insect Physiology, vol 15. Academic Press, London, pp 35-213

Lauer GJ (1969) Osmotic regulation of *Tanypus nubifer*, *Chironomus plumosus*, and *Enallagma clausum* in various concentrations of saline lake water. Physiol Zool 42:381-387

Linser PJ, Dinglasan RR (2014) Insect gut structure, function, development and target of biological toxins. In: Dhadialla TS, Gill SS (eds) Advances in insect physiology, vol. 47. Academic Press, Oxford, UK, pp 1-37

Lob DW, Silver P (2012) Effects of elevated salinity from road deicers on *Chironomus riparius* at environmentally realistic springtime temperatures. Freshwater Sci 31:1078-1087

Lockwood APM (2008) The osmoregulation of crustacea. Biol Rev 37:257-303

Lovett DL, Verzi MP, Burgents JE, Tanner CA, Glomski K, Lee JJ, Towle DW (2006) Expression profiles of Na^+, K^+ ATPase during acute and chronic hypo-osmotic stress in the blue crab *Callinectes sapidus*. Biol Bull 211:58-65

Luquet CM, Genovese G, Rosa GA, Pellerano GN (2002) Ultrastructural changes in the gill epithelium of the crab *Chasmagnathus granulates* (Decapoda: Grapsidae) in diluted and concentrated seawater. Mar Bio 141:753-760

Luquet C, Pellerano G, Rosa G (1997) Salinity-induced changes in the fine structure of the gills of the semiterrestrial estuarian crab, *Uca uruguayensis* (Nobili, 1901) (Decapoda, Ocypodidae). Tissue Cell 29: 495-501

Marshall WS (2002) Na^+, Cl^-, Ca^{2+} and Zn^{2+} transport by fish gills: retrospective review and prospective synthesis. J Exp Zool 293:264-283

Nguyen H, Donini A (2010) Larvae of the midge, *Chironomus riparius* possess two distinct mechanisms for ionoregulation in response to ion-poor conditions. Am J Physiol Regul Integr Comp Physiol 299:R762-R773

Noirot-Timothee C, Noirot C (1980) Septate and scalariform junctions in arthropods. Int Rev Cytol 63:97-141

Okech BA, Boudko DY, Linser PJ, Harvey WR (2008) Cationic pathway of pH regulation in larvae of *Anopheles gambiae*. J Exp Biol 211:957-968

Onken H, Moffett DF (2009) Revisiting the cellular mechanisms of strong luminal alkalinization in the anterior midgut of larval mosquitoes. J Exp Biol 212:373-377

Parma S, Krebs BPM (1977) The distribution of chironomid larvae in relation to chloride concentration in a brackish water region of The Netherlands. Hydrobiologia 52:117-126

Patrick ML, Aimanova K, Sanders HR, Gill SS (2006) P-type Na^+/K^+-ATPase and V-type H^+-ATPase expression patterns in the osmoregulatory organs of larval and adult mosquito *Aedes aegypti*. J Exp Biol 209:4638-4651

Patrick ML, Bradley TJ (2000) The physiology of salinity tolerance in larvae of two species of *Culex* mosquitoes: the role of compatible solutes. J Exp Biol 203:821-830

Patrick ML, Gonzalez RJ, Bradley TJ (2001) Sodium and chloride regulation in freshwater and osmoconforming larvae of *Culex* mosquitoes. J Exp Biol 204:3345-3354

Pinder LCV (1995) The habitats of chironomid larvae. In: Armitage PD, Cranston PS, Pinder LCV (eds) The chironomidae: biology and ecology of non-biting midges. Chapman and Hall, London, pp 107-135

Ramasamy R, Surendran SN (2012) Global climate change and its potential impact on disease transmission by salinity-tolerant mosquito vectors in coastal zones. Front Physiol 3:198

Scholz F, Zerbst-Boroffka I (1998) Environmental hypoxia affects osmotic and ionic regulation in freshwater midge-larvae. J Insect Physiol 44:427-436

Silver P, Rupprecht SM, Stauffer MF (2009) Temperature-dependent effects of road deicing salt on chironomid larvae. Wetlands 29:942-951

Smith KE, VanEkeris LA, Okech BA, Harvey WR, Linser PJ (2008) Larval anopheline mosquito recta exhibit a dramatic change in localization patterns of ion transport proteins in response to shifting salinity: a comparison between anopheline and culicine larvae. J Exp Biol 211:3067-3076

Sohal RS, Copeland E (1966) Ultrastructural variations in the anal papillae of *Aedes aegypti* (L) at different environmental salinities. J Insect Physiol 12:429-434

Tipsmark CK, Kiilerich P, Nilsen TO, Ebbesson LOE, Stefansson SO, Madsen SS (2008) Branchial expression patterns of claudin isoforms in Atlantic salmon during seawater acclimation and smoltification. Am J Physiol Integr Regul Comp Physiol 294:R1563-R1574

Tsai JR, Lin HC (2007) V-type H^+-ATPase and Na^+/K^+-ATPase in the gills of 13 euryhaline crabs during salinity acclimation. J Exp Biol 210:620-627

Weihrauch D, Ziegler A, Siebers D, Towle DW (2001) Molecular characterization of V-type H^+-ATPase (B-subunit) in gills of euryhaline crabs and its physiological role in osmoregulatory ion uptake. J Exp Biol 204:25-37

Weng XH, Huss M, Wieczorek H, Beyenbach KW (2003) The V-type H^+-ATPase in Malpighian tubules of *Aedes aegypti*: localization and activity. J Exp Biol 206:2211-2219

Williams DD, Williams NE (1998) Aquatic insects in an estuarine environment: densities, distribution and salinity tolerance. Freshw Biol 39:411-421

Wright DA (1975) Sodium regulation in the larvae of *Chironomus dorsalis* (Meig.) and *Camptochironomus tentans* (Fabr.): the effect of salt depletion and some observations on temperature changes. J Exp Biol 62:121-139

Xiang MA, Linser PJ, Price DA, Harvey WR (2012) Localization of two Na^+- or K^+-H^+ antiporters, AgNHA1 and AgNHA2, in *Anopheles gambiae* larval Malpighian tubules and the functional expression of AgNHA2 in yeast. J Insect Physiol 58:570-579

Yanagihashi Y, Usui T, Izumi Y, Yonemura S, Sumida M, Tsukita S, Uemura T, Furuse M (2012) Snakeskin, a membrane protein associated with smooth septate junctions, is required for intestinal barrier function in *Drosophila*. J Cell Sci 125:1980-1990

Zadeh-Tahmasebi M, Bui P, Donini A (2016) Fluid and ion secretion by malpighian tubules of larval chironomids, *Chironomus riparius*: effects of rearing salinity, transport inhibitors, and serotonin. Arch Insect Biochem Physiol 93:67-85

PART I

CHAPTER 2:

TISSUE-SPECIFIC IONOMOTIVE ENZYME ACTIVITY AND K^+ REABSORPTION REVEAL THE RECTUM AS AN IMPORTANT IONOREGULATORY ORGAN IN LARVAL *CHIRONOMUS RIPARIUS* EXPOSED TO VARYING SALINITY[1]

2.1 Summary

A role for the rectum in the ionoregulatory homeostasis of larval *Chironomus riparius* was revealed by rearing animals in different saline environments and examining: (1) the spatial distribution and activity of keystone ionomotive enzymes Na^+-K^+-ATPase (NKA) and V-type H^+-ATPase (VA) in the alimentary canal and (2) rectal K^+ transport with scanning ion-selective electrode technique (SIET). NKA and VA activity were measured in four distinct regions of the alimentary canal as follows: the combined foregut and anterior midgut (FAMG), the posterior midgut (PMG), the Malpighian tubules (MT) and the hindgut (HG). Both enzymes exhibited 10 – 20 times greater activity in the HG relative to all other areas. When larvae were reared in either ion-poor water (IPW) or freshwater (FW), no significant difference in HG enzyme activity was observed. However, in brackish water (BW) reared animals, NKA and VA activity in the HG significantly decreased. Immunolocalization of NKA and VA in the HG revealed that the bulk of protein was located in the rectum. Therefore K^+ transport across the rectum was examined using SIET. Measurement of K^+ flux along the rectum revealed a net K^+ reabsorption which was reduced four-fold in BW-reared larvae versus larvae reared in FW or IPW. Inhibition of NKA with ouabain, VA with bafilomycin and K^+ channels with charybdotoxin, diminished rectal K^+ reabsorption in FW- and IPW-reared larvae, but not BW-reared larvae. Data suggest that the rectum of *C. riparius* plays an important role in allowing these larvae to cope with dilute as well as salinated environmental conditions.

---

[1]Contributing authors: Sima Jonusaite, Scott P Kelly and Andrew Donini

Department of Biology, York University, Toronto, Ontario, Canada M3J 1P3

This chapter has been published and reproduced with permission:

Jonusaite S, Kelly SP, Donini A (2013) Tissue-specific ionomotive enzyme activity and K^+ reabsorption reveal the rectum as an important ionoregulatory organ in larval *Chironomus riparius* exposed to varying salinity. J Exp Biol 216:3637-3648

2.2 Introduction

Homeostasis of hemolymph ionic and osmotic composition in aquatic insect larvae is achieved largely by regulation of material entry through the alimentary canal and elimination through the excretory system (Bradley 1994; Dow 1986; Phillips 1981). The alimentary canal is structurally divided into the foregut, midgut, Malpighian tubules and hindgut. The foregut, encompassed by the esophagus, receives the food bolus and moves it to the midgut (Clements 1992; Dow 1986). The midgut, which is further divided into the gastric caeca, anterior midgut and posterior midgut, is important for maintaining ion, fluid and acid-base balance in aquatic insect larvae as it is the main uptake site of minerals, water and nutrients, which are ingested as or with food (Dow 1986; Clark et al. 1999; Clark et al. 2005; Khodabandeh 2006; Boudko 2012; Okech et al. 2008a; Okech et al. 2008b; Linser et al. 2009; Jagadeshwaran et al. 2010). The hindgut, which includes an ileum and a rectum, and the Malpighian tubules together constitute the excretory system. The Malpighian tubules secrete a primary urine by actively transporting Na^+, K^+ and Cl^- from the hemolymph into the tubule lumen, which in turn generates a transepithelial osmotic gradient that facilitates fluid movement (Phillips 1981; Clark and Bradley 1997; Donini et al. 2006). The ionic composition of fluid secreted by the tubules is unlike that of the hemolymph and would upset hemolymph homeostasis were it not for a selective reabsorption of ions, water and nutrients in the rectum (Phillips et al. 1986; Bradley and Philips 1977; Sutcliffe 1961; Meredith and Phillips 1973; Strange et al. 1984; Leader and Green 1978; Bradley 1994). In a freshwater (FW) environment, rectal reabsorption of ions (lumen to hemolymph) results in the production of a dilute urine, permitting larvae to conserve ions while eliminating excess water. Larvae of mosquitoes and chironomids also use externally protruding anal papillae as additional sites of ion uptake in habitats such as FW (Wigglesworth 1933; Koch 1983; Donini and O'Donnell 2005; Nguyen and Donini 2010).

Na^+-K^+-ATPase (NKA) and V-type H^+ ATPase (VA) are well known membrane energizers implicated in driving a wide variety of epithelial transport processes in insects and other animals (Emery et al. 1998; Harvey et al. 1998). Depending on physiological requirements and/or cell type, the activity of NKA and/or VA leads to the secretion or absorption of fluid, mineral ions and amino acids (Emery et al. 1998; Harvey et al. 1998). VA functions as an electrogenic pump, transporting protons from the cytoplasm to extracellular or exterior fluid and generating cell-negative membrane voltages. The membrane voltage can then serve to drive ion transport through ion-specific channels, and the electrochemical proton potential can serve to drive secondary active transport processes such as cation/H^+ exchange or anion/H^+ cotransport (Harvey et al. 1998; Harvey 2009). NKA is responsible for the maintenance of two electrochemical gradients across the plasma membrane by its electrogenic activity of exporting $3Na^+$ from the cell and importing $2K^+$ to the cell. This can power Na^+/H^+ exchange, Na^+ (or K^+):amino acid symport or give rise to K^+ and Na^+ diffusion *via* channels (Emery et al. 1998; Boudko 2012). The presence and localization of both ATPases has been established in the gut epithelia, Malpighian tubules and anal papillae of aquatic mosquito larvae, where they are proposed to play an integral role in the transepithelial movement of solutes (Patrick et al. 2006; Okech et al. 2008a; Smith et al. 2008; Xiang et al. 2012). However, to our knowledge, no studies have examined the tissue-specific activity of these keystone ionomotive enzymes in aquatic insect larvae in response to changes in environmental conditions. Nevertheless, it has been shown that there are comparatively higher levels of NKA activity in the hindgut *versus* foregut/midgut of damselfly and dragonfly larvae (Khodabandeh 2006), which supports the idea that tissue-specific alterations in ionomotive enzyme activity may play an important role in how aquatic insect larvae respond to changes in environmental ion levels.

Larvae of the chironomid *Chironomus riparius* are ubiquitous benthic inhabitants of FW environments such as lakes, rivers and ponds (Pinder 1986; Pinder 1995). However, they are also known to thrive in bodies of water with increased salinity such as brackish water (BW) ditches, coastal rock pools and intertidal zones, as well as polluted FW habitats exposed to salinated industrial effluent (Driver 1977; Colbo 1996; Parma and Krebs 1977; Bervoets et al. 1994; Bervoets et al. 1996). In these environments, parameters such as osmolarity and ionic milieu can vary greatly, and as a result, ion regulation is an important process for survival. Very little is known about the ionoregulatory responses of larval *C. riparius* to sustained changes in ambient salinity. Recently it has been shown that despite a substantial reduction in external ion levels, larvae of *C. riparius* reared in ion-poor water (IPW) maintain hemolymph NaCl and pH at the same levels as larvae reared in FW (Nguyen and Donini 2010). This was partially attributed to the anal papillae, which are sites of net NaCl absorption and H^+ secretion under ion-poor conditions (Nguyen and Donini 2010). In a more recent study that examined the effects of increased external salinity on ionoregulatory homeostasis in larval *C. riparius*, it was found that acute exposure to BW (20% seawater) increased hemolymph Na^+ and Cl^- and decreased hemolymph pH (Jonusaite et al. 2011). A decrease in whole-body NKA and VA activities in BW *versus* FW animals was also observed, and because the bulk of ionomotive enzyme activity was found to be in the alimentary canal of *C. riparius* (i.e. gut and Malpighian tubules), it was hypothesized that modulation of ionomotive enzyme activity in one or more regions of the alimentary canal may be important in order for larval *C. riparius* to acclimate to changes in environmental salinity (Jonusaite et al. 2011). With this background information in mind, the present study was aimed at investigating whether there was a role for specific segments of the gut as well as the Malpighian tubules in ion regulation of *C. riparius* larvae upon exposure to different ionic conditions. In order to do this, a novel approach was taken that focused on whether

NKA and VA activity exhibited spatial variation along the alimentary canal of larval *C. riparius* and how enzyme activity might change when larvae were reared in environments that varied in ionic composition (i.e. IPW, FW and BW). To put biochemical observations into a functional context, the scanning ion-selective electrode technique (SIET), combined with the application of ion transport inhibitors, was used to characterize transepithelial ion flux.

2.3 **Materials and Methods**

2.3.1 Experimental animals: Animals from a laboratory colony of *Chironomus riparius* (Meigen), maintained in the Department of Biology at York University, were used. Eggs were hatched in 6 liter aquaria containing a 2.54 cm deep mixture of fine and coarse grade industrial sand (K&E Industrial Sand, Wyoming, ON, Canada) and 3 liters of aerated dechlorinated municipal tap water (approximate composition of FW in μmol l^{-1}: [Na^+] 590; [Cl^-] 920; [Ca^{2+}] 760; [K^+] 43; pH 7.35). The aquaria were held at room temperature (RT, ~21°C), exposed to a 12h:12h light:dark regime and larvae were fed every second day with a dusting of ground TetraFin Goldfish Flake Food (Tetra Holding US, Blacksburg, VA, USA). The water in the aquaria was replaced weekly.

2.3.2 Rearing of experimental animals in IPW and BW: In aquaria identical to those outlined above, larvae were reared from first instar and allowed to develop to the fourth instar (~30 days) either in IPW (composition in μmol l^{-1}: [Na^+] 20; [Cl^-] 40; [Ca^{2+}] 2; [K^+] 0.4; pH 6.5) or BW (7 g l^{-1} Instant Ocean SeaSalt; United Pet Group, Blacksburg, VA, USA). FW control animals were reared in FW conditions (as outlined above) for the duration of the experimental period. Experiments were conducted on fourth instar larvae that had not been fed for 24h before collection.

2.3.3 Measurement of Na^+ and K^+ in hemolymph and BW rearing medium: Larvae were placed on tissue paper, which absorbed moisture from the surface of the insect, and then transferred to a Petri dish filled with paraffin oil (Sigma-Aldrich, Oakville, Canada). Samples of hemolymph were collected by making a small tear in the cuticle with fine forceps, causing the hemolymph to pool into a droplet. Levels of K^+ and Na^+ in collected droplets as well as BW rearing medium samples were measured as ion activities using ion-selective microelectrodes (ISMEs). The K^+ and Na^+ ISMEs were constructed as previously described (Jonusaite et al. 2011). In brief,

microelectrodes were backfilled with appropriate electrolyte solutions and front-loaded with the appropriate ionophore cocktail. The following ionophore cocktails (Fluka, Buchs, Switzerland) and back-fill solutions (in parentheses) were used: Na^+ Ionophore II Cocktail A (100 mmol l^{-1} NaCl) and K^+ Ionophore I Cocktail B (100 mmol l^{-1} KCl). The K^+ and Na^+ ISMEs were calibrated in 5 and 50 mmol l^{-1} solutions of KCl and 30 and 300 mmol l^{-1} solutions of NaCl, respectively. ISME slopes (mV) for a 10-fold change in ion concentration were (mean ± SEM): 54.8±1.56 (n = 4) for K^+ and 55.9±0.53 (n = 3) for Na^+. The circuit for voltage measurements was completed with a conventional reference electrode filled with 500 mmol l^{-1} KCl. The electrodes were connected through an ML 165 pH Amp to a PowerLab 4/30 (ADInstruments, Colorado Springs, CO, USA) data acquisition system and the voltage recordings were analyzed using LabChart 6 Pro software (ADInstruments). Calculations of hemolymph and BW rearing medium ion levels were made using the following equation as described previously (Donini et al. 2007):

$$a_h = a_c \times {}^{10\Delta V/S},$$

where a_h is the hemolymph or medium ion activity, a_c is the ion activity in one of the calibration solutions, ΔV is the difference in voltage between the hemolymph or medium and the calibration solution, and S is the slope of the electrode measured in response to a 10-fold change in ion activity.

2.3.4 Measurement of NKA and VA activity: The whole gut (complete with Malpighian tubules) or isolated regions of the gut were collected and quick-frozen in liquid nitrogen. Samples were stored at -80°C until further analysis. Four regions of the gut were isolated for examination as follows: (1) the combined foregut and anterior midgut, which included gastric cecae, (2) the posterior midgut, (3) the Malpighian tubules and (4) the hindgut. NKA and VA activities were

determined according to methods previously outlined for *C. riparius* tissues (Jonusaite et al. 2011).

2.3.5 Immunohistochemical localization of NKA and VA: Immunohistochemical localization of NKA was achieved using a mouse monoclonal antibody raised against the α-subunit of avian NKA (α5; Developmental Studies Hybridoma Bank, Iowa City, IA, USA). This antibody has been used successfully to localize NKA in other dipteran species such as mosquitoes (Patrick et al. 2006; Okech et al. 2008a; Smith et al. 2008). To localize VA, a rabbit polyclonal serum antibody raised against the B subunit of the VA of *Culex quinquefasciatus* was employed (a kind gift from S. Gill, UC Riverside) (Filippova et al. 1998). The entire gut of fourth instar larva was isolated in ice-cold physiological saline (composition in mmol l^{-1}: 5 KCl, 74 NaCl, 1 CaCl2, 8.5 MgCl2, 10.2 NaHCO3, 8.6 HEPES, 20 glucose, 10 glutamine, pH 7.0) [saline adapted from Leonard et al. (Leonard et al. 2009)] and fixed in 2% paraformaldehyde for 2 h at RT. Fixed tissue was then washed three times (3×30 min) in phosphate-buffered saline (PBS; pH 7.4) at RT and blocked for 1 h at RT with 10% antibody dilution buffer (ADB; 10% goat serum, 3% BSA and 0.05% Triton X-100 in PBS). The tissue was then thoroughly rinsed in PBS and incubated for 48 h at 4°C with anti-NKA α-subunit antibody at a dilution of 1:10 with ADB and anti-VA B-subunit antibody at a dilution of 1:1000 with ADB. As negative controls, tissues were incubated for 48 h at 4°C with ADB alone. Following incubation, tissues were washed for 2 h at RT in PBS and probed for 18 h at 4°C with either fluoresceinisothiocyanate-labelled goat or Cy2-conjugated sheep anti-mouse secondary antibodies (1:500 in ADB; Jackson ImmunoResearch Laboratories, West Grove, PA, USA). To remove unbound secondary antibody, tissues were washed twice in PBS (2×1 h) at RT and incubated with either tetramethylrhodamineisothiocyanate labelled or Alexa Fluor 594-conjugated goat anti-rabbit secondary antibodies (1:500 in ADB; Jackson ImmunoResearch Laboratories) as described above. Tissues were rinsed again in PBS and

mounted in ProLong Gold Antifade reagent (Invitrogen Canada, Burlington, ON, Canada). Images were captured using an Olympus IX71 inverted microscope (Olympus Canada, Richmond Hill, ON, Canada) equipped with an X-CITE 120XL fluorescent Illuminator (X-CITE, Mississauga, ON, Canada). Single confocal plane images were gathered using an Olympus BX-51 laser-scanning confocal microscope. All images were assembled using Adobe Photoshop CS2 software (Adobe Systems Canada, Toronto, ON, Canada).

2.3.6 SIET measurement of K^+ concentration gradient adjacent to rectum surface: The SIET methodology used in this study is described in detail elsewhere (Rheault and O'Donnell 2001; Rheault and O'Donnell 2004; Nguyen and Donini 2010). In brief, a K^+ ISME was connected to the headstage with an Ag/AgCl wire electrode holder (World Precision Instruments) and the headstage was connected to an ion polarographic amplifier (IPA-2, Applicable Electronics, Forestdale, MA, USA). A reference electrode was a 3% agar in 3 mol l^{-1} KCl bridge connected to the headstage through an Ag/AgCl half-cell (WPI) and positioned in the bulk bathing medium to complete the circuit. The K^+ ISME was constructed as described above and calibrated in 1 and 10 mmol l^{-1} solutions of KCl. The ISME slope (mV) for a 10-fold change in ion concentration was 57.3 ± 0.31 (mean ± SEM, n = 34).

An *in vitro* preparation of the rectum was constructed by first isolating the whole alimentary canal of the fourth instar larva in the physiological saline defined above (see Immunohistochemical localization of NKA and VA, above). The entire gut was then transferred to a 35 mm Petri dish containing 3 ml of fresh saline solution. All subsequent SIET measurements were performed on the posterior region of the hindgut that constitutes the rectal epithelium. For each single-point measurement of K^+ concentration gradient, the ISME was positioned 5-10 μm from the surface of the rectum and a voltage was recorded. The microelectrode was then moved a further 100 μm away, perpendicular to the tissue surface,

where a second voltage was recorded. This sampling procedure employed a wait time of 4 s between movements of the ISME (where no recording took place) and a subsequent recording time of 1 s. For each site along the rectum the sampling protocol was repeated four times. The ISME was positioned and the recorded voltage gradient was calculated using Automated Scanning Electrode Technique (ASET) software (version 2.0, Science Wares, East Falmouth, MA, USA). Control measurements to account for the mechanical disturbances in the ion gradients that arise from the movement of the microelectrode were taken 3-4 mm away from the surface of the rectum. This sampling protocol was previously established and utilized for measuring ion gradients at the anal papillae of mosquitoes and midges (see Donini and O'Donnell 2005; Del Duca et al. 2011; Nguyen and Donini 2010). K^+ measurements were chosen in part because when altered by the presence of NKA and VA inhibitors, they can provide some insight into the movement of major ions (e.g. Na^+ and Cl^-) across the rectum. Direct Na^+ and Cl^- measurements with Na^+ and Cl^- ISMEs require substantial modification of the saline such that the background NaCl in the bath is reduced by approximately fivefold. These conditions would not allow the rectum to behave in a normal manner as they would be substantially different from hemolymph.

2.3.6.1 Calculation of K^+ flux: Voltage gradients recorded by the ASET software were converted into concentration gradients using the following equation as described previously (Donini and O'Donnell 2005):

$$\Delta C = C_B \times 10^{\Delta V/S} - C_B,$$

where ΔC is the concentration gradient between the two points measured in μmol l^{-1} cm^{-3}; C_B is the background ion concentration, calculated as the average of the concentration at each point measured in μmol l^{-1}; ΔV is the voltage gradient obtained from ASET in μV; and S is the slope of

the electrode. Using the calculated concentration gradients, a corresponding flux value was then derived using Fick's law of diffusion as follows:

$$J_I = D_I(\Delta C) / \Delta x,$$

where J_I is the net flux of the ion in pmol cm^{-2} s^{-1}; D_1 is the diffusion coefficient of the ion (1.92×10^{-5} cm^2 s^{-1} for K^+); ΔC is the concentration gradient in pmol cm^{-3}; and Δx is the distance between the two points measured in cm.

2.3.7 Effect of ouabain, charybdotoxin or bafilomycin on SIET measurement of K^+ concentration gradient adjacent to rectum surface: The effects of 1 mmol l^{-1} ouabain (an NKA inhibitor; Sigma-Aldrich), 23 nmol l^{-1} charybdotoxin (ChTX; a K^+ channel blocker; Abcam, Cambridge, MA, USA) and 1 μmol l^{-1} bafilomycin (a VA inhibitor; LC Laboratories, Woburn, MA, USA) on K^+ flux at the rectum were assessed by recording K^+ concentration gradients adjacent the rectum with the SIET. The choice of ouabain and bafilomycin concentrations was based on our previous study on enzyme activity in *C. riparius* larva (see Jonusaite et al. 2011). The dose of ChTX was selected such that it equalled the highest concentration used in other insect and mammalian tissue studies (Miller et al. 1985; MacKinnon et al. 1988; Grinstein and Smith 1990; Bleich et al. 1996). Ouabain and bafilomycin were dissolved in DMSO (Sigma-Aldrich) and, prior to use, diluted to a desired concentration in saline (composition defined above in Immunohistochemical localization of NKA and VA). ChTX was dissolved and diluted in saline. Using the *in vitro* rectum preparation, initial measurements in a bath saline solution established the baseline K^+ gradient at the surface of the rectum. The ISME was removed from the saline bathing the preparation. Ouabain, ChTX or bafilomycin was added at the desired concentration and the preparation was incubated with the inhibitor for 5 min. The bathing solution with the inhibitor was replaced several times with fresh saline and the K^+ gradient at the same sites along the surface of the rectum was recorded. Controls were treated with the same protocol but received saline or DMSO

(without the inhibitor). DMSO was added at a concentration of 0.1%, which equalled the DMSO concentration that resulted from the addition of the inhibitor.

2.3.8 Statistics: Data are expressed as means ± SEM (*n*). Comparisons between treatment groups or tissues were assessed with a one-way ANOVA followed by a Tukey's or Dunn's comparison test. To examine the effects of inhibitors on the K^+ flux, data were subjected to Student's *t*-test. Statistical significance was allotted to differences with $p < 0.05$. All statistical analyses were conducted using SigmaStat 3.5 software (Systat Software, San Jose, CA, USA).

2.4 Results

2.4.1 Effect of rearing conditions on hemolymph K^+ and Na^+: Rearing the larvae in FW, IPW or BW had no effect on the hemolymph K^+ and Na^+ levels despite the changes in K^+ and Na^+ levels in the rearing media (Table 2-1). The levels of K^+ and Na^+ in the hemolymph of IPW-, FW- and BW-reared larvae ranged from 7.9 to 8.7 mmol l^{-1} and from 73.9 to 80.9 mmol l^{-1}, respectively (Table 2-1). BW rearing medium contained 7.3 mmol l^{-1} K^+ and 59.4 mmol l^{-1} Na^+.

2.4.2 NKA and VA activity profiles: In the alimentary canal of FW-reared *C. riparius* (Fig. 2-1a), NKA and VA activities of the combined foregut and anterior midgut (FAMG), the posterior midgut (PMG) and the Malpighian tubules (MT) were found to be quantitatively similar, ranging from 1.08 to 1.17 μmol ADP mg^{-1} protein h^{-1} and from 1.47 to 1.8 μmol ADP mg^{-1} protein h^{-1} for NKA and VA, respectively (Fig. 2-1b,c). In contrast, the activity of NKA and VA was ~10-20- fold higher in the hindgut at 22.76 μmol ADP mg^{-1} protein h^{-1} for NKA and 16 μmol ADP mg^{-1} protein h^{-1} for VA (Fig. 2-1b,c).

2.4.3 Effect of rearing conditions on NKA and VA activity in the alimentary canal: There was no difference in whole-gut NKA and VA activities between larvae reared in FW and IPW, but the activity of both enzymes was reduced in the whole gut of BW-reared larvae (Fig. 2-2a, Fig. 2-3a). At the level of the individual segments of the alimentary canal, the activities of both enzymes were found to be reduced by at least half in the hindgut of BW-reared larvae (Fig. 2-2e, Fig.2-3e). The rearing treatments had no effect on the NKA and VA activities in the FAMG or the MT (Fig. 2-2b,d, Fig. 2-3b,d). In the PMG, the activities of both enzymes were lower in larvae reared in IPW when compared with their FW and BW counterparts (Fig. 2-2c, Fig. 2-3c).

Given that BW rearing reduced whole-gut and hindgut NKA and VA activity, and because a reduction in whole-gut enzyme activity most likely reflects a reduction in hindgut

Table 2-1: K^+ and Na^+ levels (mmol l^{-1}) in hemolymph of *Chironomus riparius* larvae reared in ion-poor water (IPW), freshwater (FW), and brackish water (BW).

	IPW	FW	BW
$[K^+]$	7.9 ± 0.6	8.7 ± 1.2	8.5 ± 0.4
$[Na^+]$	73.9 ± 2.6	74.4 ± 1.0	80.9 ± 2.7

Hemolypmh ion levels are expressed as mean ± SEM (*n* = 11-18).

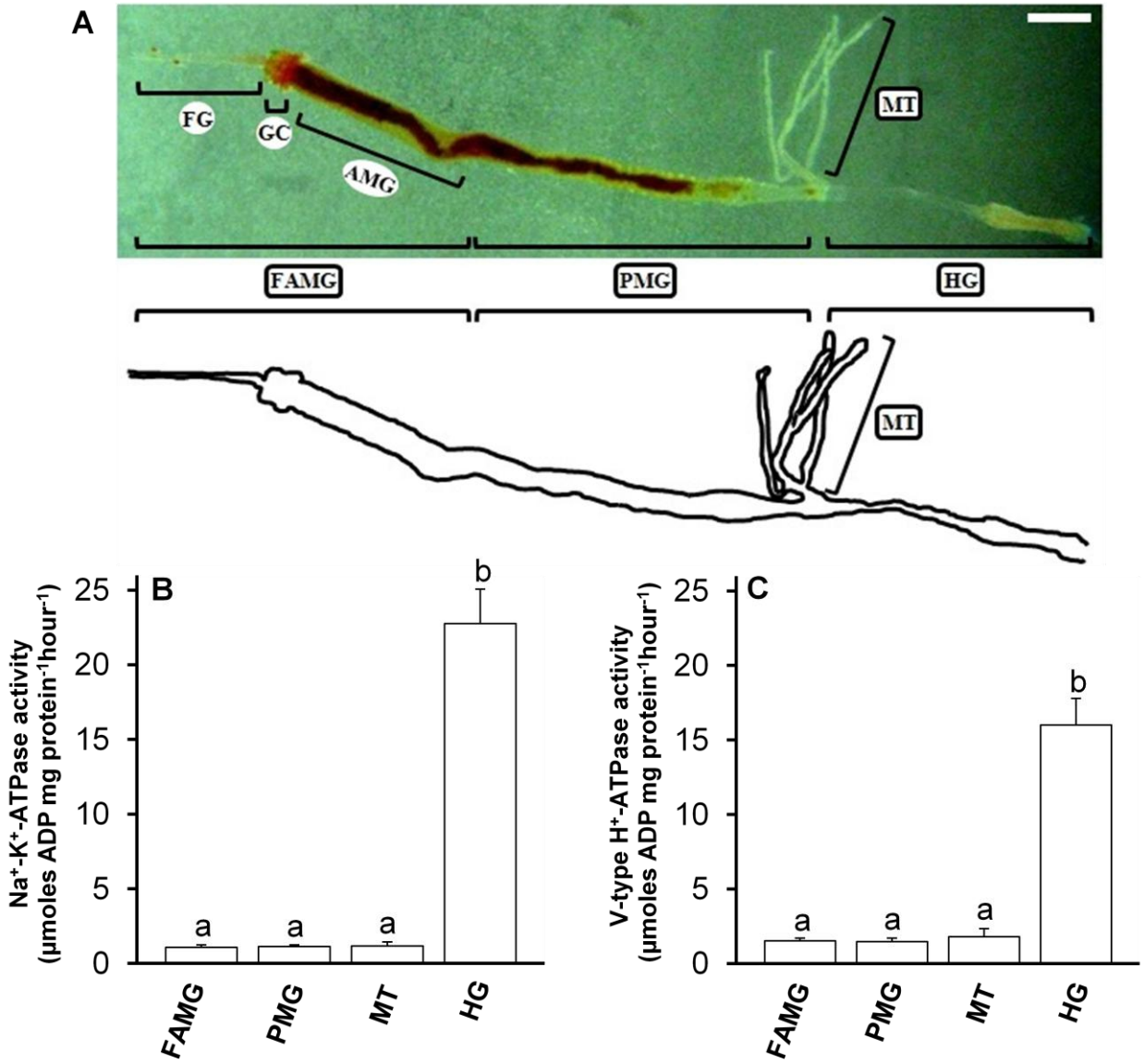

Figure 2-1: The (**a**) alimentary canal and spatial distribution of (**b**) Na^+-K^+-ATPase (NKA) and (**c**) V-type H^+-ATPase (VA) in discrete alimentary canal regions of freshwater-reared *Chironomus riparius* larva. Brackets indicate regions of the gut used for NKA and VA activity assay: FAMG, foregut (FG), gastric caeca (GC) and anterior midgut (AMG); PMG, posterior midgut; MT, Malpighian tubules; HG, hindgut. All data are expressed as mean values ± SEM (n = 6). Letters denote statistically significant differences between the segments (one-way ANOVA, Tukey's multiple comparison, $p < 0.05$). Scale bar, 1 mm.

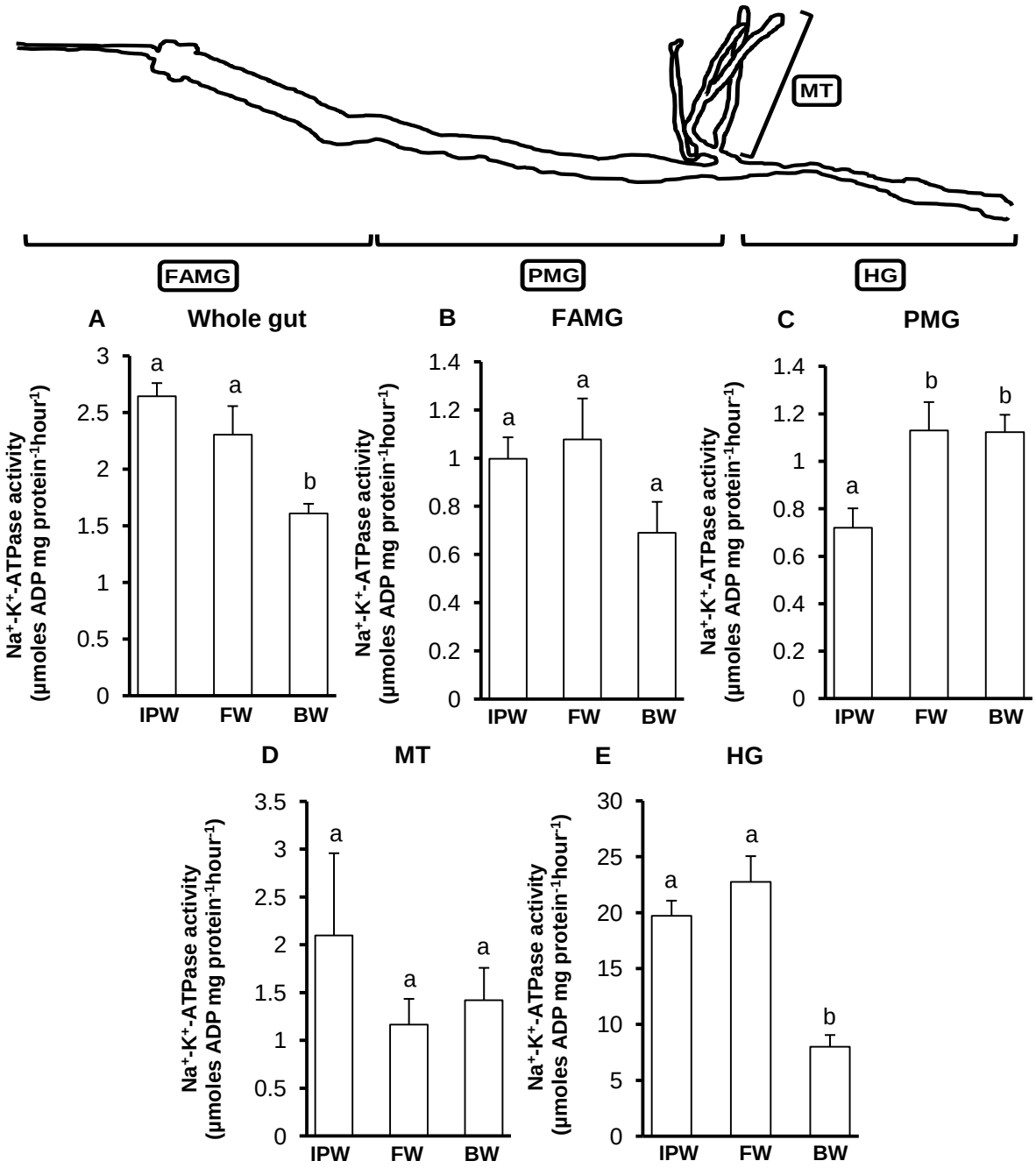

Figure 2-2: The effect of varying the ionic strength of rearing conditions on Na^+-K^+-ATPase (NKA) activity in (**a**) the entire (intact) alimentary canal, (**b**) foregut and anterior midgut (with gastric caeca; FAMG), (**c**) posterior midgut (PMG), (**d**) Malpighian tubules (MT), and (**e**) hindgut (HG) of *Chironomus riparius* larvae. Larvae were reared in either ion-poor water (IPW), freshwater (FW) or brackish water (BW; 20% seawater). All data are expressed as mean values ± SEM (n = 6). Letters denote statistically significant differences between rearing groups (one-way ANOVA, Tukey's multiple comparison, $p < 0.05$).

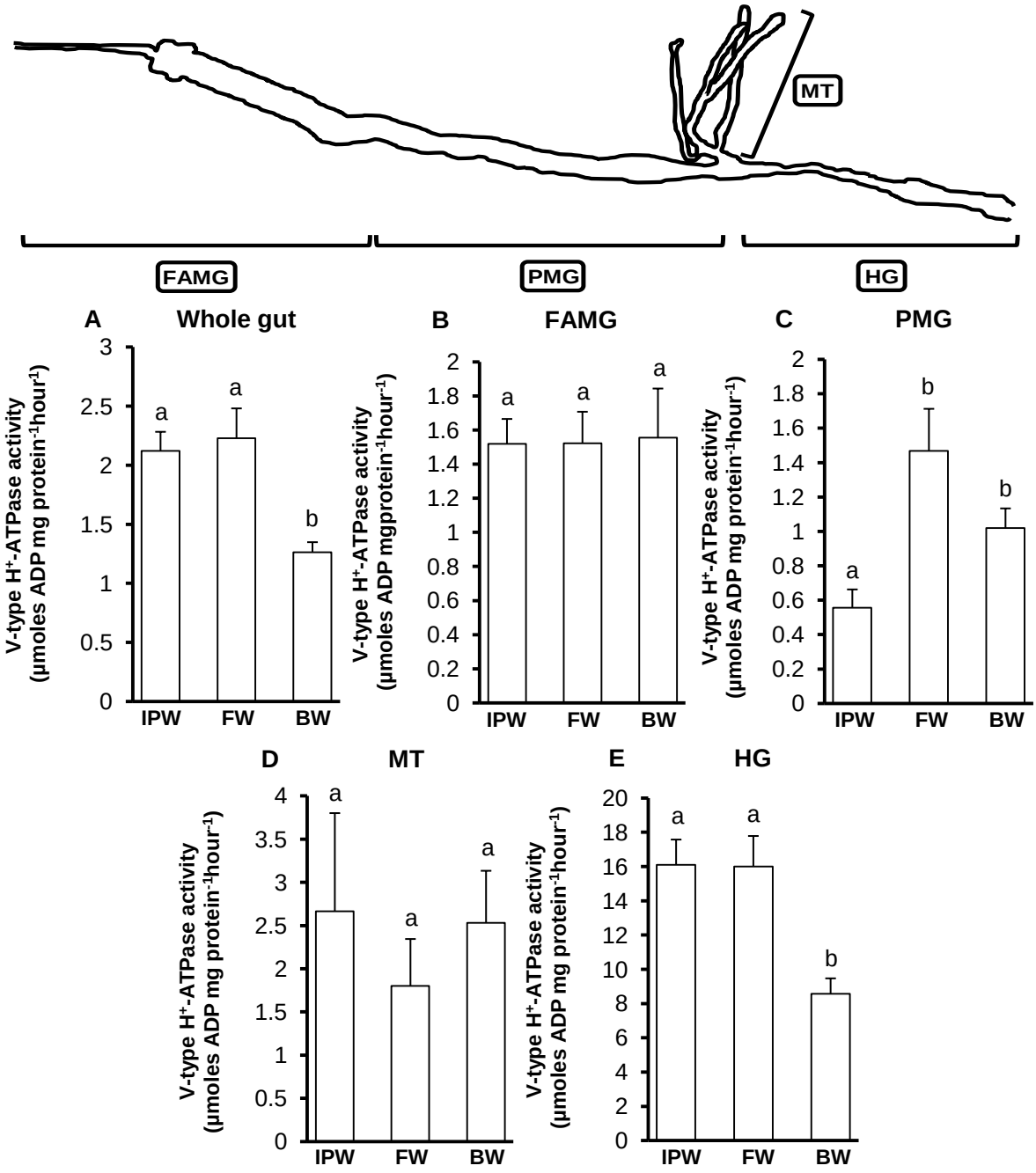

Figure 2-3: The effect of varying the ionic strength of rearing conditions on V-type H^+-ATPase (VA) activity in (**a**) the entire (intact) alimentary canal, (**b**) foregut and anterior midgut (with gastric caeca; FAMG), (**c**) posterior midgut (PMG), (**d**) Malpighian tubules (MT), and (**e**) hindgut (HG) of *Chironomus riparius* larvae. Larvae were reared in either ion-poor water (IPW), freshwater (FW) or brackish water (BW; 20% seawater). All data are expressed as mean values ± SEM (n = 6). Letters denote statistically significant differences between rearing groups (one-way ANOVA, Tukey's multiple comparison, $p < 0.05$).

NKA and VA activity (which was found to be 10-20-fold higher than any other region of the alimentary canal), the hindgut became the focus of further experiments.

2.4.4 NKA and VA immunolocalization in the hindgut: Immunohistochemical localization of NKA and VA in the hindgut of *C. riparius* revealed the presence of both enzymes in the rectum (Fig. 2-4a,c). In contrast, both ATPases were absent in the ileum (Fig. 2-4a,c). In an optical section through the whole mount rectum, rectal epithelium cells showed NKA localized to the basolateral regions of the plasma membrane (Fig. 2-4d). Immunostaining for VA was detected in subapical and cytoplasmic regions of the rectal epithelium (Fig. 2-4e). No co- localization of NKA and VA was found (Fig. 2-4f) and no signal was observed in control whole mounts that had been probed with secondary antibody only (Fig. 2-4g).

2.4.5 Effects of ouabain, ChTX and bafilomycin on K^+ efflux at the rectum: SIET measurements adjacent to the hemolymph-side surface of the rectum detected K^+ efflux (from rectal lumen to bath). K^+ efflux did not vary to any great extent spatially along the length of the rectum (see Fig. 2-5a). Rearing the larvae in FW, IPW or BW had no effect on the direction of K^+ fluxes (efflux); however, BW rearing caused a substantial reduction (approximately fourfold) in the magnitude of K^+ efflux relative to FW and IPW rearing (Fig. 2-5b).

K^+ efflux across the rectum of *C. riparius* larvae reared in BW was unaltered following the addition of ouabain, ChTX or bafilomycin to solutions bathing the tissue (Fig. 2-6a-c). In contrast, all of the inhibitors reduced the K^+ efflux measured from the rectum of IPW- and FW-reared larvae (Fig. 2-6a-c). Ouabain application resulted in a ~ 3.6 fold decrease in K^+ efflux at the rectum of larvae reared in FW or IPW. ChTX and bafilomycin decreased K^+ efflux at the rectum of FW- and IPW- reared larvae ~ 2.7 and ~ 3.4 times, respectively (Fig. 2-6b,c). No change in K^+ efflux was found at the control tissues incubated with DMSO or saline only (Fig. 2-6d,e).

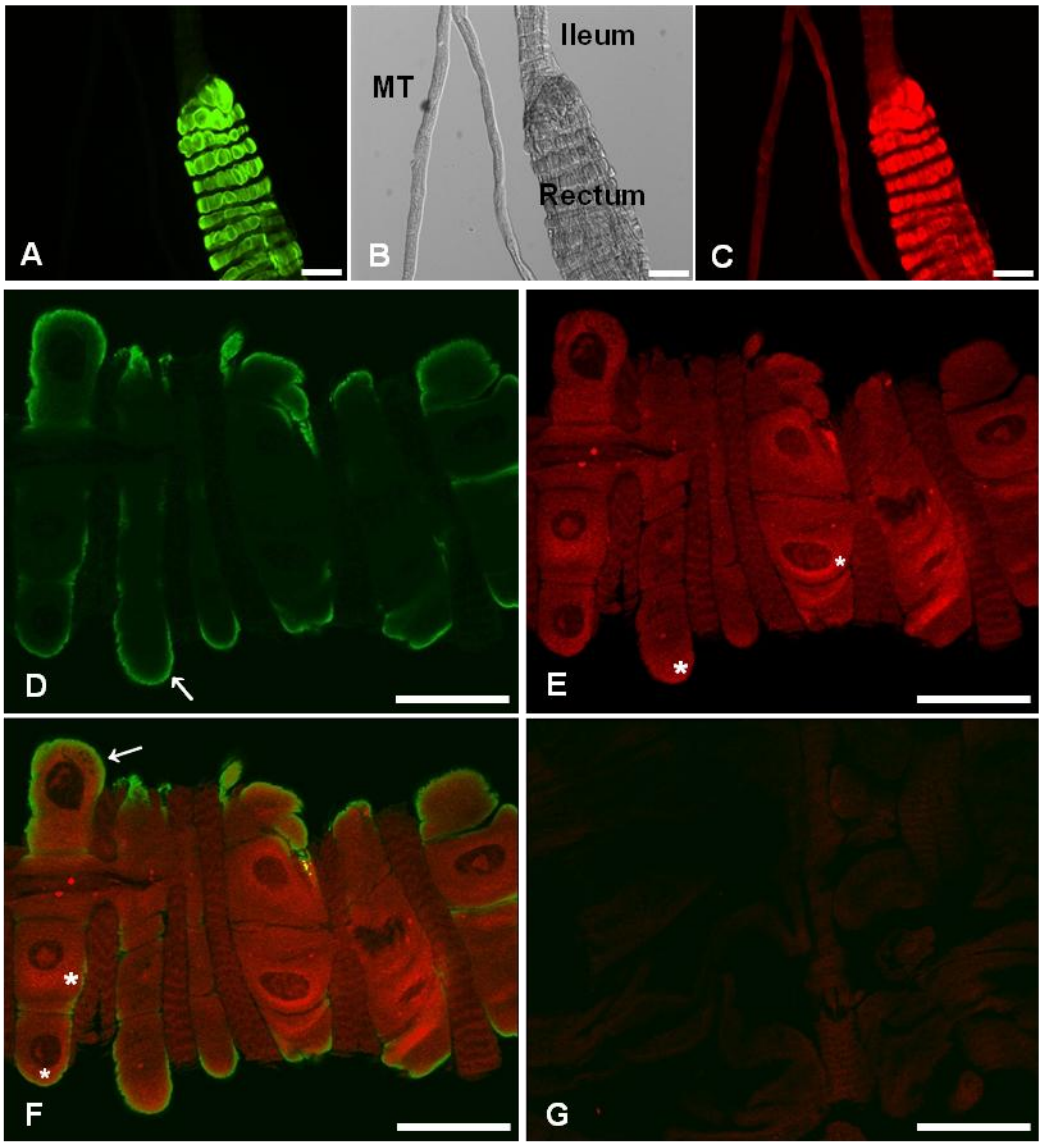

Figure 2-4: Immunolocalization of Na^+-K^+-ATPase (NKA, green) and V-type H^+-ATPase (VA, red) in the hindgut (HG) of 4th instar *Chironomus riparius* larva reared in freshwater (FW). The HG expressed high levels of NKA (**a**) and VA (**c**) in the rectum and showed little to no expression of either ATPase in the ileum (**a**, **b**). (**b**) is a bright field image of (**a**) and (**c**). NKA was localized to the basolateral membrane of rectal epithelium (**d**, **f**, white arrows) whereas VA exhibited subapical and cytoplasmic staining (**e**, **f**; asterisks). A merged image of NKA and VA immunoreactivity can be seen in **f**. Control rectal tissue processed identically to experimental tissues but probed with secondary antibody only is shown in **g**. Scale bars, (**a**-**c**) 100 µm, (**d**-**g**) 50 µm. MT, Malpighian tubules.

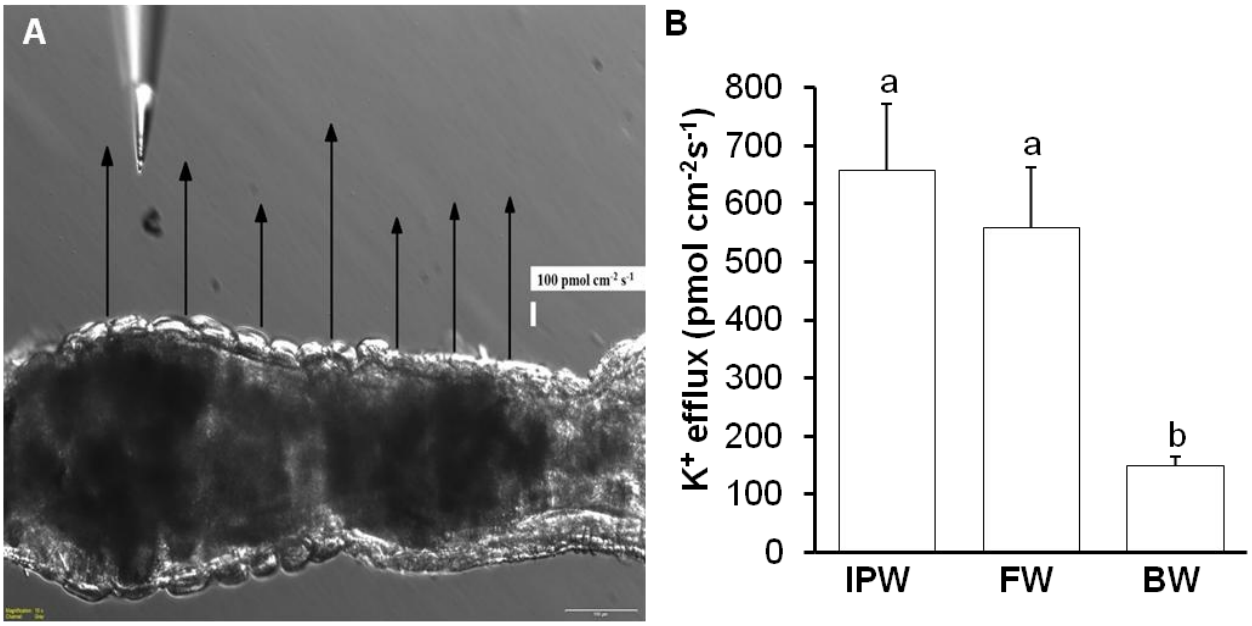

Figure 2-5: (**a**) Representative Scanning Ion-selective Electrode Technique (SIET) measurements of the K^+ voltage gradients along the surface of the rectum can be observed. K^+ voltage gradients were measured using 4th instar *Chironomus riparius* larva reared in freshwater (FW). Arrows and arrow length represent the direction and magnitude of recorded K^+ fluxes respectively, that were sampled at the base of the arrow. The scale for the magnitude of K^+ flux is denoted by the length of the thick bar below the 100 pm cm^{-2} s^{-1} label. Horizontal scale bar, 100 µm. (**b**) The effect of varying the ionic strength of rearing conditions on the average of single-point K^+ fluxes across the rectum of larval *C. riparius* reared in ion-poor water (IPW), FW or brackish water (BW; 20% seawater). Values signify the efflux of K^+ from the rectum lumen into the external bath saline. All data are expressed as mean ± SEM (n = 27-29). Letters denote statistically significant differences between K^+ flux in different rearing conditions (one-way ANOVA, Dunn's multiple comparison, $p < 0.05$).

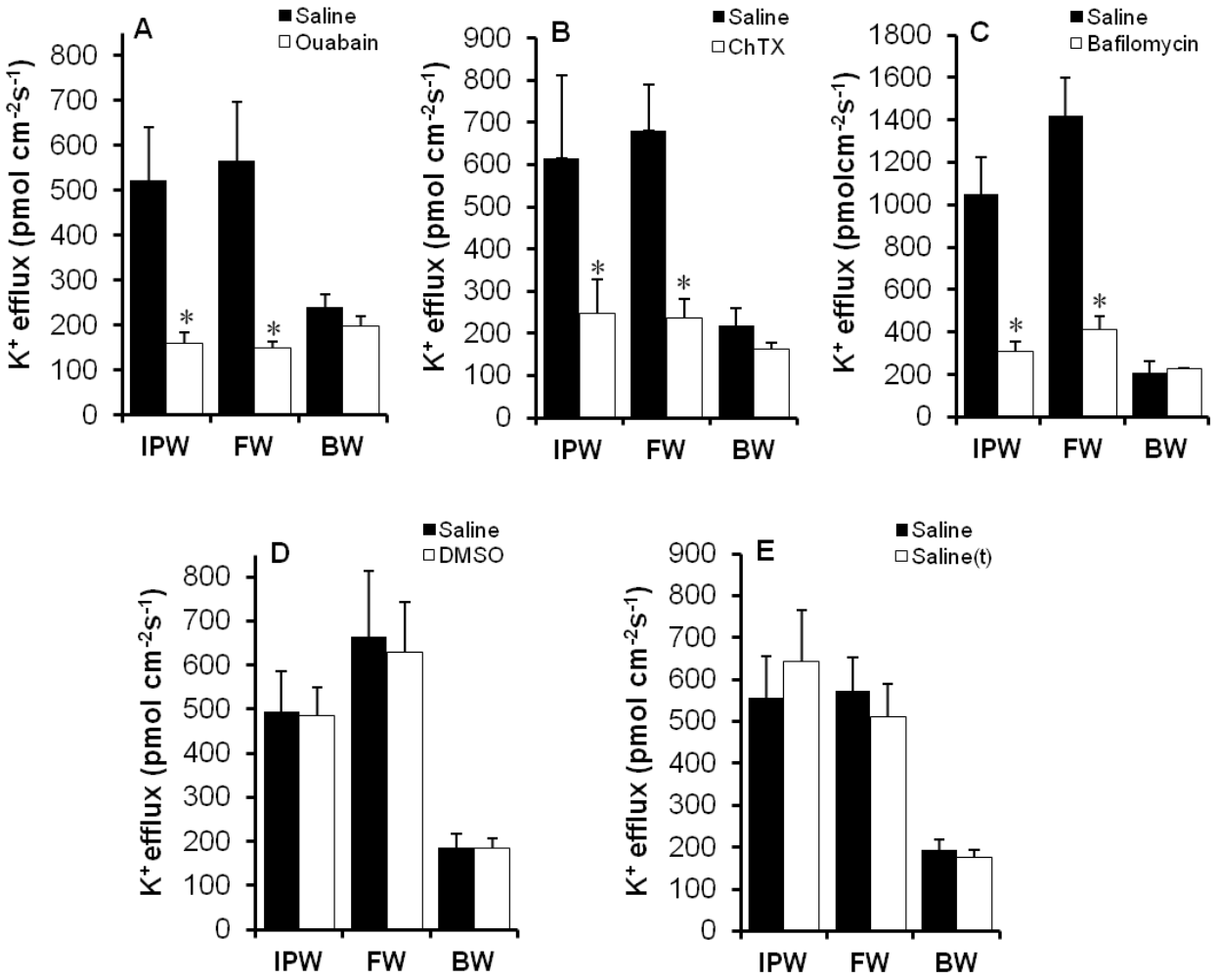

Figure 2-6: Effects of (**a**) 1mmol l^{-1}ouabain, (**b**) 23nmol l^{-1}charybdotoxin (ChTX) or (**c**) 1 µmol l^{-1} bafilomycin on K^+ efflux at the rectum of larval *Chironomus riparius* reared in ion-poor water (IPW), freshwater (FW) or brackish water (BW; 20% seawater). Values indicate K^+ efflux from the rectum lumen into the external saline bath measured immediately after the rectum was prepared and mounted on the SIET apparatus (denoted as saline) and 5 min after incubation with an inhibitor. Control measurements at the rectum incubated with DMSO and saline (saline(t)), instead of inhibitors are shown in **d** and **e**, respectively. All data are expressed as mean ± SEM (*n* = 9-19), except for BW animals in **c,** where data are mean ± SEM (*n* = 2). Asterisk denotes a statistically significant difference from the initial measurements (paired Student's *t*-test, $p < 0.05$).

2.5 Discussion

2.5.1 Overview: This study demonstrates spatial variation in the activity of NKA and VA along the alimentary canal of aquatic *C. riparius* larvae and that: (1) observed differences in tissue-specific enzyme activity and (2) environmentally induced changes in the NKA and VA activity of particular regions of the alimentary canal both point to the hindgut as an important site for iono/osmoregulation in *C. riparius* reared in water of differing ionic content. Immunolocalization of NKA and VA suggests that within the hindgut area, it is the rectum that appears to possess the bulk of ionomotive enzyme protein. Furthermore, *in situ* inhibition of NKA, VA and K^+ channels in the rectum reduces ion (K^+) reabsorption (efflux, rectal lumen to hemolymph). By providing direct insight into K^+ movement across the rectum of *C. riparius* and indirect insight into the movement of major ionic species such as Na^+ and Cl^-, these data collectively indicate overall ion reabsorption across the rectum of *C. riparius*. But inhibition of K^+ efflux can only be observed in tissues isolated from animals that are reared in hyposmotic surroundings, where ion retention is necessary in order to maintain ionoregulatory homeostasis. In contrast, animals reared in BW conditions exhibit the same pattern of spatial variation in NKA and VA activity as seen in FW- and IPW-reared *C. riparius*, but reduced NKA and VA activity in the hindgut compared with the aforementioned animals. The significance of this latter result is that these animals exhibit greatly reduced rectal K^+ efflux, which is suggestive of attenuated ion reabsorption. From a physiological perspective, this would be an appropriate strategy in saline conditions. In addition, the presence of NKA and VA inhibitors (ouabain and bafilomycin, respectively) did not further reduce K^+ efflux across the rectum of BW-reared *C. riparius*. This introduces the idea that, relative to other areas of the alimentary canal, elevated ionomotive enzyme activity in the rectum of BW-reared animals is no longer required for ion reabsorption/retention strategies such as those adopted by

FW- or IPW-reared animals, but could nonetheless be involved in other important physiological processes (e.g. acid/base balance, ammonia secretion, etc.).

2.5.2 Spatial variation in NKA and VA activity along the alimentary canal: In the alimentary canal of FW-reared *C. riparius*, NKA as well as VA activity in the FAMG, PMG and MT were quite similar (Fig. 2-1b,c). However, the hindgut was found to possess ionomotive enzyme activity levels that were ~10-20 times higher than those found in other regions (Fig. 2-1b,c). To the best of our knowledge, no other study has reported on spatial differences in VA activity in the alimentary canal of insects. However, high levels of NKA activity in the hindgut of *C. riparius*, relative to the other gut regions, are consistent with previous studies on terrestrial insects (Peacock 1976; Peacock 1977; Peacock 1981a; Peacock 1981b; Tolman and Steele 1976). Furthermore, one study has reported NKA activity in the gut of aquatic insect larvae (see Khodabandeh 2006), and in this regard, a basic separation of the gut into the foregut/midgut and the hindgut also revealed higher levels of NKA activity in the hindgut of FW damselfly and dragonfly larvae (Khodabandeh 2006). Therefore, the results of the present study are also consistent with these observations.

In the hindgut of *C. riparius*, NKA and VA immunoreactivity (staining) were found to be restricted to the rectal segment (Fig. 2-4a,c), allowing us to conclude that NKA and VA activity in the hindgut of *C. riparius* reflects ionomotive enzyme activity in the rectum. Our immunohistochemical observation of NKA expression on the basolateral membrane of the rectum of *C. riparius* (Fig. 2-4d) is similar to observations made in mosquito and other FW insect larvae, which also exhibit basolateral NKA in the hindgut (Patrick et al. 2006; Smith et al. 2008; Khodabandeh 2006). However, subapical and cytoplasmic immunostaining of VA in the rectal epithelial cells (Fig. 2-4e) may be indicative of V_1 subunits (for which the antibody was used) that have dissociated from their membrane-bound V_0 anchors (Sumner et al. 1995).

2.5.3 Differences in NKA and VA activity in different rearing environments: Epithelia of the gut may contribute to the regulation of hemolymph ionic composition either through modulated absorption of ions from water ingested along with food, or through secretion of ions from the hemolymph into the gut lumen for subsequent elimination. For example, ion transport mechanisms of the gut epithelia of larval *Drosophila* are reconfigured during dietary salt stress so that there are reductions in K^+ and Na^+ absorption and increased K^+ and Na^+ secretion (Naikkhwah and O'Donnell 2012). In the present study, we showed that NKA and VA activity in the FAMG of *C. riparius* larvae acclimated to varying salinity remain largely unaltered (Fig. 2-2b, Fig. 2-3b). These findings seem to suggest that alteration in external salt content did not trigger changes in the active transport machinery along the midgut epithelia of *C. riparius*, although this does not preclude changes in secondary ion transport processes or ultrastructural alterations of the epithelium, which may lead to alterations in ion transport function. For example, varying salinity may alter passive ion movement across the midgut because of the modulation of paracellular permeability, which is controlled by septate junctions (see Lane and Skaer 1980). In this regard, the effects of environmental salinity on the permeability of intestinal epithelia in aquatic vertebrates such as fishes are well documented (see Marshall and Grosell 2005). In addition, increased permeability of the anterior intestinal epithelium following FW to BW acclimation (without alteration in active transcellular transport processes) has also been suggested to occur in amphibians (Chasiotis and Kelly 2009). The physiological consequences of decreased NKA and VA activity in the PMG of larval *C. riparius* in response to IPW rearing are unclear (see Fig. 2-2c, Fig. 2-3c). In mosquitoes, the PMG is implicated in Na^+ absorption through VA-driven cation/amino acid symport across the apical membrane and subsequent NKA-driven Na^+ transport across the basal membrane into the hemolymph (Patrick et al. 2006; Okech et al. 2008b; Boudko et al. 2005; Rheault et al. 2007). If similar transport processes were present

in the PMG of *C. riparius*, then the observed enzymatic activity decrease in IPW rearing conditions would not be consistent with conserving ions or nutrient uptake in dilute conditions.

NKA and VA activities in the MT of *C. riparius* larvae were consistent across the three salinity rearing conditions tested (Fig. 2-2d, Fig. 2-3d). Because the activity of these pumps is thought to regulate the rate of MT secretion, the results suggest that rates of secretion are unaltered by the rearing conditions. Indeed, this is the case in the mosquito *Aedes aegypti*, where fluid secretion rates are similar between FW- and BW-reared larvae (Donini et al. 2006). This does not exclude the MT as important ionoregulatory organs involved in acclimation to different salinities because the tubules of *A. aegypti* larvae reared in BW secrete more Na^+ at the expense of K^+ to help counteract the elevated Na^+ levels in the hemolymph relative to their FW-reared counterparts (Donini et al. 2006). In contrast to the observations in *C. riparius* and *A. aegypti*, a salt-stress-induced alteration in VA activity has been shown in larval *Drosophila* (Naikkhwah and O'Donnell 2011). Specifically, rearing *Drosophila* on a KCl-rich diet results in increased VA activity in the MT, which increases the capacity of tubules to eliminate K^+ (Naikkhwah and O'Donnell 2011).

NKA and VA activity were greatly reduced in the hindgut of BW-reared larvae relative to corresponding activity in FW- and IPW-reared animals (Fig. 2-2e, Fig. 2-3e). As discussed above, the hindgut region has previously been shown to possess high NKA activity in both aquatic insect larvae and terrestrial insects (Khodabandeh 2006; Peacock 1976; Peacock 1977; Peacock 1981a; Peacock 1981b; Tolman 1976). However, we are unaware of any report on changes in hindgut ionomotive enzyme activity either in response to environmental change or alterations in systemic salt and water balance. Considering the high NKA and VA activity in the hindgut and that enzyme activity was reduced by ~50% when larvae were reared in BW, it is likely that the observed decrease in NKA and VA activities found in whole guts of BW-reared

larvae represent changes occurring in the hindgut. When taken together with immunohistochemical observations of the hindgut, where the rectum appears to be the principal site of enzyme immunoreactivity, these data suggest that the rectum plays an important role in the ability of larval *C. riparius* to cope with alterations in environmental salinity. Therefore, to address the physiological role of the rectum of larval *C. riparius* with respect to salt and water balance, *C. riparius* larvae were reared in IPW, FW or BW and K^+ fluxes were measured with SIET. In addition to providing information on transepithelial K^+ movement, alterations in K^+ flux rates in the presence of NKA and VA inhibitors can also serve as a proxy for major ion movement (for details see Materials and methods, *SIET measurement of K^+ concentration gradient adjacent to rectum surface*) across the rectal epithelium.

2.5.4 Rearing of C. riparius larvae in IPW, FW or BW and SIET measurement of K^+ concentration gradient adjacent to the rectum surface: Consistent with the notion that the rectum of FW insects selectively reabsorbs ions and metabolites to produce a dilute urine, we measured K^+ efflux (reabsorption) along the entire length of the rectum (Fig. 2-5a). Although we did not directly measure Na^+ or Cl^- fluxes, the measurements of K^+ flux could also be indicative of the general movement of NaCl across the rectum. The BW condition imposes a significant challenge to both K^+ and Na^+ regulation in the larvae. The level of K^+ in BW is ~167 times greater than its levels in FW whereas Na^+ levels increase ~100 times in BW compared with FW. Therefore, there is a greater change in external K^+ levels from FW to BW conditions relative to the change in the levels of Na^+ and as such, a greater insult to the hemolymph K^+ levels. Our observation of a fourfold reduction in K^+ efflux at the rectum of BW-reared larvae with respect to larvae reared in FW or IPW (Fig. 2-5b) suggests an important role for this tissue in the regulation of K^+ homeostasis in *C. riparius*. Hemolymph K^+ levels in FW-reared larval *C. riparius* are ~8.7 mmol l^{-1} (Table 2-1), and based on the assumption that the MT lose at least some K^+ during the

production of primary urine, under IPW and FW conditions, the larvae would require a mechanism to reabsorb K^+. Our data suggests that the rectum at least partially fulfills this role. Interestingly, the anal papillae of *C. riparius*, which are an important site of salt uptake in FW and IPW, do not take up K^+ (Nguyen and Donini 2010) and therefore reabsorption of K^+ at the rectum would be of particular importance. Under conditions of BW rearing, the amount of K^+ from imbibed medium would tend to increase K^+ hemolymph levels; however, there was no change in hemolymph K^+ levels in BW-reared larvae compared with FW- or IPW-reared animals (Table 2-1). We propose that a decrease in K^+ absorption by the rectum, as seen in BW-reared larvae, plays an important role in maintaining appropriate K^+ hemolymph levels. Furthermore, the NKA and VA activities in the rectum of IPW and FW-reared larvae coupled with the observed decrease in enzyme activities in the rectum of BW-reared larvae suggests that NKA and VA drive K^+ reabsorption in the rectal epithelium of *C. riparius* larvae. To assess the role of NKA and VA in K^+ reabsorption by the rectum we applied pharmacological transport inhibitors in conjunction with the SIET.

The presence of ouabain in tissue bathing solutions reduced K^+ reabsorption (i.e. lumen to hemolymph K^+ movement) in the rectum of both FW- and IPW-reared *C. riparius* larvae (Fig. 2-6a). Because basolateral NKA transports K^+ from the hemolymph into the cell in exchange for Na^+, and SIET detected net K^+ movement from cell to hemolymph, the latter observation suggests the presence of K^+ transport mechanisms coupled to the membrane-energizing properties of NKA. In turn, this coupling would support the lumen-to-hemolymph movement of K^+ across the epithelium. A functional link between the activities of basolateral NKA and K^+ channels in resorptive epithelia is well documented (Ehrenfeld and Klein 1997; Hurst et al. 1991; Matsumura et al. 1984; Messner et al. 1985; Kawahara et al. 1987; Sackin and Palmer 1987; Hebert et al. 2005; Warth and Bleich 2000; Hanrahan et al. 1986). In addition, ouabain inhibition

of NKA has been shown to inhibit K^+ movement through basolateral K^+ channels in the amphibian proximal tubules (Matsumura et al. 1984; Messner et al. 1985).

The addition of the K^+ channel blocker ChTX to tissue bathing solutions also inhibited K^+ absorption at the rectum of FW- and IPW-reared *C. riparius* (Fig. 2-6b). These results provide evidence for the presence of basolateral K^+ channels and suggest that basolateral NKA establishes an electrochemical gradient that supports outward movement of K^+ through these channels. ChTX is a small basic protein purified from the venom of the scorpion *Leiurus quinquestriatus* (Smith et al. 1986). It has been shown to block both large- and small-conductance Ca^{2+}-activated K^+ channels as well as Ca^{2+}-insensitive, voltage-dependent K^+ channels (Miller et al. 1985; Hermann and Erxleben 1987; MacKinnon et al. 1988; Grinstein and Smith 1990; Bleich et al. 1996). Interestingly, expression of a gene encoding the Ca^{2+}-activated K^+ channel has been localized in the ion-transporting midgut epithelial cells of *Drosophila* (Brenner and Atkinson 1997). Further characterization of the putative K^+ channels in the basolateral membrane of rectal epithelial cells of *C. riparius* will require further studies that focus on voltage-dependent and Ca^{2+}-activated K^+ channels.

Application of the VA inhibitor bafilomycin also reduced K^+ absorption by the rectum of IPW- and FW-reared larvae (Fig. 2-6c). Although we could not conclusively demonstrate apical membrane localization of VA in the rectal epithelial cells, its conspicuous absence on the basolateral membrane suggests that the pump may reside apically. If so, the observed reduction in K^+ efflux with VA inhibition suggests that K^+ transport across the apical membrane is at least in part dependent on the activity of apical VA. We propose that hyperpolarization of the apical membrane by VA drives K^+ uptake across this membrane *via* apical K^+ channels. Absorption of K^+ through channels with different properties at the apical and basolateral membranes is well documented in the desert locust (*Schistocerca gregaria*), whose rectal epithelium has both apical

VA and basal NKA (Hanrahan and Phillips 1983; Hanrahan et al. 1986; Peacock 1977; Phillips et al. 1996). Furthermore, in the hindgut of both larval and adult *Drosophila*, transcripts encoding for inwardly rectifying K^+ channels (K_{ir}) are found in abundance (Luan and Li 2012). K_{ir} channels are a special subset of K^+ channels that pass K^+ more easily into, rather than out of, the cell and are highly expressed in renal epithelial cells for ion transport (Hibino et al. 2010). The presence of such K^+ channels in the apical membrane of epithelium involved in K^+ absorption, such as the rectum of *C. riparius*, seems reasonable but does not preclude the presence of other K^+-transporting mechanisms.

The results also demonstrate that ouabain, bafilomycin and ChTX have no effect on the low K^+ absorption by the rectum of BW-reared larvae (Fig. 26a-c), which suggests that under saline conditions: (1) rectal K^+ absorption no longer requires basal membrane energization by NKA; (2) rectal K^+ absorption no longer requires apical membrane energization by VA; and (3) K^+ channels that are insensitive to ChTX are also present, the dose of ChTX used was insufficient to block all K^+ channels, or K^+ flux across K^+ channels is no longer occurring in the rectum of BW reared larvae. With regard to this final point, K^+ flux may occur through the paracellular route.

Based on the results of this study, a model for transcellular ion absorption across the rectum of *C. riparius* can be proposed as follows (see Fig. 2-7). Hyperpolarization of the apical membrane by VA drives the passive absorption of K^+ through putative K^+ channels at the apical membrane. VA-generated voltage may also be used to drive Na^+ and amino acids into the cells through a Na^+:amino acid transporter (NAT). Although we have no direct data to support the presence of NATs in the rectum of *C. riparius*, an observation that offers indirect support is that such proteins have been localized to the apical membrane of the FW mosquito rectum (Okech et al. 2008a). Basolateral NKA transports Na^+ from the cell into the hemolymph and generates an

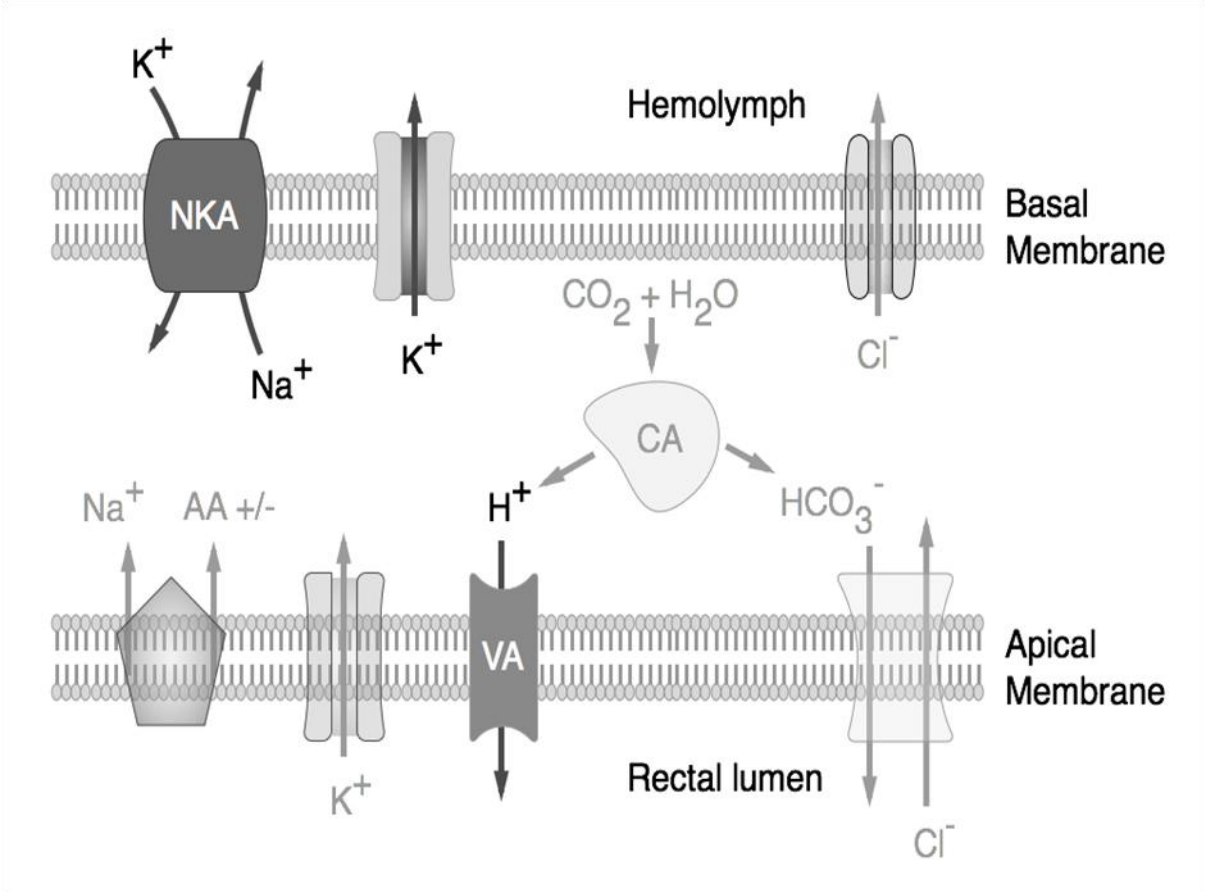

Figure 2-7: Proposed model for ion transport mechanisms across the rectum of *Chironomus riparius*. Darker shade transporters indicate proteins localized in this study; lighter shade transporters indicate postulated proteins. The V-type H^+-ATPase (VA) hyperpolarizes the apical membrane and the voltage is used to drive K^+ diffusion into the cells *via* the putative apical K^+ channels. The voltage may also be used by postulated Na^+:amino acid transporter (NAT) to drive Na^+ and amino acids into the cell. At the basolateral membrane, Na^+-K^+-ATPase (NKA) mediates Na^+ transport from the cell into the hemolymph and establishes an electrochemical gradient for K^+ diffusion to the hemolymph *via* basolateral K^+ channels. It is also suggested that Cl^- uptake may occur at the apical membrane in exchange for HCO_3^- and at the basolateral membrane *via* Cl^- channels driven by the cytosol negative potential established by basal NKA. Cytosolic carbonic anhydrase (CA) would supply H^+ to the VA and HCO_3^- to HCO_3^-/Cl^- exchangers in the apical membrane.

electrochemical gradient for the passive outward diffusion of K^+ *via* basolateral K^+ channels. Although not directly measured for the reasons stated above (see Materials and methods, SIET measurement of K^+ concentration gradient adjacent to rectum surface), Cl^- is also likely to be absorbed at the rectum of *C. riparius* and, based on studies with mosquito larvae, Cl^- most likely enters the cells at the apical membrane through apical Cl^-/HCO_3^- exchangers (Strange and Phillips 1984; Strange et al. 1984) with hydration of CO_2 by cytosolic carbonic anhydrase providing HCO_3^- for the Cl^-/HCO_3^- exchanger and H^+ for VA (Smith et al. 2008). Cl^- may leave the cell at the basal membrane through Cl^- channels driven by the cytosol negative potential established by the activity of the basolateral NKA.

2.5.5 Perspectives and significance: The larvae of *C. riparius* are ubiquitous FW benthic inhabitants that play an important role in aquatic ecosystems by feeding on detritus and thereby recycling nutrients and acting as a food source for other animals. Interestingly, studies have found larval *C. riparius* thriving in salinated bodies of water such as coastal rock pools and FW bodies that have been salinated by industrial effluent. Climate change and anthropogenic factors such as road salting are predicted to continue damaging FW ecosystems and as a result, understanding the physiological mechanisms that permit larval *C. riparius* to thrive in different environmental conditions is important. In this study we demonstrated that the rectum is of particular importance in regulating ion homeostasis by absorbing relatively high amounts of K^+ into the hemolymph under IPW and FW conditions and that the rectum responds to larval BW exposure by significantly decreasing K^+ absorption. We further demonstrated that K^+ absorption by the rectum is dependent on the activities of both NKA and VA and is at least partially mediated by K^+ channels. These findings provide a strong impetus for further identification and characterization of the major transport mechanisms in the apical and basolateral membranes of the rectal epithelium of aquatic insects. We anticipate that the epithelial model initiated in this

study will serve as a prototype for other K^+-absorptive epithelia of aquatic insects, as the frog skin has done for absorptive epithelia of vertebrates.

2.6 References

Bervoets L, Int Panis L, Verheyen, R (1994) Trace metal levels in water, sediments and *Chironomus gr. thumni*, from different water courses in Flanders (Belgium). Chemosphere 29: 1591-1601

Bervoets L, Baillieul B, Blust R, Verheyen R (1995) Evaluation of effluent toxicity and ambient toxicity in a polluted lowland river. Environ Pollut 91:333-341

Bleich M, Riedemann N, Warth R, Kerstan D, Leipziger J, Hör M, Driessche WV, Greger R (1996) Ca^{2+} regulated K^{+} and non-selective cation channels in the basolateral membrane of rat colonic crypt base cells. Pflugers Arch 432:1011-1022

Boudko DY (2012) Molecular basis of essential amino acid transport from studies of insect nutrient amino acid transporters of the SLC6 family (NAT-SLC6). J Insect Physiol 58:433-449

Boudko DY, Kohn AB, Meleshkevitch EA, Dasher MK, Seron TJ, Stevens BR, Harvey WR (2005) Ancestry and progeny of nutrient amino acid transporters. Proc Nat Acad Sci USA 102: 1360-1365

Bradley TJ (1994) The role of physiological capacity, morphology, and phylogeny in determining habitat use in mosquitoes. In: Wainwright PC, Reilly SM (eds) Ecological Morphology. The University of Chicago Press, Chicago, pp 303-318

Bradley TJ, Phillips JE (1977) Regulation of rectal secretion in saline-water mosquito larvae living in waters of diverse ionic composition. J Exp Biol 66:83-96

Brenner R, Atkinson NS (1997) Calcium-activated potassium channel gene expression in the midgut of *Drosophila*. Comp Biochem Physiol B 118:411-420

Chasiotis H, Kelly SP (2009) Occludin and hydromineral balance in *Xenopus laevis*. J Exp Biol 212:287-296

Clark TM, Bradley TJ (1997) Malpighian tubules of larval *Aedes aegypti* are hormonally stimulated by 5-hydroxytryptamine in response to increased salinity. Arch Insect Biochem Physiol 34:123-141

Clark TM, Koch A, Moffett DF (1999) The anterior and posterior 'stomach' regions of larval *Aedes aegypti* midgut: regional specialization of ion transport and stimulation by 5-hydroxytryptamine. J Exp Biol 202:247-252

Clark TM, Hutchinson MJ, Huegel KL, Moffett SB, Moffett DF (2005) Additional morphological and physiological heterogeneity within the midgut of larval *Aedes aegypti* (Diptera:Culicidae) revealed by histology, electrophysiology, and effects of *Bacillus thuringiensis* endotoxin. Tissue Cell 37:457-468

Clements AN (1992) The Biology of Mosquitoes, vol 1. Chapman & Hall, London

Colbo MH (1996) Chironomidae from marine coastal environments near St. John's, Newfoundland, Canada. Hydrobiol 318:117-122

Del Duca O, Nasirian A, Galperin V, Donini A (2011) Pharmacological characterisation of apical Na^+ and Cl^- transport mechanisms of the anal papillae in the larval mosquito *Aedes aegypti*. J Exp Biol 214:3992-3999

Donini A, O'Donnell MJ (2005) Analysis of Na^+, Cl^-, K^+, H^+ and NH_4^+ concentration gradients adjacent to the surface of anal papillae of the mosquito *Aedes aegypti*: application of self-referencing ion-selective microelectrodes. J Exp Biol 208:603-610

Donini A, Patrick ML, Bijelic G, Christensen RJ, Ianowski JP, Rheault MR, O'Donnell MJ (2006) Secretion of water and ions by Malpighian tubules of larval mosquitoes: Effects of diuretic factors, second messengers, and salinity. Physiol Biochem Zool 79:645-655

Donini A, Gaidhu MP, Strasberg D, O'Donnell MJ (2007) Changing salinity induces alterations in hemolymph ion concentrations and Na^+ and Cl^- transport kinetics of the anal papillae in the larval mosquito, *Aedes aegypti*. J Exp Biol 210:983-992

Dow JAT (1986) Insect midgut function. In: Evans PD, Wigglesworth VB (eds) Advances In Insect Physiology, vol 19. Academic Press, London, pp 187-328

Driver EA (1977) Chironomid communities in small prairie ponds: some characteristics and controls. Freshw Biol 7:121-133

Ehrenfeld J, Klein U (1997) The key role of the H^+ V-ATPase in acid-base balance and Na^+ transport processes in frog skin. J Exp Biol 200:247-256

Emery AM, Billingsley PF, Ready PD, Djamgoz MBA (1998) Insect Na^+,K^+-ATPase. J Insect Physiol 44:197-209

Filippova M, Ross LS, Gill SS (1998) Cloning of the V-ATPase B subunit cDNA from *Culex quinquefasciatus* and expression of the B and C subunits in mosquitoes. Insect Mol Biol 7:223-232

Grinstein S, Smith JD (1990) Calcium-independent cell volume regulation in human lymphocytes. Inhibition by charybdotoxin. J Gen Physiol 95:97-120

Hanrahan JW, Phillips JE (1983) Mechanism and control of salt absorption in locust rectum. Am J Physiol Regul Integr Comp Physiol 244:R131-R142

Hanrahan JW, Wills NK, Phillips JE, Lewis SA (1986) Basolateral K channels in an insect epithelium: channel density, conductance, and block by barium. J Gen Physiol 87:443-466

Harvey WR, Maddrell SHP, Telfer WH, Wieczorek H (1998) H^+ VATPases energize animal plasma membranes for secretion and absorption of ions and fluids. Amer Zool 38:426-441

Harvey WR (2009) Voltage coupling of primary H^+ V-ATPases to secondary Na^+- or K^+-dependent transporters. J Exp Biol 212:1620-1629

Hebert SC, Desir G, Giebisch G, Wang W (2005) Molecular diversity and regulation of renal potassium channels. Physiol Rev 85:319-371

Hermann A, Erxleben C (1987) Charybdotoxin selectively blocks small Ca-activated K channels in *Aplysia* neurons. J Gen Physiol 90:27-47

Hibino H, Inanobe A, Furutani K, Murakami S, Findlay I, Kurachi Y (2010) Inwardly rectifying potassium channels: their structure, function, and physiological roles. Physiol Rev 90: 291-366

Hurst AM, Beck JS, Laprade R, Lapointe JY (1991) Na pump inhibition down regulates an ATP-sensitive K channel in rabbit proximal convoluted tubule. Am J Physiol Renal Fluid Electrolyte Physiol 264:F760-F764

Jagadeshwaran U, Onken H, Hardy M, Moffett SB, Moffett DF (2010) Cellular mechanisms of acid secretion in the posterior midgut of the larval mosquito (*Aedes aegypti*). J Exp Biol 213: 295-300

Jonusaite S, Kelly SP, Donini A (2011) The physiological response of larval *Chironomus riparius* (Meigen) to abrupt brackish water exposure. J Comp Physiol B 181:343-352

Kawahara K, Hunter M, Giebisch G (1987) Potassium channels in *Necturus* proximal tubule. Am J Physiol Renal Fluid Electrolyte Physiol 253:F488-F494

Khodabandeh S (2006) Na^+,K^+-ATPase in the gut of larvae of the Zygopteran, *Ischnura elegans*, and the Anisoptera, *Libellula lydia*, (Odonata): activity and immunocytochemical localization. Zool Stud 45:510-516

Koch JH (1983) Absorption of chloride ions by anal papillae of Diptera larvae. J Exp Biol 15: 152-160

Lane NJ, Skaer HB (1980) Intercellular junctions in insect tissues. In: Berridge MJ,

Treherne JE, Wigglesworth VB (eds) Advances in Insect Physiology, vol 15. Academic Press, London, pp 35-213

Leader JP, Green LB (1978) Active transport of chloride and sodium by the rectal chamber of the larvae of the dragonfly, *Uropetala carovei*. J Insect Physiol 24:685-692

Leonard EM, Pierce LM, Gillis PL, Wood CM, O'Donnell MJ (2009) Cadmium transport by the gut and Malpighian tubules of *Chironomus riparius*. Aqua Toxicol 92:179-186

Linser PJ, Smith KE, Seron TJ, Neira Oviedo M (2009) Carbonic anhydrases and anion transport in mosquito midgut pH regulation. J Exp Biol 212:1662-1671

Luan Z, Li HS (2012) Inwardly rectifying potassium channels in *Drosophila*. Acta Physiol Sin 64:515-519

MacKinnon R, Reinhart PH, White MM (1988) Charybdotoxin block of *Shaker* K^+ channels suggests that different types of K^+ channels share common structural features. Neuron 1:997-1001

Marshall WS, Grosell M (2005) Ion transport, osmoregulation, and acid-base balance. In: Evans DH, Claiborne JB (eds) The physiology of fishes, 3rd edn. Taylor and Francis Group, Boca Raton, pp 177-210

Matsumura Y, Cohen B, Guggino WB, Giebisch G (1984) Regulation of the basolateral potassium conductance of the *Necturus* proximal tubule. J Membr Biol 79:153-161

Meredith J, Phillips JE (1973) Rectal ultrastructure in salt- and freshwater mosquito larvae in relation to physiological state. Z Zellforsch Mikrosk Anat 138:1-22

Messner G, Wang W, Paulmichl M, Oberleithner H, Lang F (1985) Ouabain decreases apparent potassium-conductance in proximal tubules of the amphibian kidney. Pfluegers Arch 404:131-137

Miller C, Moczydlowski E, Latorre R, Phillips M (1985) Charybdotoxin, a protein inhibitor of single Ca^{++}-activated K^+ channels from mammalian skeletal muscle. Nature 313:315-318

Naikkhwah W, O'Donnell MJ (2011) Salt stress alters fluid and ion transport by Malpighian tubules of *Drosophila melanogaster*: evidence for phenotypic plasticity. J Exp Biol 214:3443-3454

Naikkhwah W, O'Donnell MJ (2012) Phenotypic plasticity in response to dietary salt stress: Na^+ and K^+ transport by the gut of *Drosophila melanogaster* larvae. J Exp Biol 215:461-470

Nguyen H, Donini A (2010) Larvae of the midge *Chironomus riparius* possess two distinct mechanisms for ionoregulation in response to ion-poor conditions. Am J Physiol Reg Int Comp Physiol 299:R762-R773

Okech BA, Boudko DY, Linser PJ, Harvey WR (2008a) Cationic pathway of pH regulation in larvae of *Anopheles gambiae*. J Exp Biol 211:957-968

Okech BA, Meleshkevitch EA, Miller MM, Popova LB, Harvey WR, Boudko DY (2008b) Synergy and specificity of two Na^+-aromatic amino acid symporters in the model alimentary canal of mosquito larvae. J Exp Biol 211:1594-1602

Parma S, Krebs BPM (1977) The distribution of chironomid larvae in relation to chloride concentration in a brackish water region of The Netherlands. Hydrobiologia 52:117-126

Patrick ML, Aimanova K., Sanders HR, Gill SS (2006) P-type Na^+/K^+-ATPase and V-type H^+-ATPase expression patterns in the osmoregulatory organs of larval and adult mosquito *Aedes aegypti*. J Exp Biol 209:4638-4651

Peacock AJ (1976) Distribution of Na^+-K^+-activated ATPase in the alimentary tract of *Locusta migratoria*. Insect Biochem 6:529-533

Peacock AJ (1977) Distribution of Na^+-K^+-activated ATPase in the hindgut of two insects *Schistocerca* and *Blaberus*. Insect Biochem 7:393-395

Peacock AJ (1981a) Distribution of (Na^+-K^+)-ATPase activity in the mid- and hind-guts of adult *Glossina morsitans* and *Sarcophaga nodosa* and the hind-gut of *Bombyx mori* larvae. Comp Biochem Physiol A 69:133-136

Peacock AJ (1981b) Further studies of the properties of locust rectal Na^+- K^+-ATPase, with particular reference to the ouabain sensitivity of the enzyme. Comp Biochem Physiol C 68:29-34

Phillips JE (1981) Comparative physiology of insect renal function. Am J Physiol Regul Integr Comp Physiol 241:R241-R257

Phillips JE, Hanrahan J, Chamberlin M, Thomson B (1986) Mechanisms and control of reabsorption in insect hindgut. In: Evans PD, Wigglesworth VB (eds) Advances In Insect Physiology, vol 19. Academic Press, London, pp 329-422

Phillips JE, Wiens C, Audsley N, Jeffs L, Bilgen T, Meredith J (1996) Nature and control of chloride transport in insect absorptive epithelia. J Exp Zool 275:292-299

Pinder LCV (1986) Biology of freshwater Chironomidae. Ann Rev Entomol 31:1-23

Pinder LCV (1995) The habitats of chironomid larvae. In: Armitage PD, Cranston PS, Pinder LCV (eds) The Chironomidae: biology and ecology of non-biting midges. Chapman and Hall, London, NY, pp 107-135

Rheault MR, O'Donnell MJ (2001) Analysis of K^+ transport in Malpighian tubules of *Drosophila melanogaster*: Evidence for spatial and temporal heterogeneity. J Exp Biol 204:2289-2299

Rheault MR, O'Donnell MJ (2004) Organic cation transport by Malpighian tubules of *Drosophila melanogaster*: Application of two novel electrophysiological methods. J Exp Biol 207:2173-2184

Rheault MR, Okech BA, Keen SBW, Miller MM, Meleshkevitch EA, Linser PJ, Boudko DY, Harvey WR (2007) Molecular cloning, phylogeny and localization of AgNHA1 the first Na^+/H^+ antiporter (NHA) from a metazoan, *Anopheles gambiae*. J Exp Biol 210:3848-3861

Sackin H, Palmer LG (1987) Basolateral potassium channels in renal proximal tubule. Am J Physiol Renal Fluid Electrolyte Physiol 253:F476-F487

Smith C, Phillips M, Miller C (1986) Purification of charybdotoxin, a specific inhibitor of the high-conductance Ca^{++}-activated K^+ channel. J Biol Chem 261:14607-14613

Smith KE, Van Ekeris LA, Okech BA, Harvey WR, Linser PJ (2008) Larval anopheline mosquito recta exhibit a dramatic change in localization patterns of ion transport proteins in response to shifting salinity: a comparison between anopheline and culicine larvae. J Exp Biol 211:3067-3076

Strange K, Phillips JE (1984) Mechanisms of CO_2 transport in rectal salt gland of *Aedes dorsalis*. Ionic requirements of CO_2 secretion. Am J Physiol 246:R727-R734

Strange K, Phillips JE, Quamme GA (1984) Mechanisms of total CO_2 transport in the microperfused rectal salt gland of *Aedes dorsalis.* II. Site of Cl^-/HCO_3^-exchange and function of anterior and posterior salt gland segments. Am J Physiol 246:R735-R740

Sumner JP, Dow JAT, Earley FGP, Klein U, Jäger D, Wieczorek H (1995) Regulation of plasma membrane V-ATPase activity by dissociation of peripheral subunits. J Biol Chem 270:5649-5653

Sutcliffe DW (1961) Studies on salt and water balance in caddis larvae (Tricoptera). II. Osmotic and ionic regulation of body fluids in *Limnephilus stigma curtis* and *Anabolja nervosa* Leach. J Exp Biol 38:521-530

Tolman JH, Steele JE (1976) A ouabain-sensitive, (Na^+-K^+)-activated ATPase in the rectal epithelium of the american cockroach, *Periplaneta americana*. Insect Biochem 6:513-517

Warth R, Bleich M (2000) K^+ channels and colonic function. Rev Physiol Biochem Pharmacol 140:1-62

Wigglesworth V (1933) The function of the anal gills of mosquito larvae. J Exp Biol 10:16-26

Xiang MA, Linser PJ, Price DA, Harvey WR (2012) Localization of two Na^+- or K^+-H^+ antiporters, AgNHA1 and AgNHA2, in *Anopheles gambiae* larval Malpighian tubules and the functional expression of AgNHA2 in yeast. J Insect Physiol 58:570-579

PARTII

CHAPTER 3:

OCCLUDING JUNCTIONS OF INVERTEBRATE EPITHELIA[2]

3.1 Summary

The diversity of invertebrate architecture is remarkable. This is achieved by the organization and function of four tissue types found in most metazoan phyla – epithelial, connective, muscle and nervous tissue. Epithelial tissue is found in all extant animals (parazoan and metazoan alike). Epithelial cells form cellular sheets that cover internal or external surfaces and regulate the passage of material between separated compartments. The transepithelial movement of biological material between compartments can occur across the transcellular pathway (i.e. across cells) or the paracellular pathway (i.e. between cells) and the latter is regulated by occluding junctions that typically link cells in a subapical domain. In this review, information on occluding junctions of invertebrate epithelia is consolidated and discussed in the context of morphology, ultrastructure and physiology. In addition, an overview of what is currently known about invertebrate occluding junction proteins and their role in maintaining the integrity of invertebrate epithelia and regulating the barrier properties of these tissues is presented.

[2]Contributing authors: Sima Jonusaite, Scott P Kelly and Andrew Donini

Department of Biology, York University, Toronto, Ontario, Canada M3J 1P3

This chapter has been published and reproduced with permission:

Jonusaite S, Donini A, Kelly SP (2016) Occluding junctions of invertebrate epithelia. J Comp Physiol B 186:17-43

3.2 Introduction

Invertebrate species represent 95% of all living animals. Invertebrates have colonized all habitats on earth, resulting in a tremendous array of strategies that allow these organisms to respire, acquire and process food, maintain salt and water balance, reproduce, communicate and generally cope with the stressors of life. Yet despite this diversity, the bauplan of all invertebrates is based on the structure and organization of two or more of the four tissue types found in most metazoans - muscle, connective, nervous, and epithelial tissue (Brusca and Brusca 1990). Isolation of the body from the external environment and separation of compositionally distinct fluid compartments within the body are achieved by the epithelial tissues. This is because an epithelium is a sheet of specialized cells which adhere to one another via intercellular contacts or junctions and both cell and junctions between cells control the transepithelial passage of biological material between two environments (Cereijido et al. 2004). Indeed, the formation of an epithelium that seals and controls the composition of internal milieu is a characteristic of even the earliest metazoans (parazoans), the sponges (phylum Porifera), which highlights the importance of this tissue in multicellular organisms (Leys et al. 2009; Adams et al. 2010; Leys and Hill 2012; Leys and Riesgo 2012).

The capacity of invertebrate epithelia to 'seal' varies depending on epithelium type and in a manner that can be linked to the physiological role of a tissue as it contributes to organismal homeostasis both during and after development (Skaer and Maddrell 1987; Leys et al. 2009). The ability of an epithelium to maintain gradients of biological material and electrical differences between separated compartments depends on the transport of solutes and water across the transcellular pathway (i.e. through the cells) and passive movement of material through the paracellular pathway (i.e. between adjacent cells). With regard to the latter, epithelia are typically described as 'tight' or 'leaky' depending on the electrical resistance measured across them and the

extent to which biological material can move through the paracellular pathway (Hanrahan 1984; Skaer and Maddrell 1987). Paracellular transport or permeability of an epithelium is regulated by occluding cell-cell junctions that typically link cells in a subapical domain. In the epithelia of chordates, restriction of free solute diffusion through the paracellular route is provided by the tight junction (TJ) complex which forms at the most apical region of the lateral membranes of chordate epithelial cells and appears as focal contacts between adjacent cell plasma membranes (see Fig. 3-1a; Farquhar and Palade 1963; Georges 1979; Lane et al. 1986; Anderson and Van Itallie 2009). In TJs the focal contacts or 'kissing points' are cross-sections through TJ ribbons or strands that encircle the apical cell pole as an anastomosing network, and this provides a physical basis for paracellular occlusion (see Fig. 3-1a; Farquhar and Palade 1963). In contrast, extensive literature suggests that the epithelia of invertebrates generally lack TJs, with notable exceptions such as TJs in the rectal pads of cockroach *Periplaneta americana* (Lane 1979). Notwithstanding isolated examples, the paracellular diffusion barrier in most epithelia of invertebrates is provided by intercellular septate junctions (SJs) which tend to lie in circumferential belts around lateral cell borders on the outer or apical surface (Ledger 1975; Lord and DiBona 1976; Noirot-Timothee and Noirot, 1980; Skaer et al. 1987; Itza and Mozingo 2005; Fiandra et al. 2006; Bairati and Giora 2008). SJs were first described in the epidermis of two species of *Hydra* (phylum Cnidaria) as “septate desmosomes” (Wood 1959). Following this first description, SJs possessing similar characteristics have been identified widely in other invertebrate phyla. In cross-section, SJs exhibit little variation across invertebrates as virtually all appear as a ladder-like structure between adjacent cells with septa spanning a 15-20 nm intercellular space (Fig. 3-1b; Gilula et al. 1970; Flower and Filshie 1975). However, tracer impregnation techniques made it possible to show SJ structure in tangentially cut sections and substantial differences in the fine details of SJ intercellular elaboration were revealed. Based on tangential views, SJs have been

subdivided into several types and some animals are reported to possess multiple types of SJs specific to different epithelia (Staehelin 1974; Green 1981; Green and Bergquist 1982; Dallai et al. 1990; Xué and Romano 1992). The most obvious variation in SJs is in the conformations of the septa themselves which can be double or single and arranged in parallel linear rows, pleated sheets or anastomosing networks similar to TJ strands (see Figs. 3-2, 3-5; Green and Bergquist, 1982; Green et al. 1979). In addition, the widths of septa vary and some have side projections (Figs. 3-2-5). Both homologous and heterologous cell pairs can be connected by one type of SJ and two types of SJs can coexist within the same epithelium (Satir and Gilula 1970; Rose 1971; Flower and Filshie 1975; Dallai 1976; Bairati and Gioria 2008). Aside from septate type occluding junctions, a form of simple parallel membrane junction exists in the epithelia of sponges and a single, 'tripartite apical junction' fulfills the role of an occluding junction in the epithelia of the nematode *Caenorhabditis elegans* (Green and Bergquist 1982; Michaux et al. 2001; Asano et al. 2003; Adams et al. 2010).

Molecular and biochemical characterization of the vertebrate TJ complex has revealed that it is composed of multiple transmembrane proteins as well as cytoplasmic plaque proteins, signaling proteins, and adapters involved in cytoskeletal linkage (for a review see Anderson and Van Itallie 2009; Günzel and Fromm 2012; Günzel and Yu 2013). Among transmembrane proteins, claudins are the major structural components of TJ strands and these play a key role in determining the permeability properties of vertebrate epithelia (Günzel and Fromm 2012; Günzel and Yu 2013). However, many questions about the molecular components and assembly of invertebrate occluding junctions remain open. Conservation of genes encoding members of the claudin family as well as scaffolding proteins from the membrane-associated guanylate kinase (MAGUK) family in invertebrate occluding junctions suggest that invertebrate occluding junctions also form large multiprotein complexes, the components of which will likely impart

complex developmental and physiological plasticity (Woods and Bryant 1991; Fei et al. 2000; Michaux et al. 2001; Knust and Bossinger 2002; Behr et al. 2003; Tyler 2003; Wu et al. 2004; Lockwood et al. 2008; Fahey and Degnan 2010; Nelson et al. 2010; Simske and Hardin 2011; Ganot et al. 2015). In this review a timely consolidation of information on the diversity, morphology, and physiological properties of invertebrate occluding junctions is provided as well as an overview of what is known about the proteins that comprise invertebrate SJs. With regard to the latter topic of SJ proteins, a recent excellent review can be found which covers this topic with an emphasis on SJ proteins of *Drosophila* epithelia (Izumi and Furuse 2014).

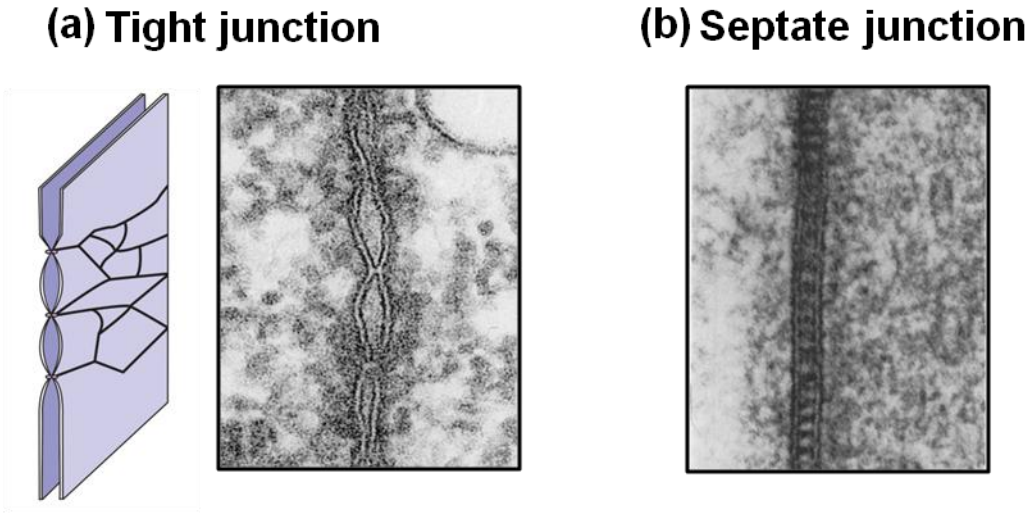

Figure 3-1: Occluding junctions of metazoans. Schematic representation and electron microscopic (EM) image of (**a**) the vertebrate tight junction (TJ) seen as focal contacts or 'kissing points' between adjacent epithelial cell plasma membranes which are cross-sections through TJ strands that encircle the apical cell pole as an anastomosing network. A common characteristic of invertebrate SJs seen in cross-section is a ladder-like appearance between adjacent cells with septa spanning a 15-20 nm intercellular space (**b**). EM images reprinted from (**a**) Furuse and Tsukita (2006), Copyright (2015), with permission from Elsevier; (**b**) Flower and Filshie (1975), Copyright (2015), with permission from The Company of Biologists Ltd.

3.3 Morphology, ultrastructure and physiology of occluding junctions in major invertebrate phyla

3.3.1 Phylum Porifera

The phylum Porifera (Sponges) contains the most ancient extant multicellular animals and these organisms are distributed throughout the world's oceans and seas at all latitudes of the globe. Recent estimates suggest that there are ~11 000 described species (see Van Soest et al. 2012). Members are organized into 4 classes, Demospongiae, Hexactinellida, Homoscleromorpha and Calcarea, based primarily on the composition and morphology of discrete skeletal-like structures called spicules. Despite a simple body plan, sponges possess a number of specialized differentiated cell types. These cells primarily arise from archeocytes which are regarded as sponge stem cells (see Funayama 2010; Funayama 2013). Archeocytes are found in a loose gelatinous matrix (mesohyl) that is contained by simple epithelia that line the external body surfaces of the sponge as well as the internal structure of the aquiferous system. The epithelium or pinacoderm that covers the external surface and incurrent canals is composed of pinacocytes (cells that line the external surfaces and in some cases internal canals of poriferans) of which there are several types. The internal canals and chambers of sponges are lined with flagellated choanocytes resulting in the choanoderm epithelium. Despite being considered the most ancient of multicellular animals, sponges exhibit substantial diversity in their physiology and this may reflect the diversity of aquatic habitats that they exploit. While the vast majority of sponge species inhabit marine environments, ~200 freshwater species are known (Manconi and Pronzato 2008; Van Soest et al. 2012) and these are also distributed throughout the globe and at all latitudes with the exception of Antarctica (Manconi and Pronzato 2008). The remarkable ability of sponges to invade inland habitats is attributed to the evolutionary development of gemmules which are a protected mass of archaeocytes that can withstand dessication and freezing

temperatures. Sponges also inhabit brackish water. For example, it is documented that the fresh water species *Ephydatia fluviatilis* can inhabit low salinity brackish water (Poirrier 1974) and estuarine species such as *Microciona prolifera* inhabit areas that range in salinity from ~10 to 30 ‰ and enter a protective dormant state in lower salinities (Fell et al. 1989).

From the description above, it is clear that sponge habitats present different challenges to the maintenance of cellular and organismal ion and water balance. It has been demonstrated that marine sponge tissues as a whole have an ionic content different from the external environment, with inward sodium and outward potassium gradients (Prosser 1967). On the other hand, the pinacocytes of freshwater sponge have a low osmolarity and possess contractile vacuoles which have been shown to actively excrete water when external solute concentration falls (Harrison 1972; Brauer 1975; Brauer and McKanna 1978). These observations suggest that the pinacoderm of both marine and freshwater sponges may regulate the internal (mesohyl) ionic composition of the animal and maintain it at levels different from that of the external environment. While specialized organelles typically associated with unicellular animal-like organisms undoubtedly play a role in this, recent evidence that the pinacoderm of freshwater sponge forms an epithelium that seals and controls the passage of ions across it was reported by Adams et al. (2010) who demonstrated that a cultured pinacoderm derived from *Spongila lacustris* exhibited a relatively high transepithelial resistance. This pinacoderm controlled membrane potential by transport of ions and limited the paracellular passage of very small tracer molecules (5 kDa ^{3}H-inulin and 0.85 kDa ruthenium red) (Adams et al. 2010). It was further concluded that paracellular occlusion was provided by parallel membrane junctions, in which the plasma membranes of adjacent pinacocytes lie parallel to one another over a long distance with 10-20 nm separation (Adams et al. 2010). Along such junctions there are regions in which cell membranes appear fused or in tight contact (Adams et al. 2010). Similar parallel membrane

junctions between the pinacocytes have been described in other freshwater as well as marine sponge species (Bagby RM 1970; Green and Bergquist 1979; Lethias et al. 1983; Pavans de Ceccatty 1986).

Ultrastructural studies provide morphological evidence for the presence of SJs between cells in a diverse range of sponges (Leys et al. 2009). Mackie and Singla (1983) described SJs with a characteristic 15 nm intercellular cleft in a cross-sectional view between the trabecular syncytium, archaeocytes and collar units of choanoblasts in hexactinellid *Rhabdocalyptus dawsoni*. Junctions with septa and electron dense regions at the membranes have been shown between the cells of the apical pole of larval epithelium in two species of homoscleromorph *Oscarella sp.* and demosponge *Corticium candelabrum* (Boury-Esnault et al. 2003; Maldonado and Riesgo 2008). By far the most distinct SJs are seen in calcareous sponges. Ledger (1975) showed images of junctions with dense septa between all sclerocytes, the cells that secrete spicules, in *Sycon ciliatum* where they are thought to provide a sealed compartment for the secretion of calcium carbonate during spiculogenesis. Green and Berquist (1979) demonstrated SJs between the choanocytes in *Clathrina*.

Although a number of genes that are homologs of SJ proteins have now been identified in some marine sponges (see section on occluding junction proteins) their molecular architecture in the SJ remains unknown. In addition, the function of these putative SJ proteins is also unknown in sponges. Efforts to understand the role of SJs in sponges and determine whether the different types of epithelia in these animals have different levels of barrier function may benefit from studying freshwater species which face the challenge of life in a hypoosmotic environment, or species that inhabit and tolerate environments such as estuaries where alterations in environmental conditions are experienced on a regular basis.

3.3.2 Phylum Cnidaria

Members of the Phylum Cnidaria are relatively simple aquatic organisms that exhibit one of two types of body form, the polyp or medusa. This group can be divided into 5 classes that include the Hydrozoa, Scyphozoa, Staurozoa, Cubozoa and Anthozoa. Cnidarians are most commonly found in a marine environment and some members of the phylum are exclusively found there (i.e. Staurazoa and Anthozoa). But some cnidarians of the Class Hydrozoa are freshwater organisms (Campbell et al. 2013) while other members of Hydrozoa as well as Scyphozoans and Cubozoans can be found in the brackish water of estuaries (Kraeuter and Setzler 1975; Primo et al. 2012). A hallmark of this phylum is the cnida which is an organelle with an eversible tube that can be ejected forcibly from within specialized cells named cnidocytes (Fautin 2009).

The epithelia of cnidarians possess SJs as sealing junctions. Three variations of SJs have been found in cnidarians (see Table 3-1; Fig. 3-2) and all appear to be unique to this phylum. In the class Hydrozoa, hydra-type or hydroid SJs have been fully described in both the gastrodermis and epidermis, where they follow a tortuous course between the apical regions of adjacent epithelial cells (Wood 1959; Overton 1963; Danilova et al. 1969; Leik and Kelly 1970; Hand and Gobel 1972; Filshie and Flower 1977; Kachar et al. 1986). When hydroid SJs are viewed in cross section, each septum is seen to extend across the 15-20 nm intercellular space between adjacent cell membranes, producing a typical SJ ladder-like image. In high-resolution micrographs, Hand and Gobel (1972) further demonstrated the presence of V-shaped projections that extend from each septum, occasionally interlinking adjacent septa. In tangential section planes that pass through junctions parallel to the cell membranes, SJs of hydroid epithelia appear to consist of 8-12 nm wide rows of straight septa that have additional fine projections on each side of the row at 4-5 nm intervals (Hand and Gobel 1972; Filshie and Flower 1977; Fig. 3-2a).

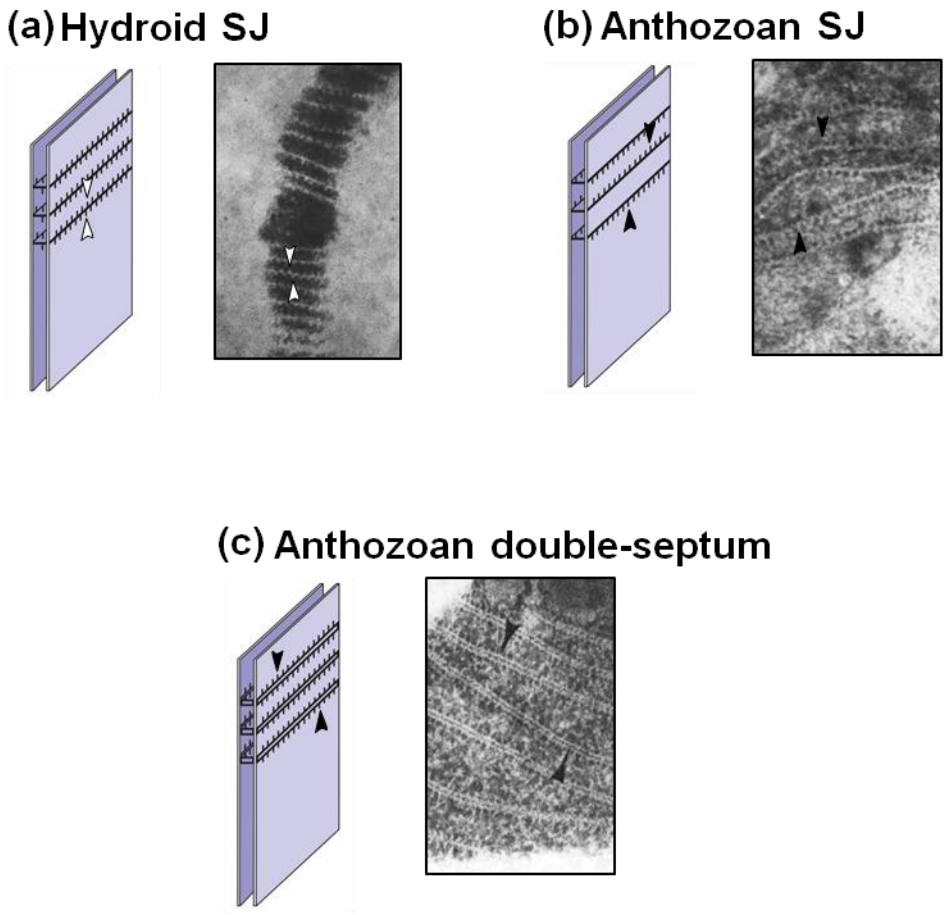

Figure 3-2: Schematic representation and electron microscopic (EM) images of septate junctions (SJs) found in the phylum Cnidaria. Illustrated tangential sections and high magnification electron micrographs are presented for (**a**) a hydroid SJ, (**b**) an anthozoan SJ and (**c**) an anthozoan double-septum. In panel (**a**), septa of the hydroid SJ are straight, 8-12 nm wide and have additional fine projections on each side (arrowheads). In epithelia of anthozoans, two SJ variants are observed. The anthozoan SJ shown in panel (**b**) is found in ectodermal tissues and the anthozoan double-septum SJ shown in panel (**c**) is present in endodermal epithelia. In oblique sections of the anthozoan SJ, septa appear as single, wavy structures with prominent side projections on one side of the septa (**b**, arrowheads). The septa of anthozoan double-septum SJs are identified as paired and straight with lateral projections protruding from the sides of the twin septa (**c**, arrowheads). EM images modified from (**a**) Filshie and Flower (1977), (**b**) Green and Flower (1980), Copyright (2015), with permission from The Company of Biologists Ltd.

In the class Anthozoa, two SJ variants have been observed (Table 3-1; Fig. 3-2b,c). When viewed in cross-section, both types of SJ show the characteristic 15-18 nm intercellular spacing and both appear around the apical circumference of epithelial cells (Green and Flower 1980). One SJ variant, the anthozoan SJ (Fig. 3-2b), seems to be restricted to ectodermal tissues such as the epidermis and the outer lining of the tentacle (Green and Flower 1980; Green and Berquist 1982). In contrast, the other SJ variant, the anthozoan double-septum (Fig. 3-2c), is seen in endodermal epithelia such as the gastrodermis and the inner lining of the sea anemone tentacles as well as between mesodermal myoepithelial cells (Green and Flower 1980; Green and Berquist 1982; Holley 1985). When SJs of anthozoan endodermal epithelia are viewed in tangential sections, the septa appear paired and straight, and are 6-7 nm apart. In many places, lateral projections up to 6 nm long (spaced about 7.5 nm apart) can be seen protruding from the sides of the twin septa (Green and Flower 1980; Green and Berquist 1982; Fig. 3-2c, arrowheads). When examining junctions between the epithelial cells of anthozoan epidermis, the septa are identified as single, long, and wavy structures. But as in the gastrodermal junction, the septa in the epidermal SJ have prominent side projections up to 7 nm long, spaced about 7 nm apart (Green and Flower 1980; Green and Berquist 1982; Fig. 3-2b, arrowheads). The main difference between the anthozoan epidermal SJ (i.e. anthozoan SJ) and the hydroid SJ is that the anthozoan epidermal SJ possess lateral projections on only one side of the septa (Green and Flower 1980; see Fig. 3-2a,b).

Despite detailed morphological descriptions of cnidarian SJs, how they contribute to the regulation of paracellular permeability and their functional importance as barriers are areas that have been largely overlooked. Variation in the number of septa has been noted by Green (1981a) who compared epidermal SJs of the freshwater hydrozoan *Chlorohydra virridissima* and a marine hydrozoan *Tubularia antennoides* and saw a larger number of cross-linked septa in the

freshwater species. Hand and Gobel (1972) found that when living *Hydra* were soaked in either horseradish peroxidase (MW 40 kDa) or cytochrome (MW 12 kDa), neither tracer penetrated beyond the fourth interseptal space in the epidermal SJs. The authors suggested that if the backbone and projections of septa bore even a weak electrical charge, a junction consisting of 30 or more septa would present a considerable barrier to the paracellular movement of a substantial number of solutes. That such considerations seem reasonable is also indicated by the electrophysiological studies of Josephson and Macklin (1967, 1969) who demonstrated that the body wall of *Hydra* maintains a 15-40 millivolts electrical potential (the inside of the animal being positive), and a high resistance to the flow of ions. SJs have also been implicated in the presence of an electrical resistance of ~ 477 Ohm cm^2 across tissues of the scleractinian coral *Stylophora pistillata*, which become less resistant to the flow of ions under hypertonic seawater conditions (Tambutté et al. 2012). On the other hand, studies on the isolated tentacle epithelia of anthozoans *Anemonia viridis* and *Heliofungia actinimorfis* suggest that both the ecto- and endodermal layers are comparatively leaky and exhibit high junctional permeability to ions such as Ca^{2+}, Na^{+} and Cl^{-} (Bénazet-Tambutté et al. 1996). The paracellular pathway of the tentacle epithelia was also found to have greater anion selectivity and was impermeable to larger molecules such as alanine and inulin, indicating charge and size selectivity (Bénazet-Tambutté et al. 1996). In this regard, it has been suggested that paracellular ion entry through the tentacle epithelia of cnidarians may play a role in a rapid renewal of the ionic pool of the coelenteron which ensures an adequate supply of calcium to the coral for building a calcified skeleton (Bénazet-Tambutté et al. 1996).

Despite the absence of a circulatory system and special organs for gas exchange as well as excretion, the ability of cnidarians to thrive in variable aquatic conditions, (including those that are freshwater, brackish and marine), presents an opportunity to consider how SJs might

contribute to the homeostasis of fluids in the cnidarian coelenteron. This circulatory system proxy is known to be involved in at least a limited circulation of nutrients and metabolic waste and is hyperosmotic to surroundings in freshwater animals (Brusca and Brusca 1990). The morphometric observations of Green (1981a) on SJs of freshwater versus marine hydrozoans suggest that significant progress could be made in our understanding of hydroid SJs if the physiology and molecular biology of this structure could be examined in a hydrozoan capable of tolerating water of different ionic strength. Moreover, it would also be of particular interest to learn more about the specific role/s for SJs in the deposition of the calcareous skeleton of corals. An area that could also be considered is what role SJs play in the physiology of complex sensory organs which are present in cubozoans. More specifically, the well developed eyes of cubomedusae, the most complex of which exhibit true epidermal cornea, a cellular lens and a multilayered retina (with a sensory, pigmented and nuclear layer) would be of comparative interest. Irrespective of functional work, an almost complete absence of information on the molecular physiology of SJs in the phylum Cnidaria (see Table 3-2 and *Putative occluding junction proteins of less derived invertebrates*) means that this area will also require attention.

3.3.3 Phylum Platyhelminthes

The Platyhelminthes (or flatworms) is a group of acoelomate worms the majority of which have adopted a parasitic lifestyle but one group, the "Turbellaria" encompass free-living worms. Free-living worms are mostly marine species with roughly one fifth being freshwater (Tyler and Tyler 1997; Schockaert et al. 2008). A characteristic of the free-living flatworms is a simple ciliated epidermis (Tyler and Hooge 2004). The larvae of the parasitic groups (including the classes Cestoda, Trematoda and Monogenea) also have a ciliated, cellular epidermis for locomotion but this is replaced by a non-ciliated syncytial epidermis once the larvae find a host and the worm transitions to the parasitic adult stage (Tyler and Tyler 1997). Because of this strategy, these

worms are collectively referred to as the neodermata (new dermis). The syncytial epidermis of neodermatans appears specialized for absorption of nutrients from the host tissues and fluids because all have microvillar-like structures that increase epidermal surface area (although these vary morphologically) (Tyler and Hooge 2004). On the other hand, the syncytium is also thought to protect the parasite from a host's defenses. For example, the morphologically distinct microvilli of Cestodes impart the parasite with a pH boundary layer that prevents host enzymes from functioning to digest it (Uglem and Just 1983). The syncytial epidermis of neodermata appears to be an ideal development for a parasitic strategy; however, some "Turbellarians" have also developed parasitic strategies without a syncytial epidermis (see Tyler and Tyler 1997). While the cellular epidermis of "Turbellarians" has both zonula adherens and SJs between epithelial cells, the syncytial epidermis is void of SJs with perhaps the exception of areas where secretory cells permeate the epidermis (Tyler and Hooge 2004).

Because of their occurrence in several lower invertebrate phyla, (e.g. Platyhelminthes, Annelida, Sipunculoidea, Bryozoa, Branchiopoda and Nemertea), SJs that seal epithelia of platyhelminthes have been described as the lower invertebrate pleated SJs (Table 3-1; Baskin 1976; Hori 1985, 1987; Green 1981a; Green and Berquist 1982; Vernet et al. 1979). The lower invertebrate pleated SJ (pSJ) (see Fig. 3-3) exhibits many features also found in hydroid SJs (Fig. 3-2a) and the pleated SJs of molluscs and arthropods (described below). In cross-sectional views, septa of this junction span a characteristic 15-18 nm intercellular space and the membranes of adjacent cells often have a slightly scalloped appearance rather than being uniformly straight (Green 1981a). Tangential sections of lower invertebrate pSJs show a narrow (~ 2 nm wide) pleated septal backbone with the periodicity of the pleating being 16-22 nm. The apices of the pleats have 3-5 nm projections which give the junction a very pronounced pleated appearance (Green 1981a; Hori 1987). Where two or more septa run very closely the apices of their pleats

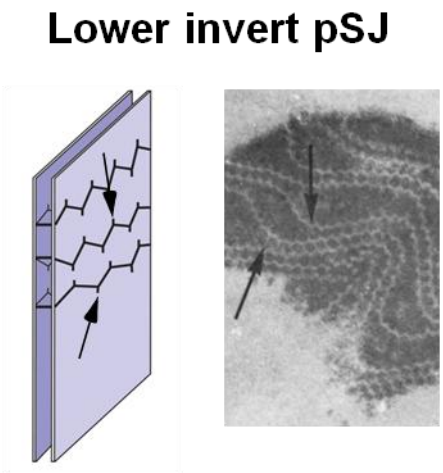

Figure 3-3: Schematic representation and an electron microscopic (EM) image of a lower invertebrate pleated septate junction (pSJ). In tangential section, lower invertebrate pSJs exhibit a narrow and pleated septal backbone with projections at the apices of the pleats (arrows) which give the junction a very pronounced pleated appearance. EM image modified from Green (1981a), Copyright (2015), with permission from Elsevier.

align and their projections fuse forming a chain of hexagonal structures (Fig. 3-3). The SJs of platyhelminths have been reported in the epidermis and gastrodermis of turbellarians (Table 3-1; Storch and Welsch 1977; Green 1981a; Hori 1987) and the uterine and protonephridial duct epithelia of parasitic platyhelminths (Table 3-1; Poddubnaya et al. 2011, 2012).

Studies on platyhelminthes have provided some information for the comparison of SJs in similar epithelia exposed to different environmental conditions. In the epidermal epithelium of a freshwater flatworm (*Neopia montana*), SJs have numerous septa, many of which are cross-linked and fused in large hexagonal arrays. In contrast, in a marine species of the genus *Pseudoceros*, the septa are fewer in number and crosslinking is less common (Green 1981a). Many cross-linked septa also occur in the epidermis of the terrestrial platyhelminthe *Bipalium* (Storch and Welsch 1977). It has been suggested that the number of septa and crosslinking vary in response to environmental stressors such as osmotic stress, which would be far greater in a freshwater environment compared to a marine setting (Green 1981a). Indeed, SJ distortion or "blister" formation has been demonstrated to occur in the epidermis of the freshwater planarian *Dugesia tigrina* when the external medium is made hypertonic, suggesting a role of SJs in the regulation of water and solute transport across this epithelium (Lord and DiBona 1976).

The SJ morphology of Platyhelminthes has been quite well described and suggestions that the epidermal SJ complex could alter the permeability of the paracellular pathway in accordance with environmental conditions (aquatic or terrestrial) have previously been discussed (Green 1981a). Further examination of this possibility would be a very interesting avenue of study, but would require a much needed first look at the molecular architecture of lower invertebrate pSJs. In addition to this, the role of lower invertebrate pSJs in the function of the flatworm protonephridial network would be a fascinating area for further work. This structure is a major advance in these triploblastic animals over previously discussed diploblastic organisms

and it is generally accepted to function in osmoregulation and, to a lesser extent, in waste excretion. Indeed it would be very interesting to see if the functional stratification (i.e. flame bulb, nephridioduct, bladder, nephridiopore) of the protonephridial network (that in different species can range from quite simple to highly complex depending on surrounding habitat) is associated with a spatial distribution of occluding junction proteins as is seen with TJ proteins in the chordate nephron.

3.3.4 Phylum Mollusca

The phylum Mollusca is a large and extremely diverse group of animals that primarily inhabit aquatic habitats but have also successfully colonized the terrestrial environment. Mollusca share several common features which are used to distinguish them as a group. These hallmarks include a muscular foot, radula feeding apparatus and a specialized dorsal epithelium (the mantle) which secretes a hard protective shell (Hohagen and Jackson 2013). There is also a cavity between the mantle and viscera (mantle cavity) which normally houses a highly versatile and multifunctional gill which can be used for gas exchange, collection of food particles, ion transport, and gamete dispersal amongst other things. Molluscs are classified into several major groups (see Haszpruner and Wanninger 2012) with Gastropoda (e.g. snails, slugs, limpets) being the most diverse and comprising ~100 000 species (or roughly 80% of all mollusca). Members of this group have successfully inhabited marine, freshwater and terrestrial habitats and display a wide diversity of feeding and reproductive strategies. Bivalvia (e.g. mussels, clams) are the second largest group and distinguished by their characteristic bivalved shell. This group comprises marine, brackish water and freshwater species and these organisms display diverse feeding strategies which also include the dependence on endosymbiotic bacteria for food (Duperron et al. 2013). Polyplacophora (chitins) is a group of marine molluscans with a modified shell consisting of eight serial plates. These animals normally inhabit rocky shores which are subjected to the daily

tidal rhythm. Cephalopoda (squid, octopus, nautilus) are predatory (or scavenger) marine molluscs possessing what is regarded as the most sophisticated invertebrate nervous system with large well developed eyes (Mather and Kuba 2013). Many species of cephalopods have internalized or lost the characteristic molluscan shell. Scaphopoda consists of small (up to 20cm in length) marine animals with tusk-shaped shells that burrow into substrate and capture prey with specialized tentacles. There are several other groups of molluscs, Solenogastres, Caudofoveata, which are worm-like and Monoplacophora which are similar to the chitins but have a single shell.

Molluscs possess a number of tissues with specialized epithelia, including the lining of their gastrointestinal tract as well as the aforementioned gills and shell-secreting mantle. In the molluscan digestive tract, morphologically and functionally distinct epithelial regions that relate to different digestive functions can be found (see Westermann and Schipp 1998), while the molluscan mantle consists of inner and outer epithelia separated by an acellular layer of connective tissue (Neff 1972). Notwithstanding the multifaceted nature of these tissues, it is the architecture and function of the molluscan gill that exhibits immense complexity (Fischer et al. 1990; Gomez-Mendikute et al. 2005; Chaparro et al. 2007). For example, the gill filaments of bivalve molluscs exhibit morphologically and functionally distinct regions, and the frontal region of the gill filament contains several epithelial cell types distinguished by their cilia (e.g. short, long, cirri, non-ciliated) (Gomez-Mendikute et al. 2005). The ciliated cells in this region are responsible for trapping and moving suspended particles as well as driving water across the filaments (Gomez-Mendikute et al. 2005). Suspension-feeding aquatic gastropods utilize a ciliated epithelium in conjunction with a mucus layer on their gill to aid in trapping and ingesting food particles (Chaparro et al. 2007), and the gills of polyplacophorans contain a simple columnar epithelium with each gill arch lamella possessing bands of ciliated cells which, based

on morphology, act to drive water between adjacent lamellae such that water flows from the outer to the inner parts of the mantle cavity (Fischer et al. 1990). Movement of water across the gill and hemolymph in the gill occurs as a countercurrent which maintains an oxygen concentration gradient for inward diffusion. This is consistent with the function of most other molluscan gills except the cephalopods. The cephalopod gills are morphologically more developed than the gills of the other molluscs. The lamellae are folded, the vascularization of the gill is relatively extensive and the surrounding epithelium has specialized regions for gas exchange and for solute transport (see Schipp et al. 1979).

Molluscs possess a well-described pSJ (Table 3-1; Fig. 3-4a), which is also characteristic of the arthropods (see following section). This type of SJ was first described by Locke (1965) in the epidermis of the caterpillar *Calpodes* and has been variously referred to as the honeycomb, pleated-sheet, or pleated-type SJ because in tangential view the septa have the shape of periodically pleated sheets, sometimes giving a honeycomb appearance (Fig. 3-4a). In molluscs, pSJs have been found in all epithelia studied to date, which include the epidermis, gill, salivary gland, digestive organs, intestine, mantle, as well as gastropod kidney sac, egg capsule gland, genital duct, and cephalopod foot epithelium, embryonic and tentacle epithelium (Table 3-1; Gilula et al. 1970; Flower 1971; Newell and Skelding 1973; Skelding 1973a; Giusti 1976; Porvaznik et al. 1979; Boucaud-Camou 1980; Green 1981a; Khan and Saleuddin 1981; Prior and Uglem 1984; Ginzberg et al. 1985; Dietz et al. 1995 Albrecht and Cavicchia 2001; Bleher and Machado 2004; Bairati and Gioria 2008). Transverse sections through positively stained molluscan pSJs show plasma membranes spaced about 15-18 nm apart that are generally joined by large number of septa. In tangentially cut sections of lanthanium-impregnated tissues, the septa are 2-3 nm wide and appear pleated with a 16-22 nm periodicity (Fig. 3-4a). These pleated

septa often run parallel in extensive arrays between epithelial cells, producing chains of hexagonal lattice (Satir and Gilula 1970; Newell and Skelding 1973).

Studies on molluscs have strengthened the notion that SJs are dynamic structures that vary in tightness in a manner that is dependent on the physiological functions of particular epithelia. Based on the permeability to different sized tracer molecules, it has been suggested that leaky SJs are present in the fluid-transporting kidney epithelium of a land snail *Achatina achatina* (Skelding 1973b). Furthermore, the complexity and size of SJs in snail kidney epithelia seem to change in response to alterations in the ion content of the external environment. Khan and Saleuddin (1981) reported that fewer septa are found in the kidney epithelium of the snail *Helisoma* when it is in a hyposmotic medium, where maximum transepithelial fluid transport is expected. In contrast, in an isosmotic medium, when transepithelial fluid transport should be minimal, many densely arranged septa are found (Khan and Saleuddin 1981). In addition, Khan and Saleuddin (1981) also reported that SJs containing fewer septa always show wide intercellular spaces, and junctions containing many septa are always associated with greatly reduced intercellular spaces. The existence and variation of intercellular spaces as a function of hemolymph osmolality has also been reported for the terrestrial slug foot epithelium which displays a rapid paracellular water uptake when a dehydrated animal is in contact with a moist surface (Prior and Uglem 1984; Uglem et al. 1985). Along with water, the paracellular movement of nonelectrolytes mannitol (182 Da) and inulin (5200 Da) is seen (Uglem et al. 1985). In the intestine of the sea slug *Aplysia juliana*, a low resistance (20 Ohm cm^2) paracellular pathway constitutes the major transport route for both Na^+ and Cl^- (Gerencser 1982). Studies on ion regulation in freshwater bivalve molluscs have suggested higher tolerance to osmotic challenges in species with gill epithelia that exhibit lower paracellular permeability to ions and solutes (Dietz et al. 1995; Zheng and Dietz 1998). Finally, it has been pointed out that the paracellular

pathway of *Anodonta cygnea* outer mantle epithelium, which is believed to be involved in the shell formation, presents a dynamic functionality with respect to Ca^{2+} transport (Coimbra and Machado 1988; Bleher and Machado 2004). Ca^{2+} may diffuse paracellularly from the hemolymph towards the extrapallial fluid and vice versa across the SJs in the outer mantle epithelium, depending on the range of Ca^{2+} concentrations in the fluids (Bleher and Machado 2004).

Studies on molluscs have revealed the dynamic nature of the pSJ of this group as it relates to alterations in the solute permeability of molluscan epithelia. A major area requiring attention is the molecular characterization of molluscan pSJs. Surprisingly it would appear that nothing is known about the molecular architecture of this structure which presents a major limitation, but also an open field for future work. That said, quite a lot is now known about the molecular biology of the arthropod pSJ, which is structurally similar (or structurally the same). So a first question might relate to how closely does the molecular architecture of the molluscan pSJ resemble the pSJ of arthropods? In many ways the paucity of information on SJs in this highly diverse, economically and medically important group (despite strong evidence to support a central role for the structure in molluscan homeostasis), encapsulates the notion that SJs and the role that they play in the physiology of invertebrates is an area that would greatly benefit from any attention. Indeed, molluscan diversity is so great that there are many areas within which future work on pSJs and their protein composite would be of considerable interest. Two in particular are what role pSJs proteins play in shell formation of molluscs and how pSJ proteins assist in the regulation of diverse molluscan gill function.

3.3.5 Phylum Annelida

The Phylum Annelida is a modest sized group of animals at ~ 15 000 species. These can be divided into three major groups, the largest is the polychaetes, while the most recognizable are

the oligochaetes (e.g. earthworms) and the hirudinea (i.e. leeches). A major characteristic of annelids is the arrangement of their body into numerous largely repetitive compartments or segments which share a common morphological structure (Westheide 1997; Purschke 2002). Each segment contains two coelomic cavities separated by a mesentery and septa at the posterior and anterior ends. In addition, each segment also contains two metanephridia or protonephridia for excretion (Bartolomaeus and Quast 2005; Bartolomaeus et al. 2005). Segments of many annelids also possess epidermal-derived articulations named chaetae, and in the case of polychaetes, lateral appendages called parapodia (Purschke 2002). Many annelids are marine and are typically benthic and/or tube dwelling but freshwater and terrestrial species also exist and have been the subject of physiological studies relevant to epithelial permeability (McHugh 2000). As in epithelia of platyhelminthes, junctions sealing the epithelia of annelids are of the lower invertebrate pleated SJ type (Fig. 3-3). This type of SJ in the annelid epithelial tissue was first reported by Baskin (1976) in the epidermis of polychaetes *Nereis* and *Cirriformia* and was later observed in the epidermis and gut endoderm of other polychaetes as well as oligochaetes (Welsch and Buchheim 1977; Bilbaut 1980; Green 1981a). Well-developed SJs are also found in the body wall epithelium of the leech (*Batracobdella picta*, Desser and Weller 1977) and a photoreceptor epithelium of *Hirudo medicinalis* (1998).

Investigation of salt homeostasis and transepithelial ion transport in annelids has provided some insight into SJ permeability of these animals. Studies conducted *in vitro* on the integument of the terrestrial oligochaete *Lumbricus* and a freshwater leech *Hirudo medicinalis*, report a very high junctional resistance in these epithelia (Schnizler et al. 2002; Krumm et al. 2005). This may not be suprising as both organisms cope with a similar problem of obligatory ion loss to the surrounding environment and in most animals that face this kind of problem, it is solved in part, by the presence of an electrically tight epithelium at the interface with the

environment. It has also been observed that paracellular Na^+ transport occurs in association with primary urine formation by the nephridial epithelium of *H. medicinalis* and any increase in fluid secretion, such as following a blood meal, requires an upregulation of junctional Na^+ transfer (Zerbst-Boroffka et al. 1997). Furthermore, the epidermis of the brackish water polychaete *Nereis diversicolor* exhibits paracellular mannitol permeability of the same order of magnitude as that reported for tight epithelia such as frog skin and toad urinary bladder (Gomme 1981), suggesting that solute movement across this tissue is tightly regulated.

Similar to many other groups of invertebrates, nothing is known about the molecular architecture of annelid SJs. As such, this area will require attention. For the most part, ultrastructural studies of annelid SJs have been performed on marine species while functional studies on the paracellular permeability of annelid epithelia have been largely performed on freshwater species. Therefore, future work could bridge these approaches using either marine or freshwater species to gain a broader understanding of annelid SJ structure and function. In addition to this, it is tempting to suggest that the homonomous metameric bauplan of many annelids is a hallmark of this group that could be exploited for mechanistic studies on the role of lower invertebrate SJs in metamere and systemic homeostasis. In addition, because the lower invertebrate pSJ appears in both annelids as well as platyhelminthes, it would be very interesting to compare the protein composition of the structure in these two groups both generally as well as in specific tissues such as the nephridia.

3.3.6 Phylum Arthropoda

The phylum Arthropoda includes such animals as insects, crabs, lobsters, shrimp, crayfish, isopods, water fleas, sea spiders, barnacles, copepods, spiders, mites, ticks, scorpions, centipedes and millipedes and more. The Arthropods make up the largest, most successful and arguably most diverse group of animals on the planet. There are ~ 1.2 million identified extant species

with another ~ 100 000 extinct species that are known from the fossil record; however, it is recognized that a great deal of species have yet to be discovered (Giribet and Edgecombe 2013). This vast group is organized into four major lineages which are sometimes referred to as subphyla, the Euchelicerata (spiders, ticks, scorpions, horseshoe crabs); Pycnogonida (sea spiders); Myriapoda (centipedes, millipedes); and Tetraconata or Pancrustacea (crabs, lobsters, shrimp, crayfish, water fleas, insects) (Giribet and Edgecombe 2013; Legg et al. 2013). The members of Pancrustacea alone make up ~ 1.1 million of the ~1.2 million identified species of arthropods with members of the class Hexapoda (insects) making up over 1 million of these species. The diversity of the arthropods is reflected in the environments that they inhabit. Arthropods are found in virtually every habitat on the planet, from deep sea hydrothermal vents, marine, brackish, and freshwater aquatic habitats, throughout terrestrial habitats and some are parasitic on other organisms (Wolff 2005; Morris 2011; Ma et al. 2014).

The diversity of arthropods is also evident in the number of specialized epithelia that they possess. The outer epidermis (or hypodermis) is highly specialized for secreting the chitinous arthropod exoskeleton (or cuticle), transferring calcium to the exoskeleton in crustaceans, synthesizing and releasing apolytic enzymes which degrade the old cuticle during moulting, and synthesizing as well as releasing a protein named Knickkopf which protects and organizes chitin of the newly secreted exoskeleton from apolytic enzymes during moulting (Halcrow 1976; Suderman et al. 2003; Elias-Neto et al. 2009; Chaudhari et al. 2011). Various arthropod gill epithelia have evolved like those found in the gills of crabs, shrimp and crayfish (Freire et al. 2008), the anal papillae (gills) of Dipteran insect larvae (Credland 1976; Nguyen and Donini 2010; Del Duca et al. 2011) and the various gut segments and Malpighian tubules of insects (Phillips et al. 1998; Shanbhag and Tripathi 2009; Vanderveken and O'Donnell 2014; Kumar 2013). In addition, there are examples of specialized tissues that function similar to the

gills in crustaceans that do not possess this organ (Aladin and Potts 1995; Johnson et al. 2014). All these epithelia are involved in solute transport functions such as salt uptake or removal, nutrient uptake and ammonia excretion and therefore these epithelia play a key role in homeostasis.

In the epithelia of arthropods, two types of SJs have been described (Table 3-1; Fig. 3-4). The most common one is the arthropod pleated SJ (pSJ, Fig. 3-4a), which is also found in molluscs and is very similar to the lower invertebrate pSJ (Locke 1965; Green 1981a). The other type has been named the smooth SJ (sSJ) because the septa appear as linear bands without periodic pleats as seen in pSJs (Flower and Filshie, 1975; Noirot-Timothee and Noirot 1980; Green et al. 1983; Dallai et al. 1990; Xué and Dallai 1992; Fig. 3-4b). Another characteristic feature of arthropod sSJs is the strict parallelism of the two adjacent membranes, in contrast to sometimes scalloped appearance observed in the pSJs (Noirot-Timothee and Noirot 1980). In tangential sections the septa of sSJs appear as linear bands, parallel sided and 5-10 nm wide (Fig. 3-4b). The disposition and course of the septa are variable, sometimes in the same junction, where they can be regularly parallel or become highly curved and form loops of various configurations (Juberthie-Jupeu 1979; Skaer et al. 1979). Some variations in the arthropod sSJs occur such as those seen in the midgut and hepatic caeca of the merostomatan horseshoe crab *Limulus* and the midgut of the sea spider (Lane and Harrison 1978; Green 1981b).

Arthropod pSJs are generally observed in epithelia of ectodermal origin such as the epidermis, foregut, hindgut, trachea, salivary gland, arachnid silk and venum gland, crayfish antennal (green) gland and crustacean gills (Table 3-1; Locke 1965; Bullivant and Loewenstein 1968; Caveney and Podgorski 1975; Shivers and Chauvin 1977; Noirot-Timothee et al. 1978; Green 1981a; Finol and Croghan 1983; Kukulies and Komnick H 1983; Flower 1986; Luquet et al. 1997; Luquet et al. 2002). The pSJs have also been observed between insect epithelial cells in

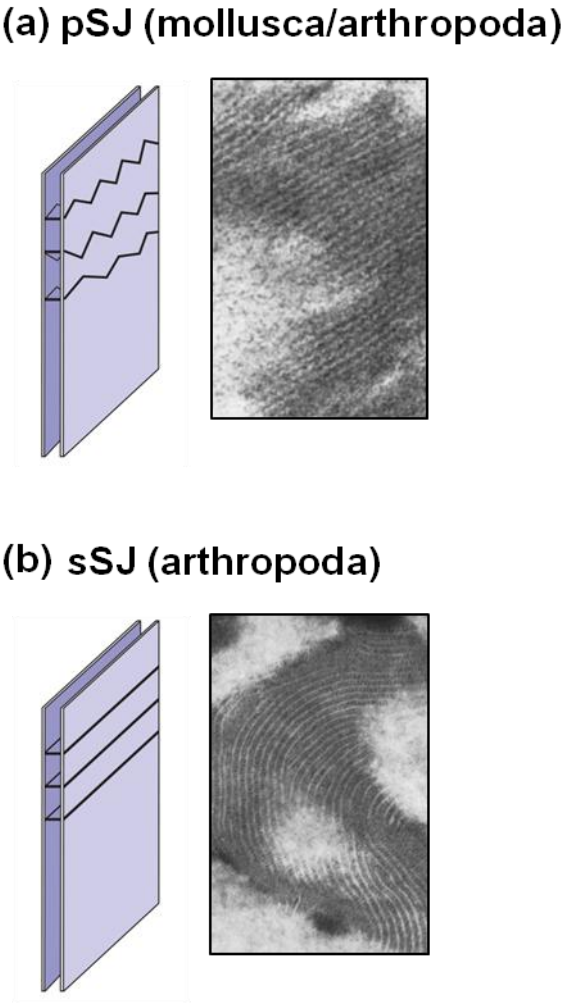

Figure 3-4: Schematic representation and electron microscopic (EM) images of (**a**) pleated septate junctions (pSJs) characteristic of molluscs and arthropods and, (**b**) smooth SJs (sSJs) which can be found in arthropods. The epithelia of molluscs possess a pSJ in which the septa are 2-3 nm wide, pleated and run parallel in extensive arrays when viewed tangentially. A pSJ of identical structure is also present in the ectodermal epithelia of arthropods. The endodermal epithelia of arthropods display sSJs, which have septa as linear bands, parallel sided and 5-10 nm wide. Electron microscopic images reprinted from (**a**) Green (1981a), Copyright (2015), with permission from Elsevier; (**b**) Flower and Filshie (1975), Copyright (2015), with permission from The Company of Biologists Ltd.

culture (Epstein and Gilula 1977; Reise Sousa et al. 1993). This junction is often distributed all along the paracellular space, from just basal to the adherens junction to the basolateral surface. Arthropod sSJs are found in tissues of endodermal origin such as the midgut, hepatic caecum and hepatopancreas of hexapods, crustaceans, myriopods, arachnids and sea spiders as well as in insect Malpighian tubules (Table 1; Hudspeth and Revel 1971; Dallai 1975; Flower and Filshie 1975; Dallai 1976; Juberthie-Jupeu 1979; Skaer et al. 1979; Lane and Skaer 1980; Noirot-Timothee and Noirot 1980; Green et al. 1980; Green 1981b, Graf et al. 1982; Green et al. 1983; Flower 1986; Dallai et al. 1990; Kachar et al. 1986; Skaer et al. 1987; Lane and Dilworth 1989; Xué and Dallai 1992; Jarial and Kelly-Worden 2011).

Despite an extensive literature on the morphological features, biological significance and permeability properties of the two types of SJs in arthropods are still not well understood largely because of a paucity of information on their functional physiology. It has been shown by Loewenstein and Kanno (1964) that pSJs in the epithelium of *Drosophila* salivary gland provide an important electrical resistance to the flow of ions between the lumen and the exterior of this tissue. On the other hand, studies on the Malpighian tubules of the insect *Rhodnius prolixus* have demonstrated that SJs of this epithelium are readily permeable to a variety of substances, such as inulin (~7000 Da), sucrose (342 Da) and polyethylene glycol (PEG; 4000 Da), suggesting a low resistance pathway for molecular flow through sSJs (O'Donnell et al. 1984; Skaer et al. 1987). A significant permeation of sSJs by a molecule as large as inulin (~5000 Da) was also observed in the gut of *Schistocerca gregaria* (Zhu et al. 2001). Similarly, low resistance sSJs (28.2 ± 2.1 Ωcm^2) have been demonstrated in the isolated midgut epithelium of *Bombyx mori* larvae (Fiandra et al. 2006). However, the latter junctions appear to be lined by fixed negative charges and display a high selectivity with respect to the size and the charge of permeating ions (Fiandra et al. 2006). Considerably greater paracellular permeability for K^+ than that for either Na^+ or Cl^- has

been demonstrated in the midgut of FW prawn *Macrobrachium rosenbergii* (Ahearn 1980) and SJs that represent a passive transport pathway for the secretion of Cl^- but not cations are characteristic of mosquito *Aedes aegypti* Malpighian tubules (Yu and Beyenbach 2001; Beyenbach and Piermarini 2011).

In addition to knowing very little about the barrier physiology of arthropod pSJs and sSJs, there is scant knowledge on how these junctions are regulated in different epithelia and/or in response to changes in environmental conditions. Pannabecker et al. (1993) demonstrated that sSJs of isolated perfused Malpighian tubules of *A. aegypti* can be modulated by a diuretic hormone leucokinin-VIII which increased paracellular Cl^- conductance in tubules in association with blood-meal initiated diuresis. Further investigations on the mode of action of leucokinin-VIII in *A. aegypti* Malpighian tubules revealed that the neuropeptide activates a signal transduction pathway which involves changes in intracellular Ca^{2+} concentration (Yu and Beyenbach 2002). It has been recently reported that in *B. mori* midgut, an increase in intracellular Ca^{2+} concentration induces a reduction in the electrical resistance of the paracellular pathway and enhances the permeability of SJs to sucrose (Fiandra et al. 2006). An increase in the paracellular permeability of the salivary gland epithelium through the modulation of intracellular Ca^{2+} has been suggested for the neurohormone serotonin-induced salivary secretion in blowfly (*Phormia regina*) (O'Doherty and Stark 1981). Lastly, salinity-induced changes in the morphology of pSJs have been reported for the gill epithelium of euryhaline crabs (Luquet et al. 1997; Luquet et al. 2002). In low-salinity acclimated crabs, the pSJs between the gill ionocytes are long, highly-developed and have numerous, closely packed septa (Luquet et al. 1997; Luquet et al. 2002). At higher salinities, the SJs of the crab gill epithelium become significantly shorter and confined to the apical region of the ionocytes, suggesting an increase in junctional permeability under high salinity conditions (Luquet et al. 1997; Luquet et al. 2002).

Although our general understanding of SJ molecular structure, regulation and function is still in its infancy, the majority of our knowledge stems from work on arthropod SJs. As a result, continuing work on arthropods is likely to have the most profound impact in terms of advancing our knowledge of invertebrate occluding junction physiology. A major hallmark of arthopods, the exoskeleton, involves the secretion of cuticle by the epidermis and moulting involves secretion of apolytic fluid that serves to digest components of the old cuticle. These processes occur at a relatively rapid rate and entail significant reorganization of the epidermis (see Elias-Neto et al. 2009) which can be expected to include the epidermal SJs. A comprehensive study of epidermal junctions during the moulting process at the molecular, structural and functional level would be of particular interest. Given that the majority of molecular information on SJs is from arthropods, these studies could provide extensive understanding on how SJs regulate epithelial integrity.

3.3.7 Phylum Echinodermata

The phylum Echinodermata (e.g. sea stars, brittle stars, sea urchins, sea cucumbers, sea lillies) is a group of marine animals with adult body plans that exhibit pentaradial symmetry. Additional hallmarks of this invertebrate phylum include a water vascular system (WVS), calcified endoskeletal plates/ossicles/spines, pedicellariae and dermal branchiae. Echinoderms do not appear to possess specialized tissues or organs for osmoregulation or excretion and internal fluids are generally isosmotic to their external marine habitat (Lange 1964; Herrera et al. 1981). In this regard, ion and water movement between seawater and internal body fluids occur via the WVS, the dermal branchiae and in Holothuroids (sea cucumbers), paired diverticula of the posterior gastrointenstinal tract refered to as the respiratory tree. The WVS is a series of internal canals which terminate in blind ended tube feet that are pressurized by the WVS fluid. This serves as a hydraulic system primarily for locomotion (Prusch 1977; Ferguson 1989). The WVS has a single opening to the exterior termed the madreporite and there is evidence that seawater enters the

madreporite to aid in maintaining internal fluid levels (Ferguson 1989). There is also evidence that the epithelium at the terminal tube feet of the WVS transports K^+ into the tube foot lumen which may create an osmotic gradient for water uptake (Prusch 1977). The tube feet are also sites of ammonia excretion along with the dermal branchiae (Khanna and Yadav 2005). Dermal branchiae are ciliated epithelia that directly interface with surrounding seawater and the cilia create a water flow across its surface that is countercurrent to the movement of internal (coelomic) fluid which is driven by underlying peritoneal tissue (Khanna and Yadav 2005). The countercurrent creates diffusional gradients that support metabolic waste excretion and oxygen uptake (Khanna and Yadav 2005). In sea cucumbers the epithelia of the respiratory tree are important for exchanging solutes and gases with the environment (Dolmatov et al. 2011). Seawater enters and exits the respiratory tree via the anus and cloaca driven by muscular expansion and contraction of the cloacal region.

In the ectodermal epithelia of this phylum, such as the tube foot epithelium as well as the larval body wall epithelium, a double-septum SJ has been identified (Table 3-1; Fig. 3-5a), while in endodermal epithelia an anastomosing SJ is present (Table 3-1; Fig. 3-5b) (Green et al. 1979; Green 1981c; Spiegel and Howard 1983; Dan-Sohkawa et al. 1995; Itza and Mozingo 2005). In both cases, junctions have the 15-18 nm intercellular spacing common to all invertebrate SJs and both occur around the apical circumference of cells lining an outside or luminal side surface. Tangential views of the echinoderm double-septum SJ reveal the septa as relatively straight, unbranched but double structures with each half being typically 2-5 nm apart (Green 1981c; Spiegel and Howard 1983; Fig. 3-5a). The two halves can be touching or have a space between them up to 3 nm wide (Fig. 3-3a, arrows). There appears to be no correlation between the total septal width, the width of the two component halves of a septum, and the gap between these halves (Green 1981c). A lack of correlation between the latter factors gives the septa of the

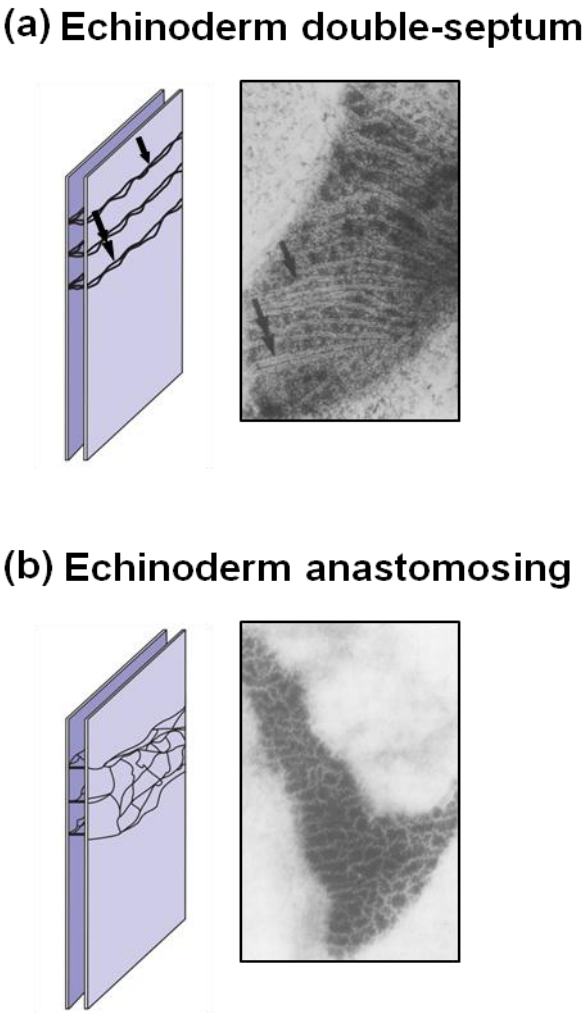

Figure 3-5: Schematic representation and electron microscopic (EM) images of (**a**) an echinoderm double-septum and (**b**) an echinoderm anastomosing septate junction (SJ). The echinoderm double-septum SJ is found in ectodermal tissues while the echinoderm anastomosing SJ is present in endodermal epithelia. In tangential section, the echinoderm double-septum SJ reveals septa as relatively straight, unbranched but double structures with the two halves touching (**a**, arrow) or being up to 3 nm apart (**a**, double arrow). The echinoderm anastomosing SJ shows an intricate network of semi-pleated 6-8 nm wide single septa (**b**). EM images reprinted from (**a**) Green (1981c), (**b**) Green et al. (1979), Copyright (2015), with permission from Elsevier.

echinoderm double-septum SJ an irregular appearance when compared to a double-septum SJ such as that found in the anthozoan gastrodermis (Green and Flower 1980; Green 1981c; see Fig. 3-2c). When seen in tangential view, the echinoderm anastomosing SJ shows an intricate network pattern similar to that of the vertebrate TJ (Green et al. 1979; Spiegel and Howard 1983; Fig. 3-5b). The anastomosing compartments are about 30-35 nm wide and are formed by 6-8 nm wide single septa which have a semi-pleated appearance with an irregular pleating periodicity (Green et al. 1979; Spiegel and Howard 1983). The echinoderm SJ extends basally to a depth of about one-third the length of the epithelial cell. The echinoderm anastomosing SJ has a wide occurrence in the endodermally derived epithelial tissues such as the pyloric caecum of the starfish, the stomach and intestine of the sea urchin, and the lining of the sea cucumber alimentary canal (Green et al. 1979; Spiegel and Howard 1983; Mashanov and Garcia-Arraras 2011).

Studies on the embryonic epithelia of echinoderms have demonstrated a strong link between the SJ structure and the ability of the epithelium to maintain a paracellular diffusion barrier. When treated with hypertonic seawater, starfish embryos exhibit simultaneous changes in SJ ultrastructure and body wall paracellular permeability (Dan-Sohkawa et al. 1995). In response to hypertonic stimuli, the SJs, which completely block the passage of cell membrane impermeable IgG under normal conditions, allow IgG to penetrate into the starfish embryo blastocoel and ultrastructural observations indicate that under these conditions septa are diffuse or disappear altogether (Dan-Sohkawa et al. 1995). Similarly, the cells of the body wall epithelium of the sea urchin embryo either lack or exhibit disorganized SJs when the paracellular permeability barrier is disrupted in response to divalent-cation-depleted seawater (Itza and Mozingo 2005). Additionally, intact SJs are reformed in embryos that exhibit a resumed paracellular barrier following recovery in normal seawater (Itza and Mozingo 2005). Lastly, and as mentioned before, the main function of the holothurian respiratory tree is gas and solute

exchange. In this regard it has been suggested that the presence of well-developed SJs in the epithelia of the respiratory tree is likely to prevent unregulated solute loss from coelemic fluid and the penetration of environmental water into the coelomic cavity (Dolmatov et al. 2011; Kamenev et al. 2013). This suggestion is supported by the observation that the osmolarity of coelomic fluid of a submerged holothurian is higher than that of the surrounding seawater (Vidolin et al. 2002).

Significant progress has been made in elucidating echinoderm SJ structure and function. With the sequencing of several echinoderm genomes including a brittle star, sea star, sea cucumber and at least two sea urchin species, it should be relatively straightforward to now focus on the molecular components of echinoderm SJs. In this regard it would be very interesting to compare the molecular composition of the two different types of SJ found in echindorems, to see whether these possess unique proteins that impart specific functional properties. Beyond this, the absence of distinct ionoregulatory or excretory organs and the stenohaline nature of echinoderms may appear to limit the tractability of these organisms as models for examining SJ physiology. However, echinoderms have proven to be incredibly useful models for understanding the ramifications of climate change and ocean acidification on marine invertebrates (e.g. Pespeni et al 2013). Therefore, opportunities may present themselves in this realm, as well as in the study of what role SJs might play in the physiology of the unique WVS.

3.4 Morphology and ultrastructuire of occluding junctions in other invertebrate phyla

3.4.1 Phylum Nematoda

Nematodes have been phylogenetically grouped with other ecdysozoans (molting animals), including arthropods (Aguinaldo et al. 1997), but the epithelia of these animals appear to lack junctions containing true septa. In the epidermis as well as the gut of the often-studied nematode *C. elegans*, only a single intercellular junction, referred to as the *C. elegans* apical junction (CeAJ), has been reported and it seems to execute both adhesive and barrier functions (Michaux 2001; Knust and Bossinger 2002; Armenti and Nance 2012). At the ultrastructural level, the CeAJ is positioned at the apicolateral membrane of adjacent cells and appears as an electron dense structure (Leung 1999; McMahon et al. 2001; Segbert et al. 2004). A detailed analysis of the pharyngeal epithelium has now identified a specialized cell-to-cell junctional region apical to the CeAJ that bears no resemblance to SJ structure (Asano et al. 2003).

There have been a few other ultrastructural studies of nematode epithelia, mainly intestine, and they have described the electron dense apical junctional region between the cells as being similar to the sSJs known from the insect midgut (Jamuar 1966; Bruce 1966; Burghardt 1980; Davidson 1983; Wright et al. 1985). Although the characteristic 15 nm spacing of adjacent plasma membranes is reported in some cases, such as between intestinal cells of *Ascaris*, no true septa are seen to span the intercellular cleft in cross sections (Bruce 1966; Burghardt 1980; Davidson 1983; Wright et al. 1985).

3.4.2 Phylum Chaetognatha

Studies on the intestine of a chaetognath *Sagitta setosa* have revealed the presence of a pSJ of the lower invertebrate pSJ type which coexists, in the same epithelium, with a paired SJ (Duvert et al. 1980; Duvert and Gros 1982). In tangential views of chaetognath pSJs, each septum is about 3nm thick and appears pleated with a periodicity of only 12 nm (compared to 16-23 nm in lower

invertebrate pSJ or mollusc-arthropod pSJ). The paired septa run in either a “loose” or “tight” formation. In the loose formation, the septa are more spaced and have rings or small segmental structures between them (Duvert et al. 1980). In the tight formation, which is less frequently seen than the loose formation, the septa run closely together in the pair with no other elements between them. Very infrequently, unpaired septa are seen associated with the tight formation of paired septa (Duvert et al. 1980).

3.4.3 Phylum Onychopora

The epithelia of Onychopora (velvet worms), of which *Peripatus* is best known, possess the SJs of smooth and pleated type found in Arthropoda (Wright and Luke 1989; Lane et al. 1994). Similar to the occurence of sSJs mainly in the endodermal epithelia in the arthropods, only the midgut of *Peripatus* has what appear to be characteristic sSJs. Junctions in the rest of the epithelial tissues studied, i.e. epidermis, mucous and salivary glands, rectum, renal organ, and testis, exhibit the characteristic features of molluscan-arthropod pSJs (Lane et al. 1994).

Table 3-1: Type and occurrence of occluding junctions in invertebrate phyla.

Phylum	Junction Type	Tissue	Reference
Porifera	Parallel membrane	Pinacoderm	Bagby 1970 Green & Bergquist 1979 Lethias et al. 1983 Pavans de Ceccatty 1986 Adams et al. 2010
	Septa-containing junction	Choanoderm, sclerocytes, larval epithelium, trabecular syncytium, archaeocytes and collar units of choanoblasts	Green & Bergquist 1979 Ledger 1975 Boury-Esnault et al. 2003 Maldonado & Riesgo 2008 Mackie & Singla 1983
Cnidaria	Hydroid SJ	Epidermis, gastrodermis	Wood 1959 Overton 1963 Danilova et al. 1972 Hand & Gobel 1972 Filshie & Flower 1977 Leik & Kelly 1970
	Anthozoan SJ	Epidermis, outer surface of the tentacle	Green & Flower 1980 Green & Bergquist 1982
	Anthozoan double-septum	Gastrodermis, inner lining of tentacle, mesenteric myoepithelium	Green & Flower 1980 Green & Bergquist 1982 Holley 1985
Platyhelminthes	Lower invertebrate pSJ	Epidermis, gastrodermis, uterine epithelium, protonephridial duct epithelium	Green 1981a Hori 1987 Poddubnaya et al. 2011, 2012
Annelida	Lower invertebrate pSJ	Epidermis, gut endoderm, leech photoreceptor epithelium	Baskin 1976 Green 1981a Aschenbrenner & Walz 1998

Table 3-1 (cont.): Type and occurrence of occluding junctions in invertebrate phyla.

Phylum	Junction Type	Tissue	Reference
Nematoda	Apical junction	Epidermis, pharynx, intestine, gonad/uterus	Leung 1999 McMahon et al. 2001 Segbert et al 2004 Michaux 2001
Mollusca	Pleated SJ (pSJ)	Epidermis, gill epithelium, digestive gland, caecum, digestive duct appendages, salivary gland, intestine, genital duct, mantle, snail kidney & egg capsule gland epithelium, cephalopod tentacle epithelium, slug foot epithelium, squid embryo	Bairati & Gioria 2008 Gilula et al. 1970 Porvaznik et al. 1979 Green 1981a Giusti 1976 Boucaud-Camou 1980 Newell & Skelding 1973 Khan & Saleuddin 1981 Flower 1971 Bleher & Machado 2004 Albrecht & Cavicchia 2001 Prior & Uglem 1984 Ginzberg et al. 1985
Arthropoda	Pleated SJ (pSJ)	Epidermis, salivary gland, trachea, foregut, hindgut, gill epithelium, crayfish, antenal gland, arachnid silk & venom gland	Locke 1965 Bullivant & Loewenstein 1968 Green 1981a Noirot-Timothee et al. 1978 Finol & Croghan 1983 Flowers 1986 Shivers & Chauvin 1977
	Smooth SJ (sSJ) (some variations exist)	Midgut, proventriculus, hepatic caecum, hepatopancreas, insect Malpighian tubules	Flowers & Filshie 1975 Juberthie-Jupeu 1979 Hudspeth & Revel 1971 Dallai 1975 Noirot-Timothee & Noirot 1980 Green et al. 1983 Lane & Harrison 1978 Skaer et al. 1987

Table 3-1 (cont.): Type and occurrence of occluding junctions in invertebrate phyla.

Phylum	Junction Type	Tissue	Reference
Chaetognatha	Chaetognath double septum SJ	Intestine	Duvert et al. 1980 Duvert & Gros 1982
	pSJ	Intestine	
Echinodermata	Echinoderm double-septum SJ	Tube foot epithelium, larval sea urchin body wall epithelium	Green 1981c Spiegel & Howard 1983
	Echinderm anastomosing SJ	Pyloric caecum, stomach, intestine	Green et al. 1979 Spiegel & Howard 1983

3.5 Proteins of invertebrate occluding junctions

Although the ultrastructure of occluding junctions in the epithelia of invertebrates is well characterized and has been known for some time, a working knowledge of the molecular components involved in establishing and regulating invertebrate occluding junction structure and function is very much in its infancy. In this regard, the molecular physiology of invertebrate occluding junctions is only known to any extent in select model organisms such as *Drosophila* and *C. elegans*. However, more recently comparative analysis of the genes known to be involved in the formation of SJs and TJs has been carried out in general assessments of the genomes of *Hydra* and the demosponge *Amphimedon queenslandica*, the EST database of the homoscleromorph *Oscarella carmela* (Chapman et al. 2010; Fahey and Degnan 2010; Nichols et al. 2006), and by *in situ* hybridization experiments in demosponge *Suberites domuncula* (Adell et al. 2004). Nevertheless, there is a tremendous amount of ground to be covered in this area of epithelial transport physiology.

3.5.1 Putative occluding junction proteins of less derived invertebrates

Although the composition of sponge septate and parallel membrane junctions is not yet known, gene accounting of SJ components in sponges has identified a Nrx IV homolog in the homoscleromorph sponge *O. carmela* and demosponge *A. queenslandica* (Nichols et al. 2006; Fahey and Degnan 2010). Also found in *A. queenslandica* are homologs of genes encoding for claudin, Scrib and Dlg and the latter has been shown to be expressed at the mRNA level in *A. queenslandica* larval epithelium (Sakaraya et al. 2007). The presence of mRNA transcript encoding the MAGUK protein MAGI in both the surface exopinacoderm and in cells of the pinacoderm lining the canals has been demonstrated for the adult demosponge *S. domuncula* (Adell et al. 2004). *A. queenslandica* claudin gene ortholog aligns well with sequences from two other sponges as well as *Drosophila* (*kune* and *sinu*), *C. elegans* and human sequences (Fahey

and Degnan 2010; Leys and Riesgo 2012). Claudin, MAGUK and NrxIV orthologs are also found in the genomes from several classes of cnidarians (Chapman et al. 2010; Ganot et al. 2015). Moreover, a MAGUK protein ZO-1 homolog has been shown to localize to the apical plasma membrane of ectodermal epithelial cells in *Hydra vulgaris* (Fei et al. 2000) and in the scleractinian coral *Stylophora pistillata*, Nrx IV homolog co-localizes with the cortical actin network at the apical border of the calicoblastic (epidermal) epithelial cells where SJs occur (Ganot et al. 2015).

3.5.2 Occluding junction proteins of C. elegans

A combination of molecular and immunochemical data of *C. elegans* embryonic epithelial CeAJ suggests that despite its organization in electron micrographs as a single, electron-dense structure, the latter junction contains at least two distinct units that have the characteristics of the adherens junction and SJ/TJ of arthropods (*Drosophila*) and vertebrates. In addition to the single, electron-dense structure, a second junctional area located more apically was discovered between cells in the isthmus portion of the digestive tube (Asano et al. 2003). Thus far no proteins have been conclusively localized to the latter junctional area; however, many proteins have been localized to the CeAJ and these proteins are a combination of homologs of adherens junctional proteins and homologs of occluding junctional proteins. Since at this point it is unclear exactly how this unique CeAJ functions we will discuss each of the proteins that have been associated with CeAJ in this section on occluding junction proteins with the caveat that some of these proteins may in fact play no role in occlusion of the paracellular pathway.

Proteins that localize at the apical-most region of the CeAJ are the adherens junction proteins E-cadherin, β-catenin, α-catenin, and p120-catenin, encoded by *hmr-1*, *hmp-2*, *hmp-1*and *jac-1*, respectively (Costa et al. 1998; McMahon et al. 2001; Pettitt et al. 2003; Segbert et al. 2004), the claudin-like protein VAB-9 (Simske et al. 2003), ZOO-1, the *C. elegans* ortholog of

Table 3-2: Molecular components of occluding junctions and tissue location in invertebrates.

	Tissue location	Function	Reference
Putative Occluding Junction Proteins of Porifera			
MAGI in demosponge (*Suberites domuncula*)	Exopinacoderm, endopinacoderm	Not known	Adell et al. 2004
Dlg in demosponge (*Amphimedon queenslandica*)	Larval epithelium	Not known	Sakaraya et al. 2007
Putative Occluding Junction Proteins of Cnidaria			
ZO-1 (*Hydra vulgaris*)	Ectodermal epithelium	Not known	Fei et al. 2000
Nrx1V (*Stylophora pistillata*)	Calicodermis (epidermis)	Not known	Ganot et al. 2015
Proteins of Nematoda (*Caenorhabditis elegans*)			
HMR-1	Epidermis, pharynx, intestine	Epithelial morphogenesis	Costa et al. 1998 Segbert et al. 2004
HMP-2	Epidermis, pharynx, intestine	Epithelial morphogenesis	Costa et al. 1998 Segbert et al. 2004
HMP-1	Epidermis, pharynx, intestine	Epithelial morphogenesis	Costa et al. 1998 Segbert et al. 2004
AJM-1	Epidermis, pharynx, intestine, gonad/uterus	Junction formation/maintenance	Köppen et al. 2001
DLG-1	Epidermis, pharynx, intestine, gonad/uterus	Junction formation/maintenance, epithelial morphogenesis	McMahon et al. 2001

Table 3-2 (cont.): Molecular components of occluding junctions and tissue location in invertebrates.

	Tissue location	Function	Reference
Proteins of Nematoda (cont.) (*Caenorhabditis elegans*)			
LET-413	Epidermis, pharynx, intestine, gonad/uterus	Junction formation/maintenance, apicobasolateral polarity	Legous et al. 2006 McMahon et al. 2001
CLD-1	Pharynx	Barrier formation	Asano et al. 2003
CLD-2	Epidermis	Barrier formation	Asano et al. 2003
VAB-9	Epidermis, pharynx, intestine, gonad/uterus	Epithelial morphogenesis, junctional adhesion	Simske et al. 2003
ZOO-1	Epidermis	Epithelial morphogenesis, junctional adhesion	Lockwood et al. 2008
MAGI-1	Epidermis, pharynx, intestine	Junctional compartmentalization	Stetak & Hajnal 2011
JAC-1	Epidermis	Epithelial morphogenesis, junctional adhesion	Pettitt et al. 2003
SRGP-1	Epidermis, pharynx	Epithelial morphogenesis, junctional adhesion	Zaidel-Bar et al. 2010
Proteins of Arthropoda (*Drosophila melanogaster*) Transmembrane Proteins			
Megatrachea/Pickel	Epidermis, salivary gland, foregut, hindgut, trachea (pSJ)	Septa/barrier formation	Behr et al. 2003
Sinuous	Epidermis, salivary gland, foregut, hindgut, trachea (pSJ)	Septa/barrier formation, tracheal tube morphogenesis	Wu et al. 2004
Kune-kune	Epidermis, salivary gland, foregut, hindgut, trachea (pSJ)	Septa/barrier formation, tracheal tube morphogenesis	Nelson et al. 2010

Table 3-2 (cont.): Molecular components of occluding junctions and tissue location in invertebrates.

	Tissue location	Function	Reference
Proteins of Arthropoda (cont.) (*Drosophila melanogaster*) Transmembrane Proteins			
Neurexin IV	Epidermis, salivary gland, foregut, hindgut, trachea (pSJ)	Septa/barrier formation, tracheal tube morphogenesis	Baumgartner et al. 1996
Bark beetle/Anakonda	Epidermis, hindgut, midgut, trachea (pSJ, sSJ)	SJ maturation, epithelial cell adhesion, tracheal tube morphogenesis	Hildebrandt et al. 2015 Byri et al. 2015
Gliotactin	Epidermis, salivary gland, foregut, hindgut, midgut, trachea, imaginal disc epithelium (pSJ, sSJ)	Septa/barrier formation, epithelial cell adhesion	Schulte et al. 2003 Byri et al. 2015
Neuroglian	Epidermis, salivary gland, foregut, hindgut, trachea, imaginal disc epithelium (pSJ)	Septa/barrier formation	Genova & Fehon 2003
Na^+/K^+ATPase subunits α and β	Epidermis, salivary gland, foregut, hindgut, trachea, imaginal disc epithelium (pSJ)	Septa/barrier formation, tracheal tube morphogenesis	Genova & Fehon 2003 Paul et al. 2007
Lachesin	Epidermis, salivary gland, foregut, hindgut, trachea (pSJ)	SJ formation, tracheal tube morphogenesis	Llimargas et al. 2004
Contactin	Epidermis, salivary gland, foregut, hindgut, trachea (pSJ)	Septa/barrier formation	Faivre-Sarrailh et al. 2004
Fasciclin III	Salivary gland, midgut, hindgut, trachea, imaginal disc epithelium (pSJ, sSJ)	Septa formation	Woods et al. 1996 Woods et al. 1997 Wu et al. 2004 Izumi et al. 2012
Melanotransferrin	Epidermis, hindgut, trachea (pSJ)	Septa formation	Tiklová et al. 2010

Table 3-2 (cont.): Molecular components of occluding junctions and tissue location in invertebrates.

	Tissue location	Function	Reference
Proteins of Arthropoda (cont.) (*Drosophila melanogaster*) Transmembrane Proteins			
Macroglobulin complement-related	Epidermis, salivary gland, foregut, hindgut, trachea, imaginal disc epithelium (pSJ)	Septa/barrier formation, tracheal tube morphogenesis	Hall et al. 2014 Bätz et al. 2014
Mesh	Proventriculus, midgut, Malpighian tubules (sSJ)	Septa/barrier formation	Izumi et al. 2012
Snakeskin	Proventriculus, midgut, Malpighian tubules (sSJ)	Septa/barrier formation	Yanagihashi et al. 2012
Proteins of Arthropoda (*Drosophila melanogaster*) Cytosolic/Scaffolding Proteins			
Coracle	Epidermis, salivary gland, foregut, hindgut, trachea, imaginal disc epithelium (pSJ, sSJ)	Septa/barrier formation	Fehon et al. 1994 Lamb et al. 1998 Izumi et al. 2012
Scribble	Epidermis, salivary gland, foregut, hindgut, trachea, imaginal disc epithelium (pSJ)	Sepat/barrier formation, apicobasal polarity, epithelial growth control	Bilder et al. 2000 Bilder & Perrimon 2000
Lethal giant larvae	Epidermis, salivary gland, proventriculus, midgut, imaginal disc epithelium (pSJ, sSJ)	Apicobasal polarity, epithelial growth control	Strand et al. 1994 Bilder et al. 2000
Varicose	Epidermis, salivary gland, hindgut, trachea (pSJ)	Septa formation, ttracheal tube morphogenesis	Wu et al. 2007

Table 3-2 (cont.): Molecular components of occluding junctions and tissue location in invertebrates.

	Tissue location	Function	Reference
Proteins of Arthropoda (cont.) (*Drosophila melanogaster*) Cytosolic/Scaffolding Proteins			
Ly6 family proteins (Boudin, Crooked, Coiled, Crimpled)	Epidermis, salivary gland, foregut, hindgut, trachea, imaginal disc epithelium (pSJ)	Septa/barrier formation, tracheal tube morphogenesis	Hijazi et al. 2009 Nilton et al. 2010 Jaspers et al. 2012
Coracle	Epidermis, salivary gland, foregut, hindgut, trachea, imaginal disc epithelium (pSJ, sSJ)	Septa/barrier formation	Fehon et al. 1994 Lamb et al. 1998 Izumi et al. 2012

pSJ = arthropod pleated septate junction; sSJ = arthropod smooth septate junction
Proteins associated with the Nematoda apical junction have been listed, but in most cases occluding function has yet to be determined

the tight junction MAGUK protein ZO-1(Lockwood et al. 2008), and SRGP-1, the *C. elegans* ortholog of mammalian Slit-Robo GTPase activating protein (srGAP) (Zaidel-BAR et al. 2010). Proteins that are found in the more basal region of the CeAJ are DLG-1, the *C. elegans* homolog of the *Drosophila* Dlg (McMahon et al. 2001), and its binding partner AJM-1 (apical junction molecule), a large hydrophilic coiled-coil domain protein with no obvious orthologs in other species (Köppen et al. 2001), as well as proteins involved in membrane trafficking (*C. elegans* homologs of the F-BAR proteins of the TOCA family) (Giuliani et al. 2009). Besides these CeAJ components, the other known junctional proteins are LET-413, which encodes a homolog of the Drosophila Scrib and is associated with the basolateral membrane of epithelial cells (Legouis et al. 2000), and a recently identified protein MAGI-1, which is a homologue of the mammalian MAGUK MAGI-1 and localizes apical to both the adherens junction complex and DLG-1/AJM-1(Stetak and Hajnal 2011). Interestingly, a homolog of *Drosophila* SJ protein Lgl has been identified in *C. elegans* (*lgl-1*) and is shown to be expressed in the basolateral cortex of embryonic epithelia, where it contributes to polarity maintenance (Beatty et al. 2010; 2013).

Adherens junctions provide robust adhesion between epithelial cells to ensure tissue integrity and correct morphogenesis (Armenti and Nance 2012). However, the classical adherens junction components of the CeAJ (HMR-1, HMP-2 and HMP-1) are not essential for general cell adhesion in the *C. elegans* embryonic epithelia and instead mediate specific aspects of morphogenetic cell shape change and actin cytoskeletal organization (Costa et al. 1998). Inactivation of the basal CeAJ components DLG-1 or AJM-1 causes defects in the formation of the electron-dense structure that corresponds to the CeAJ. In *ajm-1* mutants, large paracellular gaps or vacuoles appear between the normally closely apposed sides of the junctional complex, suggesting that AJM-1 is required to maintain the tightness of the CeAJ electron dense domain (Köeppen et al. 2001). Loss of *dlg-1* activity leads to AJM-1 mislocalization and an almost

complete disappearance of the electron-dense structure of the CeAJ, suggesting that DLG-1 is required to aggregate AJM-1 and other proteins forming the CeAJ (McMahon et al. 2001; Segbert et al. 2004). It is not clear whether mutations in *hmr-1*, *hmp-2* and *hmp-1* are also defective since junctions in these mutants have not been examined by electron microscopy.

The primary function of LET-413 is to recruit CeAJ components at a subapical position. In the absence of LET-413, the electron-dense part of the CeAJ is either discontinuous or extends more basally which corresponds to the mislocalization of AJM-1, DLG-1 and HMP-1 along the lateral membrane of embryonic epithelial cells (Legouis et al. 2000; McMahon et al. 2001). LET-413 is also required for the maintenance of apicobasal polarity (McMahon et al. 2001). A novel junctional protein MAGI-1 appears to play an important regulatory role in segregating functional domains within the CeAJ as mutually exclusive localization of the adherens junction proteins and the DLG-1/AJM-1 is lost in the epithelia of *magi-1* mutants (Stetak and Hajnal 2011).

VAB-9, which is a four-pass transmembrane molecule similar to human brain cell membrane protein (BCMP1) of the PMP22/EMP/Claudin family of cell junction proteins, colocalizes with adherens junction proteins in the epithelial CeAJ and requires HMR-1 for its initial recruitment to the cell membrane and both HMP-1 and HMP-2 for maintaining its distribution at the CeAJ (Simske et al. 2003). Morphological defects in the epidermis due to the disorganization of actin filaments at the CeAJ are observed in *vab-9* mutant embryos (Simske et al. 2003). In addition, mutations in *vab-9* enhance cell adhesion defects in embryos lacking AJM-1 or DLG-1, suggesting that VAB-9 participates in the organization of actin cytoskeleton at the CeAJ and helps to maintain proper epithelial adhesion (Simske et al. 2003). Interestingly, VAB-9 is required for the junctional localization of ZOO-1 which also colocalizes with the adherens junction proteins at the CeAJ (Lockwood et al. 2008). Similar to *vab-9* mutations, *zoo-1* knockdown results in morphological defects in the epidermis with occasional rupturing and

reduced levels of actin at the CeAJ (Lockwood et al. 2008). Loss of ZOO-1 function does not enhance *vab-9* null mutant phenotypes, suggesting that ZOO-1 functions downstream of VAB-9 to mediate strong junctional anchorage to the actin cytoskeleton during epithelial morphogenesis in *C. elegans* (Lockwood et al. 2008).

In addition to VAB-9, five more claudin-like proteins, CLC-1 to -5, have been identified in *C. elegans* by virtue of sequence identity to mammalian claudins (Asano et al. 2003; Simske et al. 2011). Two of the latter five putative *C. elegans* claudins have been further analyzed to determine the extent of their function as classical claudins. CLC-1 is expressed mainly in the pharyngeal epithelial cells of adult worm intestine where it colocalizes with AJM-1 at the CeAJ whereas CLC-2 is found in the hypodermal seam cells (lateral hypodermis) (Asano et al. 2003). Following RNAi of *clc-1* or *clc-2*, it was shown that a 10 kDa dextran is able to infiltrate to the interior of the pharynx and body cavity for *clc-1* RNAi embryos and into the body cavity for *clc-2* RNAi embryos, suggesting that both of these claudin-like proteins play arole in maintaining epithelial barrier properties (Asano et al. 2003).

3.5.3 Identification of occluding junction proteins in Drosophila

More than twenty proteins that function in the establishment and/or maintenance of epithelial SJs have been identified in *Drosophila melanogaster* (Table 3-2). The availability of powerful genetic techniques to manipulate the expression of genes in *Drosophila* was coupled with observations of SJ formation in the developing embryonic tissues to identify many of these proteins. For example, specific genetic mutants resulting in disrupted septa in embryonic epidermal epithelia led to the discovery of proteins that are important in SJ development (Genova et al. 2003; Hildebrandt et al. 2015; Baumgartner et al. 1996). Furthermore, by coupling specific genetic mutation and/or RNAi mediated knockdown with permeability assays using either injection or ingestion of a fluorescently labelled paracellular marker verified the importance of

these proteins in paracellular barrier function (Schulte et al. 2003; Faivre-Sarrailh et al. 2004). Of these proteins, fifteen are transmembrane components of the SJ complex. These include three proteins from the claudin family, i.e. megatrachea/pickel (Mega), sinuous (Sinu) and kune-kune (Kune) (Behr et al. 2003; Wu et al. 2004; Nelson et al. 2010), protein macroglobulin complement-related (Mcr), a member of the conserved α-2-macroglobulin (α2M) complement protein family (Bätz et al. 2014; Hall et al. 2014), and cell adhesion molecules or CAMs such as neurexin IV (NrxIV) (Baumgartner et al. 1996), gliotactin (Gli) (Schulte et al. 2003), neuroglian (Nrg), the α and β subunits of the Na^+/K^+ ATPase (Atpα and Nrv2) (Genova and Fehon 2003; Paul et al. 2007), lachesin (Lac) (Llimargas et al. 2004), contactin (Cont) (Faivre-Sarrailh et al. 2004), fasciclin III (FasIII) (Woods et al. 1997), the GPI-linked iron binding protein melanotransferrin (MTf) (Tiklová et al. 2010), and the putative scavenger receptor-like protein Bark beetle (Bark)/Anakonda (Aka) (Hildebrandt et al. 2015; Byri et al. 2015).

Another set of proteins that are important for the formation of SJs in *Drosophila* reside on the cytoplasmic side of the membrane. This group includes scaffolding FERM-domain protein coracle (Cora) (Fehon et al. 1994; Lamb et al. 1998), multi-PDZ and leucine-rich repeat protein scribble (Scrib) (Bilder and Perrimon 2000), WD-40 repeat protein lethal giant larvae (Lgl) (Strand et al. 1994b; Bilder and Perrimon 2000), MAGUK family proteins varicose (Vari) (Wu et al. 2007) and discs large (Dlg) (Woods and Bryant 1991; Woods et al. 1996), several members of the Ly6 family of proteins (e.g. boudin, crooked, coiled and crimpled) (Hijazi et al. 2009; Nilton et al. 2010; Jaspers et al. 2012), proteins that function in endocytosis and recycling (e.g. Rab5 and Rab11, clathrin heavy chain and dynamin/shibire) (Tiklová et al. 2010; Jaspers et al. 2012), and a SJ gene transcription factor of the Grainy head (Grh) family (Narasimha et al. 2008). Except for Dlg, Lgl, FasIII, Cora, Gli and Bark/Aka, all of the aforementioned SJ proteins have been reported to be highly or exclusively expressed in ectodermally derived epithelia such as the

epidermis, foregut, hindgut, trachea and salivary gland, which suggests that they may be pSJ-specific proteins (Baumgartner et al. 1996; Behr et al. 2003; Faivre-Sarrailh et al. 2004; Genova and Fehon 2003; Llimargas et al. 2004; Wu et al. 2004; Wu et al. 2007; Nelson et al. 2010; Bätz et al. 2014). Two *Drosophila* sSJ-specific membrane proteins, mesh and snakeskin (Ssk), have recently been discovered and are shown to be restricted to sSJ-bearing endodermal epithelia (Yanagihashi et al. 2012; Izumi et al. 2012).

3.5.4 Functions of occluding junction proteins in Drosophila

Nrx, Nrg, Cont and Cora are homologs of the vertebrate proteins NCP1 (neurexin IV/Caspr/paranodin), neurofascin, contactin and erythrocyte Band 4.1 protein, respectively, which are molecular components of the paranodal junctions (PJs) between neurons and myelinated glial cells that possess ladder-like structures similar to those observed in SJs (Bhat 2003). *Drosophila* Scrib, Dlg and Lgl constitute a distinct subgroup of proteins required for initial epithelial cell polarization during early stages of embryogenesis before SJ development (Strand et al. 1994b; Woods et al. 1996; Bilder and Perrimon 2000; Tepass et al. 2001). The latter proteins are also involved in the regulation of cell growth as *Drosophila* tumor suppressors, a finding that highlights the importance of SJs for proper cell-cell communication during epithelial morphogenesis in addition to forming paracellular barriers (Bilder 2004). *Drosophila* Gli is a single-pass transmembrane protein that belongs to the protein family known as CLAMS (cholinesterase-like adhesion molecules) and to date, it is the only known protein to localize exclusively to occluding regions of tricellular contact between neighbouring invertebrate epithelial cells, or more specifically the tricellular junction (TCJ) (Schulte et al. 2003; Gilbert and Auld 2005; Schulte et al. 2006). Gli is necessary for TCJ and SJ development in *Drosophila* ectodermal epithelia as Gli null mutation results in paralysis and embryonic lethality due to disruption of the TCJ and failure of the SJ permeability barrier (Schulte et al. 2003). The

importance of Gli to the barrier function of the SJ was shown in embryonic salivary glands using a 10 kDa rhodamine-dextran conjugate injected into the embryonic hemocoel. The rhodamine-dextran dye did not enter the salivary gland lumen in wild type embryos but permeated into the salivary gland lumen of Gli mutant embryos (Schulte et al. 2003). In polarized epithelia, Gli is tightly regulated at the cell membrane via phosphorylation, endocytosis and degradation to control its levels and localization to the TCJ as well as cell survival (Padash-Barmchi et al. 2010). Overexpression of Gli in imaginal disc epithelia causes Gli to spread away from the TCJ into the SJ domain where its interaction with Dlg leads to Dlg downregulation, tissue overgrowth and apoptosis (Schulte et al. 2006; Padash-Barmchi et al. 2010; Padash-Barmchi et al. 2013). Interestingly, Dlg is found at both the bicellular SJ and the TCJ and Gli appears to be recruited to the TCJ by Dlg (Schulte et al. 2006). Lastly, a recently characterized SJ protein encoded by the gene CG3921 was studied by two groups in parallel, and has been named *Drosophila* Bark by one group (Hildebrandt et al. 2015) and Aka by the other group (Byri et al. 2015). Bark/Aka was previously identified as an interaction partner of Mega (Jaspers et al. 2012), and is required for the maturation but not the establishment of pSJs and for controlling epithelial cell adhesion within the SJ compartment (Hildebrandt et al. 2015). During early stages of development (embryonic stages 15 and 16) *bark/aka* mutant embryos establish morphologically normal SJs (Hildebrandt et al. 2015; Byri et al. 2015). Later in embryogenesis (stage 17), Bark/Aka mutants showed rudimentary septa formation between the tracheal and epidermal cells with only sporadic appearance of the characteristic ladder like structure of SJs (Hildebrandt et al. 2015; Byri et al. 2015). Furthermore, *bark/aka* lacking embryos show cell adhesion defects such as the detachment of lateral cell membranes and formation of large gaps between the epithelial cells in this later stage of embryogenesis (Hildebrandt et al. 2015). Bark/Aka was shown to co-localize with Gli at tricellular junctions in epithelia of wild type embryos; however in Bark/Aka mutant

embryos Gli was lost from the tricellular junctions and instead spread into the bicellular junctions of the epithelia (Byri et al. 2015). By examining the vertex of three cells in RNAi Bark/Aka knockdowns it was determined that Bark/Aka expression in all three cells is required for both Bark/Aka and Gli localization in the tricellular junction (Byri et al. 2015). In contrast to pSJs, few genetic and molecular analyses have been carried out on sSJs in arthropods. Several studies have described the isolation of sSJ-enriched membrane fractions from insect midgut and lobster hepatopancreas and have demonstrated protein bands within these fractions by SDS-PAGE, but these proteins have not been characterized further (Green et al. 1983; Lane and Dilworth 1989; Baldwin and Hakim 1999). The only characterized sSJ-specific proteins are *Drosophila* mesh and Ssk. Ssk is a protein with four membrane-spanning domains and appears to be conserved only within arthropod species (Yanagihashi et al. 2012) whereas mesh is a single-pass transmembrane protein with cell adhesion activity and has orthologs in other invertebrates such as *C. elegans* and sea urchin as well as mouse (Sugahara et al. 2007; Izumi et al. 2012). Both mesh and Ssk are localized exclusively in the epithelia of proventriculus, midgut and Malpighian tubules, where sSJs reside, and are required for the paracellular barrier function in *Drosophila* midgut (Izumi et al. 2012; Yanagihashi et al. 2012). In control first instar larvae fed 10 kDa dextran labelled with Alexa-Flour 555, the dye was restricted to the gut lumen; however, in similarly treated larvae under the influence of *mesh* RNAi, the dye also accumulated in the hemocoel (Izumi et al. 2012). Similar studies using TRITC labelled dextran revealed the same results when Ssk was knocked down (Yanagihashi et al. 2012). Complete lack of Ssk expression is embryonically lethal and results in defective sSJ formation accompanied by abnormal morphology of midgut epithelial cells while compromised mesh expression causes defects in the organization of sSJs and mislocalization of Ssk, Cora, Lgl and FasIII in the midgut (Izumi et al. 2012; Yanagihashi et al. 2012). The finding that Cora, Lgl, FasIII as well as Dlg are present at

the sSJs of *Drosophila* midgut suggests that the latter proteins are components of both arthropod pSJs and sSJs, although their functions at sSJs remain unknown (Izumi et al. 2012).

3.5.5 Structural organization of occluding junction proteins of Drosophila

Compared to how much has been learned about the individual components of *Drosophila* SJs, far less is known about how these components assemble and maintain such solid structures. Mutations in most of the genes encoding SJ proteins, including *mega*, *sinu*, *kune*, *mcr*, *nrxIV*, *gli*, *nrg*, *atpα*, *nrv2*, *lac*, *cont*, *cora*, *vari*, *mesh* and *ssk* result in a structural loss or reduction of septa in the junction, a functional disruption of paracellular barrier properties in the epithelia these proteins reside and dramatic mislocalization of all other SJ components, indicating a high degree of mutual interdependence between SJ proteins (Fehon et al. 1994; Baumgartner et al. 1996; Behr et al. 2003; Genova and Fehon 2003; Schulte et al. 2003; Faivre-Sarrailh et al. 2004; Llimargas et al. 2004; Wu et al. 2004; Wu et al. 2007; Nelson et al. 2010; Izumi et al. 2012; Bätz et al. 2014). The notion that the SJ is a large and highly crosslinked protein complex was first supported by Ward et al. (1998) who showed that Cora directly interacts with the cytoplasmic tail of NrxIV. In addition, several pSJ associated proteins as well as Mesh and Ssk have been shown to coimmunoprecipitate (Genova and Fehon, 2003; Faivre-Sarrailh et al., 2004; Izumi et al. 2012; Jaspers et al. 2012) and fluorescence recovery after photobleaching (FRAP) experiments have revealed that SJ components such as CAMs and scaffolds Cora and Vari form an immobile core complex at SJs midway through embryogenesis (Laval et al. 2008; Oshima and Fehon 2011). Mutations in any of these SJ genes increase the mobility of other SJ proteins, further demonstrating the highly stable and interdependent nature of the SJ complex. FRAP analyses by Oshima and Fehon (2011) further suggested that a stable SJ requires interactions of its components not only within the plane of the membrane but also between cells. Consistent with this idea, Genova and Fehon (2003) had previously reported that NrxIV is strongly reduced in

wing imaginal epithelial wild-type cells at the membrane in contact with cells mutant for *cora* and Hall et al. (2014) observed a substantial reduction in Mcr expression in many wild-type cells just at the membrane in contact with *Mcr* knock-down cells.

3.6 Perspectives

Studies performed in recent years have greatly increased our knowledge of the morphology and functional properties of occluding junctions in the epithelia of various invertebrates. It has become clear that the most prominent invertebrate occluding junctions are the SJs and that from a morphological standpoint a great variety of these exist. Ultrastructure and molecular data suggest that SJs are established in all Porifera and that in less derived invertebrate clades SJs are not a novelty of just one or a few select groups/species. Work conducted using model organisms such as *Drosophila* and *C. elegans* has greatly expanded our knowledge of the molecular components of SJs whose homologs are present in occluding junctions that lack morphological septa. Yet despite advances through a number of studies that have examined the permeability of invertebrate occluding junctions, we are still far from understanding how the diverse morphology and barrier function of these structures are integrated and modulated in different epithelia and under different physiological conditions. Further investigations on the molecular architecture and physiology of occluding junctions in invertebrate species will be an exciting avenue for exploration and will lead to a better understanding of the physiological functions of these structures as well as their evolution across invertebrate phyla. In addition to this and in a broader sense, work on the integrative physiology of metazoan occluding junctions is dominated by investigations using mammalian systems (see Günzel and Fromm 2012; Günzel and Yu 2013), although in chordates a growing number of studies are utilizing less derived vertebrates such as fishes (see Loh et al. 2004; Chasiotis et al. 2012; Baltzegar et al. 2013; Kolosov et al. 2013). Therefore, in order to gain a truly comprehensive understanding of the comparative physiology of metazoan occluding junctions, it is imperative to consider diverse animal phyla as well as the myriad of environmental and physiological circumstances that these organisms operate within.

3.7 References

Adams EDM, Goss GG, Leys SP (2010) Freshwater sponges have functional, sealing epithelia with high transepithelial resistance and negative transepithelial potential. PLoS One 5(11):e15040

Adell T, Gamulin V, Perović-Ottstadt S, Wiens M, Korzhev M, Müller IM, Müller WE (2004) Evolution of metazoan cell junction proteins: the scaffold protein MAGI and the transmembrane receptor tetraspanin in the demosponge *Suberites domuncula*. J Mol Evol 59(1):41-50

Aguinaldo AM, Turbeville JM, Linford LS, Rivera MC, Garey JR, Raff RA, Lake JA (1997) Evidence for a clade of nematodes, arthropods and other mo*ulting animals. Nat*ure 387:489-493

Ahearn GA (1980) Intestinal electrophysiology and transmural ion transport in freshwater prawns. Am J Physiol 239(1):C1-10

Aladin NV, Potts WTW (1995) Osmoregulatory capacity of the cladocera. J Comp Physiol B 164:671-683

Albrecht EA, Cavicchia JC (2001) Permeability barrier in the mantle epithelium lining the testis in the apple-snail *Pomacea canaliculata* (Gastropoda: Ampullariidae). Tissue Cell 33(2):148-153

Anderson JM, Van Itallie M (2009) Physiology and function of the tight junction. Cold Spring Harb Perspect Biol 1

Armenti ST, Nance J (2012) Adherens junctions in *C. elegans* embryonic morphogenesis. Subcell Biochem 60:279-299

Asano A, Asano K, Sasaki H, Furuse M, Tsukita S (2003) Claudins in *Caenorhabditis elegans*: their distribution and barrier function in the epithelium. Curr Biol 13:1042-1046

Aschenbrenner S, Walz B (1998) Pleated septate junctions in leech photoreceptors: ultrastructure, arrangement of septa, gate and fence function. Cell Tissue Res 293:253:269

Bagby RM (1970) The fine structure of pinacocytes in the marine sponge *Microciona prolifera* (Ellis and Solander). Z Zellforsch 105:579-594

Bairati A, Giora M (2008) An ultrastructural study of cell junctions and the cytoskeleton in epithelial cells of the molluscan integument. J Morphol 269(3):319-331

Baldwin KM, Hakim RS (1999) Evidence for high molecular weight proteins in arthropod gap and smooth septate junctions. Tissue Cell 31:195-201

Baltzegar DA, Reading BJ, Brune ES, Borski RJ (2013) Phylogenetic revision of the claudin gene family. Mar Genomics 11:17-26

Banerjee S, Sousa AD, Bhat MA (2006) Organization and function of septate junctions: an evolutionary perspective. Cell Biochem Biophys 46:65-77

Bartolomaeus T, Purschke G, Hausen H (2005) Polychaete phylogeny based on morphological data – a comparison of current attempts. Hydrobiol 535/536:341-356

Bartolomaeus T, Quast B (2005) Structure and development of nephridia in Annelida and related taxa. Hydrobiol 535/536:139-165

Baskin DG (1976) Fine structure of polychaete septate junctions. Cell Tissue Res 174:55-67

Bätz T, Förster D, Luschnig S (2014) The transmembrane protein Macroglobulin complement-related is essential for septate junction formation and epithelial barrier function in *Drosophila*. Development 141(4):899-908

Baumgartner S, Littleton JT, Broadie K, Bhat MA, Harbecke R, Lengyel JA, Chiquet-Ehrismann R, Prokop A, Bellen HJ (1996) A *Drosophila* neurexin is required for septate junction and blood-nerve barrier formation and function. Cell 87:1059-1068

Beatty A, Morton D, Kemphues K (2010) The *C. elegans* homolog of *Drosophila* Lethal giant larvae functions redundantly with PAR-2 to maintain polarity in the early embryo. Development 137:3995-4004

Beatty A, Morton DG, Kemphues K (2013) PAR-2, LGL-1 and the CDC-42 GAP CHIN-1 act in distinct pathways to maintain polarity in the *C. elegans* embryo. Development 140(9):2005-2014

Behr M, Riedel D, Schuh R (2003) The claudin-like Megatrachea is essential in septate junctions for the epithelial barrier function in *Drosophila*. Dev Cell 5:611-620

Bénazet-Tambutté S, Allemand D, Jaubert J (1996) Permeability of the oral epithelial layers in cnidarians. Mar Biol 126:43-53

Beyenbach KW, Piermarini PM (2011) Transcellular and paracellular pathways of transepithelial fluid secretion in Malpighian (renal) tubules of the yellow fever mosquito *Aedes aegypti*. Acta Physiol (Oxf) 202:387-407

Bhat MA (2003) Molecular organization of axo-glial junctions. Curr Opin Neurobiol 13(5):552-559

Bilbaut A (1980) Cell junctions in the excitable epithelium of bioluminescent scales on a polynoid worm: a freeze-fracture and electrophysiological study. J Cell Sci 41:341-368

Bilder D (2004) Epithelial polarity and proliferation control: links from the *Drosophila* neoplastic tumor suppressors. Genes Dev 18:1909-1925

Bilder D, Perrimon N (2000) Localization of apical epithelial determinants by the basolateral PDZ protein Scribble. Nature 403:676-680

Bilder D, Li M, Perrimon N (2000) Cooperative regulation of cell polarity and growth by *Drosophila* tumor suppressors. Science 289(5476):113-116

Bleher R, Machado J (2004) Paracellular pathway in the shell epithelium of *Anodonta cygnea*. J Exp Zool A Comp Exp Biol 301(5):419-27

Boucaud-Camou E (1980) Junctional structures in digestive epithelia of a cephalopod. Tissue Cell 12(2):395-404

Boury-Esnault N, Ereskovsky A, Bezac C, Tokina D (2003) Larval development in the Homoscleromorpha (Porifera, Demospongiae). Invertebr Biol 122:187-202

Brauer EB (1975) Osmoregulation in the fresh water sponge, *Spongilla lacustris*. J Exp Zool 192: 181-192

Brauer EB, McKanna JA (1978) Contractile vacuoles in cells of a fresh water sponge *Spongilla lacustris*. Cell Tissue Res 192:309-317

Brusca RC, Brusca GJ (1990) Invertebrates. 2nd ed. Sinauer Associates, Sunderland, USA

Bruce RG (1966) The fine structure of the intestine and hind gut of the larva of *Trichinella spiralis.* Parasitology 56:359-365

Bullivant S, Loewenstein WR (1968) Structure of coupled and uncoupled cell junctions. J Cell Biol 37:621-632

Burghardt RC (1980) Intercellular junctions and exocytosis in the vas deferens of *Ascaris*. J Ultrastruct Res 71(2):162-172

Byri S, Misra T, Syed ZA, Batz T, Shah J, Boril L, Glashauser J, Aegerter-Wilmsen T, Matzat T, Moussian B, Luschnig S (2015) The triple-repeat protein anaconda controls epithelial tricellular junction formation in *Drosophila*. Dev Cell 33:535-548

Campbell RD, Iniguez AR, Iniguez AJ, Martinez DE (2013) Hydra of Hawaii: phylogenetic relationships with contintental species. Hydrobiol 713(1):199-205

Caveney S, Podgorski C (1975) Intercellular communication in a positional field. Ultrastructural correlates and tracer analysis of communication between insect epidermal cells. Tissue Cell 7(3):559-574

Cereijido M, Contreras RG, Shoshani L (2004) Cell adhesion, polarity, and epithelia in the dawn of metazoans. Physiol Rev 84:1229-1262

Chaparro OR, Montiel YA, Segura CJ, Cubillos VM, Thompson RJ, Navarro JM (2008) The effect of salinity on clearance rate in the suspension-feeding estuarine gastropod *Crepipatella dilatata* under natural and controlled conditions. Estuar Coast Shelf S 76:861-868

Chapman JA, Kirkness EF, Simakov O, Hampson SE, Mitros T, Weinmaier T, Rattei T, Balasubramanian PG, Borman J, Busam D, Disbennett K, Pfannkoch C, Sumin N, Sutton GG, Viswanathan LD, Walenz B, Goodstein DM, Hellsten U, Kawashima T, Prochnik SE, Putnam NH, Shu S, Blumberg B, Dana CE, Gee L, Kibler DF, Law L, Lindgens D, Martinez DE, Peng J, Wigge PA, Bertulat B, Guder C, Nakamura Y, Ozbek S, Watanabe H, Khalturin K, Hemmrich G, Franke A, Augustin R, Fraune S, Hayakawa E, Hayakawa S, Hirose M, Hwang JS, Ikeo K, Nishimiya-Fujisawa C, Ogura A, Takahashi T, Steinmetz PRH, Zhang X, Aufschnaiter R, Eder M-K, Gorny A-K, Salvenmoser W, Heimberg AM, Wheeler BM, Peterson KJ, Bottger A, Tischler P, Wolf A, Gojobori T, Remington KA, Strausberg RL, Venter JC, Technau U, Hobmayer B, Bosch TCG, Holstein TW, Fujisawa T, Bode HR, David CN, Rokhsar DS, Steele RE (2010) The dynamic genome of *Hydra*. Nature 464:592-596

Chasiotis H, Kolosov D, Bui P, Kelly SP (2012) Tight junctions, tight junction proteins and paracellular permeability across the gill epithelium of fishes: a review. Resp Physiol Neurobiol 184:269-281

Chaudhari SS, Arakane Y, Specht CA, Moussian B, Boyle DL, Park Y, Kramer K.J, Beeman RW, Muthukrishnan S (2011) Knickkopf protein protects and organizes chitin in the newly synthesized insect exoskeleton. PNAS 108(41):17028-17033

Coimbra J, Machado J (1988) Electrophysiology of the mantle of *Anodonta cygnea*. J Exp Biol 140:65-88

Credland PF (1976) A structural study of the anal papillae of the midge *Chironomus riparius* Miegen (Diptera: Chironomidae). Cell Tissue Res 166(4):531-540

Dallai (1975) Continuous and gap junction in the midgut of Collembola as revealed by lanthanum tracer and freeze-etching techniques. J Submicr Cytol 7:249-257

Dallai R (1976) Septate and continuous junctions associated in the same epithelium. J Submicr Cytol 8: 163-174

Dallai R, Bigliardi E, Lane NJ (1990) Intercellular junctions in myriapods. Tissue Cell 22(3): 359-369

Danilova LV, Rokhlenko KD, Bodryagina AV (1969) Electron microscopic study on the structure of septate and comb desmosomes. Z Zellforsch Mikrosk Anat 100(1):101-117

Dan-Sohkawa M, Kaneko H, Noda K (1995) Paracellular, transepithelial permeation of macromolecules in the body wall epithelium of starfish embryos. J Exp Zool 271:264-272

Davidson LA (1983) A freeze fracture and thin section study of intestinal cell membranes and intercellular junctions of a nematode, *Ascaris*. Tissue Cell 15(1):27-37

Del Duca O, Nasirian A, Galperin V, Donini A (2011) Pharmacological characterisation of apical Na^+ and Cl^- transport mechanisms of the anal papillae in the larval mosquito, *Aedes aegypti*. J Exp Biol 214:3992-3999

Desser SS, Weller I (1977) Ultrastructural observations on the body wall of the leech, *Batracobdella picta*. Tissue Cell 9(1):35-42

Dietz TH, Byrne RA, Lynn JW, Silverman H (1995) Paracellular solute uptake by the freshwater zebra mussel *Dreissena polymorpha*. Am J Physiol 269:R300-R307

Dolmatov IY, Frolova LT, Zakharova EA, Ginanova TT (2011) Development of respiratory trees in the holothurians *Apostichopus japonicas* (Aspidochirotida: Holothuroidea). Cell Tissue Res 346(3):327-338

Duperron S, Gaudron SM, Rodrigues CF, Cunha MR, Decker C, Olu K (2013) An overview of chemosynthetic symbioses in bivalves from the North Atlantic and Mediterranean Sea. Biogeosciences 10:3241-3267

Duvert M, Gros D (1982) Further studies on the junctional complex in the intestine of *Sagitta setosa*. Cell Tissue Res 225:663-671

Duvert M, Gros D, Salat C (1980) The junctional complex in the intestine of *Sagitta setosa* (Chaetognatha): the paired septate junction. J Cell Sci 42:227-246

Elias-Neto M, Soares MPM, Bitondi MG (2009) Changes in integument structure during the imaginal molt of the honey bee. Apidologie 40:29-39

Epstein ML, Gilula NB (1977) A study of communication specificity between cells in culture. J Cell Biol 75(3):769-787

Fahey B, Degnan BM (2010) Origin of animal epithelia: insights from the sponge genome. Evol Dev 12: 601-617

Faivre-Sarrailh C, Banerjee S, Li J, Hortsch M, Laval M, Bhat MA (2004) Drosophila contactin, a homolog of vertebrate contactin, is required for septate junction organization and paracellular barrier function. Development 131:4931-4942.

Farquhar MG, Palade GE (1963) Junctional complexes in various epithelia. J Cell Biol 17:375-412

Fautin DG (2009) Structural diversity, systematics, and evolution of cnidae. Toxicon 54(8):1054-1064

Fehon RG, Dawson IA, Artavanis-Tsakonas S (1994) A *Drosophila* homologue of membrane-skeleton protein 4.1 is associated with septate junctions and is encoded by the *coracle* gene. Development 120:545-557

Fei K, Yan L, Zhang J, Sarras MP Jr (2000) Molecular and biological characterization of a zonula occludens-1 homologue in *Hydra vulgaris*, named HZO-1. Dev Genes Evol 210(12):611-616

Fell PE, Knight P, Rieders W (1989) Low-salinity tolerance of and salinity-induced dormancy in the estuarine sponge *Microciona prolifera* (Ellis *et* Solander) under long-term laboratory culture. J Exp Mar Biol Ecol 133:195-211

Ferguson JC (1989) Rate of water admission through the madreporite of a starfish. J Exp Biol 145:147-156

Fiandra L, Casartelli M, Giordana B (2006) The paracellular pathway in the lepidopteran larval midgut: modulation by intracellular mediators. Comp Biochem Physiol A Mol Integr Physiol 144:464-473

Filshie BK, Flower NE (1977) Junctional structures in *Hydra*. J Cell Sci 23:151-172

Finol HJ, Croghan PC (1983) Ultrastructure of the branchial epithelium of an amphibious brackish-water crab. Tissue Cell 15(1):63-75

Fischer FP, Alger M, Ceislar D, Krafczyk H-U (1990) The chiton gill: ultrastructure in *Chiton olivaceus* (Mollusca, Polyplacophora). J Morphol 204:75-87

Flower NE (1971) Septate and gap junctions between the epithelial cells of an invertebrate, the mollusc *Cominella maculosa*. J Ultrastruct Res 37(3):259-268

Flower NE (1986) Sealing junctions in a number of arachnid tissues. Tissue Cell 18(6):899-913

Flower NE, Filshie BK (1975) Junctional structures in the midgut cells of lepidopteran caterpillars. J Cell Sci 17(1):221-39

Freire CA, Onken H, McNamara JC (2008) A structure-function analysis of ion transport in crustacean gills and excretory organs. Comp Biochem Physiol A 151:272-304

Froldi F, Ziosi M, Tomba G, Parisi F, Garoia F, Pession A, Grifoni D (2008) *Drosophila lethal giant larvae* neoplastic mutant as a genetic tool for cancer modeling. Curr Genomics 9:147-154

Funayama N (2013) The stem cell system in demosponges: suggested involvement of two types of cells: archeocytes (active stem cells) and choanocytes (food-entrapping flagellated cells). Dev Genes Evol 223:23-38

Funayama N (2010) The stem cell system in demosponges: Insights into the origin of somatic stem cells. Dev Growth Differ 52:1-14

Furuse M, Tsukita S (2006) Claudins in occluding junctions of humans and flies. Trends Cell Biol 16:181-188

Ganot P, Zoccola D, Tambutté E, Voolstra CR, Aranda M, Allemand D, Tambutté S (2015) Structural molecular components of septate junctions in cnidarians point to the origin of epithelial junctions in eukaryotes. Mol Biol Evol 32(1):44-62

Genova JL, Fehon RG (2003) Neuroglian, Gliotactin, and the Na^+/K^+ ATPase are essential for septate junction function in *Drosophila*. J Cell Biol 161:979-989

Georges D (1979) Gap and tight junctions in tunicates. Study in conventional and freeze-fracture techniques. Tissue Cell 11(4):781-792

Gerencser G (1982) Paracellular transport characteristics of *Aplysia juliana* intestine. Comp Biochem Physiol A 72(4):721-725

Gilbert MM, Auld VJ (2005) Evolution of clams (cholinesterase-like adhesion molecules): structure and function during development. Front Biosci 10:2177-2192

Gilula NB, Branton D, Satir P (1970) The septate junction: a structural basis for intercellular coupling. Proc Natl Acad Sci USA 67(1):213-220

Ginzberg RD, Morales EA, Spray DC, Bennett MVL (1985) Cell junctions in early embryos of squid (*Loligo pealei*). Cell Tissue Res 239:477-484

Giribet G, Edgecombe GD (2013) The Arthropoda: A phylogenetic framework. In: Minelli A, Boxshall G, Fusco G (eds) Arthropod Biology and Evolution - Molecules, Development, Morphology. Springer, Heidelberg, pp 17-40

Giuliani C, Troglio F, Bai Z, Patel FB, Zucconi A, Malabarba MG, Disanza A, Stradal TB, Cassata G, Confalonieri S, Hardin JD, Soto MC, Grant BD, Scita G (2009) Requirements for F-BAR proteins TOCA-1 and TOCA-2 in actin dynamics and membrane trafficking during *Caenorhabditis elegans* oocyte growth and embryonic epidermal morphogenesis. PLos Genetics 5:e1000675

Giusti F (1976) Tubular structures in the septate junction of a Gastropod. J Microsc Biol Cell 26:65-68

Gomez-Mendikute A, Elizondo M, Venier P, Cajaraville MP (2005) Characterization of mussel gill cells in vivo and in vitro. Cell Tissue Res 321:131-140

Gomme J (1981) D-Glucose transport across the apical membrane of the surface epithelium in *Nereis diversicolor*. J Membr Biol 62(1-2):29-46

Graf FC, Noirot-Timothée C, Noirot CH (1982) The specialization of septate junctions in regions of tricellular junctions. I. Smooth septate junctions (=continuous junctions). J Ultrastruct Res 78:136-151

Green CR (1981a) A clarification of the two types of invertebrate pleated septate junction. Tissue Cell 13(1):173-188

Green CR (1981b) A variation of the smooth septate junction in sea spiders (Pycnogonida). Tissue Cell 13 (1):189-195

Green CR (1981c) Fixation-induced intramembrane particle movement demonstrated in freeze-fracture replicas of a new type of septate junction in echinoderm epithelia. J Ultrastruct Res 75:11-22

Green CR, Bergquist PR (1979) Cell membrane specialisations in the Porifera. Colloq Int Cent Natl Rech Sci Biologie des Spongiaires 291:153-158.

Green CR, Bergquist PR (1982) Phylogentic relationships within the invertebrates in relation to the structure of septate junctions and the development of 'occluding' junctional types. J Cell Sci 53:279-305

Green CR, Flower NE (1980) Two new septate junctions in the phylum Coelenterata. J Cell Sci 42: 43-59

Green CR, Bergquist PR, Bullivant S (1979) An anastomosing septate junction in endothelial cells of the phylum echinodermata. J Ultrastruct Res 68(1):72-80

Green CR, Noirot-Timothee C, Noirot C (1983) Isolation and characterization of invertebrate smooth septate junctions. J Cell Sci 62:351-370

Green LF, Bergquist PR, Bullivant S (1980) The structure and function of the smooth septate junction in a transporting epithelium: the Malpighian tubules of the New Zealand glow-worm *Arachnocampa luminosa*. Tissue Cell 12(2):365-381

Günzel D, Fromm M (2012) Claudins and other tight junction proteins.Compr Physiol 2:1819-1852

Günzel D, Yu ASL (2013) Claudins and the modulation of tight junction permeability. Physiol Rev 93:525-569

Halcrow K (1976) The fine structure of the carapace integument of *Daphnia magna* Straus (Crustacea Branchiopoda). Cell Tissue Res 169(2):267-276

Hall S, Bone C, Oshima K, Zhang L, McGraw M, Lucas B, Fehon RG, Ward RE 4th (2014) *Macroglobulin complement-related* encodes a protein required for septate junction organization and paracellular barrier function in *Drosophila*. Development 141(4):889-898

Hand AR, Gobel S (1972) The structural organization of the septate and gap junctions of *Hydra*. J Cell Biol 52(2):397-408

Hanrahan JW (1984) Ionic permeability of insect epithelia. Amer Zool 24:229-240

Harrison FW (1972) The nature and role of the basal pinacoderm of *Corvomeyenia carolinensis* Harrison (Porifera: Spongillidae): A histochemical and developmental study. Hydrobiologia 39(4):495-508

Haszpruner G, Wanninger A (2012) Molluscs. Curr Biol 22(13):R510-R514

Herrera, F.C.; Herrera, M.I.; Lopez, I. (2000) Further studies on the partial double Donnan. Is isosmotic KCl solution isotonic with cells of respiratory trees of the holothurian *Isostichopus badionotus* Selenka? J Exp Mar Bio Ecol 247:139-152

Hijazi A, Masson W, Augé B, Waltzer L, Haenlin M, Roch F (2009) *boudin* is required for septate junction organisation in *Drosophila* and codes for a diffusible protein of the Ly6 superfamily. Development 136:2199-2209

Hildebrandt A, Pflanz R, Behr M, Tarp T1, Riedel D, Schuh R (2015) Bark beetle controls epithelial morphogenesis by septate junction maturation in Drosophila. Dev Biol 400(2):237-247

Hohagen J, Jackson DJ (2013) An ancient process in a modern mollusc: early development of the shell in *Lymnaea stagnalis*. BMC Dev Biol 13:27

Holley MC (1985) Changes in the distribution of filament-containing septate junctions as coelenterate myoepithelial cells change shape. Tissue Cell 17(1):1-11

Hori I (1985) A fine structural analysis of the planarian septate junction using ruthenium red staining. J Electron Microsc 34(4):422-426

Hori I (1987) Formation of the septate junction in regenerating planarian gastrodermis. J Morphol 192:205:215

Hortsch M, Margolis B (2003) Septate and paranodal junctions: kissing cousins. Trends Cell Biol 13:557-561

Hudspeth AJ, Revel JP (1971) Coexistence of gap and septate junctions in an invertebrate epithelium. J Cell Biol 50:92-101

Itza EM, Mozingo NM (2005) Septate junctions mediate the barrier to paracellular permeability in sea urchin embryos. Zygote 13(3):255-264

Izumi Y, Furuse M (2014) Molecular organization and function of invertebrate occluding junctions. Sem Cell Develop Biol 36:186-193

Izumi Y, Yanagihashi Y, Furuse M (2012) A novel protein complex, Mesh-Ssk, is required for septate junction formation in the *Drosophila* midgut. J Cell Sci 125:4923-4933

Jamuar MP (1966) Cytochemical and electron microscope studies on the pharynx and intestinal epithelium of *Nippostrongylus brasiliensis*. J Parasitol 52:1116-1128

Jarial MS, Kelly-Worden M (2011) Additional ultrastructural observations of the first segments of Malpighian tubules in *Cenocorixa bifida* (Hemiptera: Corixidae) in relation to reabsorption of solutes. Ann Entomol Soc Am 104(4):768-777

Jaspers MH, Nolde K, Behr M, Joo SH, Plessmann U, Nikolov M, Urlaub H, Schuh R (2012) The claudin Megatrachea protein complex. J Biol Chem 287:36756-36765

Jesaitis LA, Goodenough DA (1994) Molecular characterization and tissue distribution of ZO-2, a tight junction protein homologous to ZO-1 and the *Drosophila* discs-large tumor suppressor protein. J Cell Biol 124:949-961

Johnson KE, Perreau L, Charmantier G, Charmantier-Daures M, Lee E (2014) Without gills. Localization of osmoregulatory function in the copepod *Eurytemora affinis*. Physiol Biochem Zool 87(2):310-324

Josephson RK, Macklin M (1967) Transepithelial potentials in *Hydra*. Science 156 (3782):1629-1631

Josephson RK, Macklin M (1969) Electrical properties of the body wall of *Hydra*. J Gen Physiol 53:638-665

Juberthie-Jupeu L (1979) Cellular junctions of the midgut in the centipede (*Scutigerella pagesi*) as revealed by lanthanum tracer and freeze fracture technique. Tissue Cell 11(2):317-323

Kachar B, Christakis NA, Reese TS (1986) The intramembrane structure of septate junctions based on direct freezing. J Cell Sci 80:13-28

Kamenev YO, Dolmatov IY, Frolova LT, Khang NA (2013) The morphology of the digestive tract and respiratory organs of the holothurian *Cladolabes schmeltzii* (Holothuroidea, Dendrochirotida). Tissue Cell 45:126-139

Khan HR, Saleuddin AS (1981) Cell contacts in the kidney epithelium of *Helisoma* (Mollusca: Gastropoda) - effects of osmotic pressure and brain extracts: a freeze-fracture study. J Ultrastruct Res 75(1):23-40

Khanna DR, Yadav PR (2005) Biology of Echinodermata. Discovery Publishing House, New Delhi, India

Knust E, Bossinger O (2002) Composition and formation of intercellular junctions in epithelial cells. Science 298:1955-1959

Kolosov D, Bui P, Chasiotis H, Kelly SP (2013) Claudins in teleost fishes. Tiss Barrier 1:e25391

Köppen M, Simske JS, Sims PA, Firestein BL, Hall DH, Radice AD, Rongo C, Hardin JD (2001) Cooperative regulation of AJM-1 controls junctional integrity in *Caenorhabditis elegans* epithelia. Nat Cell Biol 3:983-991

Kraeuter JN, Setzler EM (1975) The seasonal cycle of scyphozoan and cubozoa in Georgia estuaries. Bul Marine Sci 25(1):66-74

Krumm S, Goebel-Lauth SG, Fronius M, Clauss W (2005) Transport of sodium and chloride across earthworm skin *in vitro*. J Comp Physiol B 175:601-608

Kukulies J, Komnick H (1983) Plasma membranes, cell junctions and cuticle of the rectal chloride epithelia of the larval dragonfly *Aeshna cyanea*. J Cell Sci 59:159-182

Kumar KPR (2013) Malpighian tubules of adult flesh fly, *Sarcophaga ruficornis* Fab. (Diptera: Sarcophagidae): An ultrastructural study. Tissue Cell 45:312-317

Lamb RS, Ward RE, Schweizer L, Fehon RG (1998) *Drosophila coracle*, a member of the protein 4.1 superfamily, has essential structural functions in the septate junctions and developmental functions in embryonic and adult epithelial cells. Mol Cell Biol 9:3505-3519

Lane NJ (1979) Tight junctions in a fluid-transporting epithelium of an insect. Science 204:91-93

Lane NJ, Dilworth (1989) Isolation and biochemical characterization of septate junctions: differences between the proteins in smooth and pleated varieties. J Cell Sci 93:123-131

Lane NJ, Harrison JB (1978) An unusual type of continuous junction in *Limulus*. J Ultrastruct Res 64: 85-97

Lane NJ, Skaer HB (1980) Intercellular junctions in insect tissues. In: Berridge MJ, Treherne JE, Wigglesworth VB (eds) Advances in Insect Physiology, vol 15. Academic Press, London, pp 35-213

Lane NJ, Campiglia SS, Lee WM (1994) Junctional types in the tissues of an onychophoran: the apparent lack of gap and tight junctions in *Peripatus*. Tissue Cell 26 (1):143-154

Lane NJ, Dallai R, Burighel P, Martinucci GB (1986) Tight and gap junctions in the intestinal tract of tunicates (Urochordata): a freeze-fracture study. J Cell Sci 84:1-17

Lange R (1964) The osmotic adjustment in the echinoderm, *Strongylocentrotus droebachiensis*. Comp Biochem Physiol 13:205-216

Laprise P, Paul SM, Boulanger J, Robbins RM, Beitel GJ, Tepass U (2010) Epithelial polarity proteins regulate *Drosophila* tracheal tube size in parallel to the luminal matrix pathway. Curr Biol 20:55-61

Laval M, Bel C, Faivre-Sarrailh C (2008) The lateral mobility of cell adhesion molecules is highly restricted at septate junctions in *Drosophila*. BMC Cell Biol 9:38

Ledger PW (1975) Septate junctions in the calcareous sponge *Sycon ciliatum*. Tissue Cell 7:13-8

Legg DA, Sutton MD, Edgecombe GD (2013) Arthropod fossil data increase congruence of morphological and molecular phylogenies. Nat Commun 4:2485

Legouis R, Gansmuller A, Sookhareea S, Bosher JM, Baillie DL, Labouesse M (2000) LET-413 is a basolateral protein required for the assembly of adherens junctions in *Caenorhabditis elegans*. Nat Cell Biol 2:415-422

Leik J, Kelly DE (1970) Septate junctions in the gastrodermal epithelium of *Phialidium*: A fine structural study utilizing ruthenium red. Tissue Cell 2(3):435-441

Lethias C, Garrone R, Mazzorana M (1983) Fine structures of sponge cell membranes: comparative study with freeze-fracture and conventional thin section methods. Tissue Cell 15(4):523-535

Leung B, Hermann GJ, Priess JR (1999) Organogenesis of the *Caenorhabditis elegans* intestine. Dev Biol 216(1):114-134

Leys SP, Hill A (2012) The physiology and molecular biology of sponge tissues. In: Becerro MA, Uriz MJ, Maldonado M, Turon X (eds) Advances in Marine Biology, vol 62. Academic Press, London, pp 1-56

Leys SP, Riesgo A (2012) Epithelia, an evolutionary novelty of metazoans. J Exp Zool (Mol Dev Evol) 318B:438-447

Leys SP, Nichols SA, Adams EDM (2009) Epithelia and integration in sponges. Integr Comp Biol 49:167-177

Llimargas M, Strigini M, Katidou M, Karagogeos D, Casanova J (2004) Lachesin is a component of a septate junction-based mechanism that controls tube size and epithelial integrity in the *Drosophila* tracheal system. Development 131:181-190

Locke M (1965) The structure of septate desmosomes. J Cell Biol 25:166-169

Lockwood C, Zaidel-Bar R, Hardin J (2008) The *C. elegans* zonula occludens ortholog cooperates with the cadherin complex to recruit actin during morphogenesis. Curr Biol 18(17):1333-1337

Loewenstein WR, Kanno Y (1964) Studies on an epithelial (gland) cell junction. I. Modifications of surface membrane permeability. J Cell Biol 22:565-586

Loh YH, Christoffels A, Brenner S, Hunziker W, Venkatesh B (2004) Extensive expansion of the claudin gene family in the teleost fish, *Fugu rubripes*. Genome Res 14:1248-1257

Lord BA, DiBona DR (1976) Role of the septate junction in the regulation of paracellular transepithelial flow. J Cell Biol 71(3):967-972

Luquet C, Pellerano G, Rosa G (1997) Salinity-induced changes in the fine structure of the gills of the semiterrestrial estuarian crab, *Uca uruguayensis* (Nobili, 1901) (Decapoda, Ocypodidae). Tissue Cell 29:495-501

Luquet CM, Genovese G, Rosa GA, Pellerano GN (2002) Ultrastructural changes in the gill epithelium of the crab *Chasmagnathus granulates* (Decapoda: Grapsidae) in diluted and concentrated seawater. Mar Bio 141:753-760

McHugh D (2000) Molecular phylogeny of the Annelida. Can J Zool 78:1873-1884

McMahon L, Legouis R, Vonesch JL, Labouesse M (2001) Assembly of *C. elegans* apical junctions involves positioning and compaction by LET-413 and protein aggregation by the MAGUK protein DLG-1. J Cell Sci 114:2265-2277

Ma L, Gu S-H, Liu Z-W, Wang S-N, Guo Y-Y, Zhou J-J, Zhang Y-J (2014) Molecular characterization and expression profiles of olfactory receptor genes in parasitic wasp, *Microplitis mediator* (Hymenoptera: Braconidae). J Insect Physiol 60:118-126

Mackie GO, Singla CL (1983) Studies on hexactinellid sponges. I Histology of *Rhabdocalyptus dawsoni* (Lambe, 1873). Philos Trans R Soc Lond B 301:365-400

Maldonado M, Riesgo A (2008) Reproductive output in a Mediterranean population of the homosclerophorid *Corticium candelabrum* (Porifera, Demospongiae), with notes on the ultrastructure and behavior of the larva. Mar Ecol 29:298-316

Manconi, R, Pronzato R (2008) Global diversity of sponges (Porifera: Spongillina) in freshwater. Hydrobiologia 595:27-33

Manfruelli P, Arquier N, Hanratty WP, Semeriva M (1996) The tumor suppressor gene, *lethal(2)giant larvae (1(2)g1)*, is required for cell shape change of epithelial cells during *Drosophila* development. Development 122: 2283-2294

Martelo MJ, Zanders IP (1986) Modifications of gill ultrastructure and ionic composition in the crab *Goniopsis cruentata* acclimated to various salinities. Comp Biochem Physiol A 84:383–389

Mashanov VS, Garcia-Arraras JE (2011) Gut regeneration in holothurians: a snapshot of recent developments. Biol Bull 221:93-109

Mather JA, Kuba MJ (2013) The cephalopod specialties: Complex nervous system, learning, and cognition. Can J Zool 91(6):431-449

Michaux G, Legouis R, Labouesse M (2001) Epithelial biology: lessons from *Caenorhabditis elegans*. Gene 277(1-2):83-100

Morris S (2011) Neuroendocrine regulation of osmoregulation and the evolution of air breathing in decapod crustaceans. J Exp Biol 204:979-989

Narasimha M, Uv A, Krejci A, Brown NH, Bray SJ (2008) Grainy head promotes expression of septate junction proteins and influences epithelial morphogenesis. J Cell Sci (6):747-752

Neff JM (1972) Ultrastructure of the outer epithelium of the mantle in the clam *Mercenaria mercenaria* in relation to calcification of the shell. Tissue Cell 4(4):591-600.

Nelson KS, Furuse M, Beitel GJ (2010) The *Drosophila* claudin Kune-kune is required for septate junction organization and tracheal tube size control. Genetics 185:831-839

Newell PF, Skelding JM (1973) Structure and permeability of the septate junction in the kidney sac of *Helix pomatia* L. Z Zellforsch 147:31-39

Nguyen H, Donini A (2010) Larvae of the midge possess two distinct mechanisms for ionoregulation in response to ion-poor conditions. Am J Physiol 299:R762-R773

Nichols SA, Dirks W, Pearse JS, King N (2006) Early evolution of animal cell signaling and adhesion genes. Proc Natl Acad Sci USA 103:12451-12456

Nilton A, Oshima K, Zare F, Byri S, Nannmark U, Nyberg KG, Fehon RG, Uv AE (2010) Crooked, coiled and crimpled are three Ly6-like proteins required for proper localization of septate junction components. Development 137:2427-2437

Noirot-Timothee C, Noirot C (1980) Septate and scalariform junctions in arthropods. Int Rev Cytol 63:97-141

Noirot-Timothee C, Smith DS, Cayer ML, Noirot C (1978) Septate junctions in insects: comparison between intercellular and intramembranous structures. Tissue Cell 10(1):125-136

O'Doherty H, Stark RJ (1981) Transmembrane and transepithelial movement of calcium during stimulus-secretion coupling. Am J Physiol (2):G150-G158

O'Donnell MJ, Maddrell SH, Gardiner BO (1984) Passage of solutes through walls of Malpighian tubules of *Rhodnius* by paracellular and transcellular routes. Am J Physiol 246:R759-R769

Oshima K, Fehon RG (2011) Analysis of protein dynamics within the septate junction reveals a highly stable core protein complex that does not include the basolateral polarity protein Discs large. J Cell Sci 124:2861-2871

Overton J (1963) Intercellular connections in the outgrowing stolon of *Cordylophora*. J Cell Biol 17(3):661-671

Padash-Barmchi M, Browne K, Sturgeon K, Jusiak B, Auld VJ (2010) Control of Gliotactin localization and levels by tyrosine phosphorylation and endocytosis is necessary for survival of polarized epithelia. J Cell Sci 123:4052-4062

Padash-Barmchi M, Charish K, Que J, Auld VJ (2013) Gliotactin and Discs large are co-regulated to maintain epithelial integrity. J Cell Sci 126:1134-1143

Pannabecker TL, Hayes TK, Beyenbach KW (1993) Regulation of epithelial shunt conductance by the peptide leucokinin. J Membr Biol 132:63-76

Paul SM, Palladino MJ, Beitel GJ (2007) A pump-independent function of the Na,K-ATPase is required for epithelial junction function and tracheal tube-size control. Development 134:147-55

Pavans de Ceccatty (1986) Cytoskeletal organization and tissue patterns of epithelia in the sponge *Ephydatia mülleri*. J Morphol 189:45-65

Pespeni MH, Barney BT, Palumbi SR (2013) Differences in the regulation of growth and biomineralization genes revealed through long-term common-garden acclimation and experimental genomics in the purple sea urchin. Evolution 67(7):1901-1914

Pettitt J, Cox EA, Broadbent ID, Flett A, Hardin J (2003) The *Caenorhabditis elegans* p120 catenin homologue, JAC-1, modulates cadherin-catenin function during epidermal morphogenesis. J Cell Biol 162:15-22

Phillips JE, Meredith J, Audsley N, Richardson N, Macins A, Ri*ng M (1998) Locust ion* transport peptide (ITP): A putative hormone controlling water and ionic balance in terrestrial insects. Amer Zool 38:461-470

Poddubnaya LG, Levron C, Gibson DI (2011) Ultrastructural characteristics of the uterine epithelium of aspidogastrean and digenean trematodes. Acta Parasitol 56 (2):131-139

Poddubnaya LG, Xylander WER, Gibson DI (2012) Ultrastructural characteristics of the protonephridial terminal organ and associated ducts of adult specimens of the Aspidogastrea, Digenea and Monogenea, with comments on the relationships between these groups. Syst Parasitol 82:89-104

Poirrier MA (1974) Ecomorphic variation in gemmoscleres of *Ephydatia fluviatilis* Linnaeus (Porifera: Spongillidae) with comments upon its systematic and ecology. Hydrobiologia 44(4):337-347

Porvaznik M, Ribas JL, Parker JL (1979) Rhombic particle arrays in gill epithelium of a mollusc, *Aplysia californica*. Tissue Cell 11(2):337-44

Primo AL, Marques SC, Falcao J, Crespo D, Pardal MA, Azeiteiro UM (2012) Environmental forcing on jellyfish communities in a small temperate estuary. Mar Environ Res 79:152-159

Prior DJ, Uglem GL (1984) Analysis of contact-rehydration in terrestrial gastropods: absorption of ^{14}C-inulin through the epithelium of the foot. J Exp Biol 111:75-80

Prosser CL (1967) Ionic analysis and effects of ions on contractions of sponge tissues. Z vergl Physiol 54:109-120

Prusch, R.D. (1977) Solute secretion by the tubefoot epithelium in the starfish *Asterias forbesi*. J Exp Biol 68:35-43

Purschke G (2002) On the ground pattern of Annelida. Org Divers Evol 2:181-196

Reise Sousa C, Howard JE, Hartley R, Earley FGP, Djamgoz MBA (1993) An insect epidermal cell line (UMBGE-4): Structural and electrophysiological characterization. Comp Biochem Physiol A 106(4):759-767

Rose B (1971) Intercellular communication and some structural aspects of membrane junctions in a simple cell system. J Membr Biol 5(1):1-19

Sakarya O, Armstrong KA, Adamska M, Adamski M, Wang IF, Tidor B, Degnan BM, Oakley TH, Kosik KS (2007) A post-synaptic scaffold at the origin of the animal kingdom. PLoS One 2(6):e506

Satir P, Gilula NB (1970) The cell junction in a lamellibranch gill ciliated epithelium: Localization of pyroantimonate precipitate. J Cell Biol 47(2):468-487

Schnizler M, Krumm S, Clauss W (2002) Annelid epithelia as models for electrogenic Na^+ transport. Biochim Biophys Acta 1566(1-2):84-91

Schockaert ER, Hooge M, Sluys R, Schilling S, Tyler S, Artois T (2008) Global diversity of free living flatworms (Platyhelminthes, "Turbellaria") in freshwater. Hydrobiol 595:41-48

Schulte J, Charish K, Que J, Ravn S, MacKinnon C, Auld VJ (2006) Gliotactin and Discs large form a protein complex at the tricellular junction of polarized epithelial cells in *Drosophila*. J Cell Sci 119:4391-4401

Schulte J, Tepass U, Auld VJ (2003) Gliotactin, a novel marker of tricellular junctions, is necessary for septate junction development in *Drosophila*. J Cell Biol 161(5):991-1000

Segbert C, Johnson K, Theres C, van Fü-rden D, Bossinger O (2004) Molecular and functional analysis of apical junction formation in the gut epithelium of *Caenorhabditis elegans*. Dev Biol 266:17-26

Shanbhag S, Tripathi S (2009) Epithelial ultrastructure and cellular mechanisms of acid base transport in the *Drosophila* midgut. J Exp Biol 212:1731-1744

Shivers RR, Chauvin WJ (1977) Intercellular junctions of antennal gland epithelial cells in the crayfish, *Orconectes virilis*. A freeze-fracture study. Cell Tissue Res 175(4):425-438

Simske JS, Hardin J (2011) Claudin family proteins in *Caenorhabditis elegans*. Methods Mol Biol 762:147-169

Simske JS, Köppen M, Sims P, Hodgkin J, Yonkof A, Hardin J (2003) The cell junction protein VAB-9 regulates adhesion and epidermal morphology in *C. elegans*. Nat Cell Biol 5:619-625

Skaer HB, Maddrell SH (1987) How are invertebrate epithelia made tight? J Cell Sci 88:139-41

Skaer HB, Harrison JB, Lee WM (1979) Topographical variations in the structure of the smooth septate junction. J Cell Sci 37:373-389

Skaer HB, Maddrell SH, Harrison JB (1987) The permeability properties of septate junctions in Malpighian tubules of *Rhodnius*. J Cell Sci 88:251-265

Skelding JM (1973a) The fine structure of the kidney sac of *Achatina achatina* (L.). Z Zellforsch Mikrosk Anat 147(1):1-29

Skelding JM (1973b) Studies on the renal physiology of *Achatina achatina* (L.). Malacologia 14:93-96

Spiegel E, Howard L (1983) Development of cell junctions in sea urchin embryos. J Cell Sci 62:27– 48

Staehelin LA (1974) Structure and function of intercellular junctions. Int Rev Cytol 39:191-283

Stetak A, Hajnal A (2011) The *C. elegans* MAGI-1 protein is a novel component of cell junctions that is required for junctional compartmentalization. Dev Biol 350:24-31

Storch V, Welsch U (1977) Septate junctions in the cephalic epidermis of turbellarians (*Bipalium*). Cell Tissue Res 184:423-425

Strand D, Raska I, Mechler BM (1994) The *Drosophila lethal giant larvae* tumor suppressor protein is a component of the cytoskeleton. J Cell Biol 127:1345-1360

Suderman RJ, Andersen SO, Hopkins TL, Kanost MR, Kramer K.J (2003) Characterization and cDNA cloning of three major proteins from pharate pupal cuticle of *Manduca sexta*. Insect Biochem Mol Biol 33:331-343

Tambutté E, Tambutté S, Segonds N, Zoccola D, Venn A, Erez J, Allemand D (2012) Calcein labelling and electrophysiology: insights on coral tissue permeability and calcification. Proc Biol Sci 279(1726):19-27

Tepass U, Tanentzapf G, Ward R, Fehon R (2001) Epithelial cell polarity and cell junctions in *Drosophila*. Annu Rev Genet 35:747-784

Tiklová K, Senti KA, Wang S, Gräslund A, Samakovlis C (2010) Epithelial septate junction assembly relies on melanotransferrin iron binding and endocytosis in *Drosophila*. Nat Cell Biol 12:1071-1077

Tyler S (2003) Epithelium – the primary building block for metazoan complexity. Integr Comp Biol 43:55-63

Tyler S, Hooge M (2004) Comparative morphology of the body wall in flatworms (Platyhelminthes). Can J Zool 82:194-210

Tyler S, Tyler MS (1997) Origin of the epidermis in parasitic Platyhelminthes. Inter J Parasitol 27(6):715-738

Uglem GL, Just JJ (1983) Trypsin inhibition by tapeworms: Antienzyme secretion or pH adjustment? Science 220:79-81

Uglem GL, Prior DJ, Hess SD (1985) Paracellular water uptake and molecular sieving by the foot epithelium of terrestrial slugs. J Comp Physiol B 156:285-289

Vanderveken M, O'Donnell MJ (2014) Effects of diuretic hormone 31, drosokinin and allatostatin A on transepithelial K^+ transport and contraction frequency in the midgut and hindgut of larval *Drosophila melanogaster*. Arch Insect Biochem Physiol 85:76-93

Van Soest RWM, Boury-Esnault N, Vacelet J, Dohrmann M, Erpenbeck D, De Voogd NJ, Santodomingo N, Vanhoorne B, Kelly M, Hooper JNA (2012) Global diversity of sponges. PlosOne 7(4):e35105

Vernet G, Rué G, Gontcharoff M (1979) Studies on the technique of impregnation with lanthanum and the ultrastructure of the body wall epithelium of *Lineus ruber* (heteronemertine). J Ultrastruct Res 67(2):225-227

Vidolin D, Santos-Gouvea IA, Freire CA (2002) Osmotic stability of the coelomic fluids of a sea cucumber (*Holothuria grisea*) and a starfish (*Asterina stellifera*) (Echinodermata) exposed to the air during low tide: a field study. Acta Biol Par 31(1-4):113-121

Ward RE, Lamb RS, Fehon RG (1998) A conserved functional domain of *Drosophila* Coracle is required for localization at the septate junction and has membrane-organizing activity. J Cell Biol 140:1463-73

Welsch U, Buchheim W (1977) Freeze fracture studies on the annelid septate junction. Cell Tiss Res 185:527-534

Westermann B, Schipp R (1998) Morphology and histology of the digestive tract of *Nautilus pompilius* and *Nautilus macromphalus* (Cephalopoda, Tetrabranchiata). Zoomorphology 117:237-245

Westheide W (1997) The direction of evolution within the Polychaeta. J Nat His 31:1-15

Willott E, Bald, MS, Fanning AS, Jameson, B, Van Itallie, C, Anderson JM (1993) The tight junction protein ZO-1 is homologous to the *Drosophila* discs-large tumor suppressor protein of septate junctions. Proc Natl Acad Sci USA 90:7834-7838

Wolff T (2005) Composition and endemism of the deep-sea hydrothermal vent fauna. Cah Biol Mar 46:97-104

Wood RL (1959) Intercellular attachment in the epithelium of *Hydra* as revealed by electron microscopy. J Biophys Biochem Cytol 6:343-352

Woods DF, Bryant PJ (1991) The *discs-large* tumor suppressor gene of *Drosophila* encodes a guanylate kinase homolog localized at septate junctions. Cell 66:451-64

Woods DF, Hough C, Peel D, Callaini, G, Bryant PJ (1996) Dlg protein is required for junction structure, cell polarity, and proliferation control in *Drosophila* epithelia. J Cell Biol 134:1469-1482

Woods DF, Wu JW, Bryant PJ (1997) Localization of proteins to the apico-lateral junctions of *Drosophila* epithelia. Dev Genet 20(2):111-118

Wright JC, Luke BM (1989) Ultrastructural and histochemical investigations of *Peripatus* integument. Tissue Cell 21(4):605-625

Wright KA, Lee DL, Shivers RR (1985) A freeze-fracture study of the digestive tract of the parasitic nematode *Trichinella*. Tissue Cell 17(2):189-198

Wu VM, Schulte J, Hirschi A, Tepass U, Beitel GJ (2004) Sinuous is a *Drosophila* claudin required for septate junction organization and epithelial tube size control. J Cell Biol 164:313-323

Wu VM, Yu MH, Paik R, Banerjee S, Liang Z, Paul SM, Bhat MA, Beitel GJ (2007) *Drosophila* Varicose, a member of a new subgroup of basolateral MAGUKs, is required for septate junctions and tracheal morphogenesis. Development 134:999-1009

Xué L, Dallai R (1992) Cell junctions in the gut of Protura. Tissue Cell 24(1):51-59

Yanagihashi Y, Usui T, Izumi Y, Yonemura S, Sumida M, Tsukita S, Uemura T, Furuse M (2012) Snakeskin, a membrane protein associated with smooth septate junctions, is required for intestinal barrier function in *Drosophila*. J Cell Sci 125:1980-1990

Yu MJ, Beyenbach KW (2001) Leucokinin and the modulation of the shunt pathway in Malpighian tubules. J Insect Physiol 47:263-276

Yu MJ, Beyenbach KW (2002) Leucokinin activates Ca^{2+}-dependent signal pathway in principal cells of *Aedes aegypti* Malpighian tubules. Am J Physiol 283:F499-F508

Zaidel-Bar R, Joyce MJ, Lynch AM, Witte K, Audhya A, Hardin J (2010) The F-BAR domain of SRGP-1 facilitates cell-cell adhesion during *C. elegans* morphogenesis. J Cell Biol 191:761-769

Zerbst-Boroffka I, Bazin B, Wenning A (1997) Chloride secretion drives urine formation in leech nephridia. J Exp Biol 200:2217-2227

Zheng H, Dietz TH (1998) Paracellular solute uptake in the freshwater bivalves *Corbicula fluminea* and *Toxolasma texasensis*. Biol Bull 194:170-177

Zhu W, Vandingenem A, Huybrechts R, Vercammen T, Baggerman G, De Loof A, Poulos CP, Valentza A, Breuer M (2001) Proteolitic breakdown of the Neb-trypsin modulating oostatic factor (Neb-TMOF) in the haemolymph of different insects and its gut epithelial transport. J Insect Physiol 47:1235-1242

CHAPTER 4:

THE RESPONSE OF CLAUDIN-LIKE TRANSMEMBRANE SEPTATE JUNCTION PROTEINS TO ALTERED ENVIRONMENTAL ION LEVELS IN THE LARVAL MOSQUITO *AEDES AEGYPTI*[3]

4.1 Summary

Septate junctions (SJs) occlude the paracellular pathway and function as paracellular diffusion barriers within invertebrate epithelia. However, integral components of SJs and their contribution to barrier properties have received considerably less attention than those of vertebrate occluding junctions. In arthropods, SJ proteins have only been identified in *Drosophila* and among these are three integral claudin-like proteins, Megatrachea (Mega), Sinuous (Sinu) and Kune-kune (Kune), as well as a receptor-like transmembrane SJ protein known as Neurexin IV (Nrx IV). In this study, *mega*, *sinu*, *kune* and *nrx IV* are identified and characterized in aquatic larvae of the mosquito *Aedes aegypti* and a role for these proteins in osmoregulatory homeostasis is considered. Transcripts encoding Mega, Sinu, Kune and Nrx IV were found in osmoregulatory tissues such as the midgut, Malpighian tubules, hindgut and anal papillae, but abundance was greater in the hindgut and anal papillae. Using immunohistochemical and western blot analysis, it was found that Kune localized to regions of intercellular contact between epithelial cells of the rectum and posterior midgut and in the apical membrane domain of the syncytial epithelium of anal papillae. To investigate a potential role for integral SJ proteins in larval *A. aegypti* osmoregulation, abundance was examined in animals reared in freshwater or brackish water (30% seawater). In osmoregulatory epithelia, larvae exhibited tissue-specific alterations in *mega* mRNA and Kune protein abundance, but not *sinu* or *nrx IV* mRNA. These studies provide a first look at the potential contribution of integral SJ components to osmoregulatory homeostasis in an aquatic invertebrate.

---

[3]Contributing authors: Sima Jonusaite, Scott P Kelly and Andrew Donini

Department of Biology, York University, Toronto, Ontario, Canada M3J 1P3

This chapter has been published and reproduced with permission:

Jonusaite S, Kelly SP, Donini A (2016) The response of claudin-like transmembrane septate junction proteins to altered environmental ion levels in the larval mosquito *Aedes aegypti*. J Comp Physiol B 186(5):589-602

4.2 Introduction

In metazoa, isolation of the body from the surrounding environment and separation of compositionally distinct fluid compartments within the body are achieved by the epithelial tissues. To accomplish their physiological roles, epithelial sheets must participate in the controlled exchange of solutes, ions, and water through and between the cells (Knust and Bossinger 2002). Movement of molecules through the epithelial cells (i.e. transcellular transport) is reliant on channels, pumps and carrier proteins present on the apical and basolateral membranes, whereas transport between the cells (i.e. paracellular transport) is driven by passive diffusion, electrodiffusion, and osmosis (Beyenbach and Piermarini 2011). Paracellular barrier function in epithelia of invertebrates is provided by the lateral plasma membrane spanning septate junctions (SJs) (for review see Chapter 3). On the other hand, paracellular transport in vertebrates is controlled by tight junctions (TJs) which are formed in the most apical region of lateral cell membranes where they mediate selective paracellular permeability depending on physiological requirements and/or cell type (Anderson and Van Itallie 2009). Electron micrograph images of SJs show a characteristic ladder-like arrangement of distinct septa, which interconnect the plasma membranes of adjacent cells keeping them apart by 15-20 nm (Green and Bergquist 1982). In insects as well as other arthropods, two main types of SJ have been described on the basis of their ultrastructural appearance in tangential section. These are the pleated SJ (pSJ) and the smooth SJ (sSJ). The pSJs form regular undulating rows of septa whereas septa in the sSJs show regularly spaced parallel lines (Lane and Skaer 1980; Flower and Filshie 1975). Furthermore, pSJs are generally observed in tissues of ectodermal origin such as the epidermis, foregut, hindgut, trachea, salivary glands, and also in the glial cells that ensheathe the peripheral and central nervous system (Noirot-Timothee and Noirot 1980; Tepass et al. 2001). On the other hand, sSJs seem to occur in tissues of endodermal origin such as the midgut and its derivatives, as well as

Malpighian tubules (Noirot-Timothee and Noirot 1980; Lane and Skaer 1980). However, in Malpighian tubules both types of SJ have been observed, sometimes coexisting side by side in the same junctional complex (Noirot-Timothee and Noirot 1980; Lane and Skaer 1980). The biological significance of two types of SJ in arthropods is not well understood largely because of the lack of information on their molecular physiology.

The core structure and permeability characteristics of invertebrate SJs are dictated by SJ proteins, and in this regard, SJ proteins that resemble the claudin (Cldn) proteins of vertebrate TJs appear to play an important role in at least some invertebrate phyla (Behr et al. 2003; Wu et al. 2004; Stork et al. 2008; Nelson et al. 2010; Chapter 3). In vertebrates, claudin (Cldn) proteins are a large family of integral membrane TJ proteins all of which are small 20- to 34-kDa proteins predicted to have four transmembrane domains, two extracellular loops (ECL1, which is larger, and a smaller ECL2), one short intracellular loop and intracellular N and C termini (Anderson and Van Itallie 2009; Angelow et al. 2008; Günzel and Yu 2013). In *Caenorhabditis elegans*, Cldn-like proteins have been shown to be necessary for controlling paracellular permeability across the gut (Asano et al. 2003). Furthermore, at least three Cldn-like proteins, Megatrachea (Mega), Sinuous (Sinu) and Kune-kune (Kune), are integral components of the pSJs in *Drosophila* (Behr et al. 2003; Wu et al. 2004; Nelson et al. 2010). All three *Drosophila* Cldn-like proteins share the tetraspan topology and W-GLW-C-C signature motif characteristic of these molecules (see Simske and Hardin 2011; Günzel and Yu 2013; Ganot et al. 2015; Nelson et al. 2010) and loss of function mutations in Mega, Sinu or Kune cause defects in the formation and barrier function of pSJs in the trachea, salivary glands, and in the blood-brain barrier (Behr et al. 2003; Wu et al. 2004; Stork et al. 2008; Nelson et al. 2010). Interestingly, Mega, Sinu and Kune appear to have unique roles in pSJ organization. A *mega* mutant *Drosophila* embryo lacks the ladder-like septa of pSJs between tracheal cells and instead shows an intercellular space filled

with unstructured electron-dense material (Behr et al. 2003). In contrast, *sinu* mutants exhibit septa of pSJs in the trachea, salivary glands and epidermis but these are significantly reduced in number and are not organized into continuous circumferential ribbons (Wu et al. 2004). Moreover, Mega is necessary for correct subcellular localization of other pSJ proteins (Behr et al. 2003) whereas Sinu is required for maintaining normal levels of other pSJ components (Wu et al. 2004). Distinct from either Mega or Sinu, Kune is important for both the localization and levels of other pSJ proteins, suggesting that it has a more central role in pSJ formation than either Sinu or Mega (Nelson et al. 2010). Proper localization of Mega to pSJs is also dependent on another integral *Drosophila* SJ protein Neurexin IV (Nrx IV) (Baumgartner et al. 1996; Behr et al. 2003). *Drosophila* Nrx IV is a member of the Caspr (Contactin associated protein) family of neuronal receptors, which have a single membrane-spanning domain, a large extracellular domain with laminin G motifs and epidermal growth factor (EGF) repeats, and an N-terminal discoidin-like domain (Baumgartner et al. 1996; Littleton et al. 1997). Nrx IV is localized to all pSJ-bearing tissues in *Drosophila* and is required for the barrier function of SJs (Baumgartner et al. 1996). Mutant *nrx IV* embryos display paralysis due to the breakdown of pSJ-maintained blood-nerve-brain barrier and ultrastructural analysis reveals the absence of pSJ septa between glial cells as well as between ectodermally derived epithelia (Baumgartner et al. 1996). Taken together, it is clear that Nrx IV and the aforementioned Mega, Sinu, and Kune are heavily involved in maintaining the integrity and function of arthropod SJs. However, it is not known to what extent (if any) these proteins may contribute to the regulation of paracellular solute movement in aquatic invertebrates that inhabit water with different solute composition (e.g. seawater, brackish water, freshwater) and during or following changes in environmental conditions that lead to alterations in solute composition.

Freshwater (FW) aquatic invertebrates are particularly prone to such alterations in the environment because they reside in bodies of water that can vary in composition as a result of climatic and anthropogenic factors. For example, FW ecosystems are becoming increasingly salinated from mining, irrigation, and in temperate regions by winter road salting (Kaushal et al. 2005; Pond et al. 2008; Williams et al 2001). These FW invertebrates which include the majority of mosquito larvae possess hemolymph that is hyper-ionic/osmotic to the natural surrounding water, and as a consequence, these mosquito larvae are adapted to cope with passive ion loss and water gain across body surfaces (Clements 1992). Therefore, in FW, mosquito larvae maintain salt and water balance in part by actively acquiring or reabsorbing ions across ionoregulatory epithelia and the transcellular ion transport mechanisms involved in this process have been examined (e.g. Bradley 1994; Donini and O'Donnell 2005; Del Duca et al. 2011). However, it seems likely that limiting passive ion loss will also play an important role in the maintenance of ionoregulatory homeostasis in FW residing mosquito larvae, as it does in other FW organisms and this represents a significant challenge for which these larvae appear well adapted to. For example, a study comparing whole body NaCl efflux and uptake in a freshwater restricted larval mosquito, *Culex quinquefasciatus*, and a euryhaline species, *Culex tarsalis*, noted reduced ion efflux in the freshwater mosquito relative to the euryhaline species (Patrick et al. 2001). Furthermore, *C. tarsalis* was able to rapidly adjust Na^+ efflux independently of Cl^- efflux when challenged with varying salinity (transfer from 30% to 50% seawater) (Patrick et al. 2001).

In addition, ultrastructural differences in crab gill epithelium SJs have been observed to occur upon exposure to alterations in water salt content (Luquet et al. 1997; Luquet et al. 2002), that would seem to be consistent with salinity induced alterations in gill TJ morphology as seen in teleost fishes (for review see Chasiotis et al. 2012b). More specifically, when acclimated to low salinity, deep, well developed SJs are present in the crab gill epithelium (Luquet et al. 1997).

In contrast, crab gill epithelium SJs are found to be shallow and less developed in animals acclimated to a high salinity (Luquet et al. 1997). Similarly, gill cells of FW teleost fishes are linked by deep TJs, whereas in the SW teleost fish gill epithelium only shallow TJs are present and link mitochondrion-rich cells and accessory cells (Duffy et al. 2011; Chasiotis et al. 2012b). Given that deep occluding junctions are typically associated with reduced passive solute movement, morphological evidence would suggest functional similarity of gill SJs and TJs with regard to salinity acclimation. In addition to ultrastructure, the molecular physiology of occluding junctions in fishes and amphibians alter in response to changes in environmental ion levels, and in 'dilute surroundings' these changes are proposed to limit ion loss (e.g. Bagherie-Lachidan et al. 2008; Chasiotis and Kelly 2009; Chasiotis et al. 2012a; Duffy et al. 2011; Kolosov et al. 2013; Kumai et al. 2011; Kwong and Perry 2013; Tipsmark et al. 2008). However, the molecular mechanisms involved in the regulation of paracellular permeability in aquatic arthropods have been entirely overlooked. Therefore, given that the vertebrate TJ complex and invertebrate SJ complex are functional counterparts, it can be hypothesized that the abundance of integral SJ proteins found in the ionoregulatory epithelia of aquatic mosquito larvae will be altered by changes in water salt content. In this case it can be speculated that the freshwater larvae of *A. aegypti* possess SJs in important iono/osmoregulatory epithelia that limit passive ion loss and water gain. Furthermore, when these larvae face abrupt or sustained increases in environmental salinity from climatic or anthropogenic events, they will face the opposing challenge of passive ion uptake. With this in mind, the goal of the current study was to break new ground in this area by identifying and characterizing genes encoding the SJ proteins Mega, Sinu, Kune and Nrx IV in the ionoregulatory tissues of larval *A. aegypti* and examine their response to differences in the salinity of rearing conditions. Mega, Sinu and Kune are of particular interest in this regard as they are Cldn-like proteins, and in aquatic vertebrates such as fishes, an important role for Cldns in the

regulation of salt and water balance continues to emerge (Bui and Kelly 2014; Kolosov et al. 2014; Kwong and Perry 2013).

4.3 Methods and Materials

4.3.1 Insects: A laboratory colony of *Aedes aegypti* (Linnaeus) was maintained in the Department of Biology at York University as previously detailed (Del Duca et al. 2011).

4.3.2 Long-term acclimation to brackish water: Eggs were hatched in plastic containers filled with FW or a 10 % seawater (SW) solution (3.5 g/l Instant Ocean SeaSalt®, United Pet Group, Blacksburg, VA, USA). Hatched 1st instar larvae were transferred from either FW to FW or from 10% SW (3.5 g/l Instant Ocean SeaSalt®) to 30% SW (10.5 g/l Instant Ocean SeaSalt®) which served as the experimental brackish water (BW) treatment. A stepwise acclimation of larvae from 10% to 30% SW is necessary because limited hatching occurs if eggs are transferred from FW directly into 30% SW. During the course of the experiment, larvae were fed daily and water (of appropriate salinity) was refreshed weekly. Experiments were conducted on 4th instar larvae that had not been fed for 24 h before collection.

4.3.3 RNA extraction and cDNA synthesis: To obtain tissues for RNA isolation, 4th instar larvae were dissected in ice-cold physiological saline as previously detailed (Ionescu and Donini 2012) Tissues of interest such as the midgut (with the gastric caecae), the Malphigian tubules, the hindgut and the anal papillae, were separated, transferred to microtubes with 200 µl of RNA*later*™ RNA stabilization reagent (QIAGEN, Toronto, ON, Canada) and stored at -20^{0}C. Tissues from 50 larvae were combined in each tube. For whole body RNA isolation, two larvae per biological sample were used. To extract total RNA, RNA*later* was removed from collected whole body or tissue samples and RNA was isolated using TRIzol® reagent (Invitrogen, Burlington, ON, Canada). Tissues were sonicated for 8 s at 5 watts using an XL 2000 Ultrasonic Liquid Processor (QSONICA, LLC, Newtown, CT, USA) and RNA extracted in TRIzol® according to manufacturer's instructions. All RNA samples were then treated with TURBO DNA-*free*™ kit (Ambion®, Life Technologies Inc., Burlington, ON, Canada). The quality and

yield of RNA were determined using a Multiskan Spectrum spectrophotometer (Fisher Scientific, Nepean, ON, Canada) and template cDNA was synthesized using iScript^{TM} cDNA synthesis kit as per manufacturer's instructions (Bio-Rad, Mississauga, ON, Canada). cDNA was stored at -20 ^{0}C.

4.3.4 SJ gene identification in Aedes aegypti: Using the National Center for Biotechnology Information (NCBI) database BLAST search engine, expressed sequence tags (ESTs) of genes encoding SJ proteins Megatrachea (Mega, *mega*), Sinuous (Sinu, *sinu*), Kune-kune (Kune, *kune)* and Neurexin IV (Nrx IV, *nrx IV*) were retrieved from the *A. aegypti* genome and confirmed to be protein coding using a reverse BLASTx. A reading frame was established using BLASTn alignment and ORF Finder (http://www.ncbi.nlm.nih.gov/gorf/). All primer sets were designed based on EST sequences using Primer3 software (v. 0.4.0) and *A. aegypti* cDNA was used to amplify amplicons for each SJ gene by reverse transcriptase PCR (RT-PCR). RT-PCR amplicon size was verified by agarose gel electrophoresis and sequence identity of PCR products was confirmed after sequencing at the York University Core Molecular Biology Facility (Department of Biology, York University, ON, Canada). Amplicon size and primer sequences are summarized in Table 4-1. Full coding sequences for *A. aegypti mega*, *sinu*, *kune* and *nrx IV* were confirmed using a BLAST search and submitted to GenBank. Sequence data for *A. aegypti kune* and *nrx IV* are available under the accession numbers KR781452 and KR781455, respectively (see Table 4-1), and sequence data for *mega* and *sinu* are available in the Third Party Annotation Section of the DDBJ/EMBL/GenBank databases under the accession numbers BK008793 and BK008794, respectively (see Table 4-1).

4.3.5 Quantitative real-time PCR analysis of SJ gene mRNA abundance in osmoregulatory tissues: Quantitative real-time PCR (qPCR) was used to examine the distribution and abundance of mRNA encoding integral SJ proteins in the iono/osmoregulatory tissues of *A. aegypti* larvae.

For expression profile studies, total RNA was extracted from the following tissues: midgut, Malpighian tubules, hindgut and anal papillae. The extraction of RNA and synthesis of cDNA from all tissues were conducted as outlined above (see *RNA extraction and cDNA synthesis*). Primers used for RT-PCR described above were also used for qPCR analysis of *A. aegypti* SJ genes. *Rp49* and *18S rRNA* were used as reference genes (see Table 4-1).

qPCR analyses of SJ protein genes and reference genes was carried out using SYBR Green I Supermix (Bio-Rad Laboratories Ltd., Mississauga, ON, Canada) and a Chromo4^{TM} Detection System (CFB-3240, Bio-Rad Laboratories Canada Ltd.). A standard curve of serially diluted whole body cDNA was constructed for each gene of interest to optimize the template cDNA concentration, check for primer efficiencies and verify that the threshold cycle (C_t) fell into an acceptable range. The following qPCR reaction conditions were used: initial denaturation, 4 min/95^{0}C; denaturation, 95^{0}C/30s; annealing, 58-59^{0}C/45s; extension, 72^{0}C/30s, 40 cycles. A melting curve analysis was performed after each run to confirm that no primer-dimers or other nonspecific products were synthesized during reactions. A reference gene was selected for normalization on the basis that it could be determined, through statistical analysis ($p < 0.05$), that the gene was unaffected by experimental variable.

4.3.6 Immunohistochemistry: Immunohistochemical localization of Kune was achieved using a rabbit polyclonal serum antibody raised against the C-terminal cytoplasmic region of *Drosophila* Kune (Nelson et al. 2010) (a kind gift from Dr. Mikio Furuse, National Institute for Physiological Sciences, Japan). For whole-mount immunohistochemistry, the entire guts of fourth instar larvae were isolated in ice-cold physiological saline and processed using methodology as previously described (see Chapter 2) and anti-Kune antibody at 1:500 in ADB. For paraffin sections of anal papillae, whole larvae were fixed in Bouin's solution and examined using methods previously outlined (Chasiotis and Kelly 2008) and anti-Kune antibody (1:500 in ADB) and mouse

monoclonal anti-Na^+-K^+-ATPase α-subunit antibody (α5, 1:10 in ADB; Douglas Fambrough, Developmental Studies Hybridoma Bank, created by the NICHD of the NIH and maintained at the University of Iowa, Department of Biology, Iowa City, IA, USA).

4.3.7 Western blot analysis: Tissues of interest (gastric caecae, anterior midgut, posterior midgut, Malpighian tubules, hindgut, anal papillae) were isolated in ice-cold physiological saline, transferred to microtubes and stored at -80^{0}C for later analysis. Tissues from 80 larvae were combined in each tube. For examination of Kune expression and/or abundance, tissue samples were thawed on ice and sonicated in a homogenization buffer containing 50 mmol l^{-1} Tris-HCl, pH 7.5, 150 mmol l^{-1} NaCl, 1% sodium deoxycholate, 1% Triton-X-100, 0.1% SDS, 1 mmol l^{-1} PMSF and 1:200 protease inhibitor cocktail (Sigma-Aldrich). All samples were sonicated for 2 x 10s, homogenates were then centrifuged at 13,000 *g* for 10 min at 4°C, and protein content of the collected supernatants was determined using the Bradford assay (Sigma-Aldrich) according to the manufacturer's guidelines. Samples (10-20 µg protein) were prepared for SDS-PAGE by heating for 5 min at 100°C in a 6x loading buffer containing 360 mmol l^{-1} Tris-HCl (pH 6.8), 12% (w/v) SDS, 30% glycerol, 600 mmol l^{-1} DTT and 0.03% (w/v) bromophenol blue. Samples were then electrophoretically separated by SDS-PAGE and western blot analysis of Kune was conducted according to a previously described protocol (Chasiotis and Kelly 2008) using anti-Kune antibody at a 1:2000 dilution. Antigen reactivity was visualized using Clarity™ Western ECL substrate (Bio-Rad, ON, Canada). After examination of Kune, blots were stripped with stripping buffer containing 20 mmol l^{-1} magnesium acetate, 20 mmol l^{-1} potassium chloride, and 0.1 mmol l^{-1} glycine (pH 2.2), and re-probed with a 1:200 dilution of mouse monoclonal anti-JLA20 antibody (J.J.-C. Lin, Developmental Studies Hybridoma Bank, Iowa City, IA, USA) for actin or a 1:1000 dilution of rabbit monoclonal anti-GAPDH (14C10) antibody (New England BioLabs, Whitby, Ontario, Canada) as loading controls. Densitometric analysis of Kune, actin and GAPDH

was conducted using Image J 1.47 v software (USA). Kune expression was expressed as a normalized value relative to the abundance of the loading control. For the samples of anal papillae, both Kune immunoreactive bands (29kDa and 75kDa) were measured and added together in the densitometric analysis.

4.3.8 Measurement of hemolymph ion levels: Larvae were placed on tissue paper which absorbed any moisture from the surface of the insect and then transferred to a petri dish filled with paraffin oil (Sigma-Aldrich, Oakville, Canada). Samples of hemolymph were collected by making a small tear in the cuticle with fine forceps causing the hemolymph to pool into a droplet. Levels of ions in collected droplets were measured using ion-selective microelectrodes (ISMEs) as previously decribed (Jonusaite et al. 2011). The following ionophore cocktail (Fluka, Buchs, Switzerland) and back-fill solution (in parentheses) were used for Ca^{2+} ISME: Ca^{2+} Ionophore I Cocktail A (100 mmol l^{-1} $CaCl_2$).

4.3.9 Statistics: Data are expressed as means ± SEM (*n*). Comparisons between groups or tissues were assessed with a one-way ANOVA followed by a Tukey's comparison test. To examine for significant differences in salinity effect on gene and protein expression/abundance, data were subjected to a Student's *t*-test. Statistical significance was allotted to differences with $p < 0.05$. All statistical analyses were conducted using SigmaStat 3.5 software (Systat Software, San Jose, USA).

4.4 Results

4.4.1 Identification and expression profiles of integral SJ protein genes in A. aegypti: Full coding sequences of the *A. aegypti* SJ genes *mega, sinu, kune,* and *nrx IV* were obtained by assembly of ESTs using NCBI EST database. To confirm the presence of a continuous message encoding for each SJ gene in *A. aegypti* larva, primers were designed to amplify regions within and across ESTs using whole body larval cDNA. Identities of assembled sequences were confirmed by performing BLAST and BLASTx searches using the full coding sequences of *mega, sinu, kune* and *nrx IV*. Primer sequences, amplicon size and related accession numbers are summarized in Table 4-1.

Transcripts encoding *mega, sinu, kune* and *nrx IV* were found in all tissues examined in this study which included the midgut, Malpighian tubules, hindgut and anal papillae of *A. aegypti* larvae (Fig. 4-1a). In addition, mRNA abundance of *mega, sinu* and *kune* were significantly greater in the hindgut and anal papillae than in the midgut or Malpighian tubules (Fig. 4-1b-d). Significantly higher *nrx IV* transcript abundance was also found in the hindgut and anal papillae compared to the Malpighian tubules (Fig. 4-1e).

4.4.2 Kune immunolocalization and protein expression: Immunohistochemical and western blot analysis of the claudin-like Kune in the osmoregulatory epithelia of *A. aegypti* larvae revealed that Kune was prominently expressed in the hindgut (Fig. 4-2a,c) where a single immunoreactive band of ~ 75 kDa resolved (Fig. 4-2d) and anal papillae (Fig. 4-2e,f) where two protein bands were detected at ~ 75 kDa and ~ 29 kDa (Fig. 4-2g). A band of ~ 29 kDa is in close agreement with the predicted mass of Kune at ~ 26 kDa while an ~ 75 kDa band would be a size consistent with a trimeric form of Kune.

In the hindgut, Kune localization was found at cell-cell contact regions between epithelial cells of the rectum (Fig. 4-2c). Histological sections of anal papillae epithelium

Table 4-1: Primer sets, amplicon size, annealing temperatures and GenBank accession numbers for *Aedes aegypti* SJ genes *mega*, *sinu*, *kune* and *nrx IV* and reference genes *18S rRNA* and *rp49*.

Gene	Primer Sequence	Amplicon length, bp	Annealing Temperature, ^{0}C	GenBank accession number
Megatrachea				
FOR	5'-CTGGTACTCTCGTGCAACTT-3'	191	59	BK008793
REV	5'-GTGTGGTCGGCTTCAGATGT-3'			
Sinuous				
FOR	5'-ACATCTTTTTGACGCAACGC-3'	210	58	BK008794
REV	5'-TTGTTCCTGTTCACCTACGG-3'			
Kune-kune				
FOR	5'-CGCTCTGCTTCACGCTATT-3'	203	62	KR781452
REV	5'-CGTTGTGTTCCCAGTTAGG-3'			
Neurexin IV				
FOR	5'-GCAAAGCAAGAAAGGCTACA-3'	192	59	KR781455
REV	5'-AGGAGGTTAGCTTTAGCTTT-3'			
18S rRNA				
FOR	5'- TTGATTCTTGCCGGTACGTG-3'	194	58	U65375
REV	5'- TATGCAGTTGGGTAGCACCA-3'			
rp49				
FOR	5'- GGCGTAAGCCGAAAGGTATT-3'	196	59	AY539746
REV	5'- CAGATGACACGGCTTTAGCG-3'			

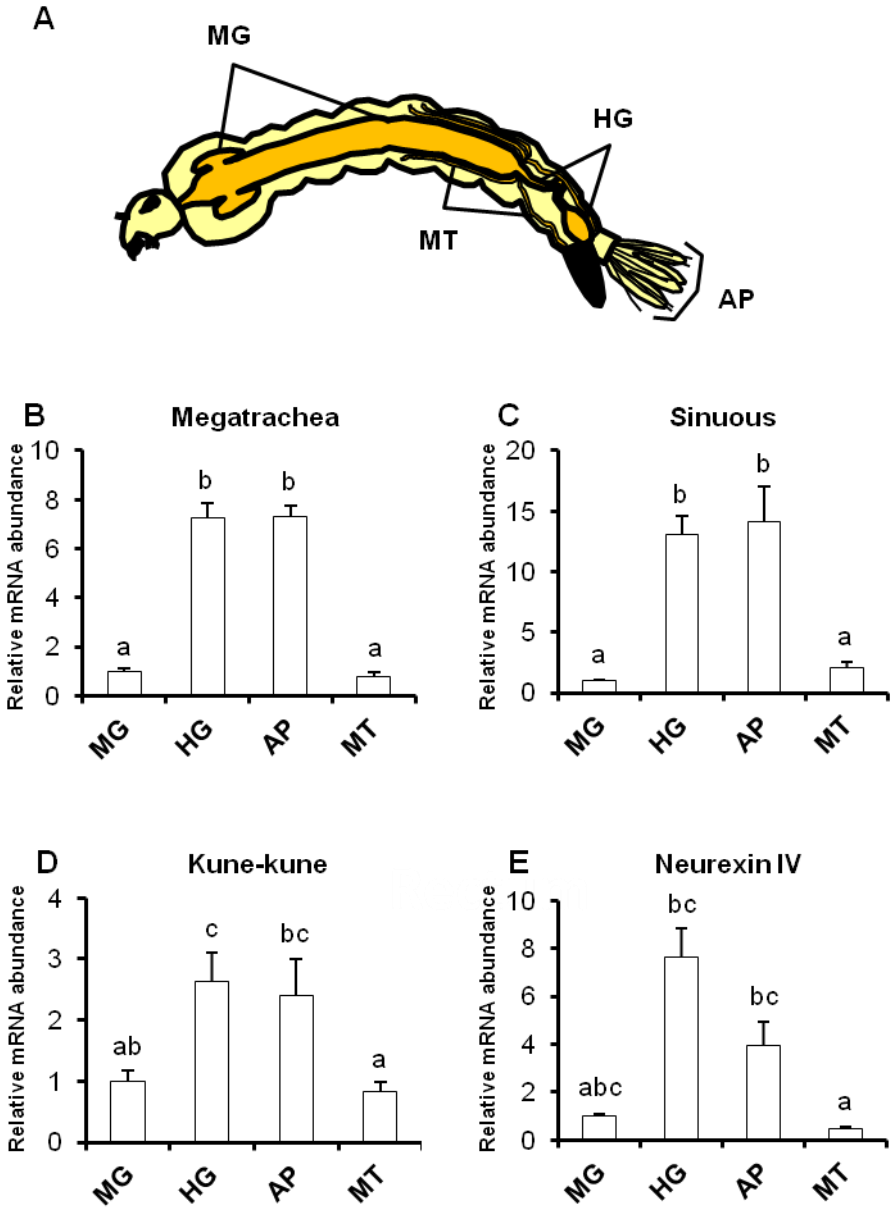

Figure 4-1: The osmoregulatory epithelia (**a**) and comparison of *mega*, *sinu*, *kune* and *nrx IV* mRNA abundance in the midgut (MG), hindgut (HG), anal papillae (AP) and Malpighian tubules (MT) of freshwater-reared *Aedes aegypti* larvae as determined by quantitative real-time PCR analysis. Each gene was normalized to *rp49* and was expressed relative to its levels in the midgut (assigned a value of 1). All data are expressed as mean values ± SEM (n = 6). Letters denote statistically significant differences between tissues (one-way ANOVA, Tukey's multiple comparison, $p < 0.05$).

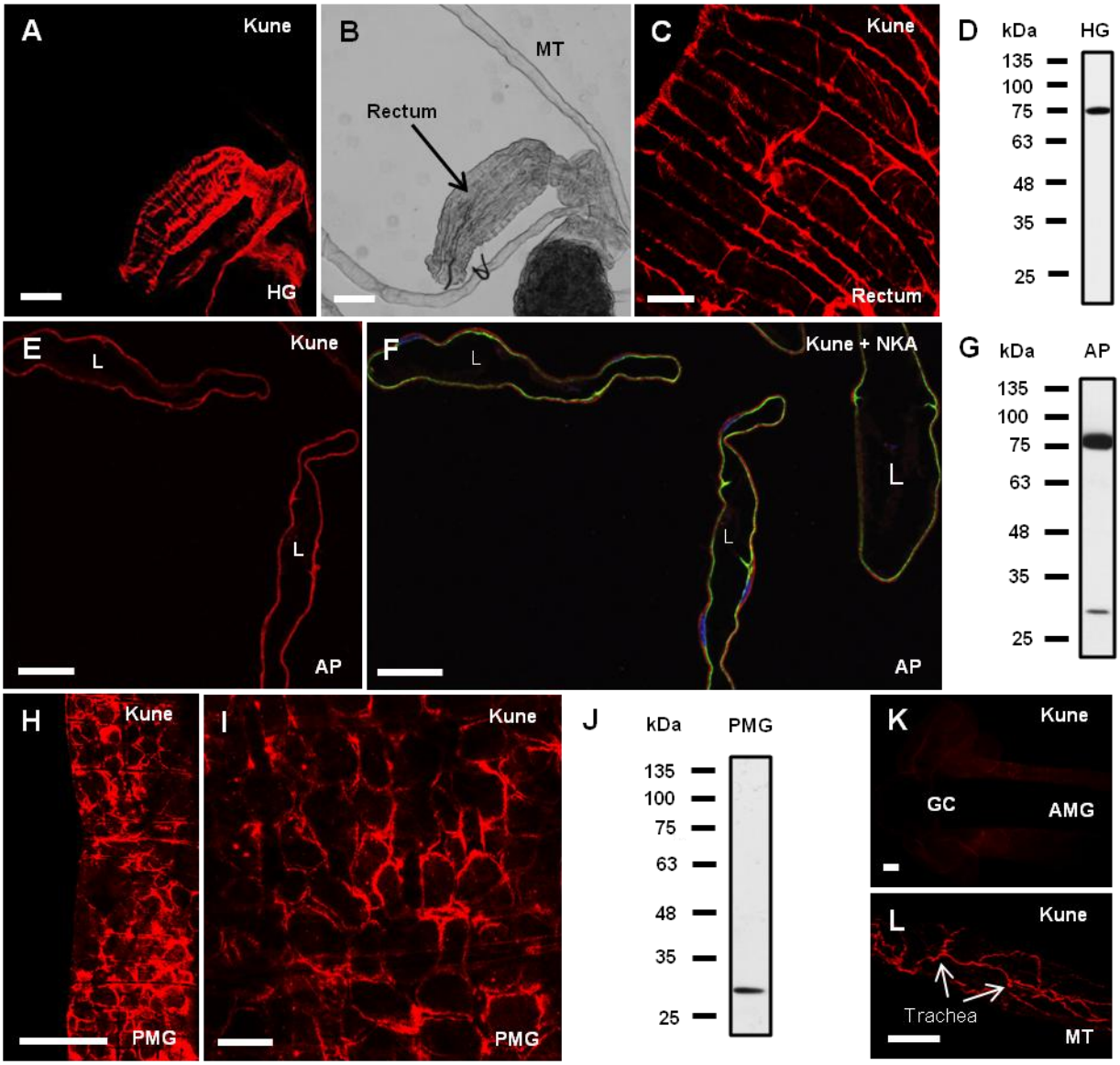

Figure 4-2: Immunolocalization and detection of Kune in the osmoregulatory epithelia of fourth instar *Aedes aegypti* larva by immunofluorescence (**a**, **c**, **e**, **f**, **h**, **i**, **k**, **l**) and western blot analysis (**d**, **g**, **j**). The hindgut (HG) showed enhanced immunostraining of Kune in the rectum (**a**) where it localized to the regions of cell-cell contact between the epithelial cells (**c**). (**b**) Brightfield image of **a**. A single immunoreactive band can be seen in HG that resolved at ~75 kDa (**d**). In the cross sections of anal papillae (AP), Kune immunoreactivity was detected in the papilla epithelium (**e**) where it localized to the apical surface and showed little to no immunolocalization with the basal membrane marker Na^+-K^+-ATPase (NKA; green) (**f**). Nuclei of AP epithelium are stained with DAPI (blue) and the lumen of papillae is labelled with the letter L in **f**. Two Kune immunoreactive bands of ~75 kDa and ~29 kDa were seen in AP. Kune was also expressed along the edges of the epithelial cells in the posterior midgut (PMG) (**h** and **i**) where a single band of ~29 kDa was detected (**j**). No immunostaining of Kune was seen in the gastric caecae (GC) and anterior midgut (AMG) (**k**) and in the Malpighian tubules (MT), Kune immunostaining was confined to the trachea (**l**, white arrows). Scale bars, (**a-c**, **i**, **k**) 100 µm, (**e**, **f**, **h**, **l**) 50 µm.

revealed that Kune immunostaining was confined to the apical surface showing little to no co-localization with Na^+-K^+-ATPase which was found to localize on the basal membrane (Fig. 4-2f). Kune expression was also detected along the edges of the epithelial cells of the posterior midgut (Fig. 4-2h,i) where a protein band of ~ 29 kDa was resolved (Fig. 4-2j). Kune showed no immunoreactivity in the gastric caecae and anterior midgut (Fig. 4-2k). In the Malpighian tubules, Kune immunostaining appeared to be restricted to tracheal branches and not cells of the tubule epithelium (Fig. 4-2l). No Kune immunoreactive bands were seen in the protein samples isolated from the gastric caecae, anterior midgut and Malpighian tubules (data not shown).

4.4.3 Effects of rearing salinity on hemolymph ion levels and pH: Rearing the larvae of *A. aegypti* in BW resulted in a significant increase in the hemolymph Na^+ and Cl^- levels and a decrease in the hemolymph K^+ levels compared to those of FW-reared animals (Table 4-2). In contrast, hemolymph Ca^{2+} levels and pH were not altered by BW rearing (Table 4-2).

4.4.4 qPCR analysis of Mega, Sinu and Nrx IV mRNA abundance in response to rearing salinity: When *A. aegypti* larvae were reared in BW, there was no significant change in the mRNA abundance of *sinu* and *nrx IV* in the midgut, Malpighian tubules, hindgut and anal papillae (Fig. 4-3). Although BW rearing did not alter transcript abundance of *mega* in the midgut, Malpighian tubules and hindgut (Fig. 4-3a-c), significantly lower *mega* mRNA abundance was found in the anal papillae of BW-reared larvae compared to FW animals (Fig. 4-3d).

4.4.5 Effects of rearing salinity on Kune mRNA and protein abundance: Rearing the larvae of *A. aegypti* in BW resulted in no significant change in the mRNA abundance of *kune* in the midgut, Malpighian tubules, hindgut and anal papillae (Fig. 4-4a). In contrast, Kune monomer protein abundance exhibited a significant increase in the posterior midgut and anal papillae in response to BW rearing (Fig. 4-4b). In addition to Kune monomer, some samples of the posterior midgut from BW-reared animals had a putative Kune trimer band of ~ 75 kDa which was absent from all

posterior midgut samples derived from FW-reared animals (data not shown). There was no change in the putative Kune trimer protein abundance in the hindgut of BW-reared larvae compared to FW animals (Fig. 4-4b). Because of lack of immunostaining and immunodetection of Kune in the anterior portion of the midgut (i.e. gastric caecae and anterior midgut) and epithelia of Malpighian tubules, Kune protein abundance was not examined in these tissues of BW-reared larvae.

Table 4-2: Ion levels **(**mmol l^{-1}) and pH in hemolymph of *Aedes aegypti* larvae reared in freshwater (FW) and brackish water (BW).

Rearing Medium	Hemolymph				
	$[Na^+]$	$[K^+]$	$[Cl^-]$	$[Ca^{2+}]$	pH
FW	73.4 ± 2.30	11.47 ± 0.66	47.7 ± 1.72	0.9 ± 0.09	8.0 ± 0.02
BW	117.0 ± 2.99*	5.63 ± 0.39*	86.5 ± 3.18*	1.0 ± 0.10	8.0 ± 0.02

Hemolymph ion levels are expressed as means ± SEM (*n* = 15-20)

*Statistically significant difference from the freshwater value

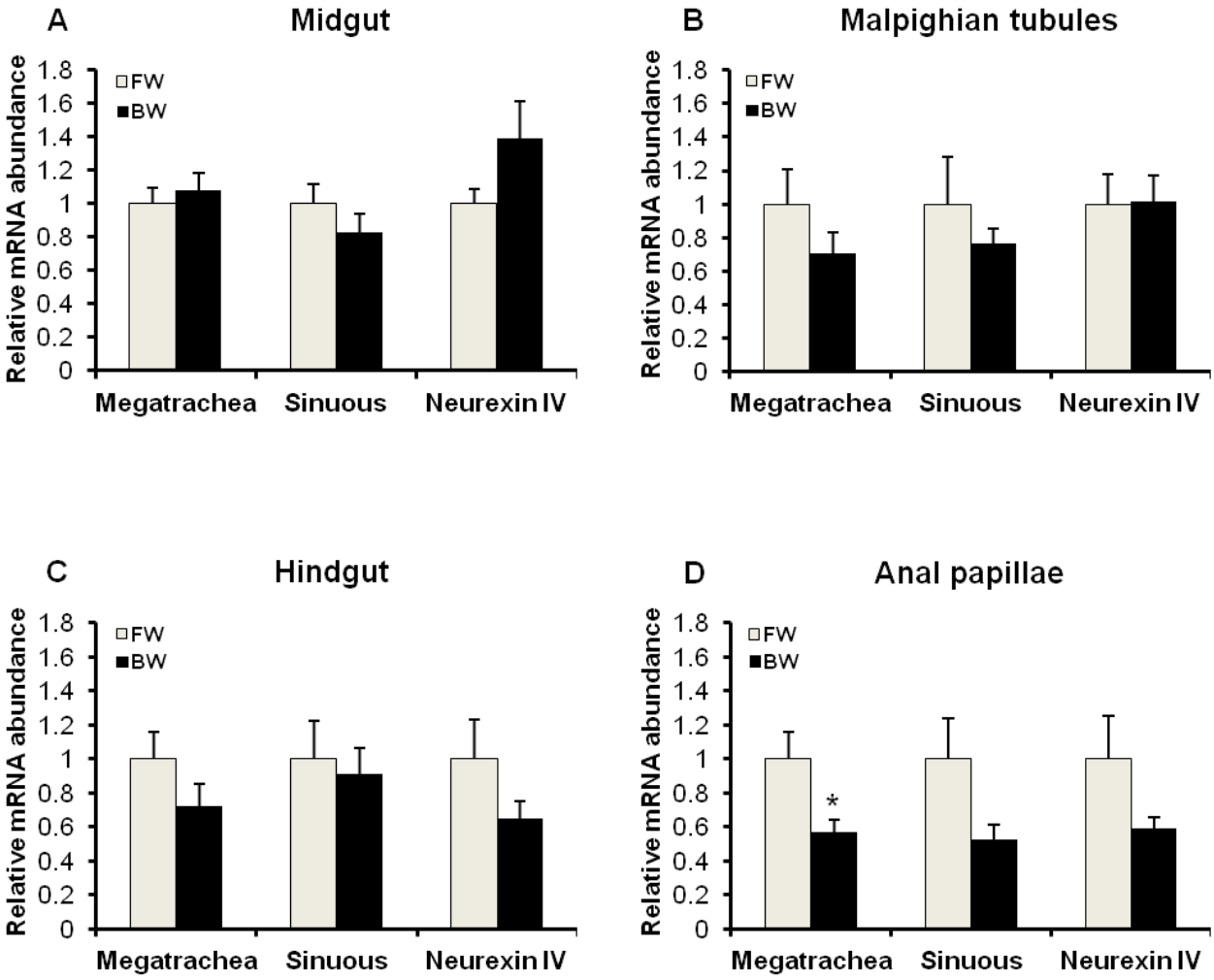

Figure 4-3: The effect of rearing salinity on mRNA abundance of *mega*, *sinu*, and *nrx IV* in the osmoregulatory epithelia of *Aedes aegypti* larvae as examined by quantitative real-time PCR analysis. The different salinities were freshwater (FW) and brackish water (BW; 30% seawater). Each SJ gene was normalized to *18S rRNA* and expressed relative to its FW value (assigned value of 1). All data are expressed as mean values ± SEM (n = 6). An asterisk denotes significant difference from FW (Student's t-test, $p < 0.05$).

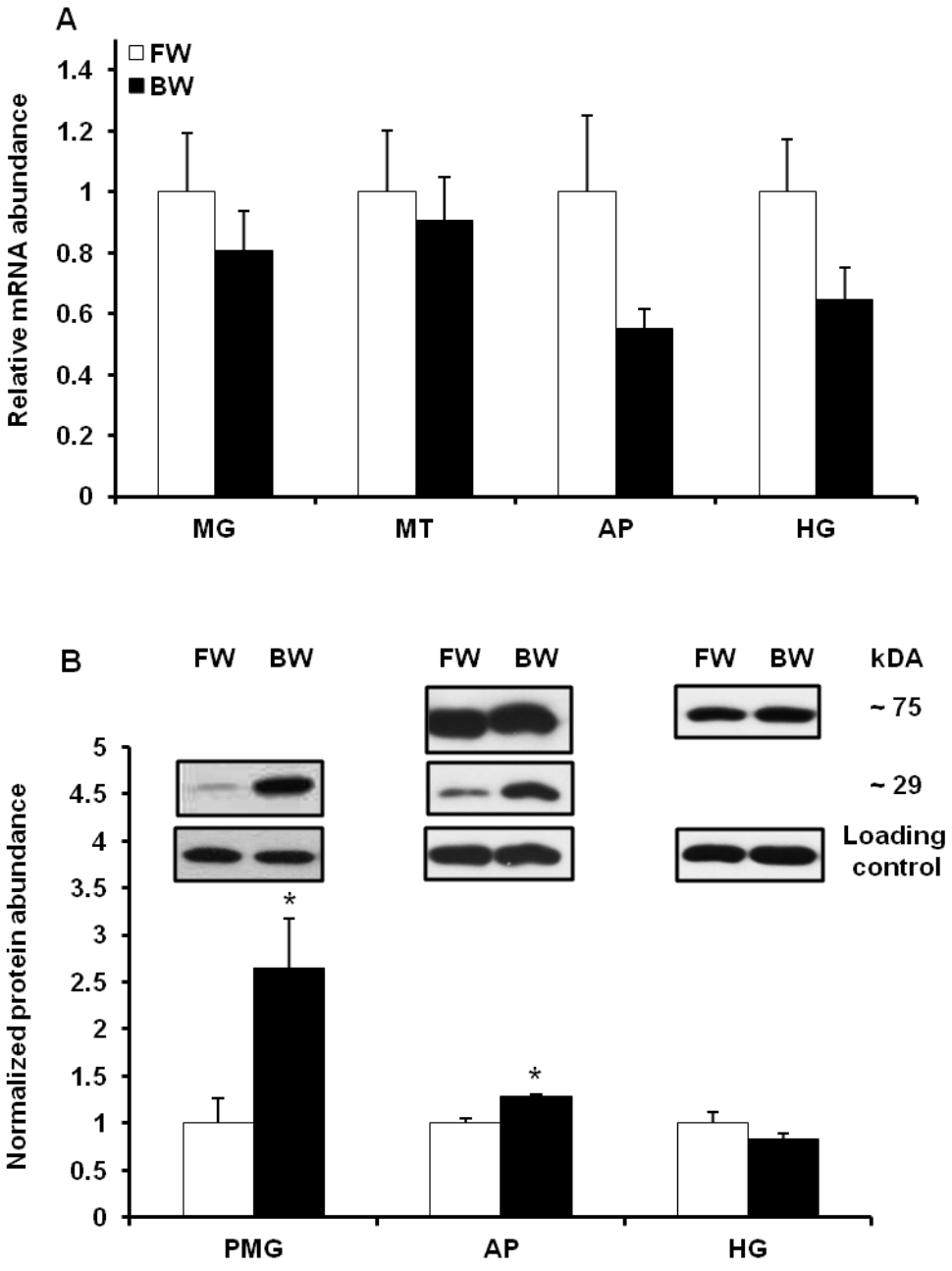

Figure 4-4: The effect of rearing salinity on Kune (**a**) mRNA and (**b**) normalized protein abundance in the osmoregulatory tissues of *Aedes aegypti* larvae as examined by quantitative real-time PCR and Western blot analysis. The different salinities were freshwater (FW) and brackish water (BW; 30% seawater). In **b**, representative western blots of Kune are ~29 kDa and ~75 kDa bands, loading controls are actin for PMG and AP, GAPDH for HG. All data are expressed as mean values ± SEM (n = 4-6)**.** An asterisk denotes significant difference from FW (Student's t-test, $p < 0.05$). MG, midgut; MT, Malpighian tubules; HG, hindgut; AP, anal papillae; PMG, posterior midgut.

4.5 Discussion

4.5.1 Tissue distribution of Mega, Sinu, Kune and Nrx IV in larval A. aegypti: When comparing the abundance of mRNA encoding Mega, Sinu, Kune and Nrx IV between different osmoregulatory tissues, all genes were more prominently expressed in the ectodermally derived epithelia such as the hindgut and anal papillae (Fig. 4-1). This observation is in general agreement with the prominent expression of Mega, Sinu, Kune and Nrx IV in the ectodermally derived tissues of larval *Drosophila* (Behr et al. 2003; Wu et al. 2004; Nelson et al. 2010; Baumgartner et al. 1996). In addition, since these SJ proteins are not expressed in the sSJ-bearing midgut and Malpighian tubules of larval *Drosophila*, they have been suggested to be pSJ-specific components (Izumi and Furuse 2014). Our finding of Mega, Sinu, Kune and Nrx IV transcripts in the midgut and Malpighian tubules in addition to the hindgut and anal papillae of *A. aegypti* larvae would suggest that these SJ proteins may be present in both pSJs and sSJs in this insect. This idea is supported, at least in part, by immunohistochemical and immunoblotting observations of Kune in the posterior midgut (see the following section). Given that all of our knowledge on these SJ components in arthropods is based on studies conducted on a single species (*Drosophila*), it is interesting and perhaps not surprising to note consistent and inconsistent observations in the appearance and localization of these genes/proteins in a second arthropod species. Furthermore, as our knowledge in this area grows, it will be interesting to consider how these differences relate to lifestyle (e.g. terrestrial versus aquatic) and the functional activities of different epithelia.

Extensive studies on the ultrastructural features of the *A. aegypti* anal papillae have revealed no evidence of lateral plasma membranes or SJs (Sohal and Copeland 1966; Edwards and Harrison 1983). Therefore, the presence of SJ proteins in this tissue, as shown in the current study (see Fig. 4-2e,f), may seem counterintuitive. One explanation for this may lie in the

additional cellular functions of these proteins such as epithelial morphogenesis and polarity (Behr et al. 2003; Wu et al. 2004; Nelson et al. 2010; Baumgartner et al. 1996; Laprise et al. 2009; Jaspers et al. 2012). Lack-of-function mutations of either Mega, Sinu, Kune or Nrx IV cause defects in the shape and size of the tracheal epithelium in *Drosophila* embryos (Behr et al. 2003; Wu et al. 2004; Nelson et al. 2010). In addition, Nrx IV mutants also show polarity defects in the embryonic epidermis as indicated by the mislocalization of the apical membrane marker Crumbs (Laprise et al. 2009). But it is important to acknowledge that all three Cldn-like proteins as well as Nrx IV are components of the tracheal SJs in *Drosophila*, and as such our gene expression results for *A. aegypti* anal papillae do not preclude the presence of *mega*, *sinu*, *kune* and *nrx IV* in the tracheolar cells that supply oxygen to the papillae epithelium (Edwards and Harrison 1983). However, immunohistochemical examination of Kune in the anal papillae clearly identifies this protein in the apical domain of the syncytium (see Fig. 4-2e,f and discussion below). Therefore, for this junction protein at least, a role in the function of an epithelium that apparently lacks occluding junctions awaits further investigation. Moreover, future experiments that localize Mega, Sinu and Nrx IV in the anal papillae would be of particular interest.

4.5.2 Localization and immunoblotting of Kune: Consistent with Kune transcript expression, Kune protein was detected in the hindgut and anal papillae of *A. aegypti* larvae. Within the hindgut, Kune immunoreactivity was found to be most prominent at junctional contact regions between epithelial cells of the rectum (Fig. 4-2a,c), suggesting that Kune is a component of pSJs in this tissue. Interestingly, Western blot analysis of Kune in the hindgut revealed a single immunoreactive band that resolved at ~ 75 kDa (Fig. 4-2d) which is about three times heavier than the predicted Kune molecular weight of ~ 26 kDa. To the best of our knowledge, no studies have reported a Western blot analysis of *Drosophila* Kune which prompts us to suggest that the ~75 kDa band in *A. aegypti* corresponds to Kune trimer. In TJs, Cldn are known to engage in

homo- and heterophilic interactions within the same cell and with Cldns of adjacent cells and by these means assemble into stable dimers and higher order oligomers (Furuse et al. 1999; Günzel and Yu 2013; Van Itallie and Anderson 2013). It has been recently shown by Suzuki et al. (Suzuki et al. 2013) that a claudin-like protein IP39 found in the plasma membrane of *Euglena gracilis* forms trimers, and these polymerize into strands similar to those of TJs. Western blotting of IP39 resolved all three forms of this protein, i.e. monomer, dimer and trimer (Suzuki et al. 2013). In the present study, bands corresponding to a putative Kune trimer as well as the monomer were detected in larval *A. aegypti* anal papillae samples (Fig. 4-2g) where Kune localization was confined to the apical membrane domain of the papillae epithelium (Fig. 4-2e,f). The role of Cldn-like Kune in a syncytial epithelium that lacks SJs (such as the anal papillae of *A. aegypti*) is unclear at present. However, non-junctional Cldn and Cldn-like protein localization has previously been reported such as Cldn-like CLC-2 in the hypodermal seam cell syncytium of *C. elegans* and select Cldns of vertebrate epithelial cells that are distributed diffusely along plasma membranes (Asano et al. 2003; Gregory et al. 2001; Furuse et al. 2002).

As shown in this study, Kune was also detected in the midgut of *A. aegypti* larvae where it could be immunoreactively visualized at SJ domains between epithelial cells of posterior midgut and as a single band resolving at ~ 29 kDa by Western blotting (Fig. 4-2h-j). The latter observation is inconsistent with *Drosophila* Kune which was reported to be absent throughout midgut epithelium (Nelson et al. 2010; Izumi and Furuse 2014). On the other hand, Kune is nondetectable in the anterior portion of the midgut (including gastric caecae), of larval *A. aegypti* (see Fig. 4-2k). *Drosophila* midgut possesses sSJs which contain at least two sSJ-specific proteins, Mesh and Snakeskin (Izumi et al. 2012; Yanagihashi et al. 2012). However, a number of proteins generally known as pSJ components have been found at the SJs between midgut epithelial cells in *Drosophila*, suggesting that SJs possess a complex molecular architecture in

this tissue (Baumann 2001; Wu et al. 2004; Izumi et al. 2012; Byri et al. 2015). The current data raise the possibility that Kune is a component of sSJs in the posterior midgut of larval *A. aegypti*. Alternatively, the cells of the posterior midgut epithelium of *A. aegypti* larvae may contain both sSJs and pSJs. The presence of cells expressing both Mesh and Kune were identified in the *Drosophila* proventriculus, suggesting the formation of hybrid junctions (Izumi et al. 2012), and both types of SJs have been observed to coexist side by side in the same junctional complex of insect Malpighian tubules (Noirot-Timothee and Noirot 1980; Lane and Skaer 1980).

Lastly, our immunohistochemical analysis of Kune in the Malpighian tubules of *A. aegypti* larvae revealed its absence in this epithelium (see Fig. 4-2a,b) which is in agreement with *Drosophila* Kune (Nelson et al. 2010). On the other hand, Kune immunoreactivity was observed in the tracheal branches that were still associated with the tubules (see Fig. 4-2l). This suggests that in contrast to observations in the anal papillae, the detection of Kune mRNA in the Malpighian tubules of larval *A. aegypti* may reflect the presence of tracheal epithelium.

4.5.3 The response of A. aegypti and transmembrane SJ proteins to BW rearing: In the current study, *A. aegypti* larvae were successfully reared in a BW condition equivalent to 30% SW strength without mortality. The larvae responded to a long-term BW exposure with an increase in hemolymph Na^+ and Cl^- levels, a decrease in hemolymph K^+ levels and no change in hemolymph Ca^+ levels or pH (see Table 4-2). The observed increase in hemolymph Na^+ levels in response to BW rearing is consistent with what has been reported for larval *A. aegypti* in a previous study (Donini et al. 2006). In addition, similar observations of elevated hemolymph Na^+ and Cl^+ levels and unaltered Ca^{2+} levels upon chronic exposure to 34% SW were made for the FW larval *C. quinquefasciatus* (Patrick and Bradley 2000). In BW media, larvae of *A. aegypti* have been shown to greatly increase drinking rates (Edwards 1982; Clements, 1992). This increased intake of fluid presumably allows the larvae to maintain body volume in the face of the osmotic loss of

water to the external medium (Clements 1992). However, ingested fluid will also contribute to the salt load that must be eliminated. As a result, larvae must modulate transport processes in the epithelia of iono/osmoregulatory tissues. Salinity-induced changes in the ion transport machinery have been suggested to occur in the epithelium of the Malpighian tubules of larval *A. aegypti* (Donini et al. 2006). Ion transport by the tubules is altered such that there is a decrease in K^+ with an apparent but not significant increase in Na^+ secretion which would help counteract elevated Na^+ levels in hemolymph when larvae are raised in BW (Donini et al. 2006). The anal papillae, which are sites of ion uptake from dilute environments, show ultrastructural changes and a decrease in Na^+ and Cl^- uptake when *A. aegypti* larvae are exposed to increased ambient salinity (Donini and O'Donnell 2005; Sohal and Copeland 1966; Donini et al. 2007). The underlying mechanisms responsible for the alterations in ion transport by the Malpighian tubules and anal papillae when larvae encounter higher salinity remain largely unclear.

In the current study, changes in Mega transcript and Kune protein abundance in the anal papillae of BW-reared *A. aegypti* larvae support the notion that these larvae utilize anal papillae to cope with differences in environmental salt levels. It is interesting to consider the response of the two Cldn-like proteins to increased environmental salinity in the tissue that lacks SJs. In short, transcript abundance of *mega* significantly reduced while *kune* was unaltered in anal papillae of BW-reared larvae. However, Kune protein levels were significantly elevated in the anal papillae of BW-reared animals (Fig. 4-3d, Fig. 4-4b) and taken together, data seem to suggest different functions for the two Cldn-like proteins in this epithelium. It seems reasonable to propose this because although Kune protein and transcript levels did not match exactly, *kune* transcript levels were not decreased as was seen with *mega*. Furthermore, lack of correlation between mRNA and protein abundance has been observed for other TJ associated proteins and such a phenomenon is postulated to be a consequence of mRNA-regulatory mechanisms or

differences in protein degradation rate (Kolosov and Kelly 2013; Fournier et al. 2010). Nevertheless, future studies would benefit from an examination of Mega protein abundance. As to what role either Kune or Mega plays in the syncytial anal papillae epithelium is difficult to speculate at this stage. In addition to their barrier function at SJs, both proteins are required for the tracheal tube size control in *Drosophila* embryos (Behr et al. 2003; Nelson et al. 2010). The lengths of tracheal tubes are increased in both *kune* and *mega* mutants which is accompanied by an increase in the dimension of the apical surface of tracheal cells (Behr et al. 2003; Nelson et al. 2010; Jaspers et al. 2012; Laprise et al. 2010). As mentioned earlier, morphological changes have been shown to occur in the epithelium of anal papillae of larval *A. aegypti* when the animals are reared in diluted seawater. More specifically, the papillae are shorter, contain fewer mitochondria and reduced apical membrane folds, suggesting a reduction in ion uptake from external environment (Sohel and Copeland 1966). If a similar role exists for Kune in the regulation of epithelial size in the trachea and anal papillae, it would be reasonable to suggest that an increase in Kune protein abundance in the anal papillae of BW-reared animals, as reported in this study, may at least be partially responsible for the reduction in the surface area of the apical plasma membrane of the papilla epithelium and presumably ion uptake in BW environment. These ideas will require further examination.

Kune protein abundance was also altered in the posterior midgut of larval *A. aegypti* in response to BW, albeit with no change in transcript abundance (Fig. 4-4). If Kune is required for the formation of paracellular barrier in the posterior midgut of *A. aegypti* larvae, increased Kune abundance in this epithelium of BW-reared larvae would suggest that the posterior midgut becomes ‘tighter’ under saline conditions. The midgut of larval *A. aegypti* is the site of nutrient absorption and ion transport (Clements 1992; Onken and Moffett 2009; Jagadeshwaran et al. 2010). Morphological and electrophysiological examination of *A. aegypti* larval midgut has

revealed regional differentiation along this segment of the alimentary canal (Clark et al. 1999; Clark et al. 2000; Clark et al. 2005; Jagadeshwaran et al. 2010). However, the precise roles of the midgut regions in absorption of nutrients and ionoregulation are not well known. It has been demonstrated that the epithelium of the posterior midgut is metabolically more active, as shown by a much greater mitochondrial density, and electrically 'leakier' compared to the epithelium of the anterior midgut (Clark et al. 2000; Clark et al. 2005). Moreover, based on the morphological features, ion substitution experiments and expression pattern of membrane transporters, larval posterior midgut has been suggested as a site of fluid secretion, active Na^+ absorption and paracellular Cl^- conductance (Clark et al. 2005; Patrick et al. 2006; Jagadeshwaran et al. 2010). If some water is secreted through the paracellular pathway in the posterior midgut, it would be tempting to speculate that increased Kune expression (and presumably decreased permeability) in this epithelium in response to BW may limit passive water movement into the lumen and that of Cl^- into the hemolymph. This would be particularly useful as it would limit water loss and salt loading in larvae exposed to saline conditions. To better characterize Kune function in the larval posterior midgut, it will require *in vitro* study of isolated posterior midgut to correlate Kune expression with measurements of paracellular permeability properties.

In contrast to Mega, mRNA abundance of genes encoding Sinu and Nrx IV did not alter in any of the osmoregulatory epithelia of larval *A. aegypti* in response to salinity (see Fig. 4-3). In *Drosophila*, both Sinu and Nrx IV are essential for the SJ formation but have different functions in this process. Nrx IV is required for the formation of the morphologically seen septa whereas Sinu has a critical role in attaining the correct number of septa and in organizing septa into contiguous circumferential ribbons (Baumgartner et al. 1996; Wu et al. 2004). Our finding of the expression of *sinu* and *nrx IV* in all the osmoregulatory tissues of *A. aegypti* larva and that they did not respond to salinity may suggest that these SJ proteins maintain baseline junctional

formation and that physiological alterations in response to environmental change may be modulated entirely by other SJ components. It has been recently demonstrated that the epithelia of a cnidarian *Stylophora pistillata* express Nrx IV homolog which localizes at the apical border of the cells where morphological SJs are observed, suggesting a conserved function of Nrx IV as a core structural component of invertebrate SJs (Ganot et al. 2015).

4.5.4 Perspectives and significance: The complex molecular architecture of occluding junctions is now broadly recognized as the major reason that these structures are so dynamic and with this comes growing recognition of a remarkable diversity as well as tremendous structural and functional plasticity of paracellular transport processes across animal epithelia. This paradigm shift in how we view the molecular physiology of transepithelial solute transport has been driven primarily by work conducted on terrestrial organisms, and more specifically mammalian models (or tissues derived from them). However, metazoans arose in an aquatic setting and large proportions of them still reside in water (or have life stages that rely on an aquatic environment). Therefore, it seems likely that a great deal is waiting to be learned about occluding junctions and their protein composite by considering their role in aquatic organism homeostasis. The regulation of salt and water balance will be a particularly fruitful avenue for further study because it occupies a dominant role in the physiology of many aquatic organisms. In addition, it involves internal epithelia that contribute to the regulation of systemic solute composition in a manner not dissimilar to that seen in terrestrial vertebrates as well as epithelia that directly interface with the surrounding environment. With regard to the latter, the importance of TJ proteins in aquatic vertebrate gill and skin permeability has become a focal point and common conclusion of recent studies (e.g. Kolosov et al. 2014; Bui and Kelly 2014). However, the physiology and barrier function of SJs remain poorly understood in invertebrates and almost completely overlooked in aquatic invertebrates (for review see Chapter 3). Therefore, observations made in the current

study provide an impetus to consider the role of SJs in salt and water balance more broadly across the invertebrate clade. In the specific case of larval *A. aegypti*, the potential contribution of SJ proteins to the maintenance of salt and water balance is of additional importance because this species is a vector of re-emerging viral diseases, Dengue and Chikungunya, and mounting evidence suggests that these animals successfully breed in salinated water in addition to FW (Ramasamy and Surendran 2012). Therefore, a more complete understanding of their iono/osmoregulatory physiology has the potential to play a part in measures that seek to control their populations.

4.6 References

Anderson JM, Van Itallie CM (2009) Physiology and function of the tight junction. Cold Spring Harb Perspect Biol 1:a002584

Angelow S, Ahlstrom R, Yu ASL (2008) Biology of claudins. Am J Physiol Renal Physiol 295:F867-F876

Asano A, Asano K, Sasaki H, Furuse M, Tsukita S (2003) Claudins in *Caenorhabditis elegans*: their distribution and barrier function in the epithelium. Curr Biol 13:1042-1046

Bagherie-Lachidan M, Wright SI, Kelly SP (2008) Claudin-3 tight junction proteins in *Tetraodon nigroviridis*: cloning, tissue-specific expression, and a role in hydromineral balance. Am J Physiol Regul Integr Comp Physiol 294:R1638-R1647

Baumann O (2001) Posterior midgut epithelial cells differ in their organization of the membrane skeleton from other *Drosophila* epithelia. Exp Cell Res 270:176-187

Baumgartner S, Littleton JT, Broadie K, Bhat MA, Harbecke R, Lengyel JA, Chiquet-Ehrismann R, Prokop A, Bellen HJ (1996) A *Drosophila* neurexin is required for septate junction and blood-nerve barrier formation and function. Cell 87: 1059-1068

Behr M, Riedel D, Schuh R (2003) The claudin-like Megatrachea is essential in septate junctions for the epithelial barrier function in *Drosophila*. Dev Cell 5:611-620

Beyenbach KW, Piermarini PM (2011) Transcellular and paracellular pathways of transepithelial fluid secretion in Malpighian (renal) tubules of the yellow fever mosquito *Aedes aegypti*. Acta Physiol (Oxf) 202:387-407

Bradley TJ (1994) The role of physiological capacity, morphology, and phylogeny in determining habitat use in mosquitoes. In: Wainwright PC, Reilly SM (eds) Ecological Morphology. The University of Chicago Press, Chicago, IL, pp 303-318

Bui P, Kelly SP (2014) Claudin-6, -10d, and -10e contribute to seawater acclimation in the euryhaline puffer fish *Tetraodon nigroviridis*. J Exp Biol 217:1758-1767

Byri S, Misra T, Syed ZA, Bätz T, Shah J, Boril L, Glashauser J, Aegerter-Wilmsen T, Matzat T, Moussian B, Uv A, Luschnig S (2015) The triple-repeat protein anakonda controls epithelial tricellular junction formation in *Drosophila*. Dev Cell 33:535-548

Chasiotis H, Kelly SP (2008) Occludin immunolocalization and protein expression in goldfish. J Exp Biol 211:1524-1534

Chasiotis H, Kelly SP (2009) Occludin and hydromineral balance in *Xenopus laevis*. J Exp Biol 212:287-296

Chasiotis H, Kolosov D, Kelly SP (2012a) Permeability properties of the teleost fish gill epithelium under ion-poor conditions. Am J Physiol Regul Integr Comp Physiol 302:R727-R739

Chasiotis H, Kolosov D, Bui P, Kelly SP (2012b) Tight junctions, tight junction proteins and paracellular permeability across the gill epithelium of fishes: a review. Resp Physiol Neurobiol 184:269-281

Clark TM, Hutchinson MJ, Huegel KL, Moffett SB, Moffett DF (2005) Additional morphological and physiological heterogeneity within the midgut of larval *Aedes aegypti* (Diptera: Culicidae) revealed by histology, electrophysiology, and effects of *Bacillus thuringiensis* endotoxin. Tissue Cell 37:457-468

Clark TM, Koch A, Moffett DF (2000) The electrical properties of the anterior stomach of the larval mosquito (*Aedes aegypti*). J Exp Biol 203:1093-1101

Clark TM, Koch A, Moffett DF (1999) The anterior and posterior ‘stomach’ regions of larval *Aedes aegypti* midgut: regional specialization of ion transport and stimulation by 5-hydroxytryptamine. J Exp Biol 202:247-252

Clements AN (1992) The Biology of Mosquitoes, vol 1. Chapman & Hall, London

Del Duca O, Nasirian A, Galperin V, Donini A (2011) Pharmacological characterisation of apical Na^+ and Cl^- transport mechanisms of the anal papillae in the larval mosquito *Aedes aegypti*. J Exp Biol 214:3992-3999

Donini A, O'Donnell MJ (2005) Analysis of Na^+, Cl^-, K^+, H^+ and NH_4^+ concentration gradients adjacent to the surface of anal papillae of the mosquito *Aedes aegypti*: application of self-referencing ion-selective microelectrodes. J Exp Biol 208:603-610

Donini A, Gaidhu MP, Strasberg D, O'Donnell MJ (2007) Changing salinity induces alterations in hemolymph ion concentrations and Na^+ and Cl^- transport kinetics of the anal papillae in the larval mosquito, *Aedes aegypti*. J Exp Biol 210:983-992

Donini A, Patrick ML, Bijelic G, Christensen RJ, Ianowski JP, Rheault MR, O'Donnell MJ (2006) Secretion of water and ions by Malpighian tubules of larval mosquitoes: Effects of diuretic factors, second messengers, and salinity. Physiol Biochem Zool 79:645-655

Duffy NM, Bui P, Bagherie-Lachidan M, Kelly SP (2011) Epithelial remodeling and claudin mRNA abundance in the gill and kidney of puffer fish (*Tetraodon biocellatus*) acclimated to altered environmental ion levels. J Comp Physiol B 181: 219-238

Edwards HA (1982) *Aedes aegypti*: Energetics of osmoregulation. J Exp Biol 101: 135-141

Edwards HA, Harrison JB (1983) An osmoregulatory syncytium and associated cells in a freshwater mosquito. Tissue Cell 15:271-280

Flower NE, Filshie BK (1975) Junctional structures in the midgut cells of lepidopteran caterpillars. J Cell Sci 17:221-239

Fournier ML, Paulson A, Pavelka N, Mosley AL, Gaudenz K, Bradford WD, Glynn E, Li H, Sardiu ME, Fleharty B, Seidel C, Florens L, Washburn MP (2010) Delayed correlation of mRNA and protein expression in rapamycin-treated cells and a role for Ggc1 in cellular sensitivity to rapamycin. Mol Cell Proteomics 9:271-284

Furuse M, Hata M, Furuse K, Yoshida Y, Haratake A, Sugitani, Y, Noda T, Kubo A, Tsukita S (2002) Claudin-based tight junctions are crucial for the mammalian epidermal barrier: a lesson from claudin-1-deficient mice. J Cell Biol 156: 1099-1111

Furuse M, Sasaki H, Tsukita S (1999) Manner of interaction of heterogeneous claudin species within and between tight junction strands. J Cell Biol 147:891-903

Ganot P, Zoccola D, Tambutté E, Voolstra CR, Aranda M, Allemand D, Tambutté S (2015) Structural molecular components of septate junctions in cnidarians point to the origin of epithelial junctions in eukaryotes. Mol Biol Evol 32: 44-62. doi: 10.1093/molbev/msu265

Green CR, Bergquist PR (1982) Phylogentic relationships within the invertebrates in relation to the structure of septate junctions and the development of 'occluding' junctional types. J Cell Sci 53:279-305

Gregory M, Dufresne J, Hermo L, Cyr D (2001) Claudin-1 is not restricted to tight junctions in the rat epididymis. *Endocrinology* 142:854-863

Günzel D, Yu ASL (2013) Claudins and the modulation of tight junction permeability. Physiol Rev 93:525-69

Ionescu A, Donini A (2012) *Aedes* CAPA-PVK-1 displays diuretic and dose dependent antidiuretic potential in the larval mosquito *Aedes aegypti* (Liverpool). J Insect Physiol 58:1299-1306

Izumi Y, Furuse M (2014) Molecular organization and function of invertebrate occluding junctions. Semin Cell Dev Biol 36:186-193

Izumi Y, Yanagihashi Y, Furuse M (2012) A novel protein complex, Mesh-Ssk, is required for septate junction formation in the *Drosophila* midgut. J Cell Sci 125:4923-4933

Jagadeshwaran U, Onken H, Hardy M, Moffett SB, Moffett DF (2010) Cellular mechanisms of acid secretion in the posterior midgut of the larval mosquito (*Aedes aegypti*). J Exp Biol 213:295-300

Jaspers MH, Nolde K, Behr M, Joo SH, Plessmann U, Nikolov M, Urlaub H, Schuh R (2012) The claudin Megatrachea protein complex. J Biol Chem 287:36756-36765

Jonusaite S, Kelly SP, Donini A (2011) The physiological response of larval *Chironomus riparius* (Meigen) to abrupt brackish water exposure. J Comp Physiol B 181:343-352

Kaushal SS, Groffman PM, Likens GE, Belt KT, Stack WP, Kelly VR, Band LE, Fisher GT (2005) Increased salinization of fresh water in the northeastern United States. PNAS 102:13517-13520

Kolosov D, Kelly SP (2013) A role for tricellulin in the regulation of gill epithelium permeability. Am J Physiol Regul Integr Comp Physiol 304:R1139-R1148

Kolosov D, Bui P, Chasiotis H, Kelly SP (2013) Claudins in teleost fishes. Tissue Barriers 1: e25391

Kolosov D, Chasiotis H, Kelly SP (2014) Tight junction protein gene expression patterns and changes in transcript abundance during development of model fish gill epithelia. J Exp Biol 217:1667-1681

Knust E, Bossinger O (2002) Composition and formation of intercellular junctions in epithelial cells. Science 298:1955-1959

Kumai Y, Bahubeshi A, Steele S, Perry SF (2011) Strategies for maintaining Na^+ balance in zebrafish (*Danio rerio*) during prolonged exposure to acid water. Comp Biochem Physiol 160A:52-62

Kwong RM, Perry SF (2013) The tight junction protein claudin-b regulates epithelial permeability and sodium handling in larval zebrafish, *Danio rerio*. Am J Physiol Regul Integr Comp Physiol 304:R504-R513

Lane NJ, Skaer HB (1980) Intercellular junctions in insect tissues. In: Berridge MJ, Treherne JE, Wigglesworth VB (eds). Advances in Insect Physiology, vol. 15. Academic Press, London, pp 35-213

Laprise P, Lau KM, Harris KP, Silva-Gagliardi NF, Paul SM, Beronja S, Beitel GJ, McGlade CJ, Tepass U (2009) Yurt, Coracle, Neurexin IV and the Na($^{+}$),K($^{+}$)-ATPase form a novel group of epithelial polarity proteins. Nature 459:1141-1145

Laprise P, Paul SM, Boulanger J, Robbins RM, Beitel GJ, Tepass U (2010) Epithelial polarity proteins regulate Drosophila tracheal tube size in parallel to the luminal matrix pathway. Curr Biol 20:55-61

Littleton JT, Bhat MA, Bellen HJ (1997) Deciphering the function of neurexins at cellular junctions. J Cell Biol 137:793-796

Luquet CM, Genovese G, Rosa GA, Pellerano GN (2002) Ultrastructural changes in the gill epithelium of the crab *Chasmagnathus granulates* (Decapoda: Grapsidae) in diluted and concentrated seawater. Mar Biol 141:753-760

Luquet C, Pellerano G, Rosa G (1997) Salinity-induced changes in the fine structure of the gills of the semiterrestrial estuarian crab, *Uca uruguayensis* (Nobili, 1901) (Decapoda, Ocypodidae). Tissue Cell 29:495-501

Nelson KS, Furuse M, Beitel GJ (2010) The Drosophila Claudin Kune-kune is required for septate junction organization and tracheal tube size control. Genetics 185:831-839

Noirot-Timothee C, Noirot C (1980) Septate and scalariform junctions in arthropods. Int Rev Cytol 63:97-141

Onken H, Moffett DF (2009) Revisiting the cellular mechanisms of strong luminal alkalinization in the anterior midgut of larval mosquitoes. J Exp Biol 212:373-377

Patrick ML, Aimanova K, Sanders HR, Gill SS (2006) P-type Na^+/K^+-ATPase and V-type H^+-ATPase expression patterns in the osmoregulatory organs of larval and adult mosquito *Aedes aegypti*. J Exp Biol 209:4638-4651

Patrick ML, Bradley TJ (2000) The physiology of salinity tolerance in larvae of two species of Culex mosquitoes: the role of compatible solutes. J Exp Biol 203:821-830

Patrick ML, Gonzalez RJ, Bradley TJ (2001) Sodium and chloride regulation in freshwater and osmoconforming larvae of *Culex* mosquitoes. J Exp Biol 204:3345-3354

Pond GJ, Passmore ME, Borsuk FA, Reynolds L, Rose CA (2008) Downstream effects of moutaintop coal mining: comparing biological conditions using family and genus-level macroinvertebrate bioassessment tools. J North Am Benthol Soc 127:717-737

Ramasamy R, Surendran SN (2012) Global climate change and its potential impact on disease transmission by salinity-tolerant mosquito vectors in coastal zones. Front Physiol 3:198

Simske JS, Hardin J (2011) Claudin family proteins in *Caenorhabditis elegans*. Methods Mol Biol 762:147-169

Sohal RS, Copeland E (1966) Ultrastructural variations in the anal papillae of *Aedes aegypti* (L) at different environmental salinities. J Insect Physiol 12:429-434

Stork T, Engelen D, Krudewig A, Silies M, Bainton RJ, Klämbt C (2008) Organization and function of the blood-brain barrier in *Drosophila*. J Neurosci 28:587-597

Suzuki H, Ito Y, Yamazaki Y, Mineta K, Uji M, Abe K, Tani K, Fujiyoshi Y, Tsukita S (2013) The four-transmembrane protein IP39 of *Euglena* forms strands by a trimeric unit repeat. Nat Commun 4:1766

Tepass U, Tanentzapf G, Ward R, Fehon R (2001) Epithelial cell polarity and cell junctions in *Drosophila*. Annu Rev Genet 35:747-784

Tipsmark CK, Kiilerich P, Nilsen TO, Ebbesson LOE, Stefansson SO, Madsen SS (2008) Branchial expression patterns of claudin isoforms in Atlantic salmon during seawater acclimation and smoltification. Am J Physiol Integr Regul Comp Physiol 294:R1563-R1574

Van Itallie CM, Anderson JM (2013) Claudin interactions in and out of the tight junction. Tissue Barriers 1:e25247

Williams WD (2001) Anthropogenic salinization of inland waters. Hydrobiol 466:329-337

Wu VM, Schulte J, Hirschi A, Tepass U, Beitel GJ (2004) Sinuous is a *Drosophila* claudin required for septate junction organization and epithelial tube size control. J Cell Biol 164:313-323

Yanagihashi Y, Usui T, Izumi Y, Yonemura S, Sumida M, Tsukita S, Uemura T, Furuse M (2012) Snakeskin, a membrane protein associated with smooth septate junctions, is required for intestinal barrier function in *Drosophila*. J Cell Sci 125: 1980-1990

CHAPTER 5:

CHARACTERIZATION OF THE SEPTATE JUNCTION PROTEINS SNAKESKIN AND MESH IN AQUATIC LARVAL MOSQUITO (*AEDES AEGYPTI*) AND THEIR CONTRIBUTION TO SALT AND WATER BALANCE

5.1 Summary

This study examined the distribution and localization of the septate junction (SJ) proteins snakeskin (Ssk) and mesh in osmoregulatory organs of larval mosquito (*Aedes aegypti*), as well as their response to altered environmental salt levels. Transcripts encoding Ssk and mesh were detected in tissues of endodermal origin such as the midgut and Malpighian tubules of *A. aegypti* larvae, but not in tissues of ectodermal origin such as the hindgut and anal papillae. Immunolocalization of Ssk and mesh in the midgut and Malpighian tubules indicated that both proteins are concentrated at regions of cell-cell contact between epithelial cells. No immunoreactivity was found in the hindgut or anal papillae. Transcript abundance of *ssk* and *mesh* was higher in the midgut and Malpighian tubules of brackish water (BW, 30% SW) reared *A. aegypti* larvae when compared with freshwater (FW) reared animals. Therefore, [^{3}H]polyethylene glycol (MW 400 kDa, PEG-400) flux was examined across isolated midgut preparations as a measure of midgut paracellular permeability, and it was found that PEG-400 flux was greater across the midgut of BW versus FW larvae. Taken together, data suggest that Ssk and mesh are found in smooth SJs (sSJs) of larval *A. aegypti* and that their abundance alters in association with changes in epithelial permeability when larvae reside in water of differing salt content. This latter observation suggests that Ssk and mesh play a role in the homeostatic control of salt and water balance in larval *A. aegypti*.

5.2 Introduction

In metazoa, epithelial tissues play important roles as barriers that isolate the body from the outer environment and form compositionally distinct fluid compartments within the body. To form a barrier, epithelial cells have specialized occluding cell-cell junctions that control the movement of biological material through the paracellular pathway. In vertebrates, paracellular transport is controlled by tight junctions (TJs) which are formed in the most apical region of lateral cell membranes and mediate selective paracellular permeability depending on physiological requirements and/or cell type (for review see Anderson and Van Itallie 2009). The epithelia of invertebrates generally lack TJs and instead, the paracellular barrier function is provided by the apicolateral plasma membrane spanning septate junctions (SJs) (for review see Chapter 3). In cross-section electron microscopy, SJs appear as ladder-like structures between adjacent cells with septa spanning a 15-20 nm intercellular space (Green and Bergquist 1982). Morphological variants of SJs exist across invertebrate phyla based on tangentially cut sections and some animals possess multiple types of SJs that are specific to different epithelia (Green and Bergquist 1982; Chapter 3). In arthropods, two morphologically different types of SJs have been described: the pleated SJs (pSJs) and the smooth SJs (sSJs). The pSJs form regular undulating rows of septa that surround the cell circumferentially whereas septa in the sSJs show regularly spaced parallel lines (Noirot-Timothee and Noirot 1980; Lane and Skaer 1980; Green and Bergquist 1982). In insects, the pSJs are generally observed in epithelia of ectodermal origin such as the epidermis, foregut, hindgut, trachea, and salivary glands, whereas sSJs seem to occur in endodermal epithelia such as the midgut and gastric caecae as well as Malpighian tubules (Noirot-Timothee and Noirot 1980; Lane and Skaer 1980; Bradley et al. 1982). The functional differences in the permeability properties of pSJs and sSJs are not well understood because of a paucity of information on their molecular physiology.

Genetic and molecular analyses in *Drosophila melanogaster* have identified more than twenty pSJ-associated components and loss-of-function mutations in most of these proteins prevent the formation of septa or SJ organization. In turn, this disrupts the transepithelial barrier properties of ectodermally derived epithelia (for review see Izumi and Furuse 2014; Chapter 3). Among these proteins, seventeen are transmembrane components of the pSJ complex (Izumi and Furuse 2014; Deligiannaki et al. 2015; Chapter 3). Another set of proteins that are important for the formation of pSJs in *Drosophila* reside on the cytoplasmic side of the membrane (see Izumi and Furuse 2014; Chapter 3). In contrast to pSJs, few genetic and molecular analyses have been carried out on sSJs. Several studies have described the isolation of sSJ-enriched membrane fractions from insect midgut and have demonstrated protein bands within these fractions by SDS-PAGE, but these proteins have not been further characterized (Green et al. 1983; Baldwin and Hakim 1999). The only characterized sSJ-specific proteins are *Drosophila* snakeskin (Ssk), mesh and tetraspanin 2A (Tsp2A) (Yanagihashi et al. 2012; Izumi et al. 2012; Izumi et al. 2016). Ssk is a protein with four membrane-spanning domains, two short extracellular loops, cytoplasmic N- and C-terminal domains, and a cytoplasmic loop and appears to be conserved only within arthropod species (Yanagihashi et al. 2012). Mesh is a single-pass transmembrane protein with a large extracellular region containing a NIDO domain, an Ig-like E set domain, an AMOP domain, a vWD domain, and a sushi domain, and has orthologs in other invertebrates such as *Caenorhabditis elegans* and sea urchin as well as vertebrates such as mouse (Sugahara et al. 2007; Izumi et al. 2012). Most recently identified Tsp2A is a tetraspanin family protein with N- and C-terminal short intracellular domains, two extracellular loops and one short intracellular turn (Izumi et al. 2016). All three proteins are localized exclusively in the epithelia of the proventriculus, midgut and Malpighian tubules, where sSJs reside. Paracellular barrier function in *Drosophila* midgut requires proper sSJ formation (Izumi et al. 2012; Yanagihashi et al. 2012;

Izumi et al. 2016). Ssk, mesh and Tsp2A form a complex with each other and show mutually dependent localizations at sSJs (Izumi et al. 2016). Compromised expression of *ssk*, *mesh* or *tsp2A* causes ultrastructural defects in the sSJs, reduces barrier function of the midgut against a 10-kDa fluorescent tracer and results in mislocalization of other SJ proteins such as coracle (Cora), lethal giant larvae (Lgl), and fasciclin III (FasIII) (Izumi et al. 2012; Yanagihashi et al. 2012; Izumi et al. 2016). The finding that usually pSJ associated Cora, Lgl, FasIII as well as discs large are present at the sSJs of *Drosophila* midgut suggests that the latter proteins are components of both arthropod pSJs and sSJs, although their functions at sSJs remain unknown (Izumi et al. 2012). Nevertheless, it is clear that similar to pSJs, sSJs function to restrict paracellular solute diffusion in *Drosophila*. Very little is known about the sSJs properties and their proteins in the epithelia of aquatic insects which live in environments that can change in parameters such as osmolarity and ionic milieu.

Habitats of freshwater (FW) larval mosquito *Aedes aegypti* are prone to changes in such parameters, especially increase in salinity, due to climatic and anthropogenic factors (Clements 1992; Ramasamy and Surendran 2012; Williams 2001; Cañedo-Argüelles et al. 2013), and as a result, ion and water regulation is an important process for survival. In FW environments, *A. aegypti* larvae possess hyper-ionic/osmotic hemolymph relative to the external water, and as a consequence, must cope with passive ion loss and water gain across body surfaces (Clements 1992). Larvae maintain salt and water balance largely by regulating material entry through the midgut and elimination through the excretory system comprised of the Malpighian tubules and hindgut (Bradley 1994; Clark et al. 2005; Donini et al. 2006). In addition, the larvae use externally protruding anal papillae as sites of ion uptake in habitats of low ionic strength (Donini and O'Donnell 2005; Del Duca et al. 2011). The contribution of SJ regulated paracellular ion and water transport to the osmoregulatory homeostasis in larval *A. aegypti* in its natural FW habitats

or upon changes in environmental ion levels is not well understood. In a recent study, which examined a role for transmembrane SJ proteins megatrachea (Mega), sinuous (Sinu), kune-kune (Kune) and neurexin IV (Nrx IV) in salt and water balance in larval *A. aegypti*, it was found that transcripts encoding these SJ proteins were present in the osmoregulatory tissues such as the midgut, Malpighian tubules, hindgut and anal papillae, and their abundance was greater in the hindgut and anal papillae (Chapter 4). In addition, Kune was immunolocalized to SJ domains between the epithelial cells of the rectum and posterior midgut and in the apical membrane domain of the syncytial anal papilla epithelium (Chapter 4). Rearing *A. aegypti* larvae in brackish water (BW) resulted in tissue-specific alterations in *mega* mRNA and Kune protein abundance, supporting the hypothesis that SJ proteins are important in the maintenance of salt and water balance in response to salinity (Chapter 4). With this background information in mind, the current study was aimed at investigating whether Ssk and mesh are sSJ proteins in larval mosquito, and if so, whether there is a role for sSJ-specific proteins such as Ssk and mesh in the osmoregulatory homeostasis of larval *A. aegypti*. It was reasoned that if Ssk and mesh participate in the regulation of salt and water balance by altering SJ permeability under different saline conditions, it can be hypothesized that differences in the transcript abundance of Ssk and mesh would be observed in animals reared in FW versus those reared in BW, and that these would occur in conjunction with changes in the paracellular permeability of the epithelia in which Ssk and mesh occur.

5.3 Methods and materials

5.3.1 Insects: A laboratory colony of *Aedes aegypti* (Linnaeus) was maintained in the Department of Biology at York University as previously described (Del Duca et al. 2011).

5.3.2 Long-term acclimation to brackish water: Hatched 1st instar larvae were reared in either FW with composition ([ion] µmol l^{-1} [Na^+] 590; [Cl^-] 920; [Ca^{2+}] 760; [K^+] 43; pH 7.35) or 30% SW (10.5 g/l Instant Ocean SeaSalt®) which served as the experimental brackish water (BW) treatment as previously detailed (Chapter 4).

5.3.3 *Identification of ssk and mesh in Aedes aegypti and quantitative real time PCR analysis:* Organs involved in the regulation of salt and water balance such as the midgut (with the gastric caecae), the Malphigian tubules, the hindgut and the anal papillae, were isolated from 4th instar *A. aegypti* larvae in ice-cold physiological saline (composition in mmol l^{-1}: L-proline, 5; L-glutamine, 9.1; L-histidine, 8.74; L-leucine, 14.4; L-arginine, 3.37; glucose, 10; succinic acid, 5; malic acid, 5; trisodium citrate, 10; NaCl, 30; KCl, 3; $NaHCO_3$, 5; $MgSO_4$, 0.6; $CaCl_2$, 5; HEPES, 25; pH 7) and RNA was extracted using TRIzol® reagent (Invitrogen, Burlington, ON, Canada) according to the manufacturer's instructions. All RNA samples were treated with the TURBO DNA-*free*™ kit (Ambion®, Life Technologies Inc., Burlington, ON, Canada) and template cDNA was synthesized using iScript™ cDNA synthesis kit as per the manufacturer's instructions (Bio-Rad, Mississauga, ON, Canada). cDNA was stored at -20 ^{0}C until subsequent use. Using the National Center for Biotechnology Information (NCBI) database BLAST search engine, expressed sequence tags (ESTs) of genes encoding snakeskin (Ssk, *ssk*) and mesh (*mesh*) were retrieved from the *A. aegypti* genome and confirmed to be protein coding using a reverse BLASTx. A reading frame was established using BLASTn alignment and ORF Finder (http://www.ncbi.nlm.nih.gov/gorf/). All primer sets were designed based on EST sequences using Primer3 software (v. 0.4.0). Primer sequences, amplicon sizes and related accession

numbers are summarized in Table 5-1. Reverse transcriptase PCR (RT-PCR) was used to examine the presence of *ssk* and *mesh* transcripts in the osmoregulatory tissues of *A. aegypti* larvae with *18S rRNA* serving as an internal control. Amplicons were resolved by gel electrophoresis and sequenced at the York University Core Molecular Facility (Depatment of Biology, York University, ON, Canada). Full coding sequences for *A. aegypti ssk* and *mesh* were confirmed using a BLAST search and submitted to GenBank. Sequence data for *A. aegypti ssk* and *mesh* are available under the accession numbers KR781453 and KR781454, respectively (see Table 5-1).

To examine transcript abundance of *ssk* and *mesh* in the midgut, Malpighian tubules, hindgut and anal papillae of *A. aegypti* larvae, quantitative real time PCR (qPCR) was performed using the primers listed in Table 5-1 and SYBR Green I Supermix (Bio-Rad Laboratories Ltd., Mississauga, ON, Canada) with a Chromo4™ Detection System (CFB-3240, Bio-Rad Laboratories Canada Ltd.) as previously outlined in Chapter 4. *18S rRNA* and *rp49* transcript abundance was used as an internal control.

5.3.4 Immunolocalization of Ssk and mesh in osmoregulatoy organs of A. aegypti larvae: Immunolocalization of Ssk and mesh in whole-mount guts and paraffin sections of anal papillae was conducted according to previously described protocols (Chapter 2 and Chapter 4) using rabbit polyclonal antibodies raised against the C-terminal cytoplasmic region of *Drosophila* Ssk (Yanagihashi et al. 2012) and mesh (Izumi et al. 2012) (a kind gift from Dr. Mikio Furuse, National Institute for Physiological Sciences, Japan) at 1:1000 in antibody dilution buffer (10% goat serum, 3% BSA and 0.05% Triton X-100 in phosphate-buffered saline). Images of sections of anal papillae were captured using an Olympus IX71 inverted microscope (Olympus Canada, Richmond Hill, ON, Canada) equipped with an X-CITE 120XL fluorescent Illuminator (X-CITE, Mississauga, ON, Canada). Whole mounts were examined using an Olympus BX-51 laser-

scanning confocal microscope. All images were assembled using Adobe Photoshop CS2 software (Adobe Systems Canada, Toronto, ON, Canada).

5.3.5 Transepithelial [^{3}H]polyethylene glycol-400 (PEG-400) flux across the midgut of A. aegypti: Paracellular permeability in the midgut epithelium of larval *A. aegypti* was determined by measuring [^{3}H]polyethylene glycol (molecular mass 400 Da; 'PEG-400'; American Radiolabeled Chemicals, Inc., Saint Louis, MO, USA) flux. An *in situ* preparation of the midgut was prepared by first removing the alimentary canal of 4th instar larvae and placing it in physiological saline. The alimentary canal was then moved onto a square piece of aluminum foil and foregut (with gastric caecae) and hindgut (with Malpighian tubules) were sealed with vaseline, leaving only the midgut segment exposed. The preparation was transferred to a 35 mm Petri dish where it was bathed in 1 ml of saline containing 0.5 µCi [^{3}H]PEG-400. After a 5h incubation, the preparation was washed (3 x with fresh saline), excess vaseline removed from the ends of the alimentary canal and the entire gut transferred into a 1.5 ml microtube with 100 µl 100 % nitric acid. Once the gut epithelium had dissolved, 450 µl of fresh saline was added and the tube was vortexed, centrifuged and 500 µl of resulting supernatant collected for radioactivity measurement. [^{3}H]PEG-400 flux rates were calculated according to the following equation:

$$P = \Delta[PEG]_{Ap} \times Volume_{Ap} / [PEG]_{Bl} \times Time \times 3600 \times Surface\ Area,$$

where P is the flux rate of the PEG-400 in cm s^{-1}; $[PEG]_{B1}$ is the measured mean radioactivity on the basolateral side; $\Delta[PEG]_{Ap}$ is the change in radioactivity on the apical side (midgut lumen) and 3600 converts time from hours to seconds. The surface area of the midgut was calculated from measurements of its length and diameter, assuming it to be a cylinder with two open ends as follows:

$$Surface\ Area = 2 \pi r l,$$

where r and l are the radius and the length of the midgut, respectively.

5.3.6 Statistics: Data are expressed as means ± SEM (*n*). For tissue comparison and to examine for significant differences in salinity effect on gene expression and midgut permeability, data were subjected to a Student's *t*-test. Statistical significance was allotted to differences with $p < 0.05$. All statistical analyses were conducted using SigmaStat 3.5 software (Systat Software, San Jose, USA).

5.4 Results

5.4.1 Identification and expression profiles of ssk and mesh: Using bioinformatic tools (i.e. NCBI, BLASTn, BLASTx), genes encoding for the SJ proteins Snakeskin (*ssk)* and Mesh (*mesh*) were identified in the *A. aegypti* genome. Transcripts encoding *ssk* and *mesh* were found in the midgut and Malpighian tubules, but were absent in the hindgut and anal papillae of *A. aegypti* larvae (Fig. 5-1).

5.4.2 Ssk and mesh immunolocalization: Immunolocalization of Ssk and mesh in the osmoregulatory organs of larval *A. aegypti* revealed that both proteins reside in epithelia of endodermal origin such as the gastric caecae (Fig. 5-2a,b) and midgut epithelium (Fig. 5-2c,d,i,j) as well as Malpighian tubules (Fig. 5-2e,f,k,l). In midgut and Malpighian tubule epithelia, Ssk and mesh were concentrated into a belt surrounding each epithelial cell where SJs occur (Fig. 5-2b,d,f,j,l). Immunoreactivity of Ssk and mesh were not detected in the hindgut (Fig. 5-2g,m) or in paraffin sections of anal papillae (Fig. 5-2h,n).

5.4.3 qPCR analysis of ssk and mesh mRNA abundance in response to rearing salinity: Rearing *A. aegypti* larvae in BW did not alter the tissue distribution of *ssk* and *mesh* mRNA, but it significantly changed their transcript abundance in the midgut and Malpighian tubules. Specifically, *ssk* and *mesh* mRNA abundance increased in both the midgut and Malpighian tubules of BW-reared larvae (Fig. 5-3a,b).

5.4.4 Effects of rearing salinity on midgut permeability: In FW-reared *A. aegypti* larvae, midgut epithelium [^{3}H]PEG-400 flux rates (efflux, basolateral to apical) were 3.47 ± 0.28 cm s^{-1} x 10^{-9} (Fig. 5-4). Rearing the larvae in BW was accompanied by an approximate doubling of PEG-400 flux across the midgut compared to values from midguts of FW reared larvae (Fig. 5-4c).

Table 5-1: Primer sets, amplicon size, annealing temperatures and GenBank accession numbers for *Aedes aegypti ssk* and *mesh* homologs and reference genes.

Gene	Primer Sequence	Amplicon length, bp	Annealing Temperature, ^{0}C	GenBank accession number
Snakeskin				
FOR REV	5'- CTGGTACTCTCGTGCAACTT-3' 5'- GTGTGGTCGGCTTCAGATGT-3'	191	59	KR781453
Mesh				
FOR REV	5'- ACATCTTTTTGACGCAACGC-3' 5'- TTGTTCCTGTTCACCTACGG-3'	210	58	KR781454
18S rRNA				
FOR REV	5'- TTGATTCTTGCCGGTACGTG-3' 5'- TATGCAGTTGGGTAGCACCA-3'	194	58	U65375
rp49				
FOR REV	5'- GGCGTAAGCCGAAAGGTATT-3' 5'- CAGATGACACGGCTTTAGCG-3'	196	59	AY539746

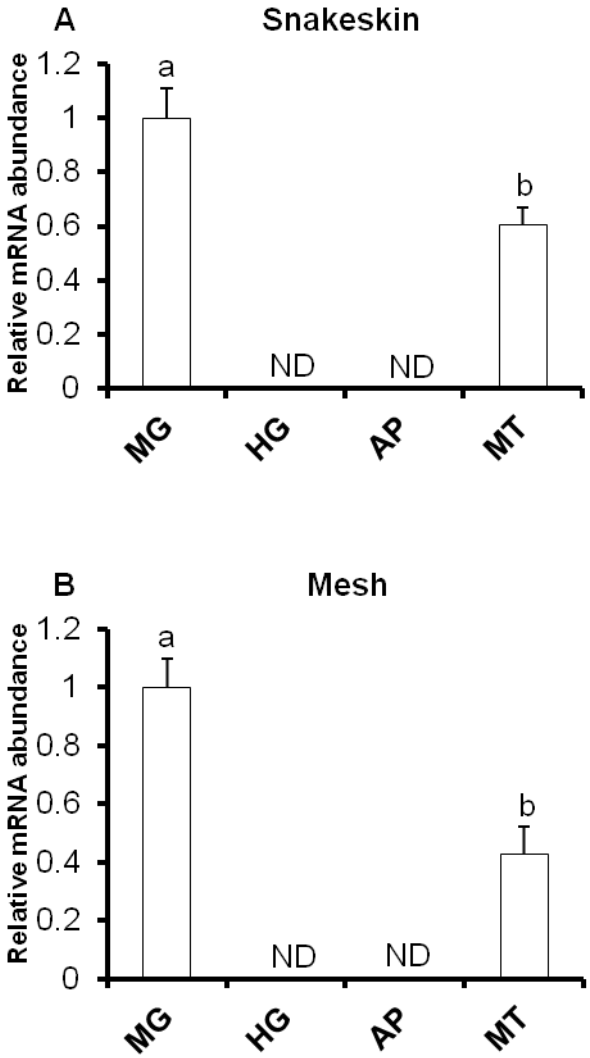

Figure 5-1: Relative mRNA abundance of (**a)** *ssk* and (**b**) *mesh* in the midgut (MG), hindgut (HG), anal papillae (AP) and Malpighian tubules (MT) of *Aedes aegypti* larvae reared in freshwater (FW). Each gene was normalized to *18S* and was expressed relative to its levels in the midgut (assigned a value of 1). All data are expressed as mean values ± SEM (n = 6). Letters denote statistically significant differences between tissues (Student's t-test, $p < 0.05$). ND, not detected.

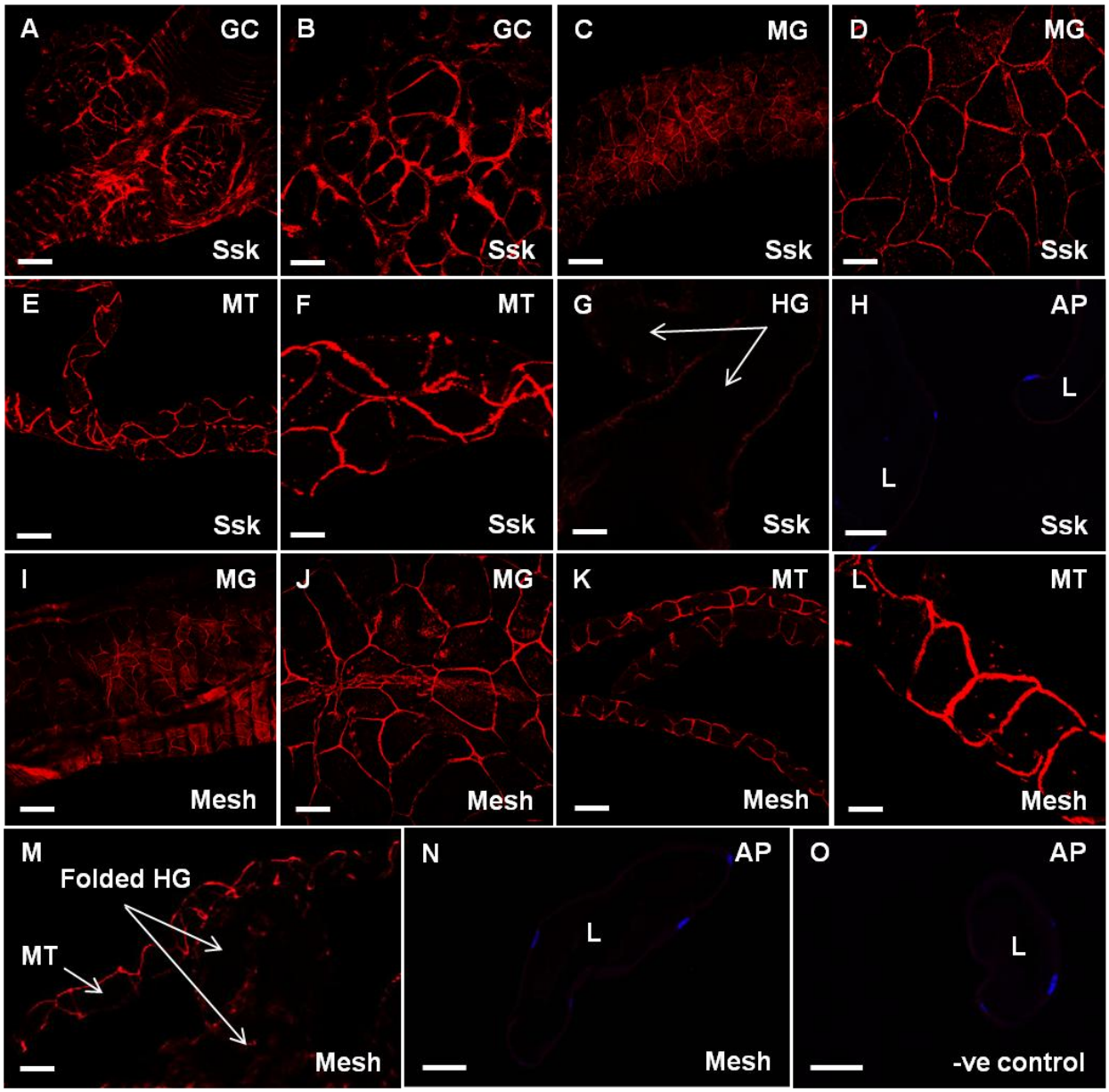

Figure 5-2: Immunofluorescence staining of snakeskin (Ssk) and mesh in the osmoregulatory tissues of fourth instar *Aedes aegypti* larva. Ssk was localized at the cell-cell contact regions in the epithelial cells of the gastric caecae (**a**, **b**). Ssk as well as mesh were also concentrated at the cell-cell contact regions in the epithelial cells of the midgut (**c**, **d**, **i**, **j**) and Malpighian tubules (**e**, **f**, **k**, **l**). **B**, **d**, **f**, **j** and **l** are higher magnification images of **a**, **c**, **e**, **i** and **k**, respectively. Ssk and mesh immunoreactivity was not detected in the hindgut (**g**, **m**; indicated by arrows) or anal papillae (**h**, **n**). **O** shows a control section of anal papillae probed with secondary antibody only. Nuclei of anal papilla epithelium are stained with DAPI (blue) in **h**, **n**, **o**. Scale bars, (**a**, **c**, **e**, **g-i**, **k**, **m-o**) 50 µm, (**b**, **d**, **f**, **j**, **l**) 20 µm.

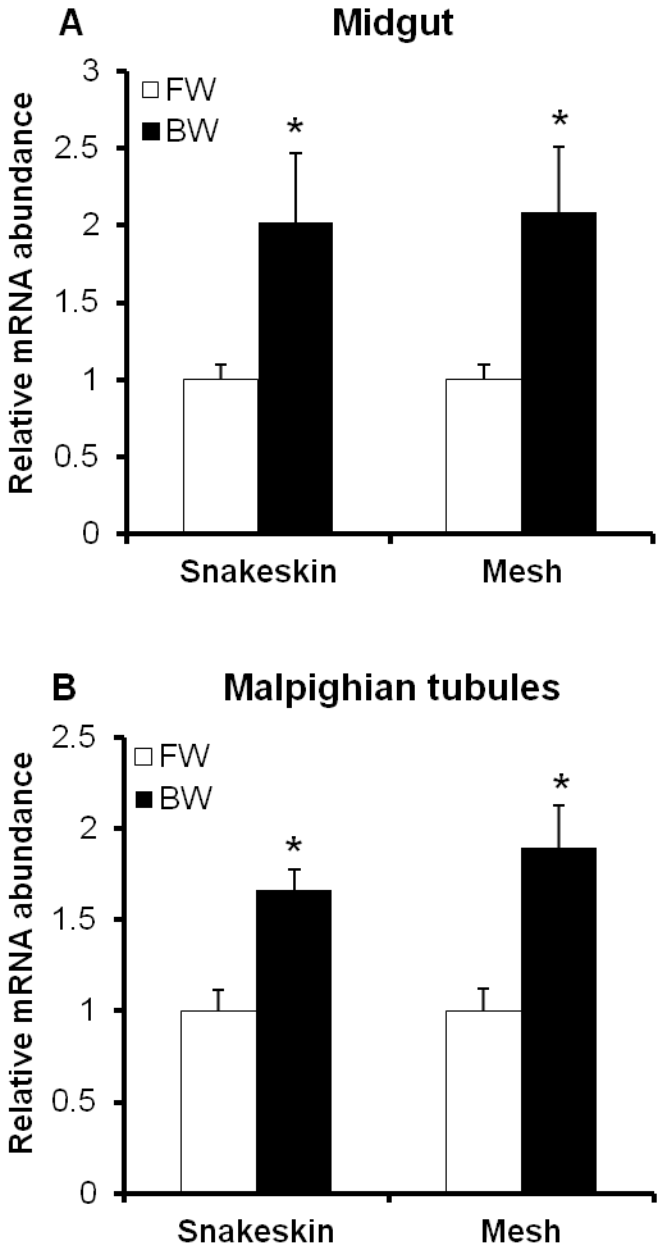

Figure 5-3: The effect of rearing salinity on mRNA abundance of *ssk* and *mesh* in (**a**) midgut and (**b**) Malpighian tubules of larval *Aedes aegypti*, as examined by quantitative real-time PCR (qRT-PCR) analysis. The different salinities were freshwater (FW) and brackish water (BW; 30% seawater). Each gene was normalized to *rp49* and expressed relative to its FW value (assigned value of 1). All data are expressed as mean values ± SEM (n = 6)**.** An asterisk denotes significant difference from FW (Student's *t*-test, $p < 0.05$).

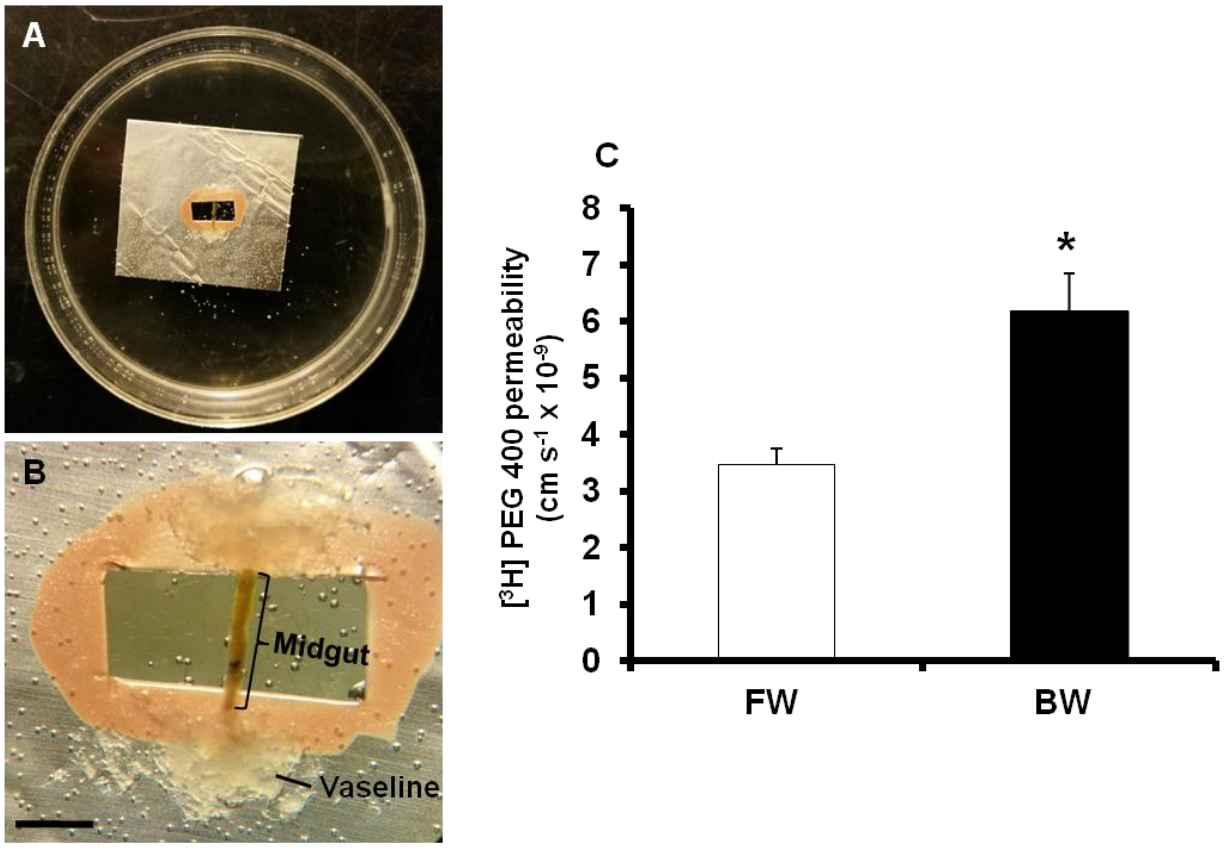

Figure 5-4: (**a**) Representative preparation of a midgut of larval *Aedes aegypti* in [^{3}H]PEG-400 containing saline bath. **B** shows a higher magnification view of the preparation displayed in **a**. Scale bar, 2 mm. (**c**) The effects of rearing salinity on [^{3}H]PEG-400 movement across the midgut epithelium of *A. aegypti* larvae. The different salinities were freshwater (FW) and brackish water (BW; 30% seawater). [^{3}H]PEG-400 flux in the midgut (from bath to midgut lumen) was measured after 5h exposure to 0.5 µCi/ml [^{3}H]PEG-400. All data are expressed as mean values ± SEM (n = 13-15). An asterisk denotes significant difference (Student's t-test, $p < 0.05$).

5.5 Discussion

5.5.1 Organ-specific expression and tissue-specific localization of Ssk and mesh in larval A. aegypti: Here we provide the first examination of organ-specific differences in the distribution of *ssk* and *mesh* mRNA as well as tissue-specific localization of Ssk and mesh in the osmoregulatory organs of an aquatic insect. It was observed that gene expression and protein immunoreactivity of both Ssk and mesh are restricted to the midgut and Malpighian tubules and are not detected in the hindgut or anal papillae of larval *A. aegypti* (see Fig. 5-1 and Fig. 5-2). In addition, immunofluorescence staining of Ssk and mesh revealed that both proteins are found at regions of cell-cell contact between the epithelial cells of the midgut and Malpighian tubules (Fig. 5-2), which is consistent with their localization to SJs. Since the epithelia of insect midgut and Malpighian tubules are generally known to possess sSJs and not pSJs (Noirot-Timothee and Noirot 1980; Lane and Skaer 1980; Bradley et al. 1982; Chapter 3), these findings suggest that Ssk and mesh are sSJ-associated proteins in larval *A. aegypti*. All the aforementioned observations are in agreement with studies in *Drosophila* (Yanagihashi et al. 2012; Izumi et al. 2012) which in turn presents further evidence that Ssk and mesh are the first two known sSJ-specific proteins conserved among Diptera. This notion is also supported by recent observations of Esquivel et al. (2016) who documented Ssk and mesh transcript in the Malpighian tubules of the adult Asian tiger mosquito *Aedes albopictus*.

5.5.2 The response of ssk and mesh transcript to BW rearing: In the current study, changes in the mRNA abundance of *ssk* and *mesh* in the midgut and Malpighian tubules of BW-reared *A. aegypti* larvae (Fig. 5-3) suggest that the paracellular transport component of these tissues plays a role in the physiological response of larvae to alterations in environmental salt levels. Our results demonstrate a similar response of Ssk and mesh to salinity such that there is greater mRNA abundance in the midgut and Malpighian tubules of BW reared larvae when compared to

FW reared larvae (Fig. 5-3). This coincides with greater Kune protein abundance in the posterior midgut and anal papillae of BW-reared larval *A. aegypti* when compared to FW reared larvae (Chapter 4). If Ssk and mesh are required for the formation of the paracellular barrier in midgut and Malpighian tubules of larval *A. aegypti*, as is the case in *Drosophila*, it could be reasoned that the increased *ssk* and *mesh* transcript abundance observed in BW-reared larvae might result in epithelia becoming 'tighter' under saline conditions. However, this is not the case as the midgut of BW-reared larvae exhibits a higher flux rate of the paracellular permeability marker PEG-400, indicating a 'leakier' epithelium (see Fig. 5-4 and discussion below), and it is reasonable to assume that the permeability of Malpighian tubules may also be increased.

5.5.3 Effect of BW rearing on midgut epithelium permeability: Since salinity induced changes in Ssk and mesh transcript abundance in the midgut of larval *A. aegypti* were observed as discussed above, we hypothesized that alteration in the permeability of the midgut epithelium may also occur. Indeed, we measured a twofold increase in the flux rate of the paracellular permeability marker PEG-400 in the midgut of BW-reared larvae compared to larvae reared in FW (Fig. 5-4c), indicating a leakier midgut epithelium under saline conditions. Increased midgut permeability might facilitate passive water movement from the midgut lumen into the hemolymph to help maintain body volume. This could be a mechanism to limit salt loading from ingested saline medium (Chapter 4; Donini et al. 2006). On the other hand, we do not preclude the presence of region-specific modulation in the permeability properties of *A. aegypti* larval midgut in response to environmental change, especially in light of a recent report on Kune localization only in the SJs of the posterior midgut epithelium and salinity induced increase in Kune abundance in this region of the alimentary canal (Chapter 4). Region-specific changes in the TJ protein abundance and/or permeability of intestinal epithelia in response to increases in external salt content have been suggested to occur in aquatic vertebrates such as fishes and amphibians (Clelland et al.

2010; Tipsmark and Madsen 2012; Chasiotis and Kelly 2009). In addition, salinity-induced modulation of SJ permeability along the midgut has been suggested for larval *Chironomus riparius* which shows no change in midgut active transcellular transport machinery when reared in BW (Chapter 2).

5.5.4 Do Ssk and mesh facilitate anion transport across the midgut and Malphigian tubules?

In the current study, data indicate that *ssk* and *mesh* transcript abundance increases in the midgut and Malphigian tubules of BW reared *A. aegypti* versus those reared in FW, and that this occurs in association with an increase in PEG-400 flux as a proxy for paracellular permeability. If we reason that changes in *ssk* and *mesh* mRNA abundance translate into an increase in protein abundance and that increased paracellular permeability occurs in BW reared Malphigian tubules as well as the midgut, the question becomes how might an increase in midgut and Malphigian tubule paracellular permeability contribute to salt and water balance in BW residing larval *A. aegypti* and how would an associated increase in Ssk and mesh abundance facilitate (or contribute to) this? Beginning with the midgut, it has been observed that the sSJs in the midgut epithelium of lepidopteran *Bombyx mori* larvae appear to be lined by fixed negative charges and display a high selectivity with respect to the size and the charge of permeating ions, suggesting that sSJ proteins can impart size and charge selectivity across the paracellular pathway of the midgut epithelium (Fiandra et al. 2006). Based on ion substitution experiments and expression of membrane transporters, larval *A. aegypti* posterior midgut has been suggested as a site of paracellular Cl^- conductance (Clark et al. 1999; Jagadeshwaran et al. 2010). If the SJs in the posterior midgut of *A. aegypti* larvae mediate selective Cl^- transport, it can be hypothesized that Ssk and mesh may play a role in modulating sSJs such that there is an increase in junctional Cl^- permeability in BW. With regard to the Malpighian tubules of larval *A. aegypti*, functional features of the paracellular pathway are currently not known, but some insight might be offered

from studies on the tubules of adult *A. aegypti*, as well as studies on larval Malpighian tubule transcellular ion transport. In this regard, it has been demonstrated that the tubule epithelium of adult *A. aegypti* has a moderate transepithelial resistance ('tightness') and that the SJs are permeable to Cl^- and impermeable to either Na^+ or K^+ which cross the epithelial cells via transcellular transport machinery (Yu and Beyenbach 2001; Beyenbach and Piermarini 2011). If a similar SJ mediated Cl^- pathway exists in the larval tubules, alteration in the paracellular Cl^- permeability may occur when larvae encounter BW. This would coincide with reported changes in transcellular transport of Na^+ and K^+ across the tubule epithelium of larvae reared in higher salinity (Donini et al. 2006). Indeed, modulation of tubule SJ permeability in response to salt loading has been recently suggested for adult female *A. albopictus*, which shows increased transcript abundance of *ssk* and *mesh* in Malpighian tubules during blood meal induced diuresis (Esquivel et al. 2016). Therefore taking all things into consideration, our view is that there is a case to be made for Ssk and mesh facilitating paracellular Cl^- movement across the midgut and Malphigian tubules of BW reared *A. aegypti* larvae and it will be very interesting to test this idea further in future studies.

5.5.5 Conclusions: Paracellular barriers have many important roles in the epithelia of insects and more broadly invertebrates (Chapter 3). Modulation of the SJ permeability in epithelia directly exposed to the external environment as well as those that line internal compartments contribute to the internal milieu. However, the physiology of SJs and the biological significance of the presence of two types of SJs in insects and other arthropods are not well understood. Observations made in the current study add to the idea that both pSJs and sSJs share a similar role in regulating paracellular permeability of the epithelia within which they occur. In addition, this work provides insight into the role of sSJ-specific components in the regulation of salt and water balance in larval mosquito and offers some evidence that sSJ proteins may be important for

altering intestinal permeability properties in response to changes in external salinity. Of particular interest is the observation that increased SJ gene transcript abundance (*ssk* and *mesh*; this study) or protein abundance (Kune; Chapter 4) coincide with increased permeability of midgut epithelium. Because compromised expression of *ssk* or *mesh* reduces barrier function of *Drosophila* midgut, it might seem logical to consider that increased Ssk and mesh abundance would enhance barrier properties of insect epithelia by making them 'tighter'. However, in this study data suggest that the opposite trend occurs with increased *ssk* and *mesh* occurring in conjunction with an increase in permeability. We believe that this might facilitate enhanced paracellular Cl^- flux in BW, but it will be necessary to test this hypothesis in future studies. Nevertheless, junction proteins that enhance anion permeability are well documented in the TJs of vertebrate epithelia (for review see Günzel and Yu 2013), and given that TJs are the functional counterpart of invertebrate SJs, a broader perspective suggests that the presence of anion selective SJ proteins should be anticipated. This study provides a new foundation on which these ideas can be built.

5.6 References

Anderson JM, Van Itallie M (2009) Physiology and function of the tight junction. Cold Spring Harb Perspect Biol 1:a002584

Baldwin KM, Hakim RS (1999) Evidence for high molecular weight proteins in arthropod gap and smooth septate junctions. Tissue Cell 31:195-201

Beyenbach KW, Piermarini PM (2011) Transcellular and paracellular pathways of transepithelial fluid secretion in Malpighian (renal) tubules of the yellow fever mosquito *Aedes aegypti*. Acta Physiol. (Oxf.) 202:387-407

Bradley TJ (1994) The role of physiological capacity, morphology, and phylogeny in determining habitat use in mosquitoes. In: Wainwright PC, Reilly SM (eds) Ecological Morphology. The University of Chicago Press, Chicago, IL, pp 303-318

Bradley TJ, Stuart AM, Satir P (1982) The ultrastructure of the larval malpighian tubules of a saline-water mosquito. Tissue Cell 14:759-773

Cañedo-Argüelles M, Kefford BJ, Piscart C, Prat N, Schäfer RB, Schulz CJ (2013) Salinisation of rivers: an urgent ecological issue. Environ Pollut 173:157-167

Chasiotis H, Kelly SP (2009) Occludin and hydromineral balance in *Xenopus laevis*. J Exp Biol 212:287-296

Clark TM, Koch A, Moffett DF (1999) The anterior and posterior 'stomach' regions of larval *Aedes aegypti* midgut: regional specialization of ion transport and stimulation by 5-hydroxytryptamine. J Exp Biol 202:247-252

Clelland ES, Bui P, Bagherie-Lachidan M, Kelly SP (2010) Spatial and salinity-induced alterations in claudin-3 isoform mRNA along the gastrointestinal tract of the pufferfish *Tetraodon nigroviridis*. Comp. Biochem. Physiol A Mol Integr Physiol 155:154-163

Clements AN (1992) The Biology of Mosquitoes, vol 1. Chapman & Hall, London.

Del Duca O, Nasirian A, Galperin V, Donini A (2011) Pharmacological characterisation of apical Na^+ and Cl^- transport mechanisms of the anal papillae in the larval mosquito *Aedes aegypti*. J Exp Biol 214:3992-3999

Deligiannaki M, Casper AL, Jung C, Gaul U (2015) Pasiflora proteins are novel core components of the septate junction. Development 142:3046-3057

Donini A, O'Donnell MJ (2005) Analysis of Na^+, Cl^-, K^+, H^+ and NH_4^+ concentration gradients adjacent to the surface of anal papillae of the mosquito *Aedes aegypti*: application of self-referencing ion-selective microelectrodes. J Exp Biol 208:603-610

Donini A, Patrick ML, Bijelic G, Christensen RJ, Ianowski JP, Rheault MR, O'Donnell MJ (2006) Secretion of water and ions by Malpighian tubules of larval mosquitoes: Effects of diuretic factors, second messengers, and salinity. Physiol Biochem Zool 79:645-655

Esquivel CJ, Cassone BJ, Piermarini PM (2016) A de novo transcriptome of the Malpighian tubules in non-blood-fed and blood-fed Asian tiger mosquitoes *Aedes albopictus*: insights into diuresis, detoxification, and blood meal processing. PeerJ 4:e1784

Fiandra L, Casartelli M, Giordana B (2006) The paracellular pathway in the lepidopteran larval midgut: modulation by intracellular mediators. Comp Biochem Physiol A Mol Integr Physiol 144:464-473

Green CR, Bergquist PR (1982) Phylogentic relationships within the invertebrates in relation to the structure of septate junctions and the development of 'occluding' junctional types. J Cell Sci 53:279-305

Green CR, Noirot-Timothee C, Noirot C (1983) Isolation and characterization of invertebrate smooth septate junctions. J Cell Sci 62:351-370

Günzel D, Yu ASL (2013) Claudins and the modulation of tight junction permeability. Physiol Rev 93:525-569

Izumi Y, Furuse M (2014) Molecular organization and function of invertebrate occluding junctions. Semin Cell Dev Biol 36:186-193

Izumi Y, Yanagihashi Y, Furuse M (2012) A novel protein complex, Mesh-Ssk, is required for septate junction formation in the *Drosophila* midgut. J Cell Sci 125:4923-4933

Izumi Y, Motoishi M, Furuse K, Furuse M (2016) A tetraspanin regulates septate junction formation in Drosophila midgut. J Cell Sci 129:1155-1164

Jagadeshwaran U, Onken H, Hardy M, Moffett SB, Moffett DF (2010) Cellular mechanisms of acid secretion in the posterior midgut of the larval mosquito (*Aedes aegypti*). J Exp Biol 213: 295-300

Lane NJ, Skaer HB (1980) Intercellular junctions in insect tissues. In: Berridge MJ, Treherne JE, Wigglesworth VB (eds) Advances in Insect Physiology, vol 15. Academic Press, London, pp 35-213

Noirot-Timothee C, Noirot C (1980) Septate and scalariform junctions in arthropods. Int Rev Cytol 63**:**97-141

Ramasamy R, Surendran SN (2012) Global climate change and its potential impact on disease transmission by salinity-tolerant mosquito vectors in coastal zones. Front Physiol 3:198

Sugahara T, Yamashita Y, Shinomi M, Yamanoha B, Iseki H, Takeda A, Okazaki Y, Hayashizaki Y, Kawai K, Suemizu H, Andoh T (2007) Isolation of a novel mouse gene, mSVS-1/SUSD2, reversingtumorigenic phenotypes of cancer cells in vitro. Cancer Sci 98:900-908

Tipsmark CK, Madsen SS (2012) Tricellulin, occludin and claudin-3 expression in salmon intestine and kidney during salinity adaptation. Comp Biochem Physiol A Mol Integr Physiol 162:378-85

Williams WD (2001) Anthropogenic salinization of inland waters. Hydrobiol 466:329-337

Yanagihashi Y, Usui T, Izumi Y, Yonemura S, Sumida M, Tsukita S, Uemura T, Furuse M (2012) Snakeskin, a membrane protein associated with smooth septate junctions, is required for intestinal barrier function in *Drosophila*. J Cell Sci 125:1980-1990

Yu MJ, Beyenbach KW (2001) Leucokinin and the modulation of the shunt pathway in Malpighian tubules. J Insect Physiol 47:263-276

CHAPTER 6:

IDENTIFICATION OF THE SEPTATE JUNCTION PROTEIN GLIOTACTIN IN THE MOSQUITO, *AEDES AEGYPTI*: EVIDENCE FOR A ROLE OF GLIOTACTIN IN INCREASED PARACELLULAR PERMEABILITY IN LARVAE

6.1 Summary

Septate junctions (SJs) regulate paracellular permeability across invertebrate epithelia. However, little is known about the function of SJ proteins in aquatic invertebrates. In this study, a role for the transmembrane SJ protein gliotactin (Gli) in the osmoregulatory strategies of larval mosquito (*Aedes aegypti*) was examined. Differences in *gli* transcript abundance were observed between the midgut, Malpighian tubules (MT), hindgut and anal papillae (AP) of *A. aegypti*, which are epithelia that participate in larval mosquito osmoregulation. Western blotting of Gli revealed its presence in monomer, putative dimer and phosphorylated forms in different larval mosquito organs. Gli localized to the entire SJ domain between midgut epithelial cells and showed a discontinuous localization along the edges of epithelial cells of the rectum as well as the syncytial AP epithelium. In the MT, Gli immunolocalization was confined to SJs between the stellate and principal cells. Rearing larvae in 30% seawater caused an increase in Gli protein abundance in the anterior midgut, MT and hindgut. Transcriptional knockdown of *gli* using dsRNA reduced Gli protein abundance in the midgut and increased the flux rate of the paracellular permeability marker, polyethylene glycol (MW 400 Da; PEG-400). Data suggest that in larval *A. aegypti*, Gli participates in the maintenance of salt and water balance and that one role for Gli is to participate in the regulation of paracellular permeability across the midgut of *A. aegypti* in response to changes in environmental salinity.

6.2 Introduction

Larval mosquitoes inhabit a variety of aquatic niches ranging from man-made containers and ditches to woodland pools and marshes. The salinity of these habitats varies from nearly salt-free freshwater (FW) to brackish water (BW) and seawater. In FW environments, the osmotic gradient between the circulating hemolymph of the larva and the external aquatic medium favors the influx of water into the body and the efflux of ions from the body. In saline conditions, the osmotic gradient is reversed and the larva is susceptible to passive water loss and excessive salt gain. The survival of mosquito larvae depends on their ability to regulate the influx and efflux of ions and water across osmoregulatory epithelia such as those of the midgut, Malpighian tubules (MT), hindgut and anal papillae (Clements 1992; Bradley 1994; Donini and O'Donnell 2005; Del Duca et al. 2011). Studies examining the role of osmoregulatory epithelia in the maintenance of salt and water balance in larval mosquitoes have generally focused on transcellular mechanisms/routes of ion movement, through which actively driven ion transport takes place (Bradley 1994; Patrick et al. 2002; Donini et al. 2006; Donini et al. 2007; Smith et al. 2008; Del Duca et al. 2011). In contrast, far less emphasis has been placed on the paracellular pathway which is regulated by the specialized cell-cell junctions known as septate junctions (SJs). As a result, the role of SJs in the maintenance of salt and water balance in mosquito larvae is poorly understood.

In cross-section electron microscopy, SJs display a characteristic ladder-like structure between adjacent cells with septa spanning a 15-20 nm intercellular space (Green and Bergquist 1982). SJs typically form circumferential belts around the apicolateral regions of epithelial cells and control the movement of biological material through the paracellular route (Chapter 3). Several morphological variants of SJs exist across invertebrate phyla and some animals possess multiple types of SJs that are specific to different epithelia (Green and Bergquist 1982; Chapter

3). Molecular analyses of insect SJs have largely been performed in *Drosophila*, where two types of SJs are present: the pleated SJ (pSJ) and the smooth SJ (sSJ), which are found in ectodermally and endodermally derived epithelia, respectively (Izumi and Furuse 2014). To date, over twenty *Drosophila* pSJ-associated proteins have been identified which include transmembrane and cytoplasmic proteins (Izumi and Furuse 2014; Deligiannaki et al. 2015; Chapter 3). Loss-of-function mutations in most of these proteins prevent the formation of septa or SJ organization which in turn disrupts the transepithelial barrier properties of ectodermally derived epithelia (for review see Izumi and Furuse 2014; Chapter 3). In addition, three *Drosophila* sSJ-specific membrane proteins, snakeskin (Ssk), mesh and Tsp2A, have recently been discovered (Yanagihashi et al. 2012; Izumi et al. 2012; Izumi et al. 2016). All three proteins are localized exclusively in the epithelia of the midgut and Malpighian tubules, where sSJs reside, and are required for the barrier function of the midgut (Izumi et al. 2012; Yanagihashi et al. 2012; Izumi et al. 2016).

Gliotactin (Gli) is a single-pass transmembrane protein that belongs to the Neuroligin family of cholinesterase-like adhesion molecules. Gli was the first *Drosophila* SJ protein to be localized exclusively to occluding regions of the tricellular junction (TCJ) which forms at regions of tricellular contact between three neighbouring epithelial cells (Schulte et al. 2003; Gilbert and Auld 2005). In addition to an extracellular cholinesterase-like domain, Gli also contains an intracellular domain with two tyrosine phosphorylation residues and a PDZ binding motif, both conserved in all Gli homologues (Padash-Barmchi et al. 2010). Gli is necessary for both TCJ and bicellular SJ development in *Drosophila* ectodermal epithelia as Gli null mutation results in paralysis and embryonic lethality due to disruption of the TCJ and failure of the SJ permeability barrier (Schulte et al. 2003). The importance of Gli to the barrier function of the SJ was shown in embryonic salivary glands using a rhodamine-labeled 10 kDa dextran injected into the embryonic

hemocoel. The fluorescent tracer did not enter the salivary gland lumen in the wild type embryos but permeated the salivary gland lumen of Gli mutant embryos (Schulte et al. 2003). In polarized epithelia, Gli is tightly regulated at the cell membrane via phosphorylation, endocytosis and degradation, and this controls Gli levels and localization to the TCJ as well as cell survival (Padash-Barmchi et al. 2010). Overexpression of Gli in imaginal disc epithelia causes Gli to spread away from the TCJ into the bicellular SJ domain where its interaction with the cytoplasmic SJ protein discs large (Dlg) leads to Dlg downregulation, tissue overgrowth and apoptosis (Schulte et al. 2006; Padash-Barmchi et al. 2010, 2013).

The effect of environmental salinity on the SJ permeability of osmoregulatory epithelia of aquatic insects and, more broadly, invertebrates is not well understood. Salinity-induced changes in the ultrastructure of pSJs have been reported for the gill epithelium of euryhaline crabs (Luquet et al. 1997, 2002). This suggests that alterations in the molecular physiology of aquatic arthropod SJs in osmoregulatory epithelia should be expected in response to changes in the ionic strength of their surroundings, and two recent studies support this hypothesis. The first (see Chapter 5) reported that the flux rate of the paracellular permeability marker PEG-400 increased across the midgut epithelium of BW-reared larval *A.aegypti* when compared to organisms reared in FW (see Chapter 5), and that this change in PEG-400 flux occured in association with increased transcript abundance of the sSJ proteins Ssk and mesh (see Chapter 5). A greater Ssk and mesh mRNA abundance was also seen in the Malpighian tubules of BW reared larvae when compared to FW animals (see Chapter 5). In a second study, a salinity-induced increase in the protein abundance of the integral SJ protein kune-kune (Kune) was observed in the posterior midgut as well as anal papillae of *A. aegypti* larva while other SJ proteins were unaltered (see Chapter 4). Taken together these observations suggest that select SJ proteins contribute to osmoregulatory homeostasis in larval *A. aegypti* (Chapter 4 and Chapter 5).

To the best of my knowledge, an osmoregulatory role for TCJs and the idea that a tricellular SJ protein might contribute to osmoregulatory homeostasis in an aquatic invertebrate have yet to be explored. In aquatic vertebrates such as fishes, the tricellular tight junction (TJ) protein tricellulin has been proposed to play a role in maintaining the barrier properties of osmoregulatory organs such as the gill (Kolosov and Kelly 2013). Therefore it seems reasonable to consider that in the functionally analogous occluding junction of an aquatic arthropod facing the same physiological problems as that of an aquatic vertebrate, a tricellular SJ protein may also contribute to salt and water balance. In this regard, it can be hypothesized that in *A. aegypti* larvae Gli will be salinity responsive in osmoregulatory organs and contribute to changes in the permeability of SJs. To address this further, the objectives of this study were to examine (1) Gli expression and localization in the osmoregulatory tissues of larval *A. aegypti*, (2) changes in Gli abundance in association with changes in environmental ion levels and (3) whether functional knock down of *gli* would alter the paracellular permeability of a larval mosquito osmoregulatory epithelium, the midgut.

6.3 Materials and methods

6.3.1 Experimental animals and culture conditions: Larvae of *Aedes aegypti* (Linnaeus) were obtained from a colony maintained in the Department of Biology at York University as previously described (Chapter 4). Hatched 1st instar larvae were reared in either FW (approximate composition in µmol l^{-1}: [Na^+] 590; [Cl^-] 920; [Ca^{2+}] 760; [K^+] 43; pH 7.35) or 30% SW (10.5 g/l Instant Ocean SeaSalt® in FW) which served as the experimental brackish water (BW) treatment. Larvae were fed daily and water of appropriate salinity was changed weekly. Experiments were conducted on fourth instar larvae that had not been fed for 24 h before collection.

*6.3.*2 *Identification of gli in Aedes aegypti and quantitative real time PCR (qPCR) analysis:* Total RNA was extracted from larval *A. aegypti* tissues (midgut with gastric ceacae, Malpighian tubules, hindgut and anal papillae) using TRIzol® reagent (Invitrogen, Burlington, ON, Canada) according to the manufacturer's instructions. Tissues from 50 larvae were pooled per one biological sample. All RNA samples were treated with the TURBO DNA-free™ kit (Ambion®, Life Technologies Inc., Burlington, ON, Canada) and template cDNA was synthesized using iScript™ cDNA synthesis kit as per the manufacturer's instructions (Bio-Rad, Mississauga, ON, Canada). Expressed sequence tags (ESTs) from *A. aegypti* genome that were similar to *Drosophila gli* (GenBank: AAC41579) were sought using the National Center for Biotechnology Information (NCBI) database BLAST search engine. Newly identified ESTs were confirmed to be protein encoding using a reverse xBLAST. A reading frame was established using BLASTn alignment and ORF Finder (http://www.ncbi.nlm.nih.gov/gorf/). A primer set for *gli* was designed based on EST sequences using Primer3 software (v. 0.4.0). Primer sequences, amplicon size and related accession numbers are summarized in Table 6-1. Expression of mRNA encoding *gli* in the whole body and osmoregulatory tissues of *A. aegypti* larvae was examined by routine reverse transcriptase PCR (RT-PCR). *18S rRNA* mRNA abundance was used as a loading control

and was amplified using primers previously described (Chapter 4). Resulting RT-PCR amplicons were resolved by agarose gel electrophoresis and sequence identities confirmed after sequencing at the York University Core Molecular Facility (Department of Biology, York University, ON, Canada). Amplified *A. aegypti gli* sequence was confirmed using a BLAST search and submitted to GenBank (accession number shown in Table 6-1). ClustalW software was used to align amino acid sequence of *A. aegypti* Gli with that of *Drosophila*. *In silico* analysis of *A. aegypti* Gli amino acid sequence was performed using EXPASY PROSITE (posttranslational modifications and protein domains), ProtParam (protein weight and stability parameters such as predicted half-life), and ProtScale and TMHMM (hydrophobicity scale and transmembrane domains). Final *A. aegypti* Gli topography was visualized using TOPO2 software.

Transcript abundance of *gli* in the midgut, Malpighian tubules, hindgut and anal papillae of *A. aegypti* larvae was examined by qPCR analysis. Reactions were carried out using the primers listed in Table 6-1 and SYBR Green I Supermix (Bio-Rad Laboratories Ltd., Mississauga, ON, Canada) with a Chromo4™ Detection System (CFB-3240, Bio-Rad Laboratories Canada Ltd.) under the following conditions: 1 cycle denaturation (95°C, 4min) followed by 40 cycles of denaturation (95°C, 30 s), annealing (59°C, 30 s) and extension (72°C, 30 s), respectively. For qPCR analyses, *gli* mRNA abundance was normalized to either *18S rRNA* or *rp49* transcript abundance. *A. aegypti 18S rRNA* and *rp49* mRNA were amplified using primers previously described (Chapter 4).

6.3.3 Western blot analysis and immunohistochemistry: Western blotting for Gli in the tissues of interest (gastric caecae, anterior midgut, posterior midgut, Malpighian tubules, hindgut, anal papillae) was performed as previously detailed (Chapter 4). A custom-made polyclonal antibody that was produced in rabbit against a synthetic peptide (GASRAGYDRSNNAS) corresponding to a 14-amino acid region of the C-terminal cytoplasmic tail of *A. aegypti* Gli (GenScript USA Inc.,

Piscataway, NJ, USA) was used at 1:500 dilution. To confirm the specificity of the custom-made *A. aegypti* Gli antibody, a comparison blot was also run with the Gli antibody pre-absorbed with 10x molar excess of the immunogenic peptide for 1 h at room temperature prior to application to blots. After examination of Gli expression, blots were stripped and re-probed with a 1:200 dilution of mouse monoclonal anti-JLA20 antibody (J. J.-C. Lin, Developmental Studies Hybridoma Bank, Iowa City, IA, USA) for actin. Densitometric analysis of Gli and actin was conducted using Image J 1.47 v software (USA). Gli abundance was expressed as a normalized value relative to the abundance of the loading control.

Immunohistochemical localization of Gli in whole-mount guts and paraffin sections of anal papillae was conducted according to previously described protocols (see Chapter 2 and Chapter 4) using a 1:50 dilution of the custom-made anti-Gli antibody described above. Whole-mount guts and paraffin sections of anal papillae were also treated with a 1:1000 dilution of a rabbit polyclonal anti-*Ae*AE antibody for SLC4-like anion exchanger (a kind gift from Dr. Peter M. Piermarini, Department of Entomology, The Ohio State University, Wooster, OH, USA)) and a 1:100 dilution of a mouse polyclonal anti-ATP6V0A1 antibody for V-type H^+-ATPase (VA; Abnova, Taipei, Taiwan), respectively. A goat anti-rabbit antibody conjugated to Alexa Fluor 594 (Jackson Immunoresearch) was used at 1:400 to visualize Gli and *Ae*AE and a sheep anti-mouse antibody conjugated to Cy-2 (Jackson Immunoresearch) was applied at 1:400 to visualize VA. Negative control slides were also processed as described above with either primary antibodies omitted or the Gli antibody pre-absorbed with 10x molar excess of the immunogenic peptide for 1 h at room temperature prior to application to tissues. Images of sections of anal papillae were captured using an Olympus IX71 inverted microscope (Olympus Canada, Richmond Hill, ON, Canada) equipped with an X-CITE 120XL fluorescent Illuminator (X-CITE, Mississauga, ON, Canada). Whole-mounts were examined using an Olympus BX-51 laser-

scanning confocal microscope. Images were assembled using Adobe Photoshop CS2 software (Adobe Systems Canada, Toronto, ON, Canada).

6.3.4 dsRNA preparation and delivery: Total RNA was extracted from the midguts of 4th instar *A. aegypti* larvae and cDNA was generated as described above. Using this cDNA template, a fragment of the *gli* gene (976 bp) was amplified by RT-PCR using primers (forward 5'-TGCTCAATCGAAACTTCGTG-3'; reverse 5'-GTTCCCACCAGAACTCCGTA-3') designed based on *gli* sequence submitted to GenBank. A fragment of *β-lactamase* (*βLac*; 799 bp) was also amplified by RT-PCR from a pGEM-T-Easy vector (kind gift from J. P. Paluzzi, York University) using the following primers: forward 5'-ATTTCCGTGTCGCCCTTATTC-3'; reverse 5'-CGTTCATCCATAGTTGCCTGAC-3'. PCR products were concentrated and purified using a QIAquick PCR Purification kit (Qiagen Inc., Toronto, ON, Canada) and used to generate double stranded (ds) RNAs by *in vitro* transcription using the Promega T7 RiboMAX Express RNAi Kit (Promega, WI, USA). dsRNA was delivered to larvae as previously described (Chasiotis et al. 2016) with slight modification. Briefly, groups of 25 4th instar larvae were incubated for 4 h in 500-600 µl PCR-grade water containing 0.5 µg µl^{-1} dsRNA and then transferred into 20 ml distilled water. To confirm reduction in *gli* transcript as a result of dsRNA treatment, total RNA was extracted and cDNA generated from larval whole body and midgut at day 1 post-dsRNA treatment. The latter cDNA templates were used in RT-PCR with the above primers. Reduction in Gli in larval midgut as a result of dsRNA treatment was examined by western blotting at days 1 and 2 post-dsRNA treatment.

6.3.5 Transepithelial [^{3}H]polyethylene glycol-400 (PEG-400) flux across the midgut of A. aegypti: Flux of the paracellular permeability marker [^{3}H]polyethylene glycol (molecular mass 400 Da; 'PEG-400'; American Radiolabeled Chemicals, Inc., Saint Louis, MO, USA) across the

midgut epithelium of larval *A. aegypti* was determined as previously described (Chapter 5). [^{3}H] PEG-400 flux rates were determined from larvae treated with *gli* or *βLac* dsRNA.

6.3.6 Statistics: Data are expressed as means ± SEM (*n*). Comparisons between tissues were assessed with a one-way ANOVA followed by a Tukey's comparison test. A Student's *t*-test was used to examine for significant differences between control and experimental groups. Statistical significance was allotted to differences with $p < 0.05$. All statistical analyses were conducted using SigmaStat 3.5 software (Systat Software, San Jose, USA).

6.4 Results

6.4.1 Gli identification and expression in larval A. aegypti: Using the NCBI EST database, a full coding sequence of the *A. aegypti* SJ gene *gli* was obtained and primers were designed to amplify regions within and across ESTs using larval cDNA. Assembled sequence identity was confirmed by performing a BLAST search using amplified coding sequence of *gli*. *A. aegypti* Gli encodes a 993 amino acid protein with a predicted molecular weight of 113 kDa that shares 68% amino acid identity with *Drosophila* Gli (Fig. 6-1a). The primary structure of *A. aegypti* Gli is similar to *Drosophila* Gli (Padash-Barmchi et al. 2010) and contains a single-pass transmembrane domain, a large extracellular region containing a carboxylesterase type-B domain, and an intracellular domain with two tyrosine phosphorylation residues and a PDZ binding motif (Fig. 6-1b).

Quantitative analysis of *gli* mRNA in the osmoregulatory organs of *A. aegypti* larvae revealed the presence of *gli* transcript in all tissues examined, i.e. the midgut, Malpighian tubules, hindgut and anal papillae but transcript abundance was highest in the midgut (Fig. 6-2a). Western blot analysis of Gli in larval osmoregulatory tissues showed that anti-Gli antibody detected three tissue-specific bands with molecular weights of ~ 115 kDa, ~ 150 and ~ 245 kDa (Fig. 6-2b). A single ~ 115 kDa band, which corresponded to the predicted Gli protein size was resolved in the Malpighian tubules. The protein of ~115 kDa was also detected in the anal papillae where an additional putative Gli dimer of ~ 245 kDa and a lower molecular mass band (<75 kDa), which most likely represents a degradation product, were seen. Antibody pre-absorption with the immunogenic peptide produced no staining of Gli in the anal papillae (Fig 6-2b, right lane). In the hindgut, three Gli products were immunodetected corresponding to the monomer, dimer and potential phosphorylated Gli form, at ~150 kDa, which were all blocked by antibody pre-absorption with the immunogenic peptide (Fig. 6-2b). In the gastric caecae and

Table 6-1: Primer information for *Aedes aegypti gli* used in RT-PCR and qRT-PCR.

Gene	Primer Sequence	Amplicon length, bp	Annealing Temperature, ^{0}C	GenBank accession number
Gliotactin				
FOR	5’-TCGGCATAGACAACAACGTC-3’	182	59	KX823345
REV	5’-CGTAGCGAGCTTTGACTTCC-3’			

(A)

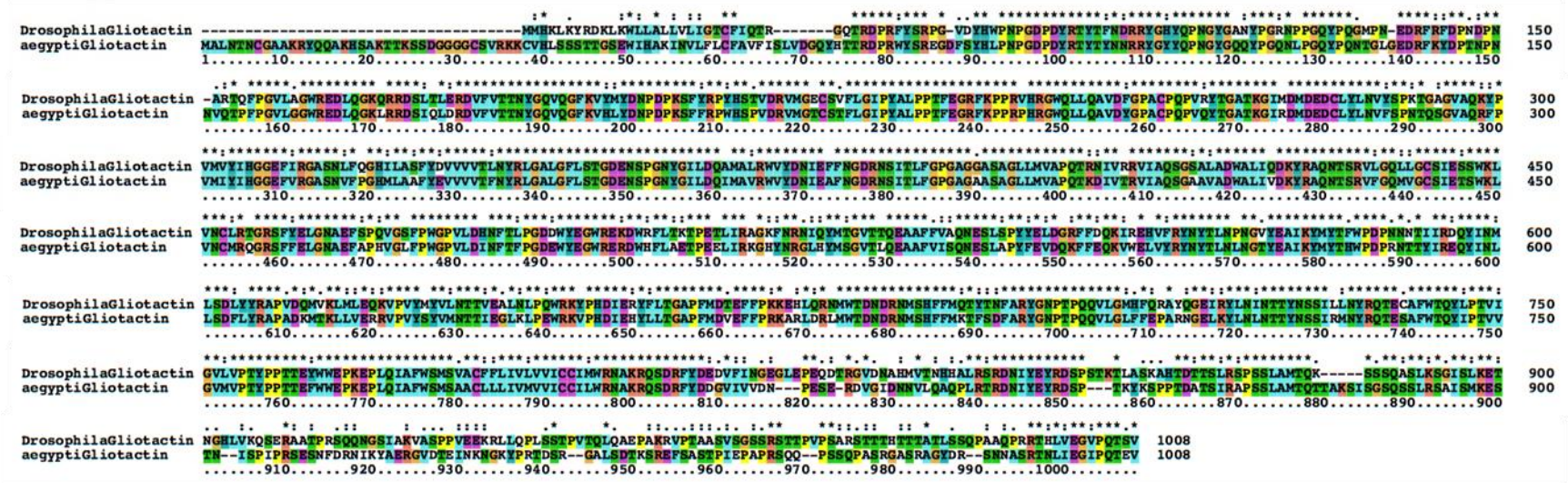

Figure 6-1: (see legend on next page).

(B)

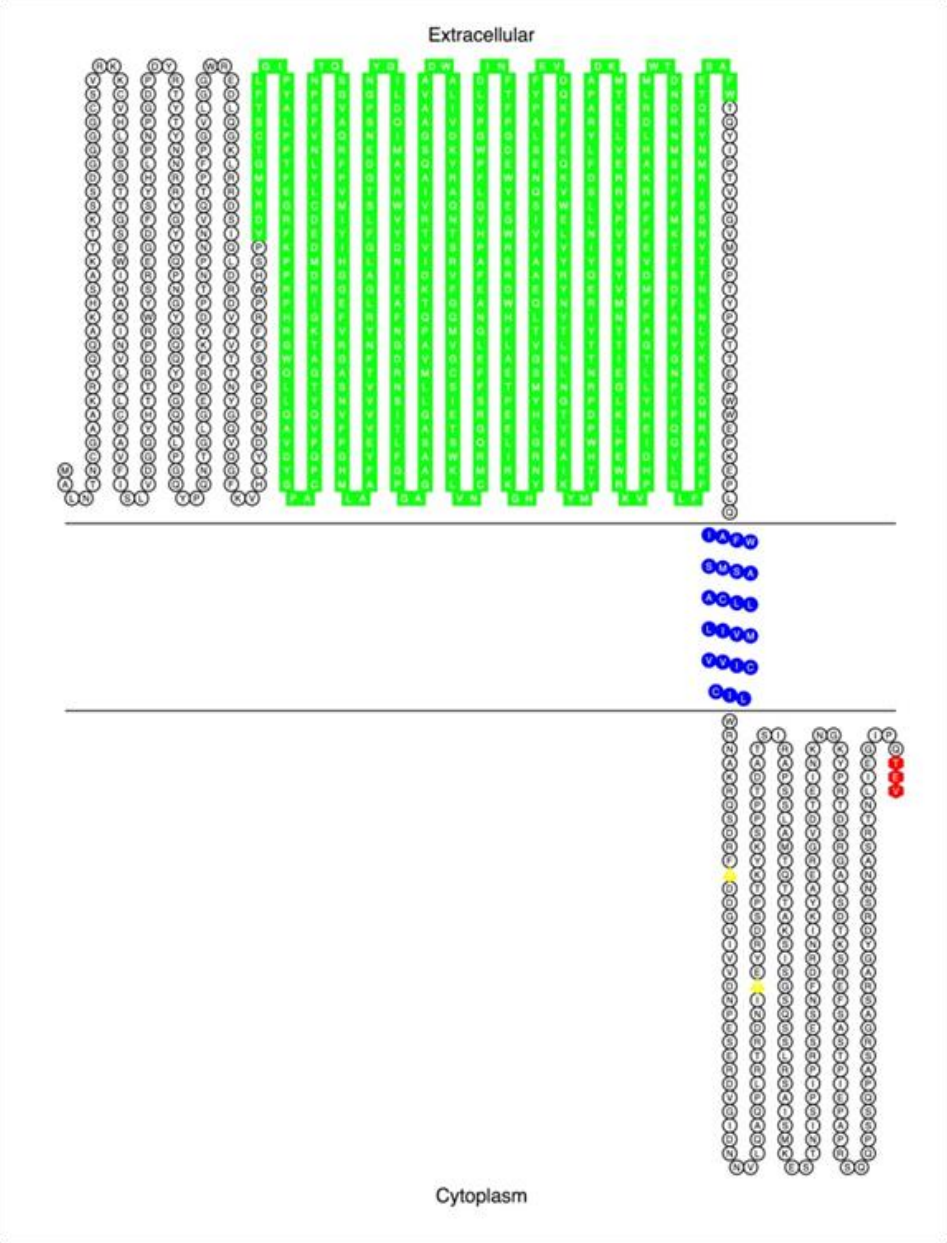

Figure 6-1: Annoted amino acid sequence of *A. aegypti* Gli. (**a**) The amino acids of *A. aegypti* Gli were aligned with those of *Drosophila* (accession no. AAC41579) using the ClustalW algorithm. "*" represents identical amino acid residues shared between *A. aegypti* Gli and *Drosophila* Gli, "**:**" conservation between two amino acid residues of strongly similar properties and "**.**" indicates conservation between two amino acid residues of weakly similar properties. (**b**) *A. aegypti* Gli has a single-pass transmembrane domain (blue), an extracellular region containing a carboxylesterases type-B domain (green), and intracellular domain with two highly conserved tyrosine phosphorylation residues (yellow) and a PDZ binding motif (red).

posterior midgut, Gli was detected as phosphorylated protein and a degradation product whereas anterior midgut samples revealed the limited presence of Gli dimer and a predominant phosphorylated form (Fig. 6-2b). A non-specific low molecular weight band (<50 kDa), which was not blocked by the immunogenic peptide, was seen in the samples from different regions of the midgut (Fig. 6-2b).

Immunostaining of Gli revealed its localization to the entire SJ domain between the epithelial cells of the gastric caecae, anterior and posterior midgut (Fig. 6-3a-d). In the Malpighian tubules, Gli immunolocalization appeared to be restricted to the cell-cell contact regions between the stellate and principal cells in the distal portion of the tubule (Fig. 6-3e-h). Little to no immunoreactivity of Gli was seen in the proximal tubule (Fig. 6-3H) which lacks stellate cells (Patrick et al. 2006; Linser et al. 2012). In addition, Gli immunostaining in the Malpighian tubules was similar to that of an established stellate cell marker *Ae*AE (Fig. 6-3i-k; Piermarini et al. 2010; Linser et al. 2012). Since both Gli and *Ae*AE antibodies were produced in rabbits, double labeling could not be performed. In the whole mount rectum and sections of anal papillae, Gli showed some punctuate staining along the edges of the rectal epithelial cells (Fig. 6-3m) and papilla epithelium (Fig. 6-3n). Within the epithelium of anal papillae, there was some overlap in immunoreactivity between Gli and apical membrane marker VA (Fig. 6-3o). Gli staining was absent in control whole mounts or sections which were probed with secondary antibodies only or with Gli antibody that was pre-absorbed with the immunogenic peptide (Fig. 6-3p; only sections of anal papillae are shown).

6.4.2 Effects of rearing salinity on gli transcript and Gli protein abundance: Rearing the larvae of *A. aegypti* in BW resulted in a significant increase in *gli* mRNA abundance as well as Gli protein abundance in the midgut and Malpighian tubules (Fig. 6-4a,b). Because of lack of

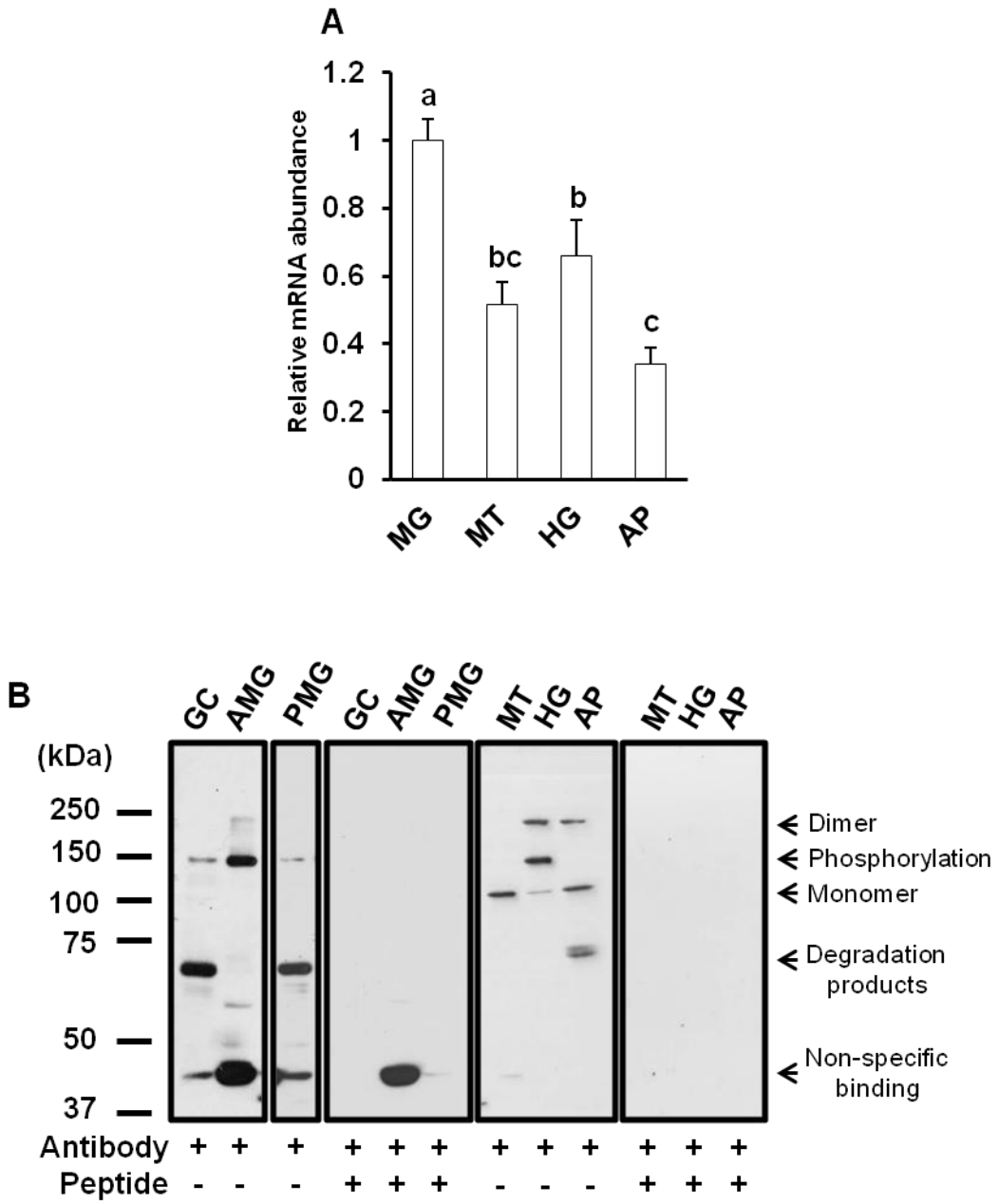

Figure 6-2: Gli transcript (**a**) and protein (**b**) expression profile in the osmoregulatory tissues of *Aedes aegypti* larvae as determined by qPCR and western blot analysis, respectively. In **a**, each gene was normalized to *18S* and was expressed relative to its levels in the midgut (assigned a value of 1). Data are expressed as mean values ± SEM (n = 6). Letters denote statistically significant differences between tissues (one-way ANOVA, Tukey's multiple comparison, $p < 0.05$). (**b**) Representative western blot of Gli in the osmoregulatory organs of larval *A. aegypti* reveals the presence of Gli monomer at ~ 115 kDa, potential phosphorylated and dimer forms (at ~ 150 kDa and 245 kDa, respectively) and some degradation products. In GC, AMG and PMG, an additional band of low molecular weight was detected which was not blocked by antibody pre-absorption with the immunizing peptide. MG, midgut; MT, Malpighian tubules; HG, hindgut; AP, anal papillae; GC, gastric caecae; AMG, anterior midgut; PMG, posterior midgut.

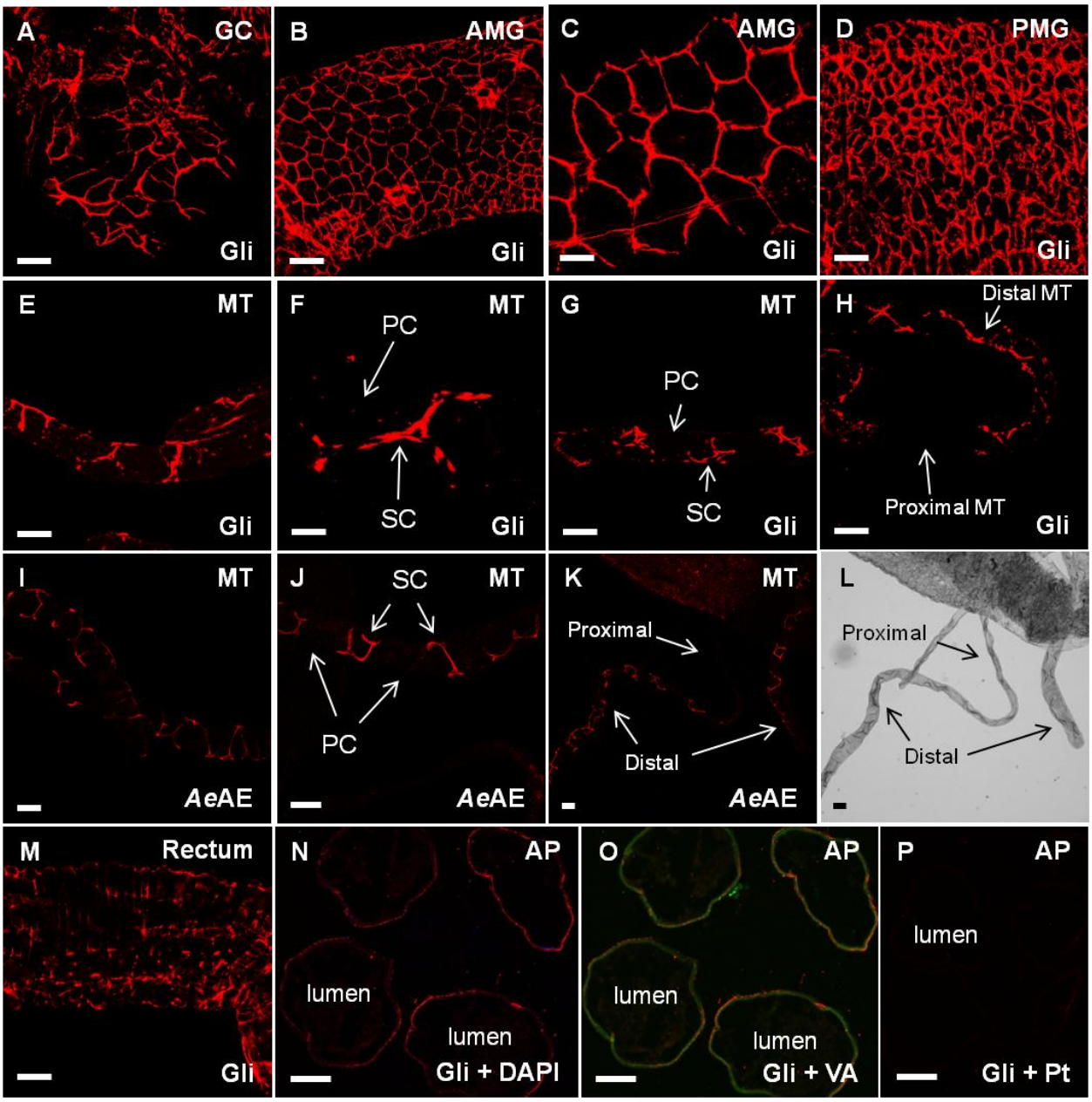

Figure 6-3: Immunofluorescence staining of Gli in the osmoregulatory tissues of *Aedes aegypti* larva. Gli was localized to regions of cell-cell contact between the epithelial cells of the gastric caecae (**a**), anterior and posterior midgut (**b**-**d**). In the Malpighian tubules, Gli immunostaining appears to be confined to the contact regions between the stellate and principal cells (SC and PC, respectively; arrows in **f** and **g**) in the distal portion of the tubule (**e**-**h**) as compared to the expression of the stellate cell marker *Ae*AE (**i**-**k**). (**l**) Brightfield image of **k**. Gli also shows some discontinuous immunostaining along the edges of the epithelial cells in the rectum (**m**) and anal papillae epithelium (**n**) where it exhibits some co-immunoreactivity with apical V-type H^+-ATPase (VA; **o**, green). Nuclei of anal papilla epithelium are stained with DAPI (blue) in **n**. (**p**) Control sections of anal papillae treated with anti-Gli antibody in the presence of immunizing peptide (Pt). Scale bars, (**a**, **c**, **d**, **f**) 20 µm, (**b**, **e**, **g**-**k**, **l**, **m**-**p**) 50 µm. GC, gastric caecae; AMG, anterior midgut; PMG, posterior midgut; MT, Malpighian tubules; AP, anal papillae.

consistent immunodetection of Gli in the posterior midgut, Gli protein abundance was examined only in the anterior midgut of FW- and BW-reared animals. Elevated Gli protein abundance was also observed in the hindgut of BW-reared larvae with no change in Gli transcript abundance in this tissue compared to FW-reared animals (Fig. 6-4a,b). While the putative phosphorylated Gli form was always detected in the samples of anterior midgut and hindgut from FW- and BW-reared animals, the potential dimer form was not consistently detected in these tissues. As a result, only the putative phosphorylated Gli form was quantified in these tissues of FW- and BW-reared larvae.

Lastly, there was no change in Gli transcript and protein monomer and dimer abundance in the anal papillae when larvae were reared in BW (Fig. 6-4a,b).

6.4.3 Effect of gli dsRNA knockdown on midgut permeability: To characterize Gli function in the osmoregulatory epithelia of larval *A. aegypti*, *gli* expression was knocked down using *gli*-targeting dsRNA. Following this, Gli protein abundance was examined as well as paracellular permeability in the midgut using the midgut permeability assay (see Chapter 5). Larvae treated with *gli* dsRNA showed a significant reduction in putative phosphorylated Gli protein abundance in the anterior midgut at day 2 post-*gli* dsRNA treatment compared to *βLac* dsRNA treated group (Fig. 6-5a,b). As such, day 2 post-*gli* dsRNA treated larvae were subjected to the midgut permeability assay. These larvae exhibited decreased PEG-400 flux (efflux, basolateral to apical) across the midgut compared to values from midguts of *βLac* dsRNA treated animals (Fig. 6-5c).

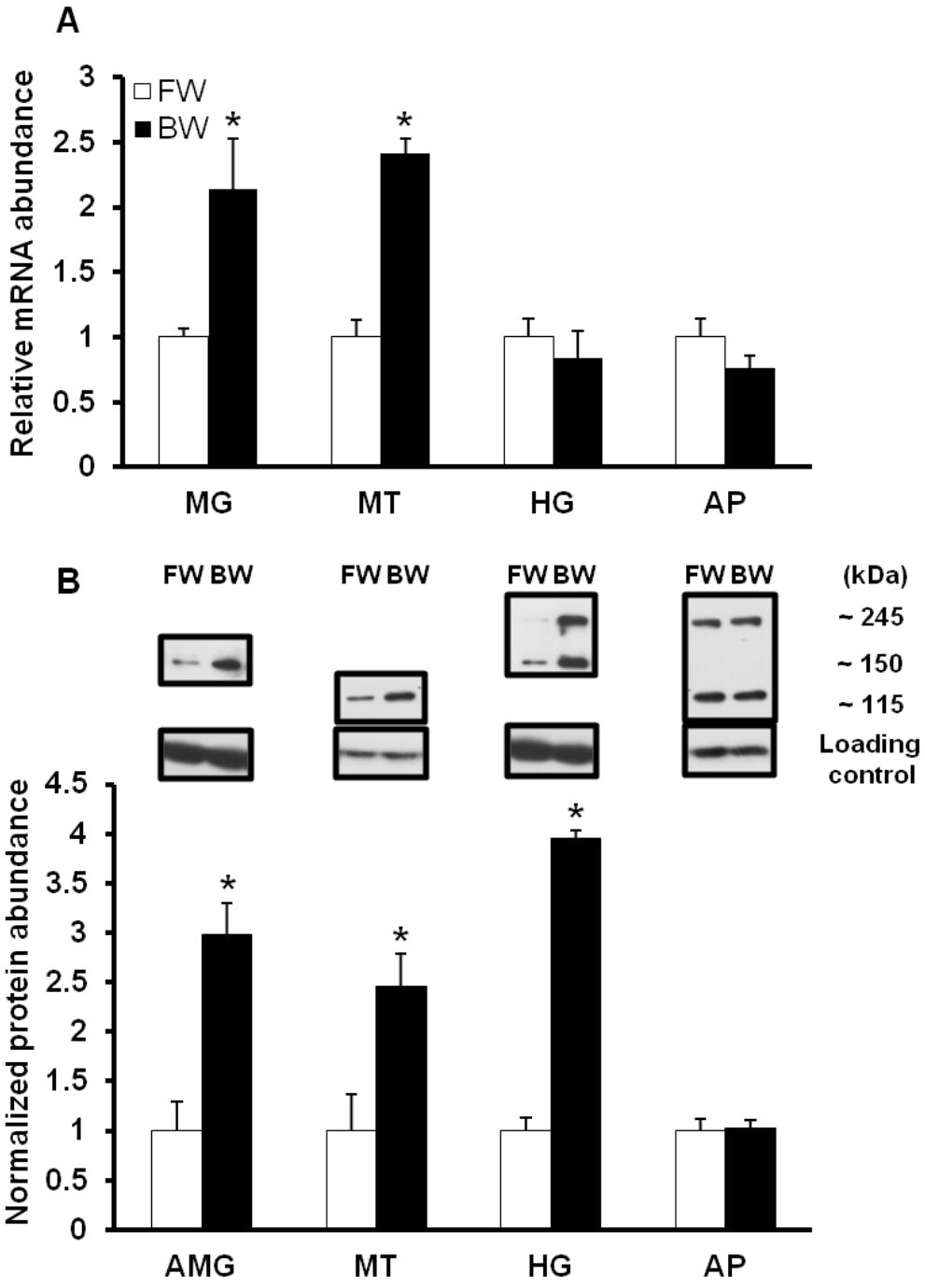

Figure 6-4: The effect of rearing salinity on Gli transcript (**a**) and normalized protein (**b**) abundance in the osmoregulatory tissues of *Aedes aegypti* larvae as examined by qRT-PCR and western blot analysis, respectively. In **a**, each gene was normalized to *rp49* and expressed relative to its FW value (assigned value of 1). In **b**, representative western blots of Gli are ~115 kDa, 150kDa and ~245 kDa bands, loading control is actin. Data are expressed as mean values ± SEM (n = 3-6)**.** An asterisk denotes significant difference from FW (Student's t-test, $p < 0.05$). MG, midgut; MT, Malpighian tubules; HG, hindgut; AP, anal papillae; AMG, anterior midgut.

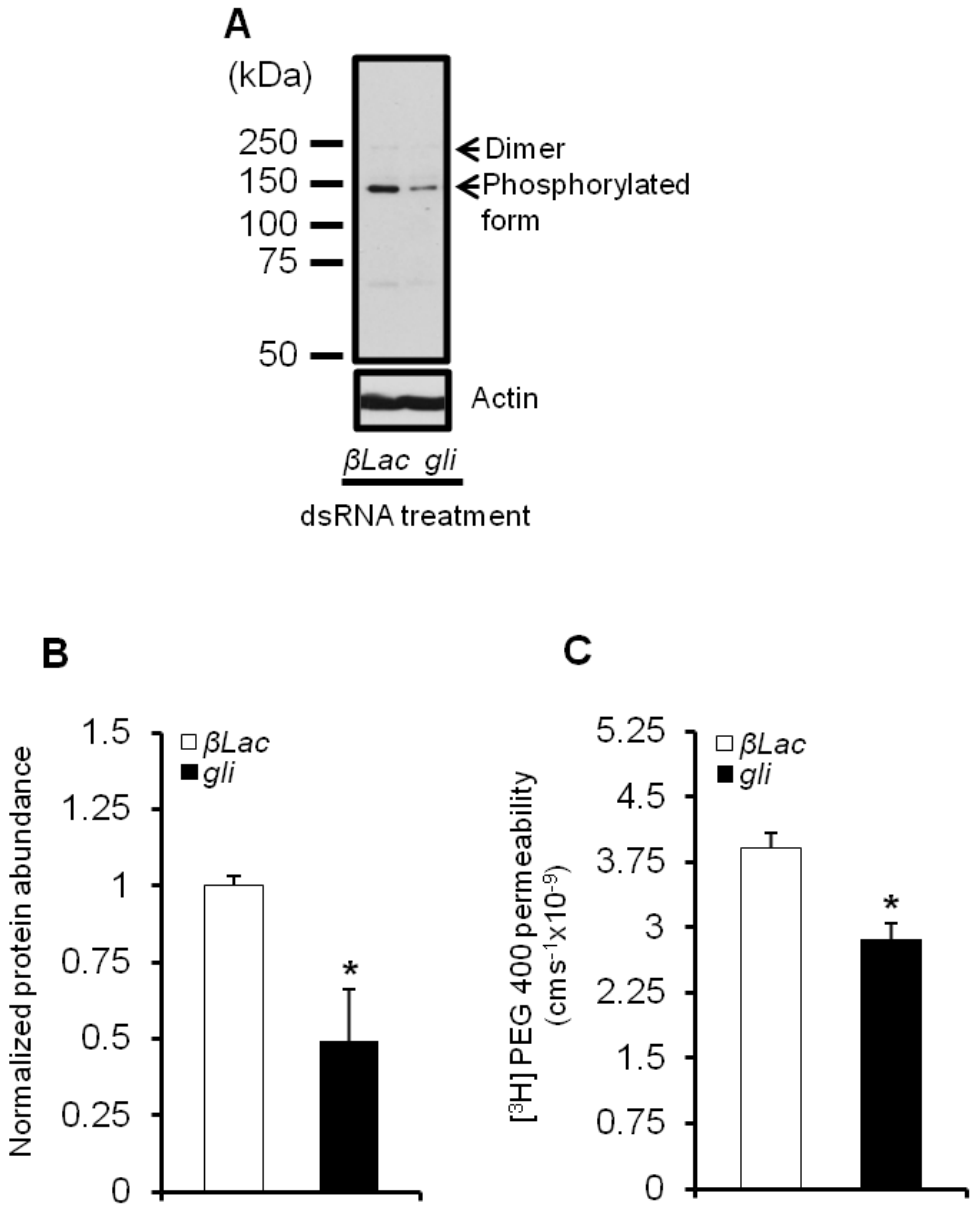

Figure 6-5: The effects of *gli* dsRNA treatment on Gli abundance and [^{3}H]PEG-400 movement across the midgut of *Aedes aegypti* larvae. (**a**) Representative western blot and (**b**) densitometric analysis of putative phosphorylated Gli form in larval anterior midgut (n = 3), and (**c**) measurements of 'PEG-400' flux across the entire larval midgut (n = 13 for *βLac* and n = 17 for *gli*) at day 2 following control *β-lactamase* (*βLac*) or *gli*-targeting dsRNA treatment. Gli abundance was normalized to actin and expressed relative to the *βLac* group. Data are expressed as mean values ± SEM. * significant difference from *βLac* group (Student's *t*-test, $p < 0.05$).

6.5 Discussion

6.5.1 Overview: In this study, we identified the *Aedes aegypti* homolog of the transmembrane septate junction protein, Gli. We hypothesized that Gli would localize to the tricellular junction complex in the epithelia of larval mosquito, as has previously been reported in *Drosophila* (see Schulte et al. 2003, 2006); however, this was not the case since in most tissues examined, Gli localized at bicellular SJs. In contrast, the hypothesis that Gli expression would respond to alterations in salinity can be accepted as Gli levels were found to exhibit an organ-specific increase in animals reared in BW. Furthermore, the hypothesis that Gli would contribute to changes in the permeability of SJs in association with salinity change is supported by changes in paracellular permeability of the midgut epithelium (as measured by [^{3}H]PEG-400 flux), which decreased following a dsRNA targeted reduction in Gli abundance. These observations suggest that Gli participates in the maintenance of salt and water balance and contributes to the regulation of paracellular permeability of osmoregulatory epithelia in the aquatic *A. aegypti* larvae. In addition, these studies make important observations that set the stage to consider, in further detail, what functional similarities and/or differences exist between Gli homologs within the SJ complex in the osmoregulatory epithelia of aquatic and non-aquatic insects.

6.5.2 Gli expression and localization in the osmoregulatory tissues of larval mosquito: An expression profile of mRNA encoding Gli revealed its presence in all larval *A. aegypti* organs examined in this study, i.e. the midgut, Malpighian tubules, hindgut and anal papillae. However, the midgut showed significantly elevated levels of Gli transcript (Fig. 6-2a). The expression of Gli in a wide range of epithelial tissues, including the midgut and hindgut, has been shown in larval *Drosophila* (Schulte et al. 2003, 2006; Byri et al. 2015). On the other hand, Gli is not expressed in the *Drosophila* Malpighian tubules (Schulte et al. 2006). As such, our observation of Gli transcript in the tubules of *A. aegypti* larvae (see Fig. 6-2a) suggests organ-specific

differences in the molecular composition of SJs between the two dipteran species. Support for this idea comes from our recent study reporting the expression of the SJ protein Kune in the posterior midgut of larval *A. aegypti* (Chapter 4). In *Drosophila*, Kune is found only in pSJ-bearing ectodermal epithelia such as the foregut and hindgut but not in the sSJ-bearing endodermal midgut epithelium (Nelson et al. 2010).

Consistent with *gli* transcript expression, Gli protein was detected by western blotting in all osmoregulatory organs of *A. aegypti* larvae. In addition, tissue-specific forms of Gli were revealed. A single Gli immunoreactive band of ~ 115 kDa, consistent with an expected molecular mass of ~ 113 kDa, resolved in Malpighian tubules (Fig. 6-2b). A Gli monomer was also found in anal papillae where an additional higher molecular mass band of ~ 245 kDa, which is about twice the weight of Gli monomer, was observed and we interpret this to be a Gli dimer. The vertebrate homologs of Gli, Neuroligins, have been shown to dimerize or oligomerize via their extracellular serine esterase-like domain (Ichtchenko et al. 1995; Ichtchenko et al. 1996) and Gli dimerization has also been suggested for *Drosophila* (Venema et al. 2004; Padash-Barmchi et al. 2013). In the present study, bands corresponding to Gli monomer, putative dimer and potential phosphorylated form at ~ 150 kDa, similar to phosphorylated *Drosophila* Gli variant (Padash-Barmchi et al. 2010, 2013), were detected in the hindgut of *A. aegypti* larvae (Fig. 6-2b). The cytoplasmic domain of all Gli homologs, including that of *A. aegypti*, has two strongly conserved tyrosine phosphorylation sites (Fig. 6-1; Padash-Barmchi et al. 2010) and in *Drosophila*, the expression level of Gli and unique localization to the TCJ are regulated through phosphorylation and subsequent endocytosis (Padash-Barmchi et al. 2010, 2013). Tight control of Gli is necessary, as its displacement away from the TCJ throughout the SJ domain leads to delamination, migration and apoptosis of columnar epithelial cells in imaginal discs (Padash-Barmchi et al. 2010, 2013). As shown in this study, the predominant putative phosphorylated Gli form was detected

throughout the midgut of larval *A. aegypti*, i.e. the gastric caecae, anterior and posterior midgut (Fig. 6-2b).

Localization of Gli revealed its presence at the cell-cell contact regions between the epithelial cells of gastric caecae, anterior and posterior midgut (Fig. 6-3a-d), suggesting that Gli is a component of bicellular SJs in these epithelia of larval *A. aegypti*. This observation is inconsistent with *Drosophila* Gli which is reported to be concentrated at the TCJs in the midgut epithelium (Byri et al. 2015). However, in the epithelia of epidermis and wing imaginal discs, *Drosophila* Gli spreads throughout the entire SJ domain and interacts with other bicellular SJ components when overexpressed (Schulte et al 2006). As mentioned above, the presence of Gli at the bicellular SJs in *Drosophila* epithelia results in tissue overgrowth and apoptosis (Padash-Barmchi et al. 2010, 2013). In addition, *Drosophila* Gli is phosphorylated at the bicellular SJs to initiate its removal through endocytosis (Padash-Barmchi et al. 2010, 2013). Hence, it is interesting to consider our observations, made in this study, of the predominant putative phosphorylated form of Gli and its localization to the bicellular SJs throughout the midgut of larval *A. aegypti* (see Fig. 6-2b and Fig. 6-3a-d). It appears that differences in the regulation and junctional localization of Gli exist between the two species. This idea is further supported by the finding of Gli in the Malpighian tubules of *A. aegypti* larvae (this study) and its absence from *Drosophila* tubules (Schulte et al. 2003, 2006). We found that Gli immunostaining appeared to be concentrated at the cell-cell contact regions between the principal and stellate cells of larval *A. aegypti* tubules, in particular, when Gli staining is compared to the staining for the stellate cell marker *Ae*-AE (Fig. 6-3e-k). sSJ specific proteins Ssk and mesh have recently been found in the Malpighian tubules of *A. aegypti* larvae where they localize to SJs between all cells (see Chapter 5). Taken together, it is not unreasonable to suggest that there is a difference in the molecular

architecture of SJs between stellate and principle cells in the Malpighian tubules of larval *A. aegypti*.

Lastly, our immunohistochemical analysis of Gli in the hindgut and anal papillae of *A. aegypti* larvae revealed its discontinuous immunostaining along the edges of rectal epithelial cells (Fig. 6-3m) and the syncytial papilla epithelium where Gli showed some co-localization with the apically expressed VA (Fig. 6-3n,o). In the embryonic hindgut of *Drosophila*, Gli is restricted to the TCJ domain between the epithelial cells (Schulte et al. 2003). However, patchy Gli staining in the epithelial cells of the dorsal epidermis has been reported for *Drosophila* embryo (Schulte et al. 2003). The finding of Gli in the anal papilla epithelium of larval *A. aegypti* (this study) which lacks SJs (Sohal and Copeland 1966; Edwards and Harrison 1983) suggests a non-junctional role for Gli in this tissue, as has been suggested for Kune (Chapter 4). In *Drosophila*, Gli is also required for parallel alignment of wing hairs in the adult wing epithelium and this Gli function is dependent on its localization to the apical cell membranes (Venema et al. 2004).

6.5.3 The response of Gli to BW rearing: In the current study, we report that an increase in external salt content triggered organ-specific changes in Gli transcript and protein abundance in *A. aegypti* larvae. Rearing larvae in BW resulted in an increase in Gli protein abundance in the anterior midgut and Malpighian tubules which was consistent with increased Gli transcript levels in these organs (Fig. 6-4a,b). In addition, there was significantly higher Gli protein abundance in the hindgut of BW-reared larvae compared to FW animals, albeit with no change in transcript abundance (Fig. 6-4a,b). Lack of correlation between mRNA transcript and protein abundance has been recently reported for *A. aegypti* Kune (Chapter 4) and such a phenomenon may occur due to mRNA-regulatory mechanisms or differences in protein degradation rate (Fournier et al. 2010). Indeed, in addition to tight control of *Drosophila* Gli protein levels by tyrosine phosphorylation and endocytosis (Padash-Barmchi et al. 2010, 2013), Gli levels are also

regulated at the mRNA level by microRNA-mediated degradation (Sharifkhodaei et al. 2016). Our observation of increased Gli abundance in *A. aegypti* larval anterior midgut and Malpighian tubules in response to salinity (see Fig. 6-4b) coincides with greater transcript abundance of Ssk and mesh in the midgut and Malpighian tubules and Kune protein abundance in the posterior midgut of BW-reared larvae when compared to FW-reared animals (Chapter 5 and Chapter 4). If Gli is required for the formation of the paracellular barrier in the midgut, Malpighian tubules and hindgut of larval *A. aegypti*, as it is in *Drosophila* salivary gland epithelium (Schulte et al. 2003), it could be suggested that increased Gli protein abundance observed in BW-reared larvae will lead to decreased paracellular permeability of these epithelia under saline conditions. However, this does not appear to be the case at least in the midgut which becomes more permeable to the paracellular permeability marker [^{3}H]PEG-400 when *A. aegypti* larvae are reared in BW (Chapter 4). Together, these observations suggest that instead of playing a role in the barrier function of SJs, Gli may contribute to a paracellular channel function, i.e. the ability of SJs to selectively allow paracellular transport of molecules of a certain size or charge or both.

Nevertheless, and in contrast to the response of Gli in the epithelia of the gut to BW condition, there was no change in Gli transcript and protein abundance in the anal papillae of BW-reared *A. aegypti* larvae compared to FW animals (6-4a,b). The role of Gli in the papillae epithelium is unclear at this stage but its lack of response to salinity is in contrast to Kune which was previously shown to be significantly elevated in this tissue upon BW rearing (Chapter 4).

6.5.4 Gli dsRNA knockdown and midgut epithelium permeability: To further explore the idea that an increase in Gli abundance may contribute to an increase in SJ permeability in the midgut, a loss of function approach was taken by targeting *gli* for knockdown using dsRNA. Knockdown of *gli* resulted in a reduction in anterior midgut Gli protein abundance as well as a corresponding, and significant, decrease in [^{3}H]PEG-400 flux across the midgut (Fig. 6-5). From a functional

standpoint, these observations are consistent with the aforementioned increase in paracellular permeability that occurs when Gli abundance is increased in BW reared larvae, suggesting that Gli is required for enhanced paracellular permeability or channel function of midgut SJs. In the TJ complex of vertebrate epithelia, the importance of select TJ proteins imparting channel or pore function is well documented (for review see Günzel and Yu 2013). More specifically, a key role in determining the permeability properties of vertebrate epithelial cells is played by transmembrane TJ proteins claudins which can either contribute to (or dictate) the barrier or channel/pore properties of an epithelium. In the case of the latter, select claudins are able to contribute to an increase in the permeability of certain ion species or molecules of a certain size (Günzel and Yu 2013). In invertebrates, it has been demonstrated that the sSJs in the midgut epithelium of *Bombyx mori* larvae display a high selectivity with respect to the size and the charge of permeating ions (Fiandra et al. 2006). But to our knowledge, no study has linked specific elements of the SJ complex with this kind of physiological process in invertebrate epithelia. How Gli contributes to increased junctional permeability in the midgut of larval *A. aegypti*, as reported in this study, and what these junctions are more permeable to when larvae are in BW (Chapter 4) remains to be answered. But it could be speculated that Gli might contribute to water transport across the midgut of *A. aegypti* larvae. For example, *A. aegypti* larvae have been shown to greatly increase drinking rates in BW conditions (Edwards 1982; Clements 1992). Increased selective paracellular midgut permeability to water movement from the midgut lumen into the hemolymph would help maintain body volume while simultaneously limiting salt loading from the ingested saline medium. The participation of claudin TJ proteins in water-selective movement across vertebrate epithelia has been described in the vertebrate kidney proximal tubule (Rosenthal et al. 2010). On the other hand, Gli might play a role in the formation of ion-selective SJs in larval *A. aegypti* as it has been recently suggested for Ssk and mesh (Chapter 5). More

specifically, it has been proposed that Ssk and mesh might facilitate paracellular Cl^- movement in the midgut and Malpighian tubules in response to salinity (Chapter 5). Given that *A. aegypti* larvae reared in BW show elevated Gli protein levels together with increased Ssk and mesh transcript abundance in the midgut and Malpighian tubules (see Fig. 6-4b and Chapter 5), it seems reasonable to suggest that all three SJ proteins are functionally involved in the maintenance of salt and water balance in BW-reared *A. aegypti* larvae, but whether they share a similar role in the SJ function, such as modulating Cl^- conductance, remains to be investigated. Regardless of the mechanism, the results are in agreement with our hypothesis that Gli plays a role in the regulation of the permeability properties of the osmoregulatory epithelia in larval *A. aegypti*.

6.5.5 Perspectives and Significance: Studies performed in *Drosophila* have greatly expanded our knowledge of the molecular components of insect SJs. Yet, we are still far from understanding the molecular physiology of SJs in other invertebrate species and in particular, how SJ barrier properties either impede solute movement or act as a selectively permeable secretory pathway. In addition, how the SJ integrates and modulates its properties in different epithelia and under different physiological, as well as environmental conditions remains poorly understood. Recent studies on larval mosquitoes (Chapter 4 and Chapter 5) have pointed toward a dynamic role for SJ proteins in the maintenance of salt and water balance in an aquatic insect. The current study provides an insight into the contribution of the SJ protein Gli to the regulation of paracellular permeability properties in osmoregulatory epithelia of mosquito larvae in accord with altered environmental conditions such as salinity. Given the complexities of SJs as well as the many challenges of an aquatic lifestyle, our understanding of the important role of the SJs and their protein machinery in the physiology of larval mosquito homeostasis seems likely to grow with further investigations.

6.6 References

Bradley TJ (1995) The role of physiological capacity, morphology, and phylogeny in determining habitat use in mosquitoes. In: Wainwright PC, Reilly SM (eds) Ecological Morphology. The University of Chicago Press, Chicago, IL, pp 303-318

Byri S, Misra T, Syed ZA, Batz T, Shah J, Boril L, Glashauser J, Aegerter-Wilmsen T, Matzat T, Moussian B, Luschnig S (2015) The triple-repeat protein anaconda controls epithelial tricellular junction formation in *Drosophila*. Dev Cell 33:535-548

Chasiotis H, Ionescu A, Misyura L, Bui P, Fazio K, Wang J, Patrick M, Weihrauch D, Donini A (2016) An animal homolog of plant Mep/Amt transporters promotes ammonia excretion by the anal papillae of the disease vector mosquito *Aedes aegypti*. J Exp Biol 219:1346-1355

Clements AN (1992) The Biology of Mosquitoes, vol 1. Chapman & Hall, London

Del Duca O, Nasirian A, Galperin V, Donini A(2011) Pharmacological characterisation of apical Na^+ and Cl^- transport mechanisms of the anal papillae in the larval mosquito *Aedes aegypti*. J Exp Biol 214:3992-3999

Deligiannaki M, Casper AL, Jung C, Gaul U (2015) Pasiflora proteins are novel core components of the septate junction. Development 142:3046-3057

Donini A, Gaidhu MP, Strasberg D, O'Donnell MJ (2007) Changing salinity induces alterations in hemolymph ion concentrations and Na^+ and Cl^- transport kinetics of the anal papillae in the larval mosquito, *Aedes aegypti*. J Exp Biol 210:983-992

Donini A, O'Donnell MJ (2005) Analysis of Na^+, Cl^-, K^+, H^+ and NH_4^+ concentration gradients adjacent to the surface of anal papillae of the mosquito *Aedes aegypti*: application of self-referencing ion-selective microelectrodes. J Exp Biol 208:603-610

Donini A, Patrick ML, Bijelic G, Christensen RJ, Ianowski JP, Rheault MR, O'Donnell MJ (2006) Secretion of water and ions by Malpighian tubules of larval mosquitoes: Effects of diuretic factors, second messengers, and salinity. Physiol Biochem Zool 79:645-655

Edwards HA (1982) *Aedes aegypti*: energetics of osmoregulation. J Exp Biol 101:135-141

Edwards HA, Harrison JB (1983) An osmoregulatory syncytium and associated cells in a freshwater mosquito. Tissue Cell 15:271-280

Fiandra L, Casartelli M, Giordana B (2006) The paracellular pathway in the lepidopteran larval midgut: modulation by intracellular mediators. Comp Biochem Physiol A Mol Integr Physiol 144:464-473

Fournier ML, Paulson A, Pavelka N, Mosley AL, Gaudenz K, Bradford WD, Glynn E, Li H, Sardiu ME, Fleharty B, Seidel C, Florens L, Washburn MP (2010) Delayed correlation of mRNA and protein expression in rapamycin-treated cells and a role for Ggc1 in cellular sensitivity to rapamycin. Mol Cell Proteomics 9:271-284

Gilbert MM, Auld VJ (2005) Evolution of clams (cholinesterase-like adhesion molecules): structure and function during development. Front Biosci 10:2177-2192

Green CR, Bergquist PR (1982) Phylogentic relationships within the invertebrates in relation to the structure of septate junctions and the development of ‘occluding’ junctional types. J Cell Sci 53:279-305

Günzel D, Yu ASL (2013) Claudins and the modulation of tight junction permeability. Physiol Rev 93:525-569

Ichtchenko K, Hata Y, Nguyen T, Ullrich B, Missler M, Moomaw C, Sudhof TC (1995) Neuroligin 1: a splice site-specific ligand for beta-neurexins Cell 81:435-443

Ichtchenko K, Nguyen T, Sudhof TC (1996) Structures, alternative splicing, and neurexin binding of multiple neuroligins. J Biol Chem 271:2676-2682

Izumi Y, Furuse M (2014) Molecular organization and function of invertebrate occluding junctions. Semin Cell Dev Biol 36:186-193

Izumi Y, Motoishi M, Furuse K, Furuse M (2016) A tetraspanin regulates septate junction formation in Drosophila midgut. J Cell Sci 129:1155-1164

Izumi Y, Yanagihashi Y, Furuse M (2012) A novel protein complex, Mesh-Ssk, is required for septate junction formation in the *Drosophila* midgut. J Cell Sci 125:4923-4933

Kolosov D, Kelly SP (2013) A role for tricellulin in the regulation of gill epithelium permeability. Am J Physiol Regul Integr Comp Physiol 304:R1139-R1148

Linser PJ, Neira Oviedo M, Hirata T, Seron TJ, Smith KE, Piermarini PM, Romero MF (2012) Slc4-like anion transporters of the larval mosquito alimentary canal. J Insect Physiol 58:551-562

Luquet CM, Genovese G, Rosa GA, Pellerano GN (2002) Ultrastructural changes in the gill epithelium of the crab *Chasmagnathus granulates* (Decapoda: Grapsidae) in diluted and concentrated seawater. Mar Biol 141:753-760

Luquet C, Pellerano G, Rosa G (1997) Salinity-induced changes in the fine structure of the gills of the semiterrestrial estuarian crab, *Uca uruguayensis* (Nobili, 1901) (Decapoda, Ocypodidae). Tissue Cell 29: 495-501

Nelson KS, Furuse M, Beitel GJ (2010) The *Drosophila* Claudin Kune-kune is required for septate junction organization and tracheal tube size control. Genetics 185:831-839

Padash-Barmchi M, Browne K, Sturgeon K, Jusiak B, Auld VJ (2010) Control of Gliotactin localization and levels by tyrosine phosphorylation and endocytosis is necessary for survival of polarized epithelia. J Cell Sci 123: 4052-4062

Padash-Barmchi M, Charish K, Que J, Auld VJ (2013) Gliotactin and Discs large are co-regulated to maintain epithelial integrity. J Cell Sci 126:1134-1143

Patrick ML, Aimanova K, Sanders HR, Gill SS (2006) P-type Na^+/ K^+-ATPase and V-type H^+-ATPase expression patterns in the osmoregulatory organs of larval and adult mosquito *Aedes aegypti*. J Exp Biol 209:4638-4651

Patrick ML, Gonzalez RJ, Wood CM, Wilson RW, Bradley TJ, Val AL (2002) The characterization of ion regulation in Amazonian mosquito larvae: evidence of phenotypic plasticity, population-based disparity, and novel mechanisms of ion uptake. Physiol Biochem Zool 75:223-236

Piermarini PM, Grogan LF, Lau K, Wang L, Beyenbach KW (2010) A SLC4-like anion exchanger from renal tubules of the mosquito (Aedes aegypti): evidence for a novel role of stellate cells in diuretic fluid secretion. Am J Physiol Regul Integr Comp Physiol 298(3):R642-R660

Rosenthal R, Milatz S, Krug SM, Oelrich B, Schulzke JD, Amasheh S, Günzel D, Fromm M (2012) Claudin-2, a component of the tight junction, forms a paracellular water channel. J Cell Sci 123:1913-1921

Schulte J, Charish K, Que J, Ravn S, MacKinnon C, Auld VJ (2006) Gliotactin and Discs large form a protein complex at the tricellular junction of polarized epithelial cells in *Drosophila*. J Cell Sci 119:4391-4401

Schulte J, Tepass U, Auld VJ (2003) Gliotactin, a novel marker of tricellular junctions, is necessary for septate junction development in *Drosophila*. J Cell Biol 161:991-1000

Sharifkhodaei Z, Padash-Barmchi M, Gilbert MM, Samarasekera G, Fulga TA, Van Vactor D, Auld VJ (2016) The Drosophila tricellular junction protein Gliotactin regulates its own mRNA levels through BMP-mediated induction of miR-184. J Cell Sci 129:1477-1489

Smith KE, VanEkeris LA, Okech BA, Harvey WR, Linser PJ (2008) Larval anopheline mosquito recta exhibit a dramatic change in localization patterns of ion transport proteins in response to

shifting salinity: a comparison between anopheline and culicine larvae. J Exp Biol 211:3067-3076

Sohal RS, Copeland E (1966) Ultrastructural variations in the anal papillae of *Aedes aegypti* (L) at different environmental salinities. J Insect Physiol 12:429-434

Venema DR, Zeev-Ben-Mordehai T, Auld VJ (2004) Transient apical polarization of Gliotactin and Coracle is required for parallel alignment of wing hairs in *Drosophila*. Dev Biol 275:301-314

Yanagihashi Y, Usui T, Izumi Y, Yonemura S, Sumida M, Tsukita S, Uemura T, Furuse M (2012) Snakeskin, a membrane protein associated with smooth septate junctions, is required for intestinal barrier function in *Drosophila*. J Cell Sci 125:1980-1990

CHAPTER 7:

EFFECTS OF SALINITY AND LEUCOKININ ON THE PARACELLULAR PERMEABILITY OF THE MALPIGHIAN TUBULES OF LARVAL *AEDES AEGYPTI*

7.1 Summary

This study examined the effects of brackish water (BW) rearing of larval *Aedes aegypti* on Malpighian tubule fluid secretion and paracellular permeability to [^{3}H]PEG-400. It was found that unstimulated tubule secretion rates were not affected by the salinity of the rearing medium. However, the tubules isolated from the larvae reared in BW showed a twofold decrease in the permeability to PEG-400 compared to FW larval tubules. We also examined the response of larval Malpighian tubules to the neuropeptide leucokinin-VIII (LKVIII), known to increase the transepithelial fluid secretion and junctional permeability in the Malpighian tubules of adult *A. aegypti*. It was found that LKVIII stimulated fluid secretion by tubules isolated from FW- and BW-reared larvae and the extent of stimulation was similar for both. However, LKVIII treatment revealed a salinity-dependent effect on tubule permeability, i.e. the tubules from FW-reared larvae showed a significant decrease in PEG-400 permeability whereas BW tubules were more permeable to PEG-400 in response to LKVIII. Taken together, data suggest that changes in rearing salinity lead to alterations in larval *A. aegypti* tubule permeability which is further modulated by the actions of leucokinin.

7.2 Introduction

Regulation of insect hemolymph composition is critical for survival, and the mechanisms involved should reflect the environmental challenges faced by the insect. Mosquito larvae are aquatic and regulate hemolymph ionic concentrations over a range of salinities. Larvae of freshwater (FW) species, such as *Aedes aegypti*, live in water more dilute than their hemolymph and must therefore conserve ions and eliminate excess water. However, larval habitats may become salinated due to climatic or anthropogenic factors which presents the opposing challenge of passive ion gain.

The primary urine in insects is produced by the Malpighian tubules. The Malpighian tubule of *A. aegypti* larva is a one-cell thick epithelium made up of two types of cells, the principal and stellate cells (Clements 1992). There are two routes for ion and water transport across the tubule epithelium: the transcellular path through either principal or stellate cells, and the paracellular route through smooth septate junctions (sSJs) between cells (Bradley et al 1982; Chapter 5). Studies examining the role of Malpighian tubules in the regulation of salt and water balance in larval *A. aegypti* have generally focused on transcellular routes of ion movement and suggested regulation of active transcellular transport of major cations Na^+ and K^+ (Clark and Bradley 1996, 1997; Donini et al. 2006). Far less is known about the contribution and functional features of the paracellular pathway of larval *A. aegypti* tubules. It has been recently reported that the Malpighian tubules of *A. aegypti* larva express sSJ-specific proteins snakeskin (Ssk) and mesh which localize to the junctions between all cells (Chapter 5). In addition, larval tubules were also shown to express the transmembrane SJ protein gliotactin (Gli) which was confined to the junctional domains between the stellate and principal cells (Chapter 6). These studies further demonstrated that brackish water (BW) rearing caused an increase in Gli protein and Ssk and mesh transcript abundance in the Malpighian tubules and these observations lead to the

hypothesis that modulation of tubule SJ permeability occurs in the larvae, particularly during conditions of altered environmental salinity (Chapter 5 and 6).

In Malpighian tubules of adult *A. aegypti*, the SJs are permselective to Cl^- (Pannabecker et al. 1993). This junctional Cl^- permeability provides a paracellular pathway for Cl^-, allowing Cl^- to serve as a counterion for the cations Na^+ and K^+ that are secreted across the epithelium by energy dependent transcellular pathways (Beyenbach and Piermarini 2011). Paracellular Cl^- permeability in adult tubules increases in the presence of the neuropeptide leucokinin-VIII (LKVIII) which in turn increases the transepithelial Na^+, K^+ and fluid secretion (Pannabecker et al. 1993; Yu and Beyenbach 2001, 2004). Moreover, it has been shown that LKVIII changes the Malpighian tubule of adult *A. aegypti* from a moderately tight epithelium (58 Ω cm^2) to a leaky epithelium (10 Ω cm^2) (Pannabecker et al. 1993) and increases junctional permeability to paracellular permeability markers inulin and sucrose (Wang et al. 1996).

Therefore, the objectives of the present study were to 1) determine whether there is a difference in the paracellular permeability of Malpighian tubules isolated from *A. aegypti* larvae reared in different salinities, and 2) examine a potential role for LKVIII in the regulation of larval tubule permeability.

7.3 Materials and methods

7.3.1 Insects: A laboratory colony of *Aedes aegypti* (Linnaeus) was maintained in the Department of Biology at York University as previously described (Chapter 4).

7.3.2 Salinity rearing: Eggs were hatched in plastic containers filled with FW with composition ([ion] µmol l^{-1} [Na^+] 590; [Cl^-] 920; [Ca^{2+}] 760; [K^+] 43; pH 7.35) or 30 % seawater (SW) solution (10.5 g/l Instant Ocean SeaSalt®, United Pet Group, Blacksburg, VA, USA) which served as the experimental brackish water (BW) treatment. Hatched larvae were allowed to grow to the 4th instar. Larvae were fed daily and water of appropriate salinity was changed weekly.

7.3.3 Malpighian tubule secretion assay: The tubule secretion assay used in this study was based on the assay described by Donini et al. (2006). Malpighian tubules of 4th instar larvae were dissected in ice-cold physiological saline (composition in mmol l^{-1}: L-proline, 5; L-glutamine, 9.1; L-histidine, 8.74; L-leucine, 14.4; L-arginine, 3.37; glucose, 10; succinic acid, 5; malic acid, 5; trisodium citrate, 10; NaCl, 30; KCl, 3; $NaHCO_3$, 5; $MgSO_4$, 0.6; $CaCl_2$, 5; HEPES, 25; pH 7). After ~15 min, tubules were transferred to a dish with 15 individual 20 µl saline drops that were suspended in paraffin oil (Fisher Scientific) and contained 0.5 µCi [^{3}H]polyethylene glycol (molecular mass 400 Da; 'PEG-400'; American Radiolabeled Chemicals, Inc., Saint Louis, MO) or 0.5 µCi PEG-400 and 1 µmol l^{-1} leucokinin-VIII (LKVIII; sequence GASFYSWG-amide; Phoenix Pharmaceuticals, Inc., Burlingame, CA, USA) . The severed end of the tubule, which had been attached to the gut, was pulled out of the saline drop with a fine glass rod and wrapped around the sharp tip of a fine steel insect pin under oil. Droplets of secreted fluid formed on the tip of the insect pin and could be readily collected under oil with a fine glass probe. After 3 h, the secreted fluid droplets were collected, pooled into one, and the diameter of a pooled droplet measured with an ocular micrometer for the determination of volume. The droplet was subsequently transferred to a scintillation vial containing 500 µl of saline to which 5ml

scintillation fluid (National diagnostics, Atlanta, Georgia, USA) was added for radioactivity measurement. The length and diameter of the tubule segment inside the saline drop were also measured for the determination of the surface area of the tubule available for the transport of PEG-400.

The rate of fluid secretion was determined by calculating the volume of a pooled droplet as $4/3\pi r^3$, where r is the radius of the droplet, and dividing the volume by the time over which the droplet formed and the number of tubules that produced the pooled droplet.

PEG-400 flux rate was calculated according to the following equation:

$$P = \Delta[PEG]_{Ap} \times Volume_{Ap} / [PEG]_{Bl} \times Time \times 3600 \times Surface\ Area,$$

where $[PEG]_{B1}$ is mean radioactivity on the basolateral side (saline drop); $\Delta[PEG]_{Ap}$ is the change in radioactivity on the apical side (secreted droplet) and 3600 converts time from hours to seconds. The surface area of the tubules was calculated from measurements of their length and diameter, assuming them to be a cylinder with two open ends as follows:

$$Surface\ Area = 2\ \pi\ r\ l,$$

where r and l are the radius and the length of the tubules, respectively.

7.3.4 Statistics: Data are expressed as means ± SEM (n). To examine for significant differences in salinity or LKVIII effect on tubule fluid secretion and PEG-400 permeability, an unpaired Student's *t*-test was used. The effect of rearing salinity and LKVIII on fluid secretion and PEG-400 permeability was assessed with two-way ANOVA followed by Bonferroni multiple comparison test. Statistical significance was allotted to differences with $p < 0.05$. All statistical analyses were conducted using SigmaStat 3.5 software (Systat Software, San Jose, USA).

7.4 Results

7.4.1 Effects of rearing salinity on unstimulated Malpighian tubule secretion and [^{3}H]PEG-400 permeability: Fluid secretion rates of Malpighian tubules isolated from *A. aegypti* larvae were similar for larvae reared in either FW or BW (Fig. 7-1a). In contrast, the permeability of the tubules to PEG-400 was significantly lower in BW-reared larvae, at 20.14 cm s^{-1} x 10^{-9}, compared to FW group, at 42.2 cm s^{-1} x 10^{-9} (Fig. 7-1b).

7.4.2 Effects of leucokinin-VIII on Malpighian tubule secretion and [^{3}H]PEG-400 permeability: Fluid secretion rates of Malpighian tubules isolated from *A. aegypti* larvae were similar for larvae reared in either FW or BW in the presence of LKVIII (Fig. 7-2a). In contrast, LKVIII increased PEG-400 permeability of the tubules from BW-reared larvae compared to FW group (Fig. 7-2b).

7.4.3 Interactive effects of rearing salinity and leucokinin-VIII on Malpighian tubule secretion and [^{3}H]PEG-400 permeability: Fluid secretion rates of tubules isolated from either FW or BW increased significantly in response to LKVIII (7-3a). There was no significant interaction between rearing salinity and LKVIII effect on fluid secretion rate (two-way ANOVA, $p = 0.94$). For tubules isolated from *A. aegypti* larvae reared in FW, there was a significant decrease in PEG-400 permeability in response to LKVIII (Fig. 7-3b). In contrast, the tubules isolated from BW-reared larvae showed a significant increase in PEG-400 permeability when treated with LKVIII (Fig. 7-3b). There was a significant interaction between rearing salinity and LKVIII effect on tubule permeability to PEG-400 (two-way ANOVA, $p < 0.05$).

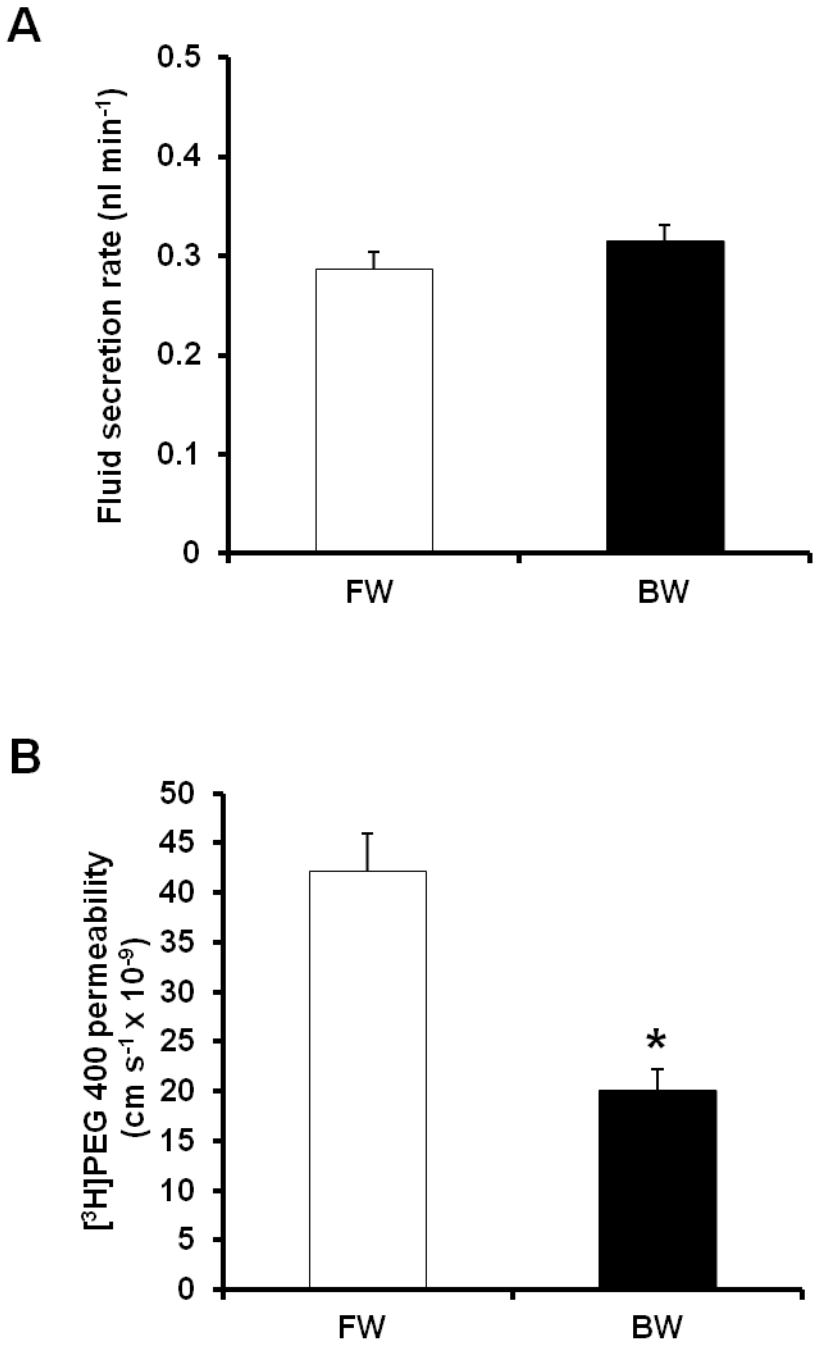

Figure 7-1: Effects of rearing salinity on fluid secretion (**a**) and [^{3}H]PEG-400 permeability (**b**) in Malpighian tubules of larval *Aedes aegypti*. The different salinities were freshwater (FW) and brackish water (BW; 30% seawater). All data are expressed as mean values ± SEM (n = 20 for FW and n = 25 for BW). An asterisk denotes statistically significant difference from FW (Student's t-test, $p < 0.05$).

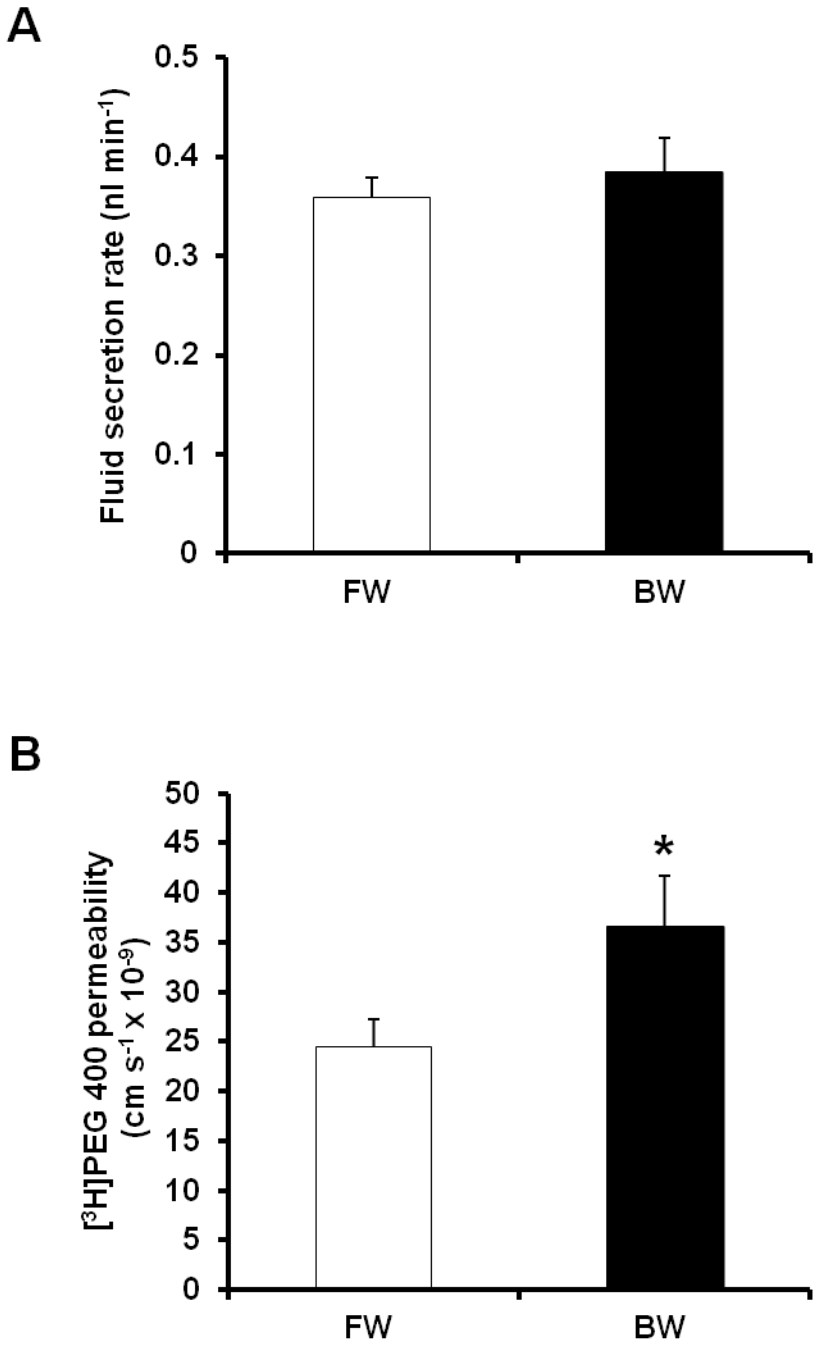

Figure 7-2: Effects of 1 µmol l^{-1} leucokinin-VIII (LKVIII) on fluid secretion (**a**) and [^{3}H]PEG-400 permeability (**b**) in Malpighian tubules of larval *Aedes aegypti* reared in freshwater (FW) or brackish water (BW; 30% seawater). All data are expressed as mean values ± SEM (n = 21 for FW and n = 16 for BW). An asterisk denotes statistically significant difference from FW (Student's t-test, $p < 0.05$).

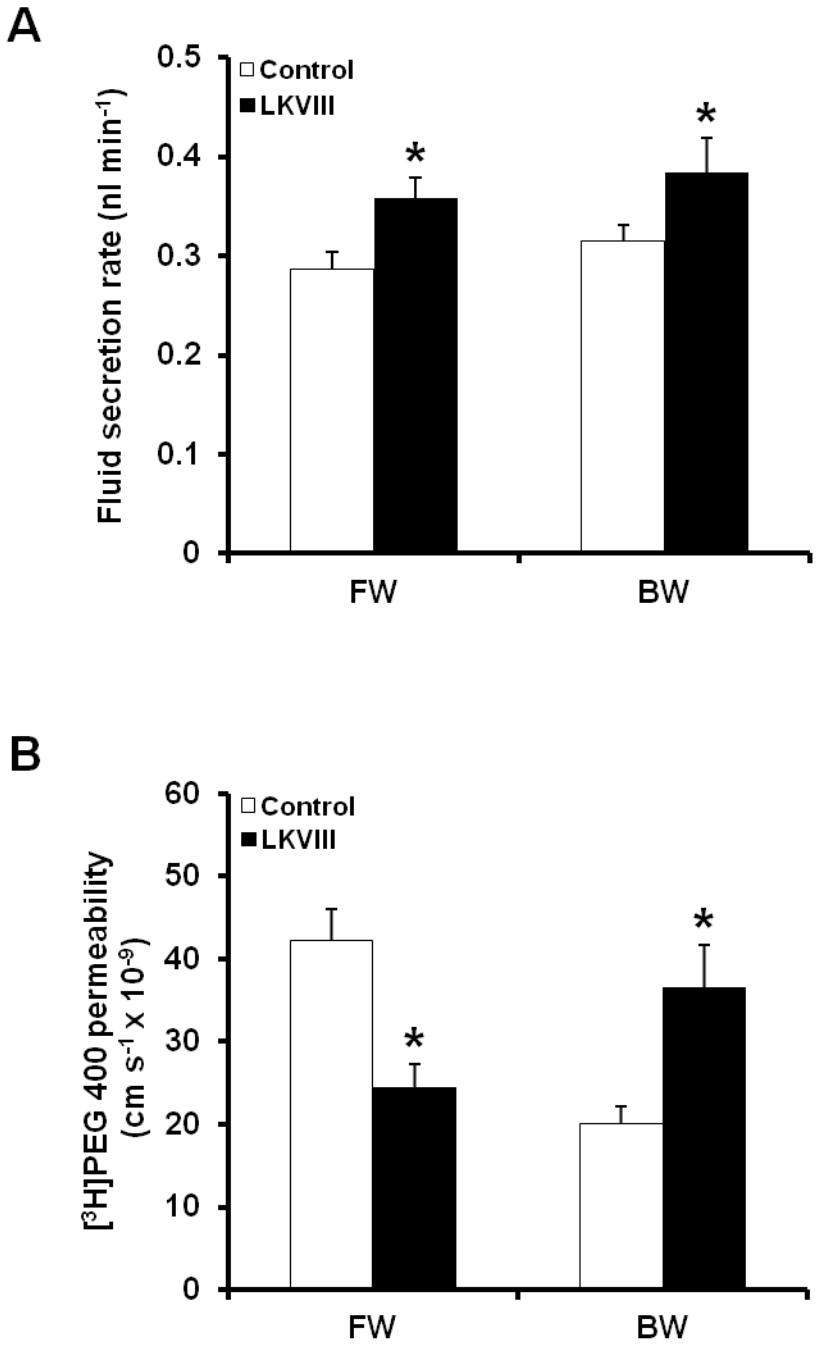

Figure 7-3: Effects of rearing salinity and 1 µmol l^{-1} leucokinin-VIII (LKVIII) on fluid secretion (**a**) and [^{3}H]PEG-400 permeability (**b**) in Malpighian tubules of larval *Aedes aegypti*. The different salinities were freshwater (FW) and brackish water (BW; 30% seawater). All data are expressed as mean values ± SEM (n = 16-25). An asterisk denotes statistically significant difference between control and treatment groups (two-way ANOVA, Bonferroni multiple comparison, $p < 0.05$).

7.5 Discussion

7.5.1 Overview: Over the past 30 years, many studies on mosquito Malpighian tubules have demonstrated a variety of mechanisms (e.g. ion transporters, neurohormonal factors, intracellular second messengers) that regulate and mediate fluid secretion and ion transport (Beyenbach KW 2003; Donini et al. 2006; Coast 2009; Beyenbach and Piermarini 2011; Esquivel et al. 2016). However, our understanding of how mosquito Malpighian tubules contribute to salt and water balance is limited, especially for an aquatic larval stage. Even less is known about the functional properties and regulation of the paracellular pathway in mosquito tubules. Our results obtained from the current study suggest that changes in environmental conditions such as salinity induce alterations in the paracellular permeability of unstimulated tubules isolated from the larval *A. aegypti* mosquito. In addition, this study provides the first evidence of the modulation of larval tubule SJ permeability by leucokinin, which is in agreement with the observations made for adult *A. aegypti* tubules (Pannabecker et al. 1993; Wang et al. 1996). Taken together, the data allow us to accept our original hypothesis that differences in Malpighian tubule paracellular permeability would be observed in larvae reared in different salinities and that hormonal regulation of the tubule paracellular permeability takes place.

7.5.2 Effect of rearing salinity and LKVIII on larval tubule secretion and permeability: Fluid secretion rates by the Malpighian tubules isolated from larval *A.aegypti* reared in FW and BW (30% SW) have previously been measured (Donini et al. 2006). In the aforementioned study, unstimulated tubule secretion rates were not affected by changing the rearing salinity from FW to BW and were ~0.22 and ~0.23 nl min^{-1} for FW and BW tubules, respectively. The latter observations are in agreement with the results of this study, reporting similar secretion rates for tubules isolated from FW- and BW-reared larvae at ~0.28 and ~0.3 nl min^{-1}, respectively (Fig. 7-1a).

Rearing salinity affected the paracellular permeability of larval *A. aegypti* tubules. Specifically, tubules isolated from BW-reared larvae showed a twofold decrease in the permeability to PEG-400 compared to FW tubules (Fig. 7-1b), suggesting a tighter tubule epithelium under saline conditions. Interestingly, it has been recently reported that the midgut epithelium of larval *A. aegypti* becomes leakier in BW, as revealed by a twofold increase in the permeability to PEG-400 (Chapter 5). It is also interesting to note that the tubule epithelium of FW-reared *A. aegypti* larvae is much more permeable to PEG-400 compared to the epithelium of the midgut (this study and Chapter 5) and this may suggest potential differences in the functions of the two epithelia, i.e. secretion versus absorption, respectively. The differences in junctional permeability properties of these epithelia may also lie in the complex nature of molecular SJ architecture. Although both the Malpighian tubules and entire midgut of larval *A. aegypti* express sSJ-specific proteins Ssk and mesh (Chpater 5), only larval posterior midgut exhibits junctional expression of SJ protein Kune which is absent in the tubules (Chapter 4). In addition, the SJ component Gli appears to be restricted to the junctions between the stellate and principal cells in the larval tubules while expressed in junctional domains between all epithelial cells in the midgut (Chapter 6).

In this study, we also found that fluid secretion rates by leucokinin treated Malpighian tubules of *A. aegypti* larvae were not affected by the change in rearing salinity. Tubules isolated from FW- and BW-reared larvae showed a similar fluid secretion rate in the presence of LKVIII (Fig. 7-2a). In addition, LKVIII had a salinity-independent stimulatory effect on larval tubules as an increase in fluid secretion was observed for FW- and BW-tubules in response to LKVIII (Fig. 7-3a). These observations are in line with previously reported diuretic effects of LKVIII on larval *A. aegypti* tubules (Donini et al. 2006).

Rearing *A. aegypti* larvae in BW was associated with increased tubule permeability to PEG-400 in response to LKVIII compared to tubules isolated from FW-reared larvae (Fig. 7-2b), which is in contrast to the observations made for unstimulated tubules (see Fig. 7-1b). Previous studies on adult *A. aegypti* Malpighian tubules have demonstrated that in parallel with an increase in transepithelial fluid secretion, LKVIII increases tubule permeability to paracellular permeability markers inulin and sucrose (Pannabecker et al. 1993; Wang et al. 1996). As discussed above, in this study, LKVIII stimulated increase in fluid secretion was observed for both FW and BW larval tubules (see Fig. 7-3a). However, the LKVIII effect on larval tubule permeability to PEG-400 was salinity-dependent, i.e. the tubules isolated from BW-reared larvae showed an increase in permeability to PEG-400 whereas those of FW-reared animals had reduced PEG-400 permeability in response to LKVIII (Fig. 7-3b). Taken together. these results suggest that rearing salinity affects the way LKVIII modulates the paracellular pathway in larval *A. aegypti* tubules.

7.5.3 Role of paracellular transport in larval tubules: In the present study, data suggest that in the absence of hormonal factors, the Malpighian tubules of larval *A. aegypti* respond to an increase in environmental salt content by decreasing the paracellular permeability with no change in transepithelial water transport. Donini et al. (2006) has also shown a decrease in transepithelial K^+ secretion with no change in Na^+ transport by the tubules isolated from BW-reared *A. aegypti* larvae. Given that Cl^- serves as a counterion for K^+ and Na^+ secretion in the tubules, it seems reasonable to suggest that the transepithelial Cl^- transport would also be attenuated in the tubules of BW-reared *A. aegypti* larvae. As such, reduced tubule permeability to PEG-400 under BW conditions (see Fig. 7-1b) may indicate a decrease in paracellular Cl^- transport. Selective junctional Cl^- permeability is well established for adult *A. aegypti* tubules (Pannabecker et al. 1993; Yu and Beyenbach 2004; Beyenbach and Piermarini 2011). Reduced paracellular Cl^-

conductance in the tubules of *A. aegypti* larvae reared in BW would at least in part contribute to the elevated hemolymph Cl^- levels in response to BW rearing (Chapter 4; Donini et al. 2006) which might serve as a mechanism to reduce salt loading from ingested saline water.

It is interesting to consider the potential physiological consequences of the effects of LKVIII on larval *A. aegypti* tubule permeability. If decreased larval tubule permeability to PEG-400 is a consequence of reduced junctional Cl^- transport, it can be postulated that the decrease in PEG-400 flux, and thus Cl^-, across FW tubules in response to LKVIII (see Fig. 7-3b) may provide a mechanism to conserve hemolymph Cl^- under dilute conditions. On the other hand, increased tubule permeability to PEG-400 in response to LKVIII in BW (see Fig. 7-3b) would suggest increased junctional Cl^- conductance which in turn would help to remove the excess Cl^- when larvae encounter higher salinity. These speculations will require studies on Cl^- flux across larval tubules under conditions of abolished transcellular transport to resolve them.

7.5.4 Conclusions: Septate junctions define the properties of the paracellular pathway in the insect Malpighian tubules, but our understanding of the contribution of this pathway to salt and water balance as well as its regulation and the mechanism of action of hormonal factors remains elusive. This study has shown that alterations in environmental salinity have profound effects on the paracellular permeability and the actions of leucokinin in larval mosquito tubules. Further electrophysiological studies as well as investigations of the molecular architecture of SJs are needed to reveal the functional characteristics of the SJ complex and mechanisms that couple leucokinin to the modulation of junctional permeability of Malpighian tubules.

7.6 References

Beyenbach KW (2003) Transport mechanisms of diuresis in Malpighian tubules of insects. J Exp Biol 206:3845-3856

Beyenbach KW, Piermarini PM (2011) Transcellular and paracellular pathways of transepithelial fluid secretion in Malpighian (renal) tubules of the yellow fever mosquito *Aedes aegypti*. Acta Physiol (Oxf) 202:387-407

Bradley TJ, Stuart AM, Satir P (1982) The ultrastructure of the larval malpighian tubules of a saline-water mosquito. Tissue Cell 14(4):759-773

Clark TM, Bradley TJ (1996) Stimulation of Malpighian tubules from larval *Aedes aegypti* by secretagogues. J Insect Physiol 42:593-602

Clark TM, Bradley TJ (1997) Malpighian tubules of larval *Aedes aegypti* are hormonally stimulated by 5-hydroxytryptamine in response to increased salinity. Arch Insect Biochem Physiol 34:123-141

Clements AN 1992 The Biology of Mosquitoes, vol 1. Chapman & Hall, London

Coast GM (2009) Neuroendocrine control of ionic homeostasis in blood-sucking insects. J Exp Biol 212:378-386

Donini A, Patrick ML, Bijelic G, Christensen RJ, Ianowski JP, Rheault MR, O'Donnell MJ (2006) Secretion of water and ions by Malpighian tubules of larval mosquitoes: Effects of diuretic factors, second messengers, and salinity. Physiol Biochem Zool 79:645-655

Esquivel CJ, Cassone BJ, Piermarini PM (2016) A de novo transcriptome of the Malpighian tubules in non- blood-fed and blood-fed Asian tiger mosquitoes *Aedes albopictus*: insights into diuresis, detoxification, and blood meal processing. PeerJ 4:e1784

Pannabecker TL, Hayes TK, Beyenbach KW (1993) Regulation of epithelial shunt conductance by the peptide leucokinin. J Membr Biol 132:63-76

Wang S, Rubenfeld AB, Hayes TK, Beyenbach KW, (1996) Leucokinin increases paracellular permeability in insect Malpighian tubules. J Exp Biol 199:2537-2542

Yu MJ, Beyenbach KW (2001) Leucokinin and the modulation of the shunt pathway in Malpighian tubules. J Insect Physiol 47:263-276

Yu MJ, Beyenbach KW (2004) Effects of leucokinin-VIII on *Aedes* Malpighian tubule segments lacking stellate cells. J Exp Biol 207:519-526

CHAPTER 8: Summary and future directions

8.1 Summary

At the beginning of this research, relatively little was known of the contribution of transcellular and paracellular solute movement to the osmoregulatory homeostasis of FW larval Dipterans such as chironomids and mosquitoes. New studies in this area have appeared since then. An insight into the mechanism of ion and water transport by the Malpighian tubules of FW chironomid larvae has been provided along with their role in salt and water balance under different environmental conditions (Zadeh-Tahmasebi et al. 2016). Several septate junction (SJ) proteins, including smooth SJ(sSJ)-specific components snakeskin (Ssk) and mesh, have been identified in the Malpighian tubules of adult mosquito where they have been proposed to play a role in regulating the permeability of the paracellular pathway in response to salt loading (Esquivel et al. 2016). However, the collection of studies presented in this dissertation provide a more detailed molecular and functional characterization and more profound understanding of the osmoregulatory roles of active transport machinery in the alimentary canal of FW larval chironomid and SJ proteins in the osmoregulatory epithelia of FW larval mosquito. Regarding the specific objectives of these studies (as outlined in Chapter 1), major findings are summarized below.

8.1.1 A role for active ion transport in FW larval chironomid osmoregulation

To establish a role for active ion transport machinery in the regulation of salt and water balance in FW larval chironomid, the activity and localization of key ionomotive enzymes Na^+/K^+-ATPase (NKA) and V-type H^+-ATPase (VA) were determined along the gut epithelia of *C. riparius* exposed to varying salinity (Chapter 2). The results pointed to the rectum as having the highest ionomotive enzyme activity in IPW- and FW-reared larvae which was significantly reduced in response to BW rearing (Chapter 2). Using the scanning ion-selective electrode

technique, combined with the application of ion transport inhibitors, it was further revealed that the rectum is a site of NKA and VA driven K^+ reabsorption in IPW and FW conditions and that this rectal K^+ reabsorption is greatly reduced in BW-reared larvae (Chapter 2).

Taken together, these studies provide novel information on tissue-specific actions of NKA and VA in aquatic insect larvae in response to changes in environmental conditions and support the notion of the functional conservation for the rectum in regulating ion homeostasis in aquatic insects under both dilute and saline conditions. In the specific case of FW larval *C. riparius*, attenuated rectal ion reabsorption is likely to contribute to the larva's ability to thrive in natural BW environments as well as polluted FW habitats (Colbo 1996; Bervoets et al. 1996).

8.1.2 Transmembrane SJ proteins in FW larval mosquito

8.1.2.1 Kune, Ssk, mesh and Gli are components of SJs in osmoregulatory tissues of larval *A. aegypti*

Using molecular techniques, full sequences of genes encoding transmembrane SJ proteins kune-kune (Kune), megatrachea (Mega), sinuous (Sinu), neurexin IV (Nrx IV), snakeskin (Ssk), mesh and gliotactin (Gli) from *A. aegypti* were identified (Chapter 4, 5 and 6). Transcripts of Kune, Gli, Mega and Nrx IV were detected in all of the osmoregulatory epithelia of larval *A. aegypti* such as the midgut, Malpighian tubules, hindgut and anal papillae but tissue-specific differences in transcript abundance of these SJ proteins were observed (Chapter 4 and 6). On the other hand, transcript expression of Ssk and mesh was found only in the mosquito larval midgut and Malpighian tubules, which possess sSJs, and this was consistent with immunolocalization of Ssk and mesh proteins to the SJs of these epithelia alone (Chapter 5). Immunohistochemical analysis of Kune distribution in the osmoregulatory tissues of *A. aegypti* larvae revealed its expression within the SJs in the posterior portion of the midgut as well as rectum and in the apical membrane domain of the syncytial anal papilla epithelium (Chapter 4). Immunostaining patterns of Gli

within larval osmoregulatory epithelia were also characterized (Chapter 6). For example, Gli immunolocalization was confined to the SJs between the stellate and principal cells in the Malpighian tubules and between midgut epithelial cells (Chapter 6).

Collectively, these data present the first description of the molecular characterization of SJ complex in an aquatic arthropod despite an extensive literature on the ultrastructure of SJs in the epithelia of arthropods (for review see Chapter 3). The molecular physiology of arthropod SJs is known to some extent in a non-aquatic insect such as *Drosophila* (Chapter 3). Based on the information on SJ components in larval *Drosophila* epithelia and the observations made in the current studies on larval *A. aegypti*, similarities and differences in the SJ architecture have emerged between the two species. More specifically, both animals express Ssk and mesh only in the midgut and Malpighian tubules, where sSJs occur, suggesting that Ssk and mesh are sSJ-specific components conserved among Diptera (Chapter 5; Yanagihashi et al. 2012; Izumi et al. 2012). On the other hand, Gli is not found in the Malpighian tubules of *Drosophila* and is a component of tricellular junctions in the epithelia that express it (Schulte et al. 2003; Byri et al. 2015) which is unlike observations made for *A. aegypti* larvae where Gli is a component of bicellular SJs in the tubules as well as the midgut (as described above).

8.1.2.2 A role for Kune, Ssk, mesh and Gli in larval *A. aegypti* osmoregulation

To establish a potential role for SJ proteins in the regulation of salt and water balance in FW larval mosquito, Kune, Mega, Sinu, Nrx IV, Ssk, mesh and Gli abundance in the osmoregulatory epithelia was determined for FW- and BW-reared *A. aegypti* larvae. In response to BW rearing, SJ protein abundance was shown to alter in a tissue-specific manner (Chapter 4, 5 and 6). For example, Gli protein and Ssk and mesh transcript abundance was significantly elevated in the Malpighian tubules of BW-reared larvae (Chapter 5 and 6). In addition, increased Ssk and mesh transcript and Gli and Kune protein abundance was found in the BW larval midgut (Chapter 4, 5

and 6). It is noteworthy that Kune protein abundance in larval anal papillae was also shown to elevate in response to BW rearing (Chapter 4). Extensive studies on the ultrastructure of the *A. aegypti* anal papilla epithelium have revealed no evidence of lateral plasma membranes or SJs (Sohal and Copeland 1966; Edwards and Harrison 1983). Thus, the presence of Kune as well as Gli (Chapter 6) in this tissue and salinity-induced alterations in Kune abundance suggest additional non-junctional functions for SJ proteins.

Since the abundance of a number of transmembrane SJ proteins (as discussed above) as well as cytoplasmic SJ components (Appendix A.1) changed in larval *A. aegypti* midgut and Malpighian tubules in response to BW condition, it was postulated that the paracellular permeability of these epithelia would also be altered. Indeed, upregulation of Kune and Gli protein and Ssk and mesh transcript levels in the midgut of BW-reared *A. aegypti* larvae occurred in conjunction with increased midgut permeability to the paracellular permeability marker PEG-400 (Chapter 5). In addition, increased Gli protein and Ssk and mesh transcript abundance in the Malpighian tubules of BW larvae (Chapter 5 and 6) was associated with decreased tubule permeability to PEG-400 (Chapter 7). Taken together, these observations appear to indicate that Kune, Gli, Ssk and mesh play a role in larval *A. aegypti* osmoregulation by modulating the permeability of the osmoregulatory epithelia such as the midgut and Malpighian tubules.

The Malpighian tubules of adult female *A. aegypti* are known to have SJs that are permselective to Cl^- (Pannabecker et al. 1993). This junctional Cl^- permeability in adult tubules is modulated by the neuropeptide leucokinin to help rid of the unwanted salts and water of the blood meal (Pannabecker et al. 1993; Beyenbach and Piermarini 2011). It was postulated that leucokinin might also modulate larval *A. aegypti* tubule permeability in different salinities (Chapter 7). Indeed, in addition to differences in larval tubule permeability in FW and BW (as discussed above), salinity-dependent leucokinin effects on tubule permeability were observed, i.e.

the tubules isolated from BW-reared larvae showed an increase in permeability to PEG-400 whereas those of FW-reared animals had reduced PEG-400 permeability in response to leucokinin (Chapter 7). Collectively, these results suggest that leucokinin may enhance the function of larval mosquito Malpighian tubules during acclimation to varying salinities by increasing SJ permeability to Cl^- to help remove excess hemolymph Cl^- in higher salinity and by reducing junctional Cl^- conductance in FW to conserve hemolymph Cl^-. In addition, these studies appear to indicate the conservation of leucokinin as a modulator of junctional permeability in the Malpighian tubules of adult and larval mosquito and support the idea of leucokinin regulation of SJ proteins (Beyenbach and Piermarini 2011). In the case of larval mosquito tubules, salinity-responsive Gli, Ssk and mesh are good candidates for such regulation.

8.1.2.3 Gli contributes to increased larval *A. aegypti* midgut permeability

To determine a functional role for Gli in the regulation of the paracellular permeability in the midgut epithelium, *gli*-targeting double stranded RNA (dsRNA) was used to knockdown Gli expression in the midgut of *A. aegypti* larvae (Chapter 6). dsRNA-mediated reduction in Gli abundance resulted in a corresponding and significantly decreased midgut permeability to PEG-400 (Chapter 6). Since Gli abundance is increased in BW-reared larvae and this occurs in conjunction with an increase in midgut permeability (as discussed above; Chapter 5 and 6), collectively, these observations suggest that Gli is required for enhanced paracellular permeability or channel function of midgut SJs. In the epithelia of vertebrates, the importance of select tight junction proteins imparting channel or pore function is well documented (for review see Günzel and Yu 2013). It is possible that Gli contributes to water transport across the midgut of *A. aegypti* larvae. These larvae have been shown to greatly increase drinking rates in BW condition (Edwards 1982; Clements 1992) and increased selective paracellular midgut permeability to water would help maintain body volume while simultaneously limiting salt

loading from ingested saline medium. On the other hand, Gli might facilitate paracellular Cl^- movement in the midgut in response to salinity, considering that Gli protein levels are also elevated in BW larval Malpighian tubules (Chapter 6) where salinity-induced increase in junctional Cl^- conductance has been suggested (Chapter 7). Taken together, these studies provide evidence that one role for Gli is to participate in the regulation of paracellular permeability of larval mosquito osmoregulatory epithelia in response to changes in environmental salinity.

8.2 Future directions

The regulation of salt and water balance is a particularly fruitful avenue for research because it occupies a dominant role in the physiology of many aquatic organisms. The present studies have greatly contributed to our fundamental knowledge of the molecular physiology of transepithelial solute transport and its role in the regulation of salt and water balance in FW larval Dipterans. Significant insight into the function of active transport components NKA and VA in the rectum of larval chironomid has been gained and the findings provide a strong impetus for further identification and characterization of the major transport mechanisms in the apical and basolateral membranes of the rectal epithelium of aquatic insects. New insights into the contribution of SJ proteins, particularly Gli, to the maintenance of salt and water balance in larval mosquito have been provided. However, the permeability properties of SJs in larval mosquito osmoregulatory epithelia are still unclear. For example, although dsRNA-mediated reduction in Gli abundance increased midgut permeability to uncharged PEG-400 (Chapter 6), the question remains whether Gli regulates the paracellular movement of certain ion species or molecules of a certain size or both. Future studies on Gli knockdown larvae using paracellular markers that vary in charge and size are warranted.

Future loss-of-function studies utilizing dsRNA would help to ascertain Kune, Ssk and mesh roles in the regulation of SJ permeability in the osmoregulatory epithelia of mosquito

larvae. Ssk and mesh are known to form a complex and are mutually interdependent for their correct localization and barrier function in *Drosophila* midgut (Izumi et al. 2012). Future studies using co-immunoprecipitation assay would be helpful for determining if Ssk and mesh function together in the formation of sSJs in larval mosquito.

Future work examining Cl^- flux across larval *A. aegypti* Malpighian tubules under conditions of abolished transcellular transport would certainly help to determine if larval tubules are permselective to Cl^- and whether leucokinin regulates this junctional Cl^- permeability. In addition, studies utilizing Gli, Ssk and mesh knockdown larvae would clarify if the observed effect of leucokinin on larval tubule permeability (Chapter 7) and alteration in Gli, Ssk and mesh abundance in the tubules in response to salinity (Chapter 5 and 6) is in part due to leucokinin regulation of these SJ components.

Although the transmembrane SJ proteins were the primary focus of this research, several cytoplasmic SJ components, i.e. coracle, scribble, lethal giant larvae and discs large, were identified and appear to play a role in larval *A. aegypti* osmoregulation (see Appendix A.1). Loss-of-function studies on these proteins would help to further delineate the molecular architecture and permeability properties of both sSJs and pSJs in the osmoregulatory tissues of larval mosquito.

8.3 References

Bervoets L, Baillieul B, Blust R, Verheyen R (1995) Evaluation of effluent toxicity and ambient toxicity in a polluted lowland river. Environ Pollut 91:333-341

Beyenbach KW, Piermarini PM (2011) Transcellular and paracellular pathways of transepithelial fluid secretion in Malpighian (renal) tubules of the yellow fever mosquito *Aedes aegypti*. Acta Physio (Oxf) 202:387-407

Byri S, Misra T, Syed ZA, Batz T, Shah J, Boril L, Glashauser J, Aegerter-Wilmsen T, Matzat T, Moussian B, Luschnig S (2015) The triple-repeat protein anaconda controls epithelial tricellular junction formation in *Drosophila*. Dev Cell 33:535-548

Clements AN (1992) The Biology of Mosquitoes, vol 1. Chapman & Hall, London

Colbo MH (1996) Chironomidae from marine coastal environments near St. John's, Newfoundland, Canada. Hydrobiologia 318:117-122

Edwards HA (1982) *Aedes aegypti*: energetics of osmoregulation. J Exp Biol 101:135-141

Edwards HA, Harrison JB (1983) An osmoregulatory syncytium and associated cells in a freshwater mosquito. Tissue Cell 15:271-280

Esquivel CJ, Cassone BJ, Piermarini PM (2016) A de novo transcriptome of the Malpighian tubules in non-blood-fed and blood-fed Asian tiger mosquitoes *Aedes albopictus*: insights into diuresis, detoxification, and blood meal processing. PeerJ 4:e1784

Günzel D, Yu ASL (2013) Claudins and the modulation of tight junction permeability. Physiol Rev 93:525-569

Izumi Y, Yanagihashi Y, Furuse M (2012) A novel protein complex, Mesh-Ssk, is required for septate junction formation in the *Drosophila* midgut. J. Cell Sci 125:4923-4933

Schulte J, Tepass U, Auld VJ (2003) Gliotactin, a novel marker of tricellular junctions, is necessary for septate junction development in *Drosophila*. J Cell Biol 161:991-1000

Sohal RS, Copeland E (1966) Ultrastructural variations in the anal papillae of *Aedes aegypti* (L) at different environmental salinities. J Insect Physiol 12:429-434

Yanagihashi Y, Usui T, Izumi Y, Yonemura S, Sumida M, Tsukita S, Uemura T, Furuse M (2012) Snakeskin, a membrane protein associated with smooth septate junctions, is required for intestinal barrier function in *Drosophila*. J Cell Sci 125:1980-1990

Zadeh-Tahmasebi M, Bui P, Donini A (2016) Fluid and ion secretion by malpighian tubules of larval chironomids, *Chironomus riparius*: effects of rearing salinity, transport inhibitors, and serotonin. Arch Insect Biochem Physiol 93:67-85

APPENDIX A: Supplementary data

A.1 Cytoplasmic septate junction proteins coracle, scribble, lethal giant larva and discs large: expression profile and response to salinity

A.1.1 Rational and methodology: As described in Chapter 3, another set of proteins that are important for the formation of septate junctions (SJs) in *Drosophila* reside on the cytoplasmic side of the membrane. Among those are scaffolding/regulatory proteins such as FERM-domain protein coracle (Cor, *cor*), multi-PDZ and leucine-rich repeat protein scribble (Scrib, *scrib*), WD-40 repeat protein lethal giant larvae (Lgl, *lgl*), and MAGUK family protein discs large (Dlg, *dlg*). *Drosophila* Scrib, Dlg and Lgl constitute a distinct subgroup of proteins required for initial epithelial cell polarization during early stages of embryogenesis before SJ development. The latter proteins are also involved in the regulation of cell growth as *Drosophila* tumor suppressors, a finding that highlights the importance of SJs for proper cell-cell communication during epithelial morphogenesis in addition to forming paracellular barriers (Chapter 3).

In this section, a potential role for Cor, Scrib, Lgl and Dlg in the regulation of salt and water balance in larval *A. aegypti* was considered. Transcript expression of *cor*, *scrib*, *lgl* and *dlg* was examined in the osmoregulatory epithelia of larval *A. aegypti* and localization of Cor, Scrib and Lgl were further determined using custom made *A. aegypti* anti-Cor, anti-Scrib and anti-Lgl antibodies. Lastly, effects of changes in rearing salinity on transcript abundance of *cor*, *scrib*, *lgl* and *dlg* in the osmoregulatory tissues of *A. aegypti* larvae were investigated.

As outlined in Chapter 4, gene-specific primers for *cor*, *scrib*, *lgl* and *dlg* (see Table A-1) were designed based on expressed sequence tags (ESTs) from *A. aegypti* genome available on the National Center for Biotechnology Information (NCBI) database. Larval rearing, tissue RNA extraction, cDNA synthesis and qRT-PCR analysis were conducted according to methods described in Chapter 4. Immunohistochemical processing of larval *A. aegypti* tissues was

Table A-1: Primer sets, amplicon size, annealing temperatures and GenBank accession numbers for *Aedes aegypti* SJ genes *cor*, *scrib*, *lgl* and *dlg*.

Gene	Primer Sequence	Amplicon length, bp	Annealing Temperature, ^{0}C	Accession #
Coracle				
FOR REV	5'- CACAGTAGTCGGCCTTCTTC-3' 5'- CCAGTCGTTCTCTTCCTTGC-3'	207	59	XM_001652916.1
Scribble				
FOR REV	5'- GATATGACTTGGGCTCGGGG-3' 5'- ATACGCCACGTTGAAAACTG-3'	198	59	XM_001661311.1
Lethal giant larva				
FOR REV	5'- TATTAGCTTTTCGTGGTCGG-3' 5'- GCTCACGAGTCCGATGTTGG-3'	191	59	XM_001654062
Discs large				
FOR REV	5'- CCACATCGACTAGACGTCCG-3' 5'- CCTCTTCCTGTAGGTCTTGG-3'	204	59	DV383935

performed according to the methods detailed in Chapter 4 using custom synthesized polyclonal *A. aegypti* anti-Cor (epitope sequence CRYDEDPSAHARDKE), anti-Scrib (epitope sequence HPKELKLKAHKLFAKEC) and anti-Lgl (epitope sequence QFDPYSDDPRLAVK) antibodies at 1:100 dilution for Cor and Scrib, and 1:50 dilution for Lgl.

A.1.2 Results and discussion: Transcripts encoding *cor, scrib, lgl* and *dlg* were found in all tissues examined such as the midgut, Malpighian tubules, hindgut and anal papillae of *A. aegypti* larvae (Fig. A-1) which is consistent with broad tissue expression of these SJ proteins in larval *Drosophila* (see Chapter 3). Transcript abundance of *cor* and *scrib* was somewhat lower in the Malpighian tubules relative to the other tissues (Fig. A-1a,b) and significantly higher *lgl* mRNA abundance was found in the midgut compared to the hindgut, Malpighian tubules and anal papillae (Fig. A-1c). On the other hand, *dlg* mRNA abundance was highest in the hindgut in comparison to the other tissues (Fig. A-1d).

Immunohistochemical analysis of Cor, Scrib and Lgl in *A. aegypti* larvae revealed that all three proteins are expressed in all of the osmoregulatory tissues. These proteins were localized to the cell-cell contact regions in the epithelial cells of the gastric caecae, midgut, Malpighian tubules and rectum (Fig. A-2 a-d, i-l, p-w). Immunostaining of Cor was also prominent in the epithelium of anal papillae (Fig. A-2e) where it exhibited co-immunoreactivity with the apical membrane marker VA and little to no colocalization with the basal membrane marker NKA (Fig. A-2f and g, respectively). Immunofluorescence labelling of Scrib and Lgl within the sections of anal papillae showed immunoreactivity of both proteins in the epithelium as well as inside the lumen of the papillae (Fig. A-2m and x, respectively). Within the epithelium of anal papillae, Scrib and Lgl appeared to co-immunolocalize with VA (Fig. A-2n and y, respectively).

It was also found that rearing *A. aegypti* larvae in BW induced changes in *cor, scrib, lgl*, and *dlg* mRNA abundance. This manifested as an increase in *cor, scrib, lgl* and *dgl* transcript

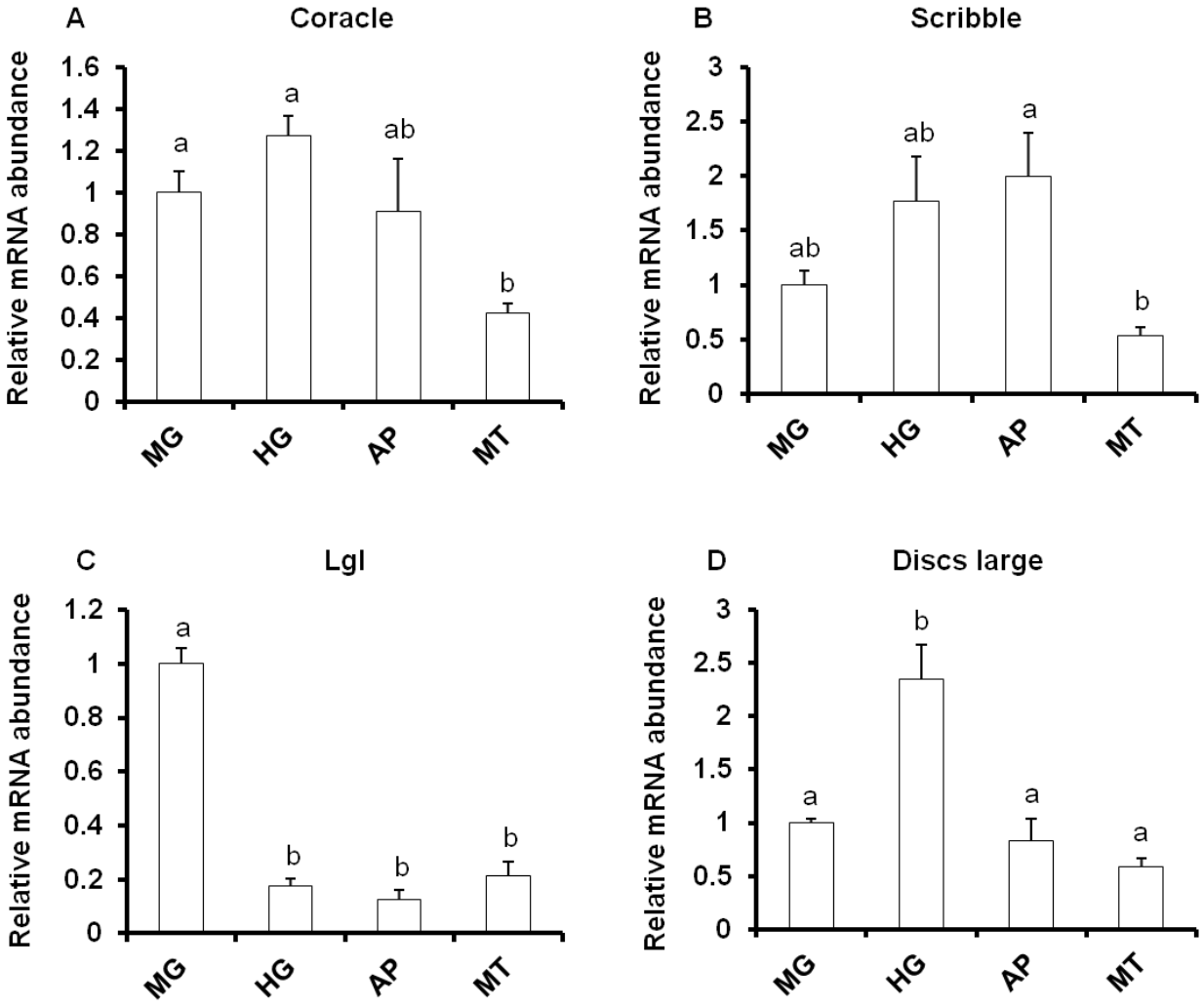

Figure A-1: Comparison of *cor*, *scrib*, *lgl* and *dlg* mRNA abundance in the midgut (MG), hindgut (HG), anal papillae (AP) and Malpighian tubules (MT) of FW reared *Aedes aegypti* larvae. Each gene was normalized to *rp49* and was expressed relative to its levels in the midgut (assigned a value of 1). All data are expressed as mean values ± SEM (n = 5-6). Letters denote statistically significant differences between tissues (one-way ANOVA, Tukey's multiple comparison, $p < 0.05$).

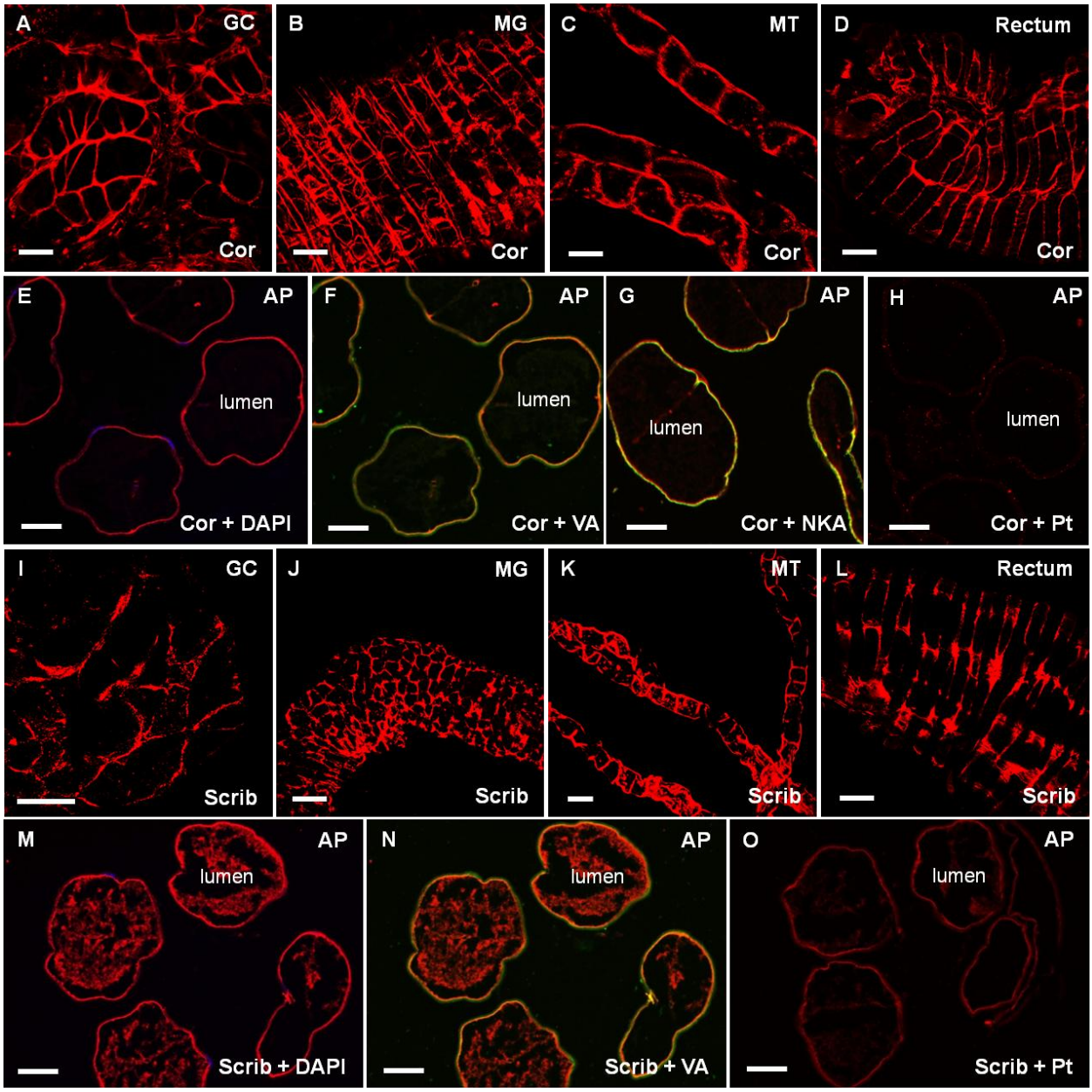

Figure A-2: (see legend on next page).

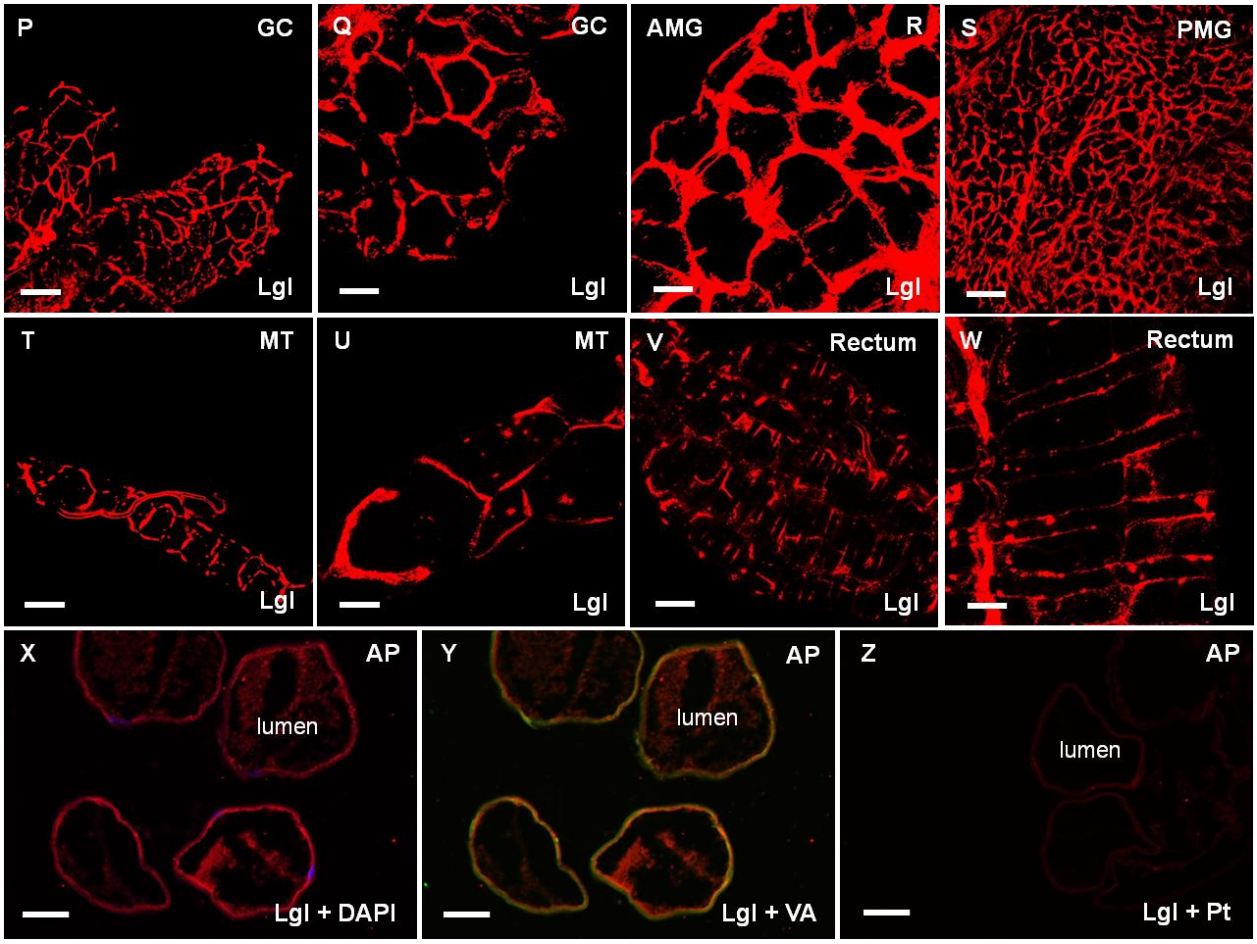

Figure A-2: Immunofluorescence staining of coracle (Cor), scribble (Scrib) and lethal giant larva (Lgl) in the osmoregulatory tissues of *Aedes aegypti* larvae. All three proteins were concentrated at regions of cell-cell contact between the epithelial cells of the gastric caecae (**a**, **i**, **p**, **q**), midgut (**b**, **j**, **r**, **s**), Malpighian tubules (**c**, **k**, **t**, **u**) as well as rectum (**d**, **l**, **v**, **w**). **Q**, **u** and **w** are higher magnification images of **p**, **t** and **v**. Immunostaining of Cor is also prominent in the epithelium of anal papillae (**e**, red) where it shows some colocalization with apical V-type H^+-ATPase (VA; **f**, green) and little to no co-immunoreactivity with basal Na^+/K^+-ATPase (NKA; **g**, green). Immunofluorescence of Scrib and Lgl was also detected in the anal papillae (**m** and **x**, respectively), where both proteins showed some co-immunostaining with VA in the epithelium and immunoreactivity inside the lumen of the papilla section (**m**, **n**, **x**, **y**). Nuclei of anal papilla epithelium are stained with DAPI (blue) in **e**, **m** and **x**. **H**, **o** and **z** show control sections of anal papillae treated with primary antibody in the presence of immunizing peptide (Pt). Scale bars, (**a**, **b**, **i**, **q**-**s**, **u**, **w**) 20 µm, (**c**, **d**-**h**, **j**-**p**, **t**, **v**, **x**-**z**) 50 µm. GC, gastric caecae; AMG, anterior midgut; PMG, posterior midgut; MT, Malpighian tubules; AP, anal papillae.

abundance in the midgut (Fig. A-3a) and a decrease in *cor* and *scrib* mRNA levels in the hindgut and anal papillae (Fig. A-3b,c). There was an increase in *scrib* transcript abundance in the Malpighian tubules of BW-reared larvae compared to FW animals (Fig. A-3d).

The observed increase in *cor* and *scrib* mRNA abundance in the midgut and a decrease in their transcript levels in the hindgut and anal papillae in response to BW rearing (see Fig. A-3a-c) would seem to suggest tissue-specific functions for these SJ proteins in the osmoregulatory tissues of *A. aegypti* larvae. Multiple roles for Cor have been suggested in the epithelia of larval *Drosophila* (Lamb et al. 1998; Izumi et al. 2012). Cor is required for the formation of septa and the paracellular barrier in ectodermally derived epithelia of *Drosophila* larvae (Lamb et al. 1998). However, in the endodermal tissue such as the midgut, Cor has been suggested to function in the organization of sSJs and/or regulation of epithelial polarity as morphological sSJs are still present in *cor* mutant larvae (Izumi et al. 2012). With regards to *Drosophila* Scrib, it is present only in ectodermal epithelia where it serves as an early marker for the site of future SJs and is required for the proper localization of other SJ proteins (Bilder and Perrimon 2000). Interestingly, it has been shown that a mammalian homolog of Scrib associates with tight junction (TJ) protein ZO-1 and is required for the assembly of TJs and integrity of epithelial barrier in human intestinal epithelium (Ivanov et al. 2010).

The finding of a similar response of *lgl* and *dlg* to salinity, i.e. increase in their mRNA abundance only in the midgut of BW-reared *A. aegypti* larvae (see Fig. A-3) may suggest a functional relationship between Lgl and Dlg in the midgut epithelium. In *Drosophila*, *dlg* encodes a multifunctional protein involved in the regulation of cell proliferation, maintenance of SJs and the apicobasal polarity of epithelial cells (Woods et al. 1996). The Lgl is a SJ component shown to participate in the cytoskeletal network via its direct association with the nonmuscle myosin heavy chain (Strand et al. 1994a; Strand et al. 1994b). Loss of Lgl activity leads to cell-

shape changes and hyperthrophy of the midgut of larval *Drosophila* (Manfruelli et al. 1996). Interestingly, *Drosophila dlg* mutants also exhibit a similar hypertrophied midgut phenotype (Izumi et al. 2012). At this stage, it is difficult to speculate whether *lgl* and *dlg* expression in the midgut of larval *A. aegypti* is related but their similar response to salinity may suggest that *lgl* and *dlg* function together to modulate midgut permeability of *A. aegypti* larvae. Interestingly, the knockdown of mammalian *lgl* promotes the TJ integrity and barrier function in the Sertoli cells (Su et al. 2012). This is mediated by reorganization of the actin filament network at the Sertoli cell-cell interface, which in turn affects changes in the localization and/or distribution of other TJ proteins (Su et al. 2012). In light of the direct association of *Drosophila* Lgl with the cytoskeletal network, it would be conceivable to suggest a similar function of invertebrate Lgl in modulating SJ integrity. This could at least in part explain the observed changes, i.e. increase in *lgl* expression (this report) and paracellular permeability (Chapter 5) in the midgut of larval *A. aegypti* in response to BW rearing.

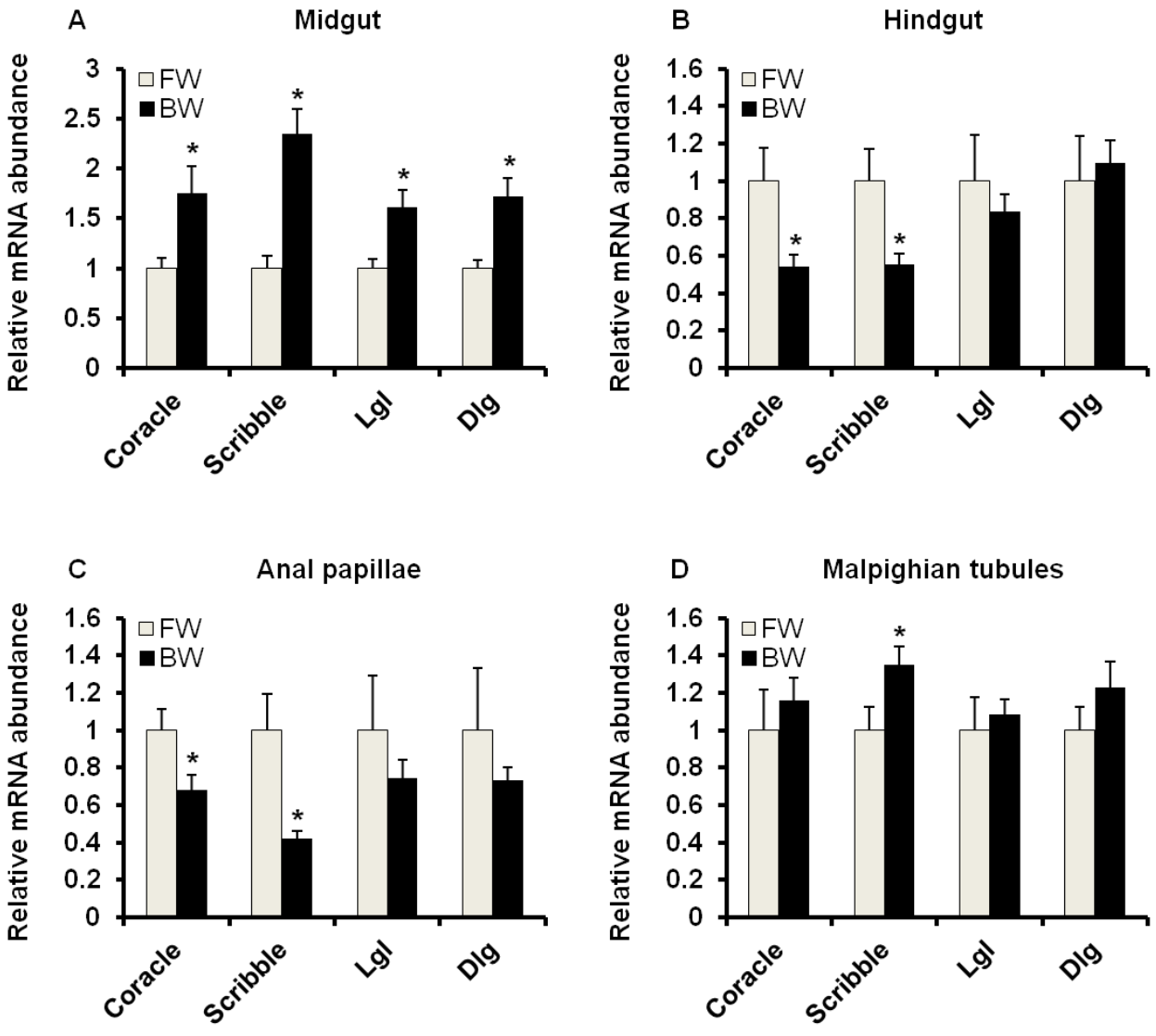

Figure A-3: The effect of salinity on mRNA abundance of *cor*, *scrib*, *lgl* and *dlg* in (**a**) midgut, (**b**) hindgut, (**c**) anal papillae, and (**d**) Malpighian tubules of larval *Aedes aegypti* as examined by qRT-PCR analysis. Each SJ gene was normalized to *18S rRNA* and expressed relative to its FW value (assigned value of 1). All data are expressed as mean values ± SEM (n = 5-6)**.** An asterisk denotes significant difference from FW (Student-t test, $p \leq 0.05$).

A.2 References

Bilder D, Perrimon N (2000) Localization of apical epithelial determinants by the basolateral PDZ protein Scribble. Nature 403:676-680

Ivanov AI, Young C, Den Beste K, Capaldo CT, Humbert PO, Brennwald P, Parkos CA, Nusrat A (2010) Tumor suppressor scribble regulates assembly of tight junctions in the intestinal epithelium. Am J Pathol 176:134-145

Izumi Y, Yanagihashi Y, Furuse M (2012) A novel protein complex, Mesh-Ssk, is required for septate junction formation in the *Drosophila* midgut. J Cell Sci 125:4923-4933

Lamb RS, Ward RE, Schweizer L, Fehon RG (1998) *Drosophila coracle*, a member of the protein 4.1 superfamily, has essential structural functions in the septate junctions and developmental functions in embryonic and adult epithelial cells. Mol Cell Biol 9:3505-3519

Manfruelli P, Arquier N, Hanratty WP, Semeriva M (1996) The tumor suppressor gene, *lethal(2)giant larvae (1(2)g1)*, is required for cell shape change of epithelial cells during Drosophila development. Development 122:2283-2294

Strand D, Jakobs R, Merdes G, Neumann B, Kalmes A, Heid HW, Husmann I, Mechler BM (1994a) The *Drosophila lethal(2)giant larvae* tumor suppressor protein forms homo-oligomers and is associated with nonmuscle myosin II heavy chain. J Cell Biol 127:1361-1373

Strand D, Raska I, Mechler BM (1994b) The Drosophila lethal(2)giant larvae tumor suppressor protein is a component of the cytoskeleton. J Cell Biol 127:1345-1360

Su W, Wong EWP, Mruk DD, Cheng CY (2012) The Scribble/Lgl/Dlg polarity protein complex is a regulator of blood-testis barrier dynamics and spermatid polarity during spermatogenesis. Endocrinology 153:6041-6053

Woods DF, Hough C, Peel D, Callaini G, Bryant PJ (1996) Dlg protein is required for junction structure, cell polarity, and proliferation control in *Drosophila* epithelia. J Cell Biol 134:1469-1482